

École Doctorale des Sciences de la Terre et de l'Environnement (ED413)
Institut de Physique du Globe de Strasbourg (UMR7516)

THÈSE présentée par :

Jordi MIRÓ PADRISA

Soutenue le : 13 octobre 2020

Pour obtenir le grade de : **Docteur de l'Université de Strasbourg et**
l'Universitat de Barcelona

Discipline/ Spécialité : **Sciences de la Terra – Géologie - Tectonique**

Rift-inheritance, segmentation and reactivation of the North Iberian rift system in the Basque - Cantabrian Pyrenees

Thèse dirigée par :

Pr. MANATSCHAL Gianreto
Pr. MUÑOZ DE LA FUENTE Josep Anton

Université de Strasbourg (FR)
Universitat de Barcelona (ES)

Rapporteurs:

Pr. TEIXELL Antonio
Pr. SOTO Juan Ignacio

Universitat Autònoma de Barcelona (ES)
Bureau of Economic Geology (USA)

Autres membres du jury :

Dr. LE POURHIET Laetitia
Dr. PEDREIRA David
Dr. ROWAN Mark
Dr. ZAMORA Gonzalo

Institut des Sciences de la Terre de Paris (FR)
Universidad de Oviedo (ES)
Rowan Consulting Inc. (USA)
Repsol (ES)

UNIVERSITÉ DE STRASBOURG & UNIVERSITAT DE BARCELONA

THESIS presented by: **Jordi MIRÓ PADRISA**

Within the **OROGEN** project



TOTAL



Géosciences pour une Terre durable

brgm

To obtain the grade of Ph.D. by:

Université de Strasbourg & Universitat de Barcelona

Rift-inheritance, segmentation and reactivation of the North Iberian rift system in the Basque - Cantabrian Pyrenees

Thesis supervises by:

Pr. MANATSCHAL Gianreto

Pr. MUÑOZ DE LA FUENTE Josep Anton

Université de Strasbourg (FR)

Universitat de Barcelona (ES)

Examiners:

Pr. TEIXELL Antonio

Pr. SOTO Juan Ignacio

Universitat Autònoma de Barcelona (ES)

Bureau of Economic Geology (USA)

Other members of the jury :

Dr. LE POURHIET Laetitia

Dr. PEDREIRA David

Dr. ROWAN Mark

Dr. ZAMORA Gonzalo

Institut des Sciences de la Terre de Paris (FR)

Universidad de Oviedo (ES)

Rowan Consulting Inc. (USA)

Repsol (ES)

Invited members:

Dr. MASINI Emmanuel

Dr. CALASSOU Sylvain

M&U sas (FR)

Total R&D (FR)

ABSTRACT

The processes responsible for the formation of oceans and mountain ranges represent an essential part of research in tectonics. These processes were characterized and defined throughout the Wilson Cycle in the 1960s, despite some ideas were developed in previous works, mainly based on direct observations in orogenic systems. During the last decades, knowledge on the formation of orogens but also on the passive margins has increased significantly, favoured by the development of new concepts as well as new data acquisition techniques. Thus, the processes that control the formation of rift margins and orogens are well known and understood by the respective communities. However, many studies addressing the inheritance concept have been published in the last years, aiding the understanding of many scientific problematics unresolved until then. Recent investigations involving the role of large and small-scale inheritance in extensive or compressive regimes has contributed significantly to a better understanding of the Wilson Cycle. This thesis focuses on the importance of inheritance in the formation of polyphase and multi-stage rift systems as well as on their reactivation and incorporation into orogens.

The Basque – Cantabrian Pyrenees represent an excellent natural laboratory to address the above outlined topics since the Pyrenean Orogen results from the reactivation of ancient hyperextended rift system/passive margin. Indeed, this system results from the development of different episodes (“multistage”) of Mesozoic rifting leading to a final polyphase extension, resulting into exhumation of sub-continental mantle during the Middle Cretaceous in most distal domains. The last extensional event (i.e. polyphase rifting) was later reactivated and incorporated into the Pyrenean mountain range from the Middle Santonian to the Oligocene. The temporal and spatial evolution of these processes is well preserved in the syn-extensional and syn-compressional sedimentary sequences which are widely documented by field observations but also by the quantity of geophysical data available in the region: seismic reflection and refraction, borehole, magnetic and gravity data. Access to such a complete dataset makes the Basque – Cantabrian Pyrenees a unique place to study the role of rift inheritance for the formation of orogens.

The first objective of this thesis is to understand the present-day structure and architecture of the Basque – Cantabrian Pyrenees, which is currently debated as indicated by the existence of numerous publications offering different geological interpretations. Later, restoring the Basque – Cantabrian Pyrenees to its pre-orogenic stage, the architecture of the rift can be deciphered being possible to determine its evolution from the Triassic to present-day. The second objective of this work is to study the transition from thick- to

thin-skin structural domains influenced by complex inherited templates (combining pre-existing basement structures and pre-rift salt decoupling horizon) during the formation and reactivation of proximal rift domains. This objective was developed during the 2nd year of this project in collaboration with the University of Barcelona, in its analogue modelling laboratory. Finally, the third goal of this thesis is to analyse the reactivation of the North Iberian rift system in order to understand how an orogen develops from a hyperextended rift system, in particular during the initial deformation phases, and to what extent this evolution is controlled by the different decoupling levels inherited from the extension phase.

The introduction summarizes the main concepts addressed in this thesis: the Wilson Cycle and inheritance. The first part, addressing extensional systems, explains the evolution of knowledge from the first observations and data acquisitions to the first models of rifted margins, as well as their classification and evolution in time and space (e.g. the multistage and polyphase rift systems). The second part focuses on compressional systems by explaining the evolution of knowledge and the fundamental concepts of orogens and fold-and-thrust belts, such as: the different types and classification of orogens, the main architecture of fold-and-thrust belts, and their evolution and the different formation models (thick- vs thin-skinned structural style). The third part of the introduction localizes the case study by describing the state of the art of the Pyrenees, the terminology used in this work, the geodynamic context and the open debates that remain in the scientific community. Finally, the methods used to carry out this thesis are explained as well as the scientific questions and objectives by describing the organization of the manuscript.

The first chapter of this thesis focuses on the Basque – Cantabrian Pyrenees and aims to describe (1) the present-day architecture, and (2) the rift template. Also, the role of the rift inheritance and the factors controlling the early phases of reactivation of hyperextended rift systems are discussed. Scientific discrepancies exist on the interpretation of this area, divided into two main schools: the first, propose a “thick-skinned” structural style controlling the architecture of the area where the basement is coupled with the sedimentary cover and as a result the basement structures mainly control the tectonic evolution. The second school suggests a “thin-skinned” architecture where the inherited Late Triassic salt unit plays an important role decoupling the sedimentary cover from the basement, which is non or slightly reactivated. We present a series of field observations and seismic interpretations combined with borehole data and seismic refraction data to demonstrate the “thin-skinned” character of the central Basque – Cantabrian Pyrenees. However, the observation in the western termination of the study area shows both “thin-skinned”

and “thick-skinned” modes of deformation combined. Thus, the results of this work can reconcile the two schools and show the importance of the pre-compressional architecture in controlling the “thin-skinned” vs. “thick-skinned” domains. The understanding of present-day architecture of the Basque – Cantabrian Pyrenees as well as the restoration of hyperextended rift systems, the inheritance concept, and how reactivation initiates in such a system are major results of this first part. Moreover, we show that the distribution and evolution of “polyphase” rift structures will have a strong influence on the reactivation and final architecture of the orogen. The reactivation is initiated and localized in the most mature rift domains (exhumed mantle domains).

The second chapter deals with the formation and reactivation of proximal rift domains characterized by a complex inherited template combining basement structures and a pre-rift decoupling horizon (i.e. salt), as observed in the transition between the Basque – Cantabrian Pyrenees and the Asturian Massif. The aim is to understand the transition from thick- to thin-skinned structural domains and how deformation is linked in between. Such investigations were carried out by preparing an experimental program using physical models during the one-year stay in Barcelona. By controlling the modelling parameters, analogue models can provide 3D, structurally balanced, and scaled solutions enabling the understanding and interpretation of complex areas by testing scenarios. The results confirm the similarities between the “thick-skinned” domain of the model and the field observations reported in the Asturian Massif, and the concordances between the “thin-skinned” domain of the analogue model with the Basque – Cantabrian Pyrenees. Nevertheless, the highlight results of the experiment become the transitional domain formed in the linking zone. This area is characterized by oblique structures which position depends on the active structures in both thick and thin-skinned domains but which orientation is determined by the presence of salt instead of following the basement structures underneath. Therefore, the inherited basement structures may determine the distribution of the salt and the position of structures, but the final orientation will be mainly controlled by the thin-skinned deformation.

The third chapter studies the reactivation of hyperextended rift systems and its incorporation into orogens, focusing on the initial phases which are so far poorly understood, possibly due to the lack of observations and field examples. The Basque – Cantabrian Pyrenees represent in this sense a unique case study where three different sections induced by a strong control of the syn-rift architecture are characterized. The Western Basque – Cantabrian Pyrenees, connected to the Bay of Biscay, are characterized by an embryonic subduction of the exhumed and serpentized mantle under the

Iberian plate, mainly suggesting a “thick-skinned” structural style. The Central Basque – Cantabrian Pyrenees run through the central part of a reactivated hyperextended rift segment governed by a thin-skinned structural style due to the Upper Triassic decollement. While the Iberian plate underlies the European plate, the deformation is characterized mainly by the folding and thrusting of the detached sedimentary cover. Finally, the section through the Eastern Basque – Cantabrian Pyrenees crosses an accommodation zone, where two rift segments overlap spatially, surrounding a crustal block (Basque Massif), and typically represents the type of deformation occurring in a segmented zone. By restoring the three sections, we can build a map of the rift domains at the end of the extensional deformation but also at the onset of compression. We show that during the initial stages of convergence, the deformation is segmented and localized, using the serpentinized mantle as the level of decoupling where underthrust initiates by pulling down the fresh and denser mantle beneath the serpentinized and hyperextended crust. However, a competition is established between the different levels of decoupling inherited from the rift system [i.e. serpentinized mantle, middle crust and intra-basin decoupling horizons (i.e. salt)]. When the serpentinized mantle is consumed by subduction or become less efficient, mid-crust decoupling levels can be used. Finally, when the salt is present, depends on its distribution, it can be reactivated since early stages, allowing a very effective detachment of the sedimentary cover.

In conclusion, this work helps to answer the main questions raised at the beginning of this thesis. It reveals the current architecture of the Basque – Cantabrian Pyrenees as well as the former rift template. It helps to understand the role of structural and compositional inheritance during the formation and reactivation of the rift systems and more important how different structural domains links. Finally, it proposes a generic model of reactivation of hyperextended rift systems and their integration into orogenic systems.

In general, this work has implications for the understanding of the Pyrenees – Bay of Biscay system, highlighting the influence of the inheritance associated with the rift, whether it is orthogonal or parallel to the rift axis, for the reactivation and the formation of the orogen. The methodology developed during this thesis as well as the main results could be applied and integrated to other similar orogenic chains in the world (e.g. Alps, Colombian Central Cordillera).

RÉSUMÉ ÉTENDU

Les processus responsables de la formation des océans et des chaînes de montagnes représentent une part essentielle de la recherche en tectonique. Ces processus ont été associés et définis à travers le *Cycle de Wilson* au cours des années 60, alors même que les idées ont été développées lors de travaux précédents, principalement basées sur des observations directes dans les chaînes orogéniques (Fig. R.1).

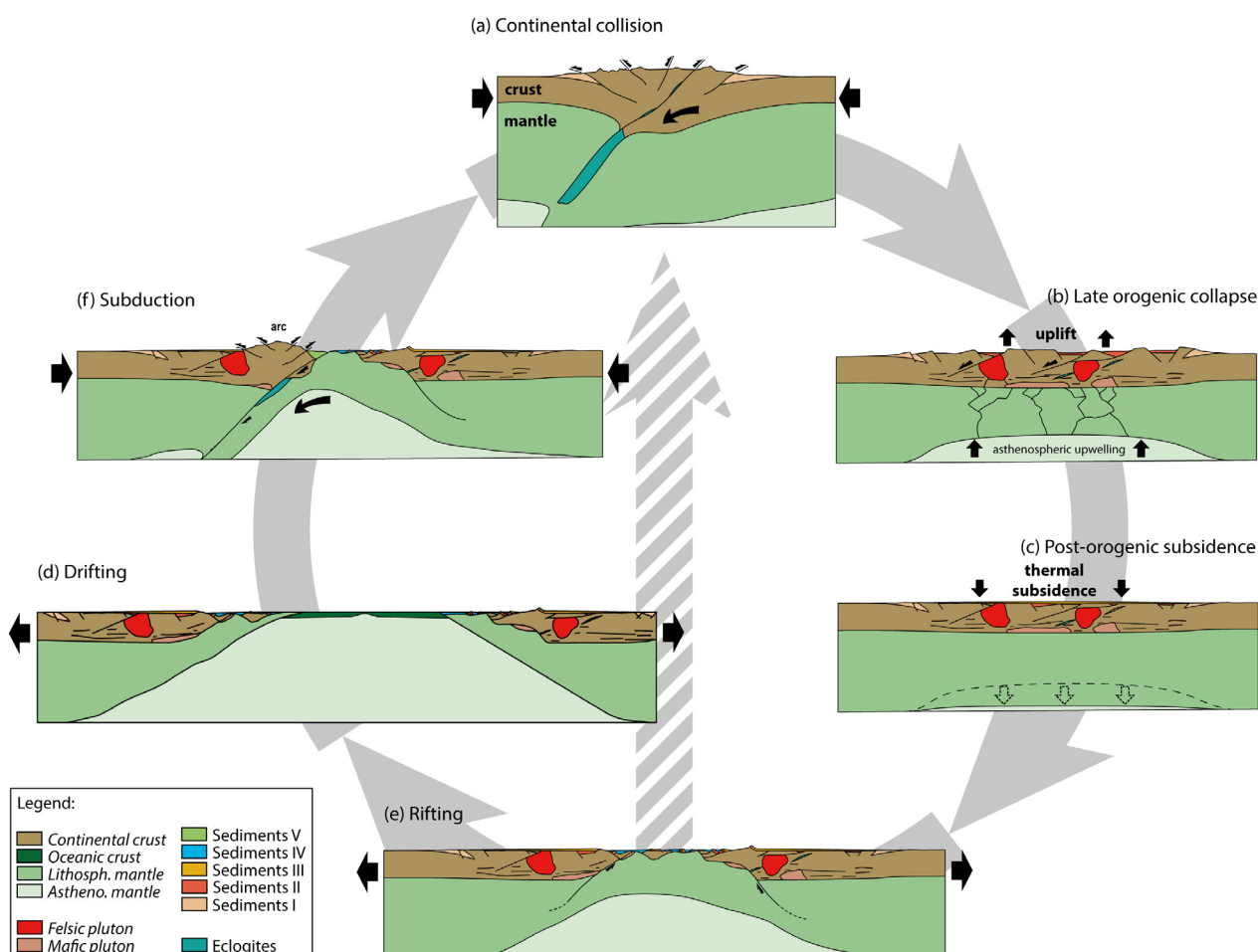


Figure R.1 : Cycle de Wilson ainsi qu'une possible évolution alternative (flèche hachurée). Modifiée d'après Petri (2014) et Chenin et al. (2019).

Au cours des dernières décennies, les connaissances sur la formation des orogènes mais aussi sur les marges passives ont augmenté de manière significative, favorisées par le développement de nouveaux concepts ainsi que de nouvelles techniques d'acquisition de données. Ainsi, les processus qui régissent la formation des marges de rifts et des orogènes sont bien connus et compris par les communautés respectives. Cependant, au cours des dernières années, de nombreuses études soulignant l'importance de l'héritage ont émergé, permettant notamment de débloquent de nombreux verrous scientifiques auparavant inexplicables. Ainsi, les récentes recherches impliquant le rôle de l'héritage, à

grande et à petite échelle, dans les régimes extensif ou compressif ont considérablement contribué à une meilleure compréhension du Cycle de Wilson. Cette thèse porte sur l'importance de l'héritage dans la formation des systèmes de rifts polyphasés et multi-étapes ainsi que sur leur réactivation et leur incorporation dans les orogènes.

Les Pyrénées Basco – Cantabriques représentent un excellent laboratoire naturel pour répondre aux questions ci-dessus puisqu'il s'agit d'une chaîne orogénique formée à partir de la réactivation d'anciens rifts hyper-étirés et de marges passives. En effet, ce système résulte du développement de différentes épisodes (« multistage ») de rifting mésozoïque à évolution polyphasée (« polyphase »)(Fig. R.2), menant à l'exhumation du manteau sous-continentale pendant le Crétacé moyen. Ce dernier a ensuite été réactivé et incorporé dans la chaîne de montagnes des Pyrénées à partir du Santonien Moyenne jusqu'au Oligocène.

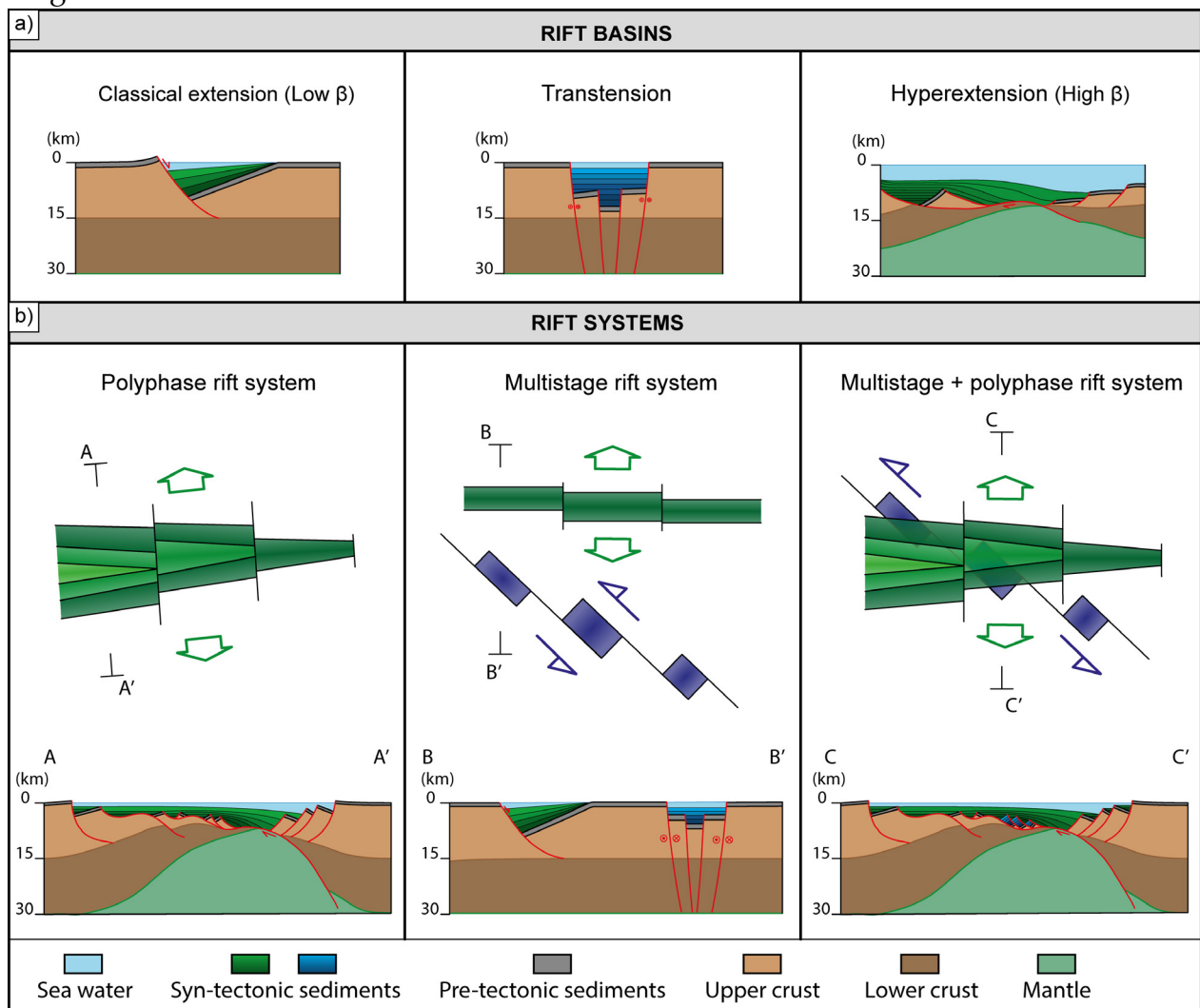


Figure R.2 : a) Classification des différents types de bassins de rift. b) Schéma théorique montrant la variabilité des systèmes de rift (voir chapitre 1 pour plus de détails).

L'évolution temporelle et spatiale de ces processus est bien préservée dans les séquences sédimentaires syn-extensives et syn-compressives qui sont non seulement largement accessibles mais également bien documentées par la quantité de données géologiques et géophysiques disponibles dans la région, notamment des données de réflexion et réfraction sismiques, de forage, ou encore de relevés magnétiques et gravimétriques. L'accès à un ensemble de données complet fait des Pyrénées Basco – Cantabriques un lieu unique pour l'étude du rôle de l'héritage du rift dans les systèmes orogéniques (Fig. R.3).



Figure R.3 : Carte tectono-stratigraphique des Pyrénées Basque – Cantabriques avec la localisation des différentes lignes sismiques et des puits illustrés dans ce travail ainsi que la position des sections présentées dans cette étude. BCB: Bassin Basque – Cantabrique ; CB: Bassin de Cabuérniga; PB: Bassin de Polientes

Le premier objectif de cette thèse est de comprendre la structure et l'architecture actuelles des Pyrénées Basco – Cantabriques, qui sont actuellement débattues comme l'indique l'existence de nombreuses publications proposant des interprétations géologiques très différentes. Ainsi, en restaurant le système Basco – Cantabrique à son stade pré-orogénique, l'architecture du rift peut être déchiffrée et permettre de déterminer son évolution du Trias à aujourd'hui. Le deuxième objectif de ce travail est d'étudier l'influence de modèles hérités complexes (combinant les structures héritées du socle et le découplage du sel à la base des séries syn-rift) lors de la formation et la réactivation des domaines de rift proximaux. Cet objectif a été développé au cours de la 2e année de la thèse en collaboration avec l'Université de Barcelone et son laboratoire de modélisation analogique. Enfin, le troisième objectif principal est d'analyser la réactivation du système de rift nord ibérique afin de comprendre comment une orogène se développe à partir d'un rift hyper-étiré, en

particulier lors des phases de déformations initiales, et dans quelle mesure cette évolution est contrôlée par les différents niveaux de découplage hérités de la phase d'extension.

L'introduction résume les principaux concepts génériques abordés dans cette thèse : le Cycle de Wilson et l'héritage. La première partie, traitant des systèmes extensifs, résume l'évolution des connaissances depuis les premières observations et acquisitions de données jusqu'aux modèles de formation des marges de rift, ainsi que leur classification et leur évolution dans le temps et l'espace (c'est-à-dire les systèmes « multistage » et « polyphase ») (Fig. R.2). La deuxième partie se concentre sur les systèmes compressifs en expliquant l'évolution des connaissances et les concepts fondamentaux des orogènes et des chaînes plissées (« fold-and-thrust belts »), tels que : les différents types et la classification des orogènes, l'architecture principale des « fold-and-thrust belts », leur évolution et les différents modèles de formation. La troisième partie de l'introduction aborde le domaine d'étude en décrivant l'état de l'art sur les Pyrénées, la terminologie utilisée dans ce travail, le contexte géodynamique et les questions scientifiques majeures qui animent la communauté des sciences de la Terre. Enfin, les méthodes utilisées pour développer cette thèse sont expliquées ainsi que les questions et objectifs scientifiques de cette thèse en décrivant l'organisation du manuscrit.

Le premier chapitre de ma thèse se concentre sur les Pyrénées Basco – Cantabriques (Fig. R.3) et a pour objectif de décrire (1) l'architecture actuelle, et (2) l'architecture du rift. En outre, le rôle de l'héritage de rift et les mécanismes en jeu lors des premières phases de réactivation d'un système de rift hyper-étiré. D'importantes confrontations scientifiques existent dans l'interprétation de cette zone, divisée en deux écoles principales: la première propose une architecture « thick-skinned » de la zone où les structures du socle contrôlent principalement l'évolution tectonique de la zone et l'architecture actuelle, tandis que la deuxième école suggère une architecture « thin-skinned » où le sel hérité joue un rôle important dans le découplage entre la couverture sédimentaire et le socle, qui est lui, pas ou peu réactivé. Nous présentons une série d'observations de terrain et d'interprétations sismiques combinées aux données de forage et aux données de sismique réfraction pour démontrer le caractère « thin-skinned » de la déformation dans la partie centrale des Pyrénées Basco – Cantabriques (Fig. R.4a). Cependant, l'observation de la terminaison ouest de la zone d'étude montre à la fois des modes de déformations « thin- » et « thick-skinned ». Ainsi, les résultats de ma thèse peuvent partiellement concilier les deux écoles et montrent l'importance de l'architecture pré-convergence dans le contrôle de la réactivation « thin-skinned » vs. « thick-skinned » (Fig. R.4b). Ainsi, l'introduction du concept d'héritage de rift et la compréhension du système de rift sur lequel s'initie la

réactivation (c'est-à-dire un rift « multistage » vs « polyphase »), est fondamentale et représente un résultat majeur de cette première partie. Dans cette étude, nous montrons que la distribution et l'évolution des structures de rift « polyphase » auront une forte influence sur la réactivation et l'architecture finale de l'orogène. Ainsi, la réactivation s'initie et se localise dans les zones du rift les plus matures (domaines de rift les plus distaux).

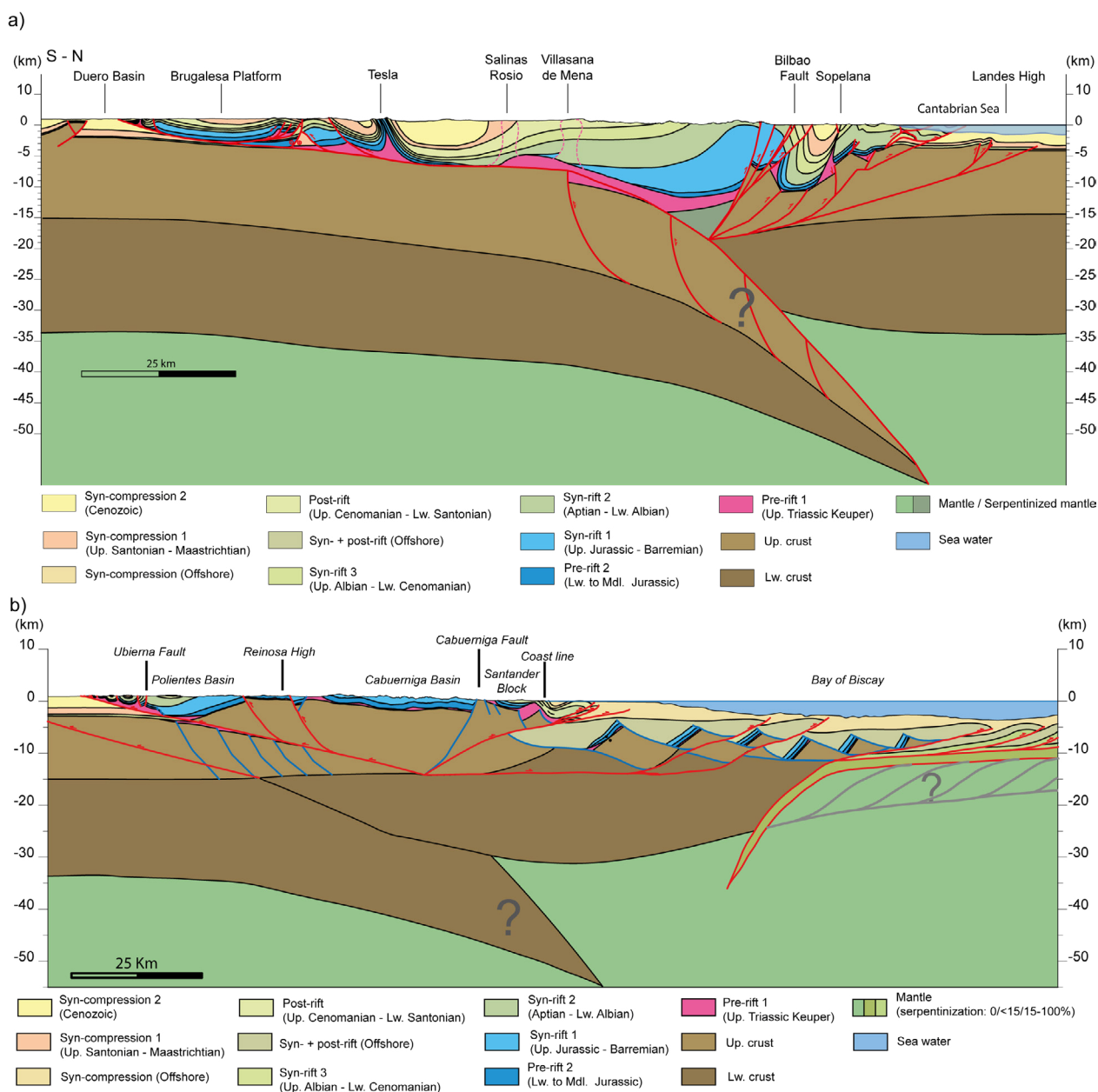


Figure R.4 : Coupe régionale à travers les Pyrénées Basque – Cantabriques centrales (modifiée à partir de Muñoz, 2019). b) Coupe régionale à travers les Pyrénées Basque – Cantabriques occidentales jusqu'au golfe de Gascogne.

Le deuxième chapitre traite de la formation et de la réactivation des domaines de rift proximaux caractérisés par un héritage complexe combinant des structures de socle et un niveau de découplage dans le sel pré-rift, tel qu'observé dans la zone de transition entre les Pyrénées Basco – Cantabriques et le Massif Asturien. L'objectif est de comprendre la transition de domaines « thick-skinned » a « thin-skinned » et comment la déformation est liée entre les deux. Ces investigations ont été menées en préparant un programme expérimental utilisant des modèles physiques pendant le séjour d'un an à Barcelone. En contrôlant les paramètres de modélisation, les modèles analogiques peuvent fournir des solutions 3D, structuralement restaurable, et à l'échelle permettant la compréhension et l'interprétation de zones complexes en testant différents scénarios. Les résultats confirment les similitudes entre le domaine « thick-skinned » du modèle et les observations de terrain rapportées dans le Massif Asturien, et les concordances entre le domaine « thin-skinned » du modèle analogique avec les Pyrénées Basco – Cantabriques caractérisées par le développement de différentes structures salifères telles que les diapirs (Fig. R.5).

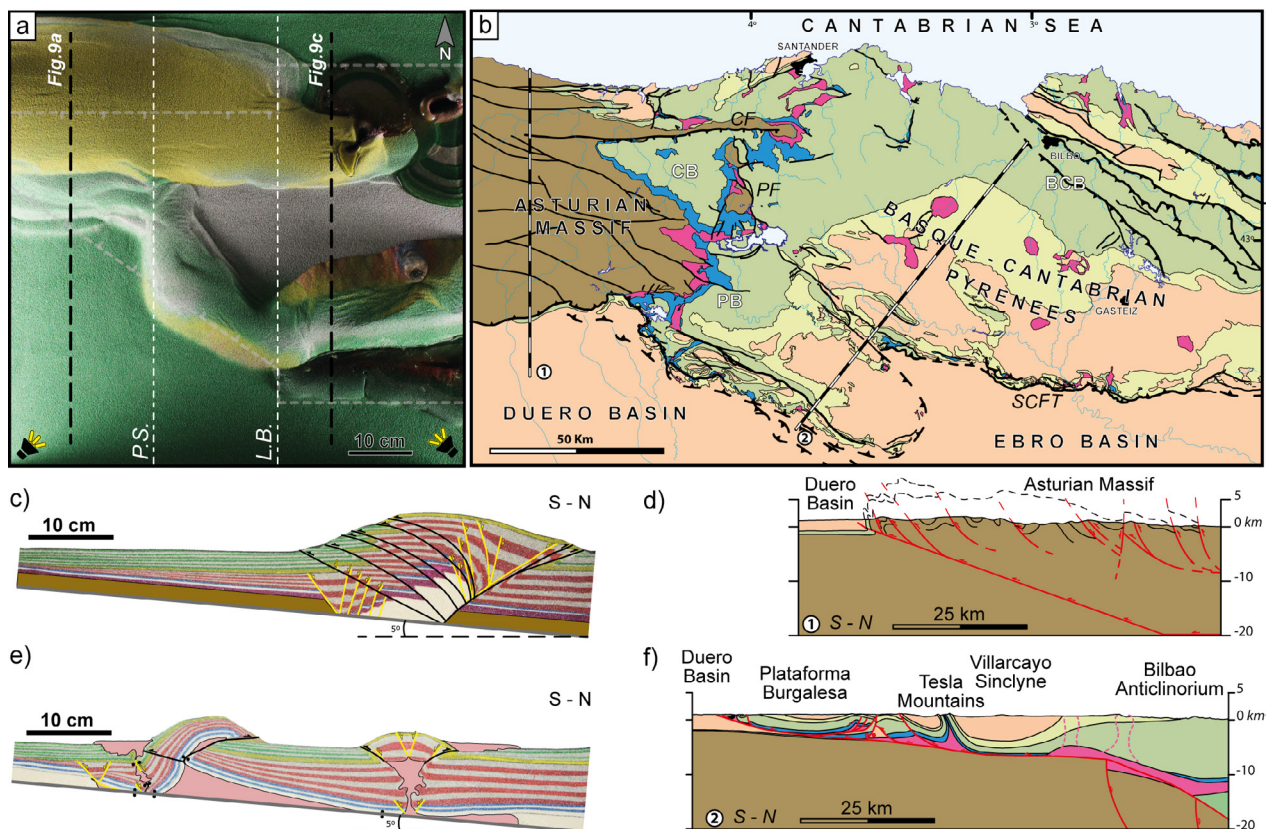


Figure R.5 : a) Vue du dessus du Model-3 à la fin de la compression. b) Carte tectono-stratigraphique de la jonction Pyrénées Basque-Cantabriques – Massif Asturien. c) Coupe transversale du domaine couplé montrant l'architecture « thick-skinned » dans le Modèle-3. d) Coupe transversale à travers le Massif Asturien montrant l'architecture « thick-skinned » similaire à celle observée dans le modèle. e) Coupe à travers le domaine découplé dans le Modèle-3. f) Coupe géologique à travers le sud des Pyrénées Basque-Cantabriques montrant le caractère « thin-skinned » de la déformation

Néanmoins, les résultats plus remarquables des modèles deviennent le domaine de transition formé dans la zone de liaison. Cette zone est caractérisée par des structures obliques dont la position dépend des structures actives à la fois dans les domaines « thick- » et « thin-skinned », mais dont l'orientation est déterminée par la présence de sel au lieu de suivre les structures du sous-sol en dessous. Par conséquent, les structures de sous-sol héritées peuvent déterminer la distribution du sel et la position des structures, mais l'orientation finale sera principalement contrôlée par la déformation « thin-skinned ».

Le troisième chapitre étudie la réactivation d'un système étiré et son incorporation dans la chaîne orogénique, en se concentrant sur les étapes initiales qui sont mal comprises jusqu'à présent, probablement en raison du manque d'observations et du peu d'analogues de terrain. Les Pyrénées Basco – Cantabriques représentent en ce sens un lieu d'étude unique car elles permettent de décrire et de définir trois sections différentes induites par un fort contrôle de l'architecture syn-rift (Fig. R.6). Les Pyrénées Basco – Cantabriques occidentales, connectées au Golfe de Gascogne, sont caractérisés par une subduction embryonnaire du manteau exhumé et serpentinisé sous la plaque Ibérique, suggérant principalement un style structural « thick-skinned ». Les Pyrénées Basco – Cantabriques centrales traversent la partie centrale d'un segment de système de rift hyper-étiré réactivé avec découplage de la déformation le long du sel pré-rift. Alors que la plaque Ibérique sous-charrie la plaque Européenne, la déformation se caractérise principalement par le plissement et le chevauchement de la couverture sédimentaire décollée (déformation « thin-skinned »). Enfin, la section du Pyrénées Basco – Cantabriques orientale traverse une zone d'accommodation, où deux segments de rift se superposent spatialement de part et d'autre d'un haut structural, et représente typiquement le type de déformation se produisant dans une zone segmentée. Ainsi, en restaurant les trois sections, nous pouvons construire une carte des domaines de rift de la zone à la fin de la déformation extensive mais aussi au début de la compression. Nous montrons que lors des étapes initiales de la convergence, la déformation est segmentée et localisée, utilisant le manteau serpentinisé exhumé comme niveau de découplage où s'initie le sous-charriage et éventuellement la subduction. Cependant, une compétition s'établit entre les différents niveaux de découplage hérités du système de rift (c.-à-d. manteau serpentinisé, croûte moyenne ductile et interface couverture-socle salifère ou non). Ainsi, lorsque le manteau serpentinisé est consumé par la subduction ou est devenu moins efficace, les niveaux de découplage en milieu de croûte peuvent être utilisés. Enfin, lorsque le sel est présent, il est réactivé dès les premiers stades, permettant un décollement très efficace de la couverture sédimentaire.

En conclusion, cette étude permet de répondre aux principales questions soulevées au début de cette étude. Elle révèle l'architecture actuelle des Pyrénées Basco – Cantabriques ainsi que l'organisation structurale du rift. Elle permet de comprendre le rôle de l'héritage structural et compositionnel lors de la formation et la réactivation du système de rift. Enfin elle propose un modèle générique de réactivation des domaines de rift hyper-étirés et leur intégration dans la chaîne orogénique.

De manière générale, ce travail a des implications pour la compréhension du système Pyrénées - Golfe du Gascogne, soulignant l'influence de l'héritage associé au rift, qu'il soit orthogonal ou parallèle à l'axe du rift, pour la réactivation et la formation de l'orogène. La méthodologie développée pendant cette thèse ainsi que les principaux résultats pourraient être appliqués et intégrés à d'autres chaînes orogéniques similaires dans le monde (ex: Alpes, Cordillère Centrale Colombienne).

ACKNOWLEDGEMENTS

Acknowledgements

Many people have been part of this thesis in one or another way and I will try to mention all of them. But just to make it clear from the beginning, those who know me also know about my memory and therefore I want to thank all this people who helped me during my PhD.

At first, I would like to mention my supervisors, starting by Josep Anton Muñoz. I still remember the first field trip in the Pyrenees where I attended to the amazing show you gave us as undergraduate students. At this time, it became clear at my mind that I wanted to do a PhD on tectonics with you. Luckily (because in life, apart from being at the right time at the right place, there is always a bit of luck) I called to your door at the precise moment. Almost next time we met, we were going to Pau for a meeting with Gianreto Manatschal (supervisor from Strasbourg), Manu and Sylvain (managers of Orogen Project) to introduce myself into the project (what an exciting and nervous trip! But also an amazing one crossing through the Portalet pass). The first step was achieved: I was starting my PhD where I wanted, with the group I wanted, on a place I love. But still it could be improved! For that is necessary to call also Gianreto Manatschal, excellent scientific and geologist and even better person. Since day one I saw that it was going to be a great and successful project if I was doing my part. I want to deeply thank Gianreto and Anton for guide me during this three exciting years, for teaching me so many things, to be patient when needed but more important for all the time we spent together discussing, working or just enjoying conversations.

Second, I must dedicate some words to the Orogen Project and the project managers (Sylvain Calassou, Emmanuel Masini, Isabelle Thinon and Olivier Vidal), not only for giving me the opportunity to do my PhD thesis on their behalf and the financial support, but also for all the people I met in there, the numerous project meetings and “orogen schools” we have had the pleasure to attend, geology discussions and many laughs when needed. In that case, I want to dedicate a special mention to Manu Masini as a great leader who always made me feel comfortable and supported by the project.

In the third place, I would like to give a special attention to the “Orogen dream-team” composed by Rodolphe Lescoutre (the papi) and Patricia Cadenas. But also I need to mention all these people both from Strasbourg and Barcelona (actually from many places in the world) who helped me either with logistic issues, scientific discussions, personal talks, etc.: Nicolo Incerpi (grandpa), Simon Tomasi, Chao Peng, Gianluca Frasca, Lulu Prieto, Pierre-Olivier, Benoit Petri, Charlotte Ribes, Maria-Eva, Antoine, Paul, Julie Tugend, Michael Nirrengarten, Júlia Gómez, Oriol Giménez, Maria Roma, Oriol Pla, Frede

Escosa, Pablo Granado, Pablo Santolaria, Esther Izquierdo, Marco Snidero, Marco de Matteis, Patricia Cabello, Rodolfo Uranga, Elisabeth Wilson, Núria Carrera and even more important, Òscar Gratacós for his help in multiple tasks (software issues, presentations, logistics, etc.) and Oriol Ferrer, my somehow third supervisor while being in Barcelona and “living” in the Analog Modelling Laboratory. To all of them and the people who I probably forget while texting, many thanks! I am very happy to have met all of you and shared with you some great moments during my thesis. No doubt all those moments helped me to improve this work and to finish the PhD in a good mood.

Moltes gràcies també a tots els meus amics i amigues, perquè cada un d’ells/elles han aportat el seu granet de sorra ja sigui en animar, desconnectar o simplement, ser-hi. Especialment als Lluços, per tots els moments viscuts durant aquests anys: pedalades, caminades, esquíades, xais, tiberis, “arboools” gaudits... però sobretot per fer-me gaudir de la vida permetent-me desconnectar de la recerca, de vegades massa intensa, i per no fer oblidar les coses que de veritat són importants i ens fan feliços. M’agradaria mencionar expressament al Gerard (sociu) per l’ajuda en la recta final amb la maquetació del volum. I també als Pendejos (Sebas i Taio) perquè malgrat la distància sempre han estat presents per animar i transmetre esperança i perseverança.

A la meva família, Mercè, Joan i Pau. Moltes gràcies per la paciència, l’estima, el suport i la comprensió. Han estat tres anys intensos i complicats però que finalment han vist la llum. I si ha estat així, també ho ha estat en bona part per vosaltres! I finalment i de manera molt especial, ja que és la persona qui ha pogut experimentar de més a prop com algú es fa doctor, infinites gràcies a la Jana. Sempre amb energia, un somriure, ànims i coratge, m’ha animat i ajudat a arribar fins aquí de manera exitosa sense deixar-me sol en cap moment, fins i tot invertint gairebé un any per acompanyar-me a Estrasburg a viure un dels millors anys de la meva vida. Senzillament, moltes gràcies.

Thank you all!

TABLE OF CONTENTS

Table of Contents

ABSTRACT	7
RÉSUMÉ ÉTENDU	11
ACKNOWLEDGEMENTS	21
INTRODUCTION	31
A. The extensional cycle: evolution of concepts	34
B. Convergent cycle: orogens and fold and thrust belts	39
C. The Pyrenean natural laboratory.	43
D. Open debates	51
E. Data and methodology	52
F. Scientific questions.	55
CHAPTER 1: REACTIVATION OF A HYPEREXTENDED RIFT SYSTEM: THE BASQUE-CANTABRIAN PYRENEES CASE	61
Abstract	61
1.1. Introduction	62
1.2. Geological setting	66
1.3. Observations in the Basque – Cantabrian Pyrenees: seismic interpretations and geological cross sections	68
1.4. Crustal architecture: geophysical constraints	76
1.5. Discussion	78
1.6. Conclusion	88
Acknowledgements.	89
CHAPTER 2: ROLE OF INHERITANCE IN A THICK- TO THIN-SKIN TRANSITION: INSIGHTS FROM ANALOGUE MODELLING AND BASQUE – CANTABRIAN PYRENEES	93
Abstract	93
2.1. Introduction	93
2.2. Geological setting	95
2.3. Analogue modelling	99
2.4. Experimental results	102
2.5. Discussions.	111
2.6. Conclusions	117
CHAPTER 3: CONTROL OF RIFT-INHERITANCE ON THE NUCLEATION AND GROWTH OF AN OROGEN: INSIGHTS FROM THE PYRENEAN OROGEN	121
Abstract	121
3.1. Introduction	121
3.2. The Basque – Cantabrian Pyrenees (BCP)	123
3.3. The North Iberian Rift System.	124
3.4. The Inversion of the North Iberian Rift System	124
3.5. From a hyperextended system to a collisional orogen	128
3.6. Conclusions	130
Acknowledgements.	130

GENERAL SYNTHESIS AND DISCUSSION	135
CONCLUSIONS	145
OUTLOOKS	151
REFERENCES	157
ANNEX 1: THE BASQUE - CANTABRIAN PYRENEES: REPORT OF DATA ANALYSIS	187
Abstract	187
Résumé.	188
1.1. Introduction	189
1.2. Geological framework	191
1.3. Data	194
1.4. Geological map of the Basque – Cantabrian region	195
1.5. Composite section across the Basque – Cantabrian Pyrenees	198
1.6. Summary	202
Acknowledgements.	202
ANNEX 2	204
Annex 2.1 reflexion seismic lines information	204
Annex 2.2 drill holes information	205
Annex 2.3 1:50.000 maps references.	206
Annex 2.4 tecton-stratigraphic map of the basque - cantabrian pyrenees	217
ANNEX 3: STRIKE-SLIP CORRIDORS IN MICROPLATE KINEMATICS: THE IBERIA RESTORATION PARADIGM REVISED (PEER REVIEW)	218
LIST OF FIGURES	240
LIST OF TABLES	247





INTRODUCTION

The cover photo of the Introduction depicts the Doniene Gaztelugatxeko hermitage, facing the Cantabrian Sea (Bizkaia province). The island is made of Albian breccias in the eastern limit of the Bakio diapir.

INTRODUCTION

John Tuzo Wilson wrote once “[*these features (i.e. mountains, mid-ocean ridges, and transform faults) [] are connected into a continuous network of mobile belts around the Earth, which divide the surface into several large rigid plates*]” (Wilson, 1965 in K. Burke, 2011). Later, he realized that “[*each stage (i.e. evolution of oceanic basins from embryonic to relic scar stage) has its own characteristics on rock types, sediments and dominant motions (Table 1 of Burke, 2011)*]” (Wilson, 1968). The development of these ideas would become the base of the Plate Tectonic theory, known as the “Wilson Cycle” (i.e. opening and closure of oceans). But even if at present the theory takes the name of J.T. Wilson, many scientists did a crucial progress before, which helped J.T. Wilson to get the final theory and consensus.

One of the important names, when thinking about Plate Tectonics, is Arthur Holmes, who suggested in the early XIX century, that crustal motion was driven by radioactivity coming from the core of the Earth and the resulting heat would generate the mantle convection responsible for the continental drift. This idea was consistent with the current thoughts, similar to the ideas of Alfred Wegener from the beginning of the same century. Some years later during the 1930s, F.V. Meinesz observed that the gravitational field of the Earth was weaker than expected above the deepest regions of the oceans and debated that with H. Hess. However, it was H. Hess and the P.M.S. Blackett and K. Runcorn who suggested that the Earth magnetic field was related to the rising of mantle, i.e. convection cells, that were also responsible to move the overlying ocean floor resulting in the separation of continents (called sea-floor spreading by R. Dietz). Progress continued evolving later with scientists like Vine and Matthews or L. Moreley working on sea floor spreading and magnetic stripes related to the Earth’s magnetic field, or T. Atwater and M. Tharp addressing the continental drift, volcanism, and seismicity. In any case, all those ideas were at the origin of what became later the Wilson Cycle (Dewey & Burke, 1974), a concept broadly accepted at present across the Earth Science community (Fig. I.1).

However, the theory of Wilson Cycle is not accomplished everywhere like in Western Europe where most of the Variscan sutures were not reactivated during the Mesozoic extensional phase. Another example might be that of only around 45% of the rifted margins of Gondwana supercontinent were parallel to the former sutures, and more than 20.000 km of pre-existing orogens did not rift (Krabbendam & Barr, 2000). Or the Pyrenean case, where the drifting phase and steady-state seafloor spreading were never developed, evolving directly to collision from the rifting phase (Fig. I.1) (Chenin et al., 2017, 2019).

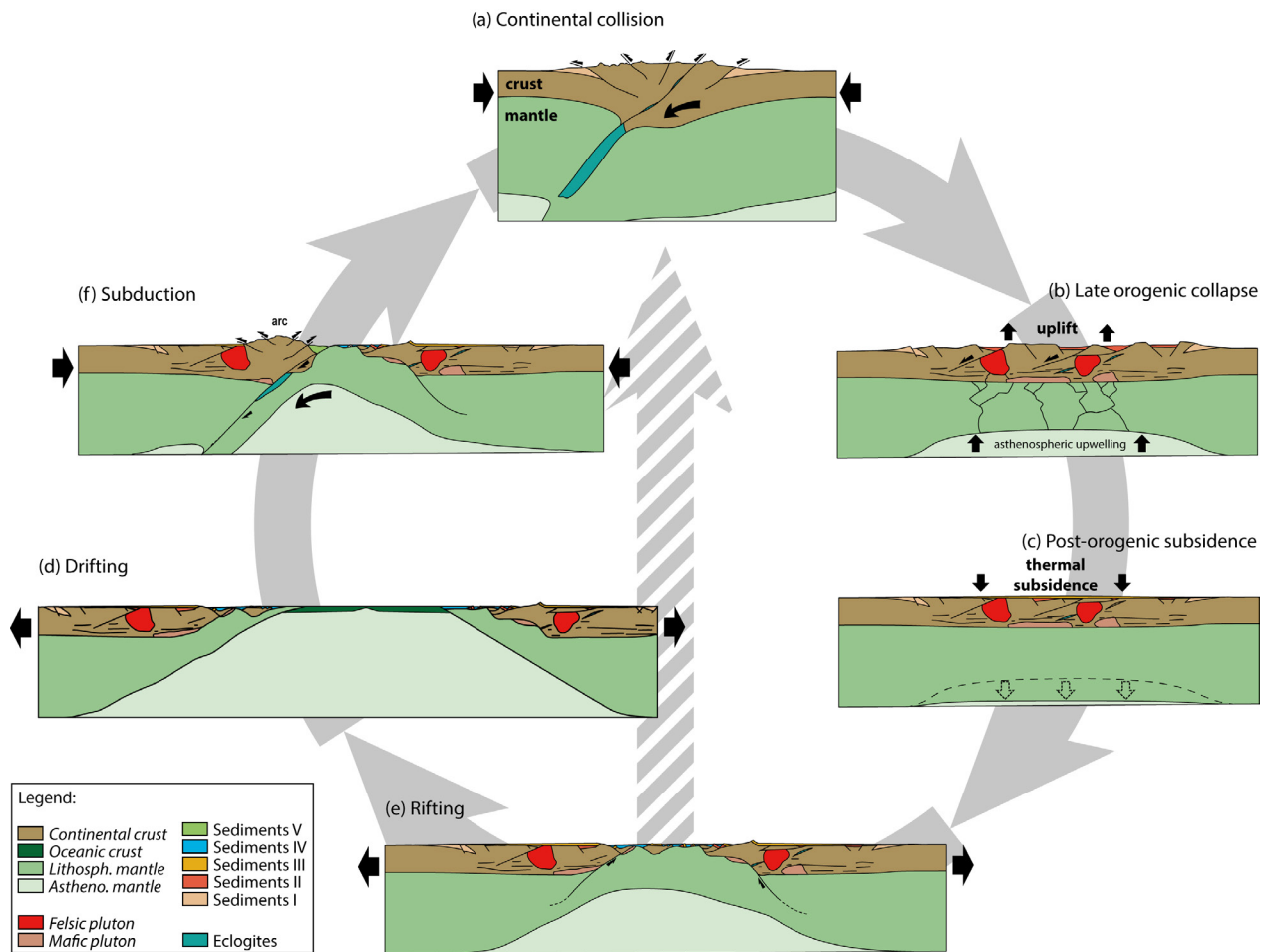


Figure I.1 : Classical view of the Wilson Cycle with possible short-cuts (stripped line). Modified after Petri (2014) and Chenin et al. (2019).

In the meantime, inheritance was a concept with an increasing interest as the evolution of the Wilson cycle did not follow always the weakest and expected parts of the system for the subsequent deformation phases. Already in the 70's, Dewey & Bird (1970) started to investigate the structural inheritance due to the strain partitioning observed in collisional belts as a key component of the evolution of mountain belts and continental lithosphere in general. Many authors have recognized the importance of inheritance either at a large scale (e.g. Lindholm, 1978; Jackson, 1980) or at a more local scale (e.g. Cohen, 1982; Lowell, 1995). More recently, an interesting debate came out about the inheritance concept and its implications (Krabbendam & Barr, 2000) resulting in the idea that inheritance may be controlled by a wide range of components not only structural features [e.g. rock fabrics (Jammes & Lavier, 2019), composition of lithosphere or thermal state (Manatschal et al., 2015)] (Fig. I.2). Although yet little understood, it appears that understanding “inheritance” which may also be referred to as the initial conditions of a system for the subsequent tectonic evolution has a major importance, in particular to understand the early stages.

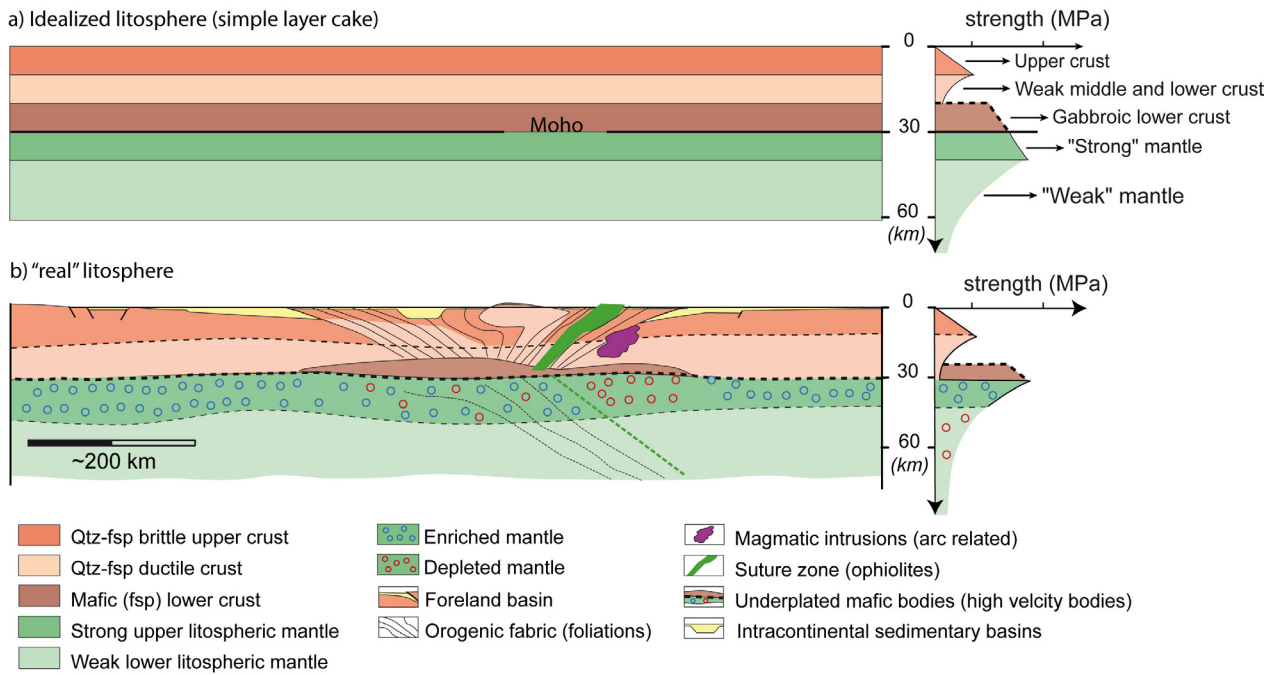


Figure I.2 : Lithospheric scale sections showing (a) an idealized lithosphere made of a thermally equilibrated layer cake and (b) a “real” post-orogenic lithosphere showing inherited structural and compositional complexity. From Manatschal et al. (2015).

During the last years an increasing interest has focused on the role of inheritance in different tectonic settings such as: the impact of orogenic inheritance on rifted margins (Manatschal et al., 2015; Chenin et al., 2015), influence of the architecture of magma-poor rifted margins on orogens (Tugend et al., 2014; Chenin et al., 2017), the interaction of inheritance and segmentation during formation and reactivation of rifted margins (Lescoutre, 2019), among others. Yet, many questions remain poorly understood, such as: Does a rift template influence the reactivation and the distribution of compressional deformation? What is the link between rift domains and orogenic evolution (i.e. deformation phases)? How does a segmented rift system gets involved into a continuous orogen?

In this thesis, the role of rift inheritance is addressed by studying the Bay of Biscay - Pyrenean system during the Alpine cycle, from the onset of extensional event at Triassic times to till the end of compression during Miocene. Considering the necessity of looking through both extensional and compressional settings, a brief introduction to some of the fundamental concepts and terminology will be introduced hereafter.

A. THE EXTENSIONAL CYCLE: EVOLUTION OF CONCEPTS

The study and understanding of extensional systems (i.e. rifted margins) is strongly linked to the data acquisition in the present-day margins. In that sense, the World Wars as well as the Cold War became an important step on the progress of the knowledge of the Earth due to mineral and hydrocarbon necessities but also for mobility issues. As such, methods, quality, and quantity of data increased a lot during those decades resulting in big datasets of mainly magnetic, gravity and seismic data. This allowed the scientists to link observations done in the field with offshore data, doing a big progress. As an example, field observations in the Alps pointing out the presence of extensional basins controlled by normal faults older than the Alpine orogeny (e.g. Argand, 1916; Bernoulli, 1964) were linked with the first tilted block imaged by seismic data in the Western Approaches Margin (De Charpal et al., 1978; Lemoine et al., 1987). This sort of observations enabled to develop the first coherent model to explain the lithospheric extensional mechanisms and the associated extensional basins. The first thermo-mechanical model, known as the McKenzie model or pure shear model, explains horizontal extension and thinning by a depth uniform relationship ($1/\beta$ crust = $1/\beta$ mantle) and in consequence both conjugate margins are symmetric (McKenzie, 1978) (Fig. I.3a). This model was useful to explain the extension and resulting structures in the proximal margins, i.e. areas with low β values, but could not explain the subsidence history and magma production in the more distal parts where thinning is depth-dependant. Later, during the 80's, a second model was developed by Wernicke (1981, 1985) inspired from field work in the Basin and Range where the extension was controlled by low angle detachment faults creating an asymmetric extensional system (Fig. I.3b). By using this model, the depth-dependent thinning could be predicted by the presence of a big detachment fault responsible of an important extension and the exhumation of the mantle.

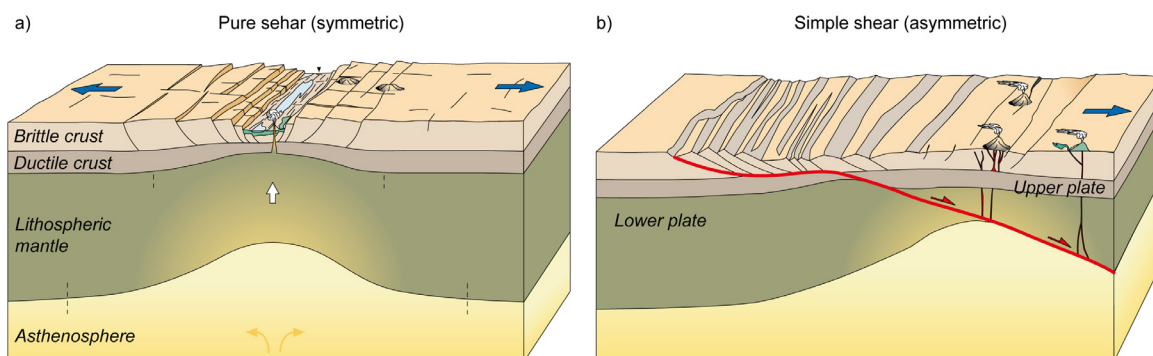


Figure I.3 : 3D block to schematize a (a) pure shear extension (symmetric) and (b) a simple shear extension (asymmetric). Modified after Frisch et al. (2010)

However, no example of lithosphere-scale dip-slip fault or shear zone cross-cutting a thermally equilibrated crust (35 ± 5 km thick) from the surface down into the upper mantle has ever been observed (Kusznir & Matthews, 1988). Therefore, neither the pure-shear (McKenzie, 1978) or the simple-shear models (Wernicke, 1985) can individually explain lithosphere deformation during rifted margin formation, which suggests that other lithosphere-scale deformation processes may play an important role (Fletcher et al., 2009).

Further studies addressing the lithospheric extension on distal margins and mantle exhumation (e.g. Boillot et al., 1987; Whitmarsh et al., 2001), the role of serpentinization (e.g. Reston & Pérez-Gussinyé, 2007), magmatism (e.g. Whitmarsch et al., 2001; Minshull et al., 2001) and their geophysical properties (Minshull, 2009) showed that the transition between continental crust and oceanic crust is in fact gradual in the absence of magma (e.g. magma-poor margins) and not abrupt as suggested previously. Moreover, the thinning of the crust from an initial 35 ± 5 km thick normal crust to less than 10 km commonly observed in the distal parts of rifted margins is also gradual (Manatschal et al., 2001). Therefore, the major crustal thinning between the proximal and the distal domains need to occur spatially in between, along the so-called necking domains (thinning domains) (Contrucci et al., 2004; Péron-Pinvidic & Manatschal, 2009; Mohn et al. 2012; Chenin et al., 2018). Different models have been proposed to explain the thinning processes most of which were inspired by offshore geophysical and onshore field observations that made it possible to conceptualize the rheological and structural evolution in the necking domains (e.g. Mohn et al., 2012). The crustal thinning in the necking domains can be reached by a system of conjugate concave downward faults instead of multiple planar normal faults as previous models argued (Lavie & Manatschal, 2006). New models suggest that necking is controlled by the failure of the strongest level in the lithosphere (in equilibrated orogenic lithosphere as exemplified in Western Europe it is the upper mantle) that induces a localization of the deformation in the overlying crust resulting in necking (e.g. Chenin et al. 2020).

At present, the passive margins can be classified into magma-poor rifted margins and magma-dominated (also called magma-rich) rifted margins depending on the amount of magma present in the system (Reston, 2009) (Fig. I.4). In fact, the classification of rifted margins can be more complex (Reston & Manatschal, 2011) as they can have magma focusing resulting in uneven distribution of magma (Chalmers & Pulvertaft, 2001) or evolve from magma-poor to magma-rich margins through time (Osmundsen & Ebbing, 2008) or along strike (Hopper et al., 1992). In this introduction we will focus on magma-poor rifted margins.

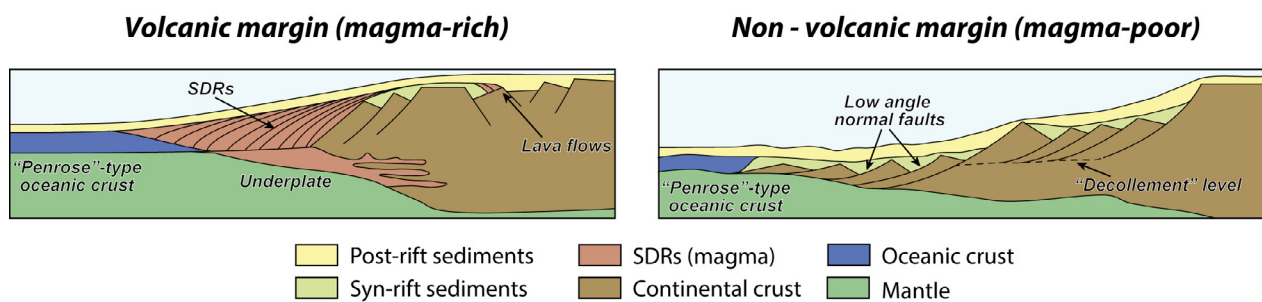


Figure I.4 : First order architecture of a volcanic margin (left) and a non-volcanic margin (right). From Péron-Pinvidic et al. (2019).

The evolution and architecture of the magma-poor rifted margins is well known by the combination of marine geophysical observations (Reston, 2009 and references therein) and fossil examples observed in collisional orogens (e.g. Mohn et al., 2012; Masini et al., 2012; Ribes et al., 2019). Magma-poor rifted margins develop as the result of a polyphase evolution, which is characterized by a sequence of phases that are from early to late referred to as: stretching, thinning, exhumation and seafloor spreading [see for its characterization Lavier & Manatschal (2006) and Péron-Pinvidic & Manatschal (2009)] (Fig. I.5). The final architecture of a margin is described by different characteristic domains as a response of the polyphase evolution, from low to high β as: proximal, necking, hyperextended, exhumed mantle and oceanic (Sutra et al., 2013 and Tugend et al., 2014b) for a detailed characterization of each domain) (Fig. I.6). Recent studies have applied the previous concepts of rifted margins into the Pyrenees – Bay of Biscay in an attempt to establish the rift domains and restore the extensional template developed during Mesozoic, prior to the Alpine orogeny (Tugend et al., 2014a, 2015; Masini et al., 2014; Lescoutre, 2019).

The polyphase rift evolution, as described above, is a well-known evolution of a rifted margin with a specific terminology that has been developed during the last years (e.g. Péron-Pinvidic & Manatschal, 2009). However, recent investigations proposed an additional complexity defined as the multistage rift evolution (Cadenas et al., accepted). A multistage evolution refers to the different rift systems (i.e. stages) that are developed in an area through time and as a result of different extensional episodes. Thus, whereas the polyphase concept addresses the evolution of a single rift system (Fig. I.7a), the multistage concept links and describes the stacking of different either polyphase or monophasic rift systems (Fig. I.7b). The complexity of the final rift template is lower when the case study is monostage and high in the case of polyphase systems (e.g. Galicia – Newfoundland rifted margin) (Fig. I.7c, e.g. Bay of Biscay – Pyrenean system). Therefore, identifying and characterizing rift systems (i.e. rift domains for each rift system) and the crustal architecture associated will be fundamental to correctly interpret the evolution of an area

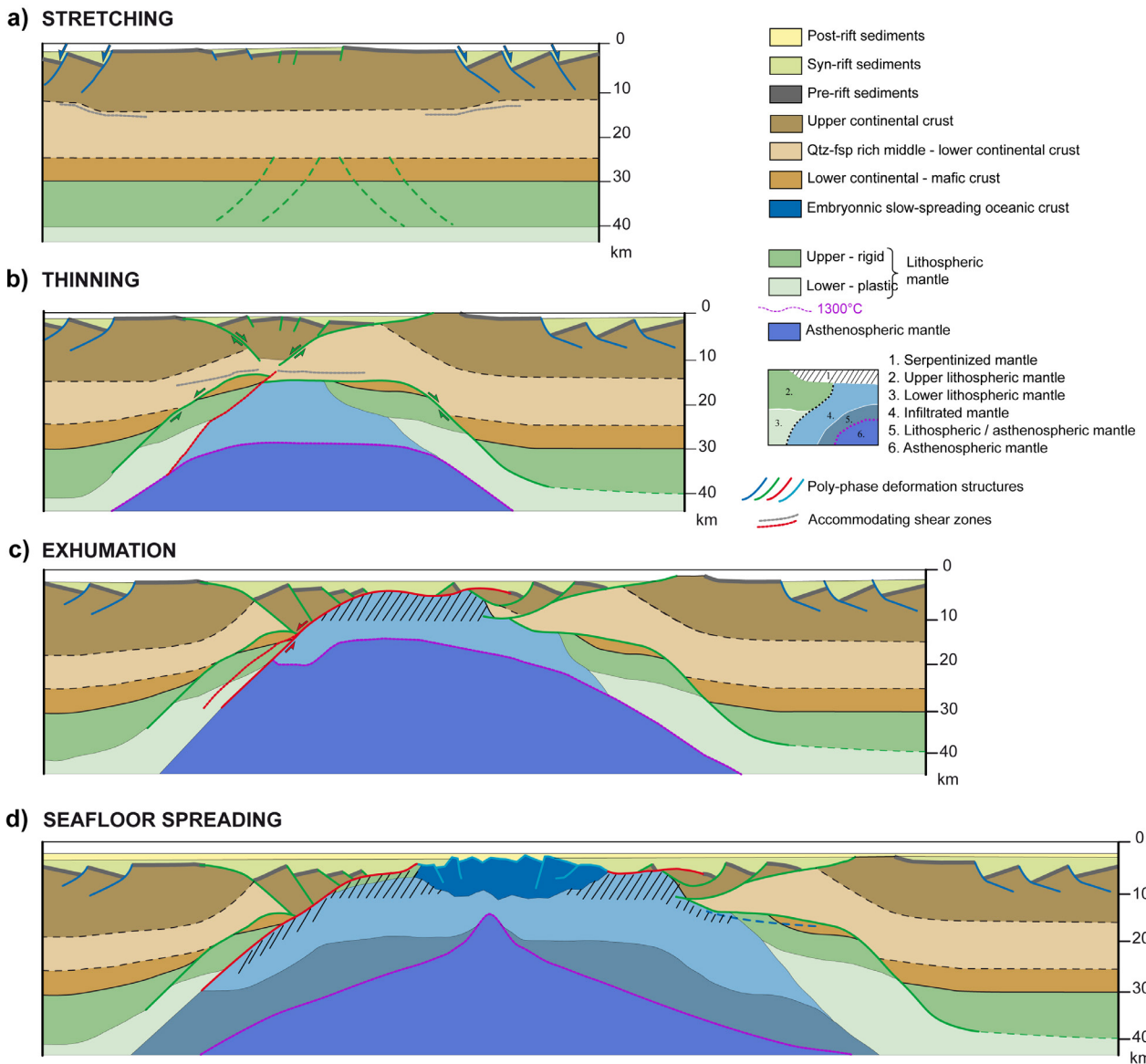


Figure I.5 : Conceptual model of the evolution of a polyphase rifting. (a) Stretching mode characterized by high angle normal faults associated to half-graben subsidence. Continental crust may be slightly stretched, and sedimentary basins developed independently from each other. (b) Thinning phase is characterized by a conjugate decoupling system of detachment faults that accommodated exhumation of deeper crustal levels. Deformation goes from a distributed to localized extension. (c) Exhumation phase is observed where detachment faults crosscut the embrittled crust and exhume serpentinized mantle rocks. (d) Sea floor spreading is the final phase where a proto-ridge is developed. Modified after Peron-Pinvidic and Manatschal (2009).

This section provided a short summary of how the knowledge of rifts and rifted margins evolved over the last years. The increasing interest of the industry for the exploration of natural resources in rifts and rifted margins was a major driver in the development of the new concepts and the technology that enabled to get new and better data that can image the extensional systems. However, this topic is still far behind and less mature than the compressional systems (i.e. orogens) as the latter are more accessible in the past and their study started earlier and asked for less technical support (imaging and drilling).

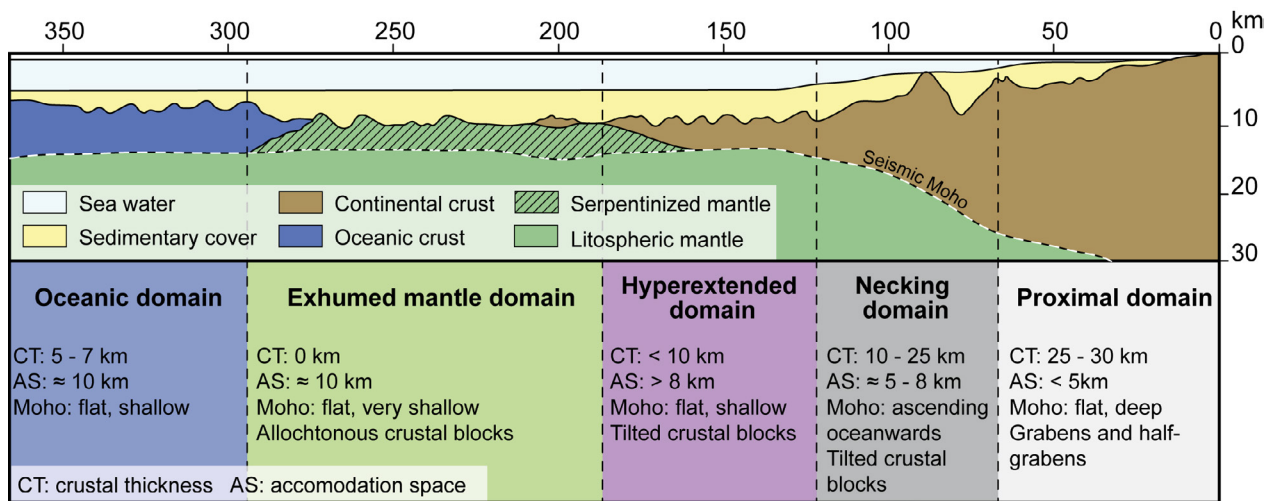


Figure I.6 : Simplified architecture of a passive margin hyperextended with the characterized domains and its main characteristics. Modified after Tugend (2013).

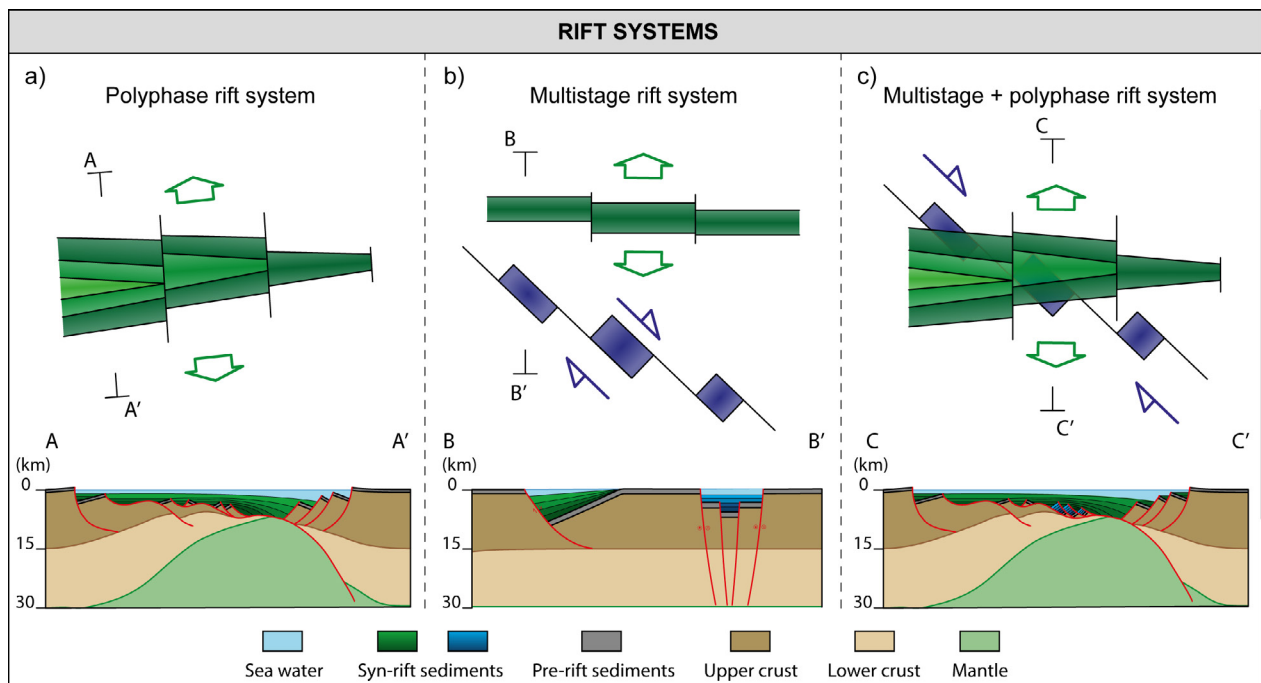


Figure I.7 : Conceptual model of (a) polyphase rift system, (b) multistage rift system and (c) multistage and polyphase rift system in both map view (upper part) and section view (lower part).

B. CONVERGENT CYCLE: OROGENS AND FOLD AND THRUST BELTS

Most of the concepts related to the convergent cycle have been developed in the 70's to 90's and are therefore more mature relative to those of the extensional cycle. One of the factors that helped the successful evolution of knowledge was the onset of reflection seismic during the 70's in the Rocky Mountains fold and thrust belt, an important moment for the community. Due to the wide knowledge and terminology referred to convergent margins [see Roeder et al. (2013) and references therein for extensive review], this section will be focused to some concepts regarding orogens and fold and thrust belts used in this thesis.

B.1. OROGENS

Despite the amount of worldwide observations and evolution of knowledge during the last centuries, we start this summary with the debate around the formation of mountain ranges occurring in the mid XIX century, which could be simplified in three main schools of thinking: 1) the fixists who visualized the mountain building as the result of an asthenospheric diapirism, which would activate gravitational mechanisms to explain thrusts and folds (Belousov, 1962; Belousov & Milanovsky, 1977; Price, 1971, 1973); 2) the expanding earth school that saw mountain building similar to the fixists but differing on the formation of oceans, accepting the accretion and spreading processes in the mid-ocean ridges recording an expansion of the earth (Carey, 1975, 1978); and 3) the Plate Tectonic school, that saw mountain building as the result of subduction processes on converging plate boundaries. Therefore, thrusts and folds are of compressional origin and represent excess sediments slices of the underlying crystalline crust (Wilson, 1966, 1968). It was the last one that became generally accepted as it was best confirmed by the observations and existing data sets.

However, during the last fifty years, different approaches have been developed to increase the understanding of orogenic processes: (1) conceptual models, linking observations from different settings such as passive margins and collisions (e.g. Dewey & Bird, 1970; Vanderhaeghe, 2012); (2) physical experiments with analogue materials bringing insights into simple tectonic processes and geometries (e.g. Malavielle, 1984, see Graveleau et al., 2012, for a review of experimental modelling of orogenic wedges), and (3) numerical models dealing with elements such as strain, heat transfer, mass transport, among others (e.g. Beaumont et al., 1996, 2004; Gerya & Stockhert, 2006). As a result, a wide range of orogen types can be described in function of different factors (see Roeder et al., 2013 for detailed explanation).

Introduction

There are many factors that may be used to organize or classify orogens, one of which, broadly used for the orogens, is the magnitude vs temperature state, meaning the size of the mountain building as well as the material that constitutes the orogen. In that case the orogens can be divided into small and cold orogens, transitional orogens and large and hot orogens (Fig. I.8).

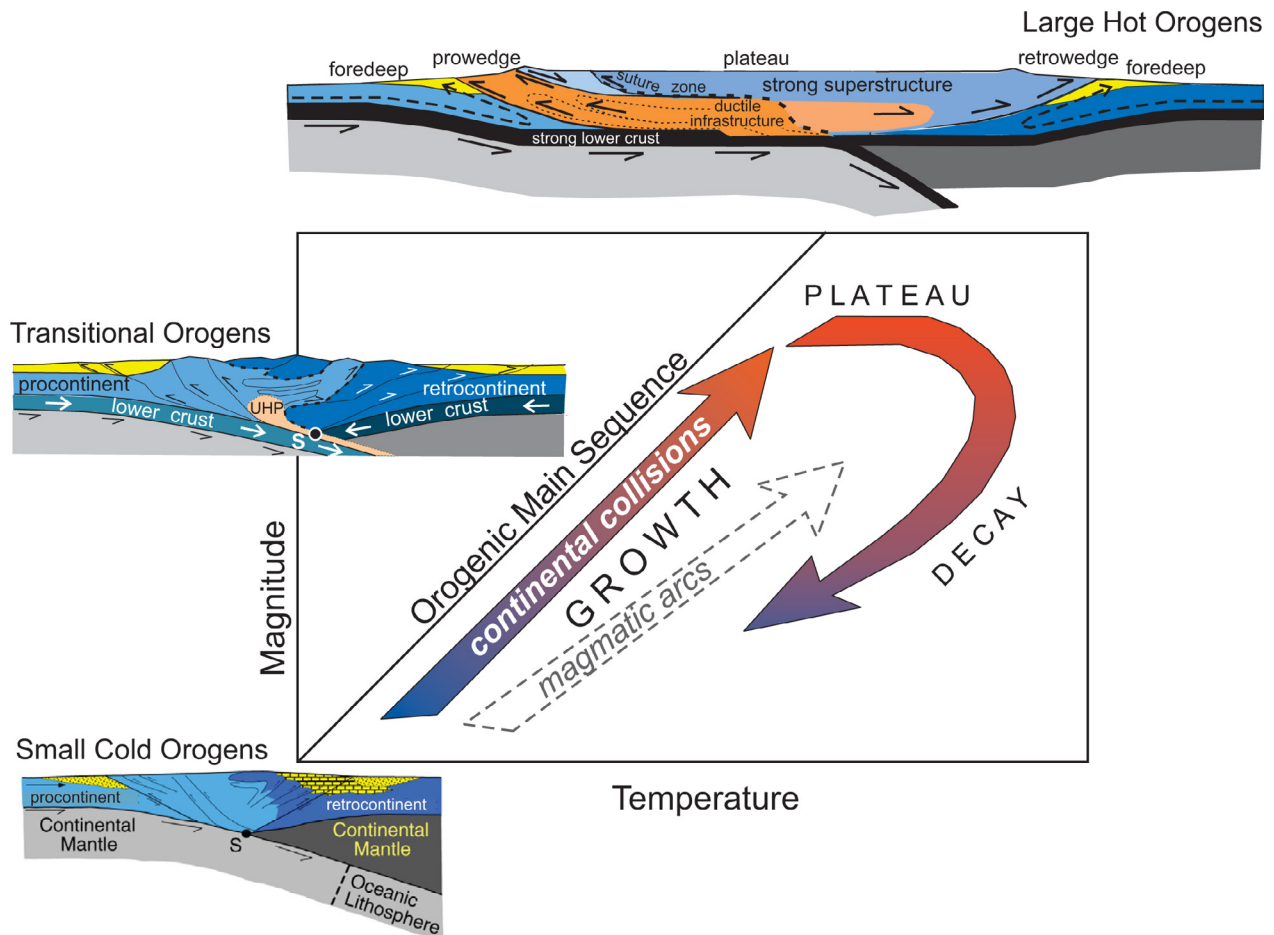


Figure I.8 : Diagram showing a possible classification of orogens by temperature and magnitude. From Jamieson and Beaumont (2013).

The Pyrenean orogen addressed in this study is a typical example of a small and cold orogen. This type of orogen develops above subduction zones where they form an accretionary wedge architecture (Fig. I.9). In a first order, its kinematic can be simplified in a 2-D mechanical model framework in which the crustal domain consists of single or double verging critical wedges and where lithospheric mantle underthrust asymmetrically beneath the orogen (e.g. Pyrenees, Fig. I.9). In the small and cold orogens, the underthrusting is typically given with little deformation and therefore the interior of the orogen remains cold and strong, i.e. ductile deformation is totally or almost absent.

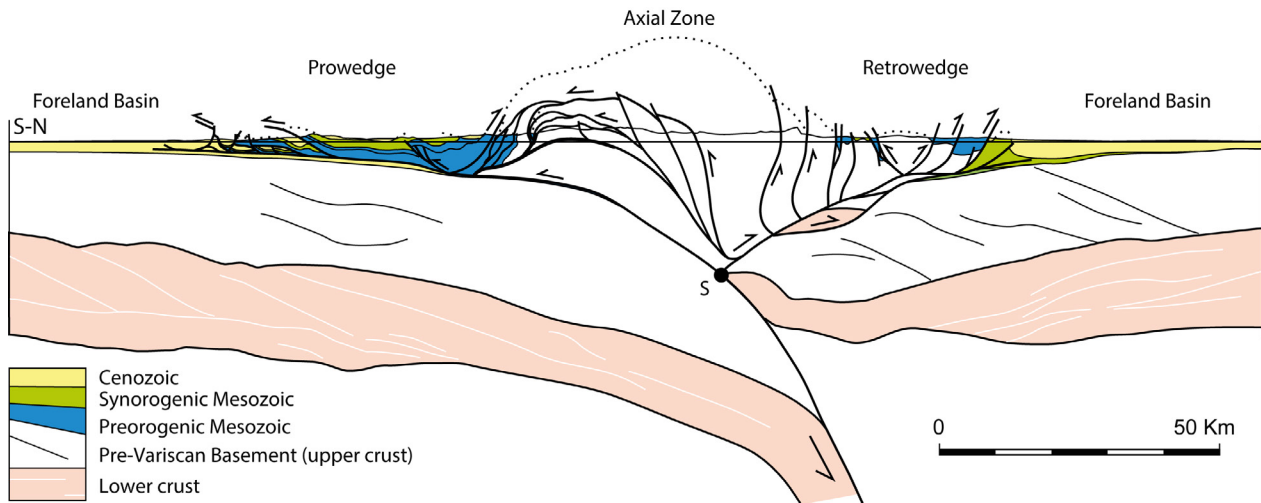


Figure I.9 : Geological sketch of the ECORS geological cross section of the Central Pyrenees with the main terminology of a fold and thrust belt. From Muñoz et al., (2018).

B.2.FOLD AND THRUST BELTS

Orogens evolve from the contractional reactivation of a passive margin (e.g. Alps, Andes, Pyrenees) or intracratonic rift systems (e.g. Atlas, Palmyrides) and related sedimentary basins, but the fold and thrust belts are commonly resulting from the reactivation of the proximal part or of little extended (i.e. low β) systems. The rift systems developed during extension form the crustal weakness which act as a precursor for the localization of the subsequent compressional deformation. Thus, the rift basins become the volume of rocks that will be later incorporated into the orogenic building together with the syn-orogenic sediments. In such a way, fold and thrust belts are formed usually at the final stages of compression in mature orogenic systems, typically in the outer part of the orogens connecting to foreland basins.

Fold and thrust belts are classically divided into two endmembers by structural geologists: (1) thick-skinned structural style fold and thrust belts, characterized by steep thrust faults involving basement coupled with the sedimentary cover which cut across the entire upper crust (sometimes even lower crust). The basement of the foreland use to be tilted or folded into a syncline adjacent to the thrust front [e.g. Laramide Rocky Mountains (Erslev et al., 1999); Cordillera Oriental in Andes (Carrera et al., 2006)] (Fig. I.10). (2) Thin-skinned structural style where the sedimentary cover is detached from the underlaying and usually undeformed basement. This structural style is commonly represented by a thrust system affecting the sedimentary succession where the thrusts merge down into a mechanically weak decollement horizon where the main displacement is accommodated. The basement of the adjacent foreland basin uses to be tilted to the hinterland below the frontal thrust [e.g. Canadian Rockies (Dahlstrom, 1970); Sevier (Camilleri & Chamberlain,

1997); Bolivian Andes (McQuarrie & DeCelles, 2001)] (Fig. I.10). However, intermediate positions where both styles of deformation are mixed is also usually observed, and this has been referred as basement-involved thin-skinned tectonic model (Pfiffner, 2006, 2016).

In general, passive margins with post-rift sedimentary prisms tapering out onto the non-rifted cratons favour the thin-skinned style, whereas intracratonic rift systems tend to produce thick-skin structural styles inverting the half-graben basement faults (Nemock et al., 2013). Nevertheless, the presence of salt or thick shale deposits influence significantly the style of deformation being more complex than just summarized before. As a result, many fold and thrust belts exhibit both thin- and thick-skin structural styles in different portions of the belt either in strike variations such as the Andes (Allmendinger et al., 1997) and Pyrenees (Roca et al., 2011; Muñoz et al., 2013) or in their internal vs external parts such as the Laramide Rocky Mountains (Hamilton, 1988).

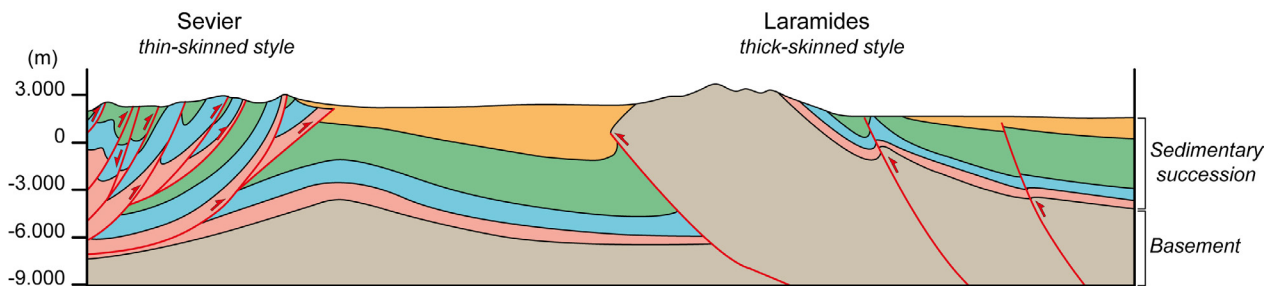


Figure I.10 : Geological sketch of the Sevier and Laramides orogens in North America to illustrate a thin-skinned structural style vs a thick-skinned structural style. Modified after Wyoming State Geological Survey (2020).

Fold and thrust belts have been extensively analysed using different methodologies such as physical models (e.g. Malavieille, 2010; Granado et al., 2017; Izquierdo-Llavall et al., 2018; Pla et al., 2019), and numerical models (e.g. Ellis et al., 1998; Beaumont et al., 2000). See Dahlen (1990), McClay et al. (2004) and Buiter (2012) for an extended review of compressional wedge models. But the kinematics of a fold and thrust belt can be explained in a simplified way by using the critical wedge mechanics theory (Chapple, 1978; Davis et al., 1983; Dahlen et al., 1984; Dahlen, 1984, 1990; Suppe, 2007; Buiter, 2012) that give an explanation for the basic geometry and stress state in accretionary wedges. Considering them analogous to wedges of snow or sand in front of moving bulldozer: The material in front of the bulldozer will deform until it reaches a so-called critical taper. If no further material is encountered, the wedge will slide stably along the base, without internal deformation. If new material is encountered, the wedge will grow self similarly at its critical taper value [see Buiter (2012) for a detailed explanation]. However, this theory requires few assumptions: (1) the wedge consists of brittle/frictional material which is on the verge of failure everywhere, (2) rock strength is time-invariable and determined

by the Coulomb criterion, (3) material properties are constant in time, homogeneous in space, and isotropic, (4) the base is cohesionless, and (5) the strength of the base cannot exceed the strength of the interior.

In cross section, fold and thrust belts shows a wedge-shape deformed area overlying a basal detachment, which dips towards the hinterland whereas the topography slopes towards the deformation front (Fig. I.11). Deformation within the wedge is usually organized by thrust faults verging towards the front [e.g. Canadian Rockies (Bally et al., 1966), Southern Appalachians (Roeder & Witherspoon, 1978); central Pyrenees s.s. (Muñoz et al., 2018)].

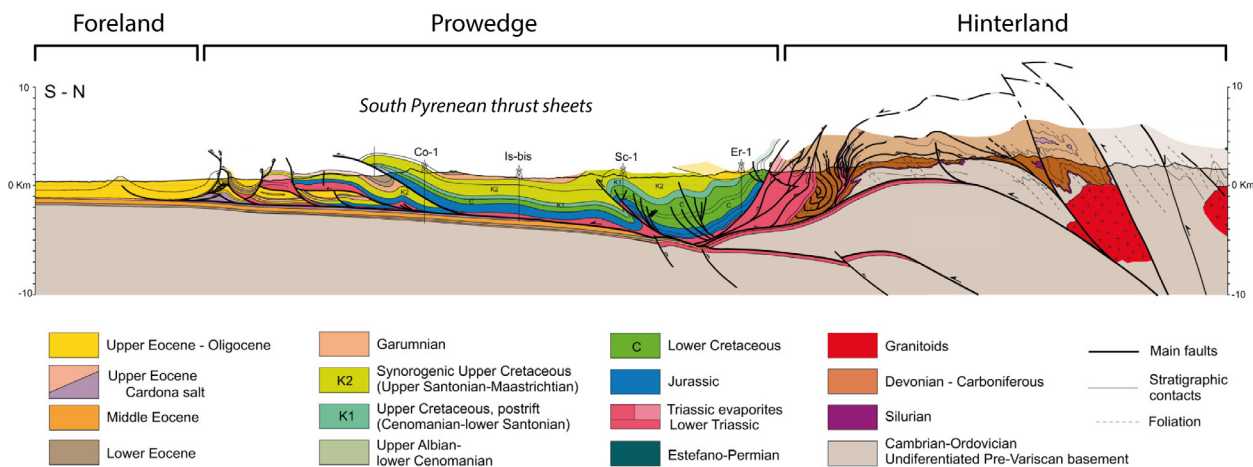


Figure I.11 : Geological cross section along the Pallaresa valley (central Pyrenees s.s.) based on the ECORS-Pyrenees cross section. From Muñoz et al. (2018).

C. THE PYRENEAN NATURAL LABORATORY

The Pyrenees are one of the most studied fold and thrust belts on the planet due to the preservation of the syn-tectonic materials, the lack of metamorphic overprint developed during compression, the amount of geophysical data available and last, but not least, the quality of the outcrops as well as the good accessibility. Therefore, the Pyrenees represent a perfect natural laboratory to study the formation and reactivation of rift systems and the evolution of orogens (i.e. fold and thrust belts). The previous mentioned reasons as well as the involvement of this thesis in the Orogen Project (TOTAL – CNRS – BRGM: www.orogen-project.com) that has as a main interest deciphering genesis of mountain belts, became a great opportunity to investigate the formation and reactivation of a multistage and polyphase rift system using the Basque – Cantabrian Pyrenees as a case study.

The Pyrenees, geologically speaking, constitute an orogenic system located in between the Iberian/Ebro and European plates but not restricted to, as this mountain belt continues to the east connecting to the Alps, Carpathians and subsequent mountain chains up to the Himalayas (Fig. I.12).

Within the Pyrenees, the stratigraphic record and the structural style changes significantly along strike and as a result, different physiographic units can be identified along the mountain belt (Fig. I.13). This fact has been captured in the literature with a wide range of names both geographical and geological being used to refer to the same areas. Therefore, in the Fig. I.14 a compilation of the most used terminology in the Pyrenees is summarized as well as the one that will be used in this work from now onwards to avoid any further confusion.

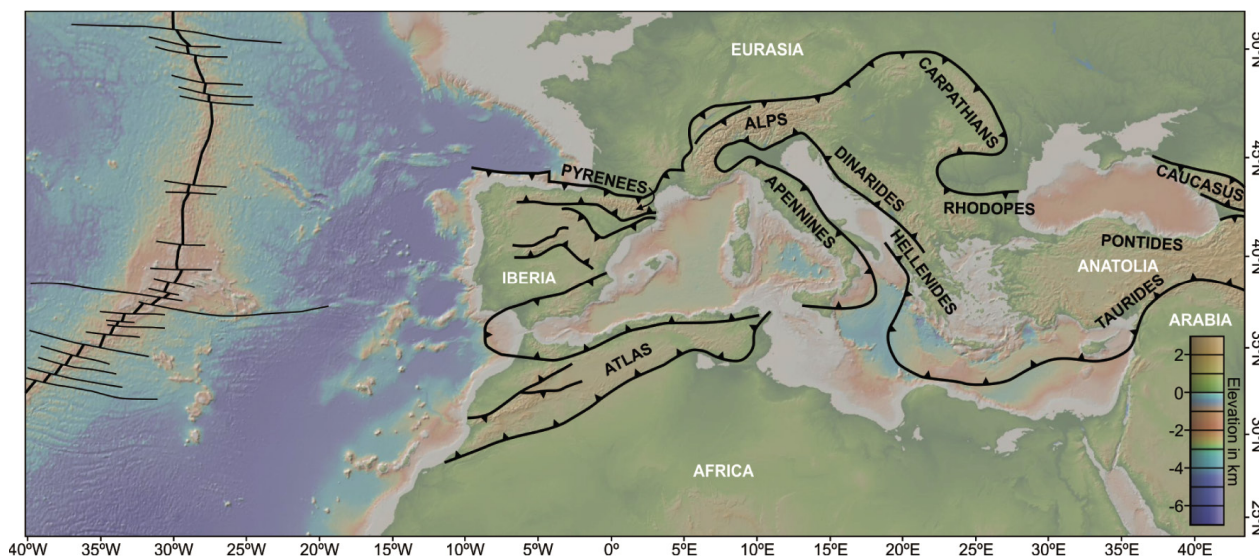


Figure I.12 : Mountain belts of the western portion of the Himalayan – Alpine orogenic system labelled in black and main tectonic plates labelled in white. From Carola (2014).

The Pyrenees formed as a result of the inversion of a hyperextended rift system, i.e. the North Iberian Rift System, and related passive margin, i.e. Northern Iberian Margin, developed during Late Jurassic to Early Cretaceous all along the northern Iberian plate (Tugend et al., 2015; Cadenas et al. 2020). Such domains connected the Atlantic and Alpine Tethys oceans (Stamfli & Hochard 2009). At present, the Pyrenees constitute an asymmetric double vergent orogenic wedge formed due to the collision between the Iberian/Ebro and European plates from Late Cretaceous to Miocene times (Roest & Srivastava, 1991; Rosenbaum et al., 2002). Such collision occurred above the subduction of the Iberian/Ebro plate beneath the European plate (Choukroune & ECORS Team, 1989; Muñoz, 1992; Pedreira et al., 2003; Campanyà et al., 2012; Chevrot et al., 2015).

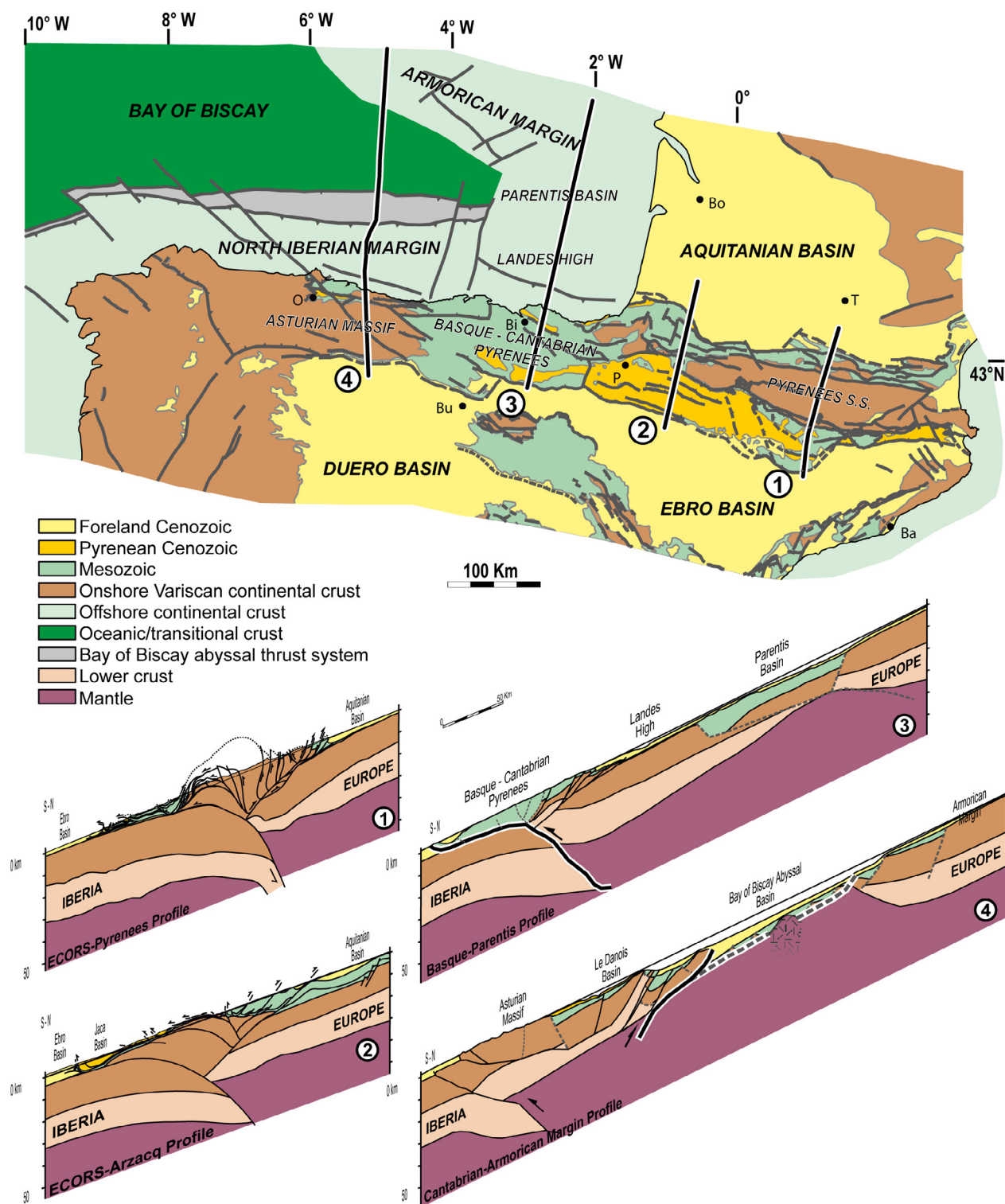


Figure I.13 : Crustal scale geological cross section along the Pyrenean Orogen showing the main architecture along strike. (1) ECORS-Pyrenees, (2) ECORS-Arzacq, (3) Basque-Cantabrian Pyrenees – Parentis and (4) Asturian Massif – Armorican Margin. Modified after Muñoz (2019).

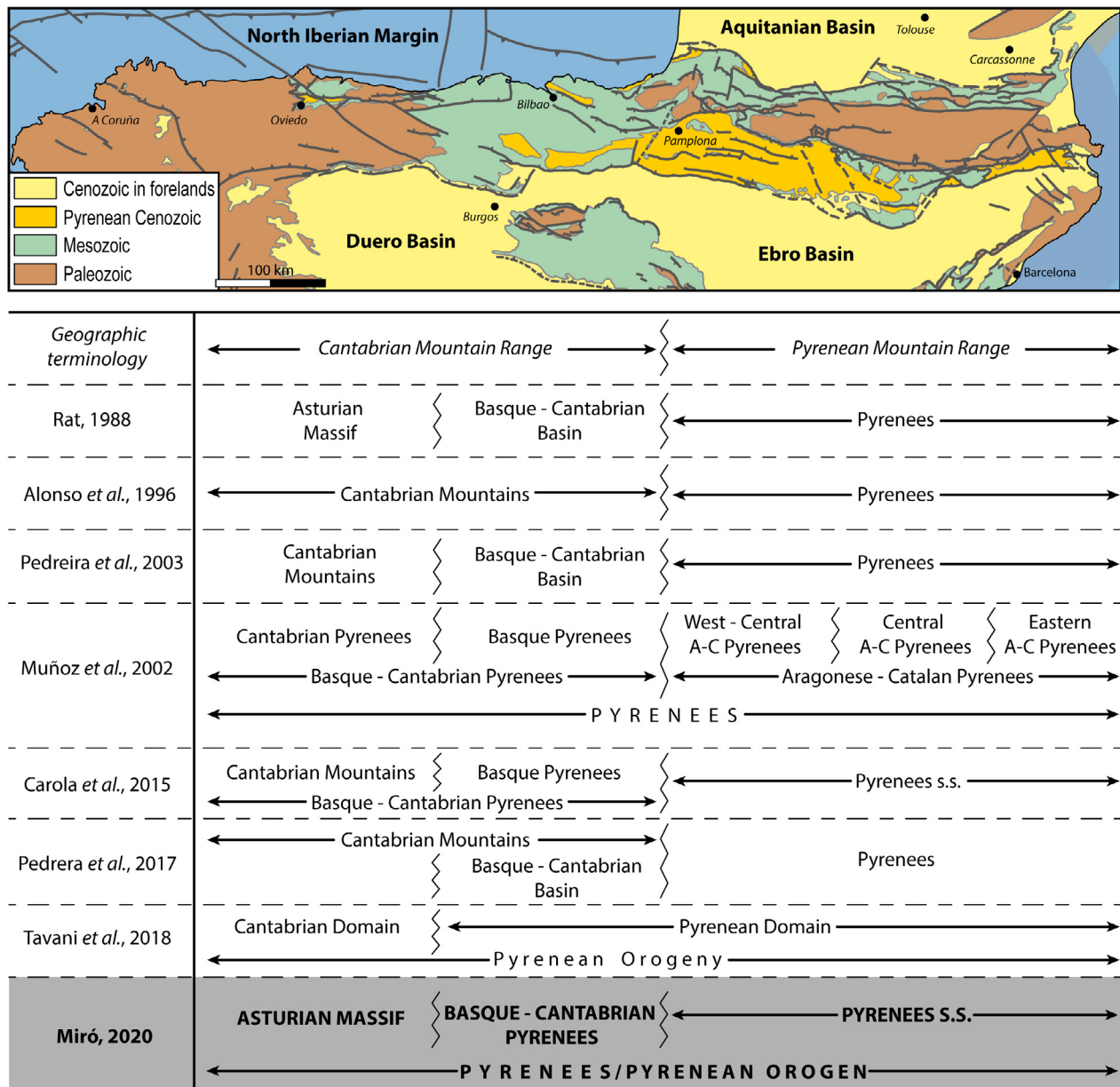


Figure I.14 : Common terminology used in the literature to refer to different parts of the Pyrenean orogen. Modified from Barnolas and Pujalte (2004).

C.1. GEODYNAMIC CONTEXT

The Variscan cycle

Many questions remain concerning the Variscan cycle and its paleogeographic interpretation, but it is accepted that the Variscan orogeny (480 to 290 Ma) resulted from the collision of two main continents, Gondwana to the south and Baltica to the north (Matte, 2001). However, small microplates have been recognized in between by using paleomagnetic, paleobiostratigraphic and geological observations (i.e. observation of oceanic sutures) such as Avalonia (Matte, 1991; Cochelin, 2016) (Fig. I.15). The Variscan collision developed an intense high temperature metamorphism and magmatism that resulted in the emplacement of the plutons observed in the hinterland (Ballèvre et al., 2014; Martínez – Catalán et al., 2007) contemporaneous with the bending of the orogen that finished with the orocline shape observed at present-day in the north-west of Iberia (Fig. I.15).

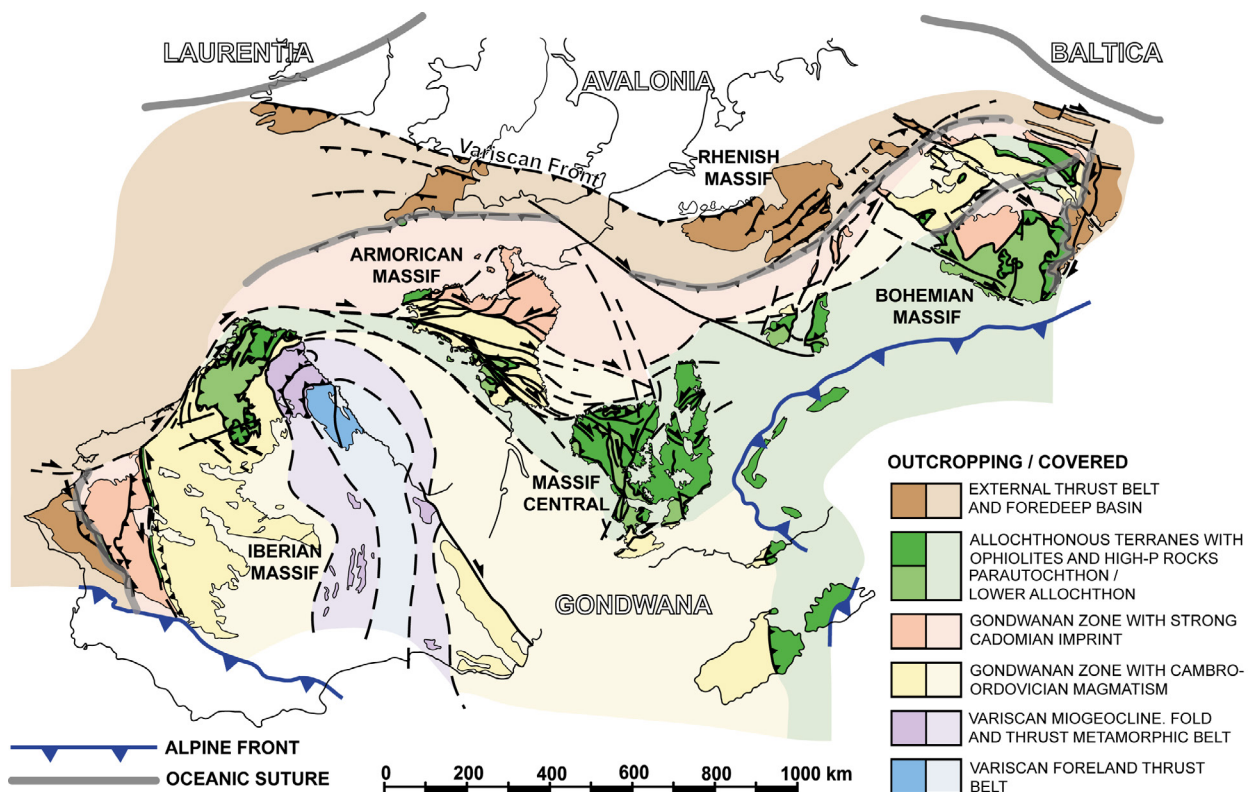


Figure I.15 : Map of the Variscan orogeny in the western Europe with the main sutures identified and the different tectonic plates involved. Modified after Martínez-Catalán et al. (2007).

At the end of the Variscan cycle, the Late Permian to Triassic period corresponds to a moment with erosion and peneplanation of the Variscan relief all across the Western Europe (Arthur & Matte, 1977; Doré et al., 1999). This period is characterized by continental sedimentation in half graben basins controlled by a transtensional regime (Bixel & Lucas, 1987). The most typical facies in Western Europe are the Germanic Buntsandstein (Stevaux

& Winnock, 1974) that unconformably overlies the Permian basins and Paleozoic basement. The Triassic period is associated with the onset of rifting related to the breakup of the Pangea supercontinent in the Tethys and Central- Atlantic (Fig. I.16a) (Stampfli & Borel, 2002). The Late Triassic period shows a thermal and magmatic event resulting in the formation of evaporitic layers of heterogeneous distribution often with the presence of tholeiitic dolerites (also called ophites).

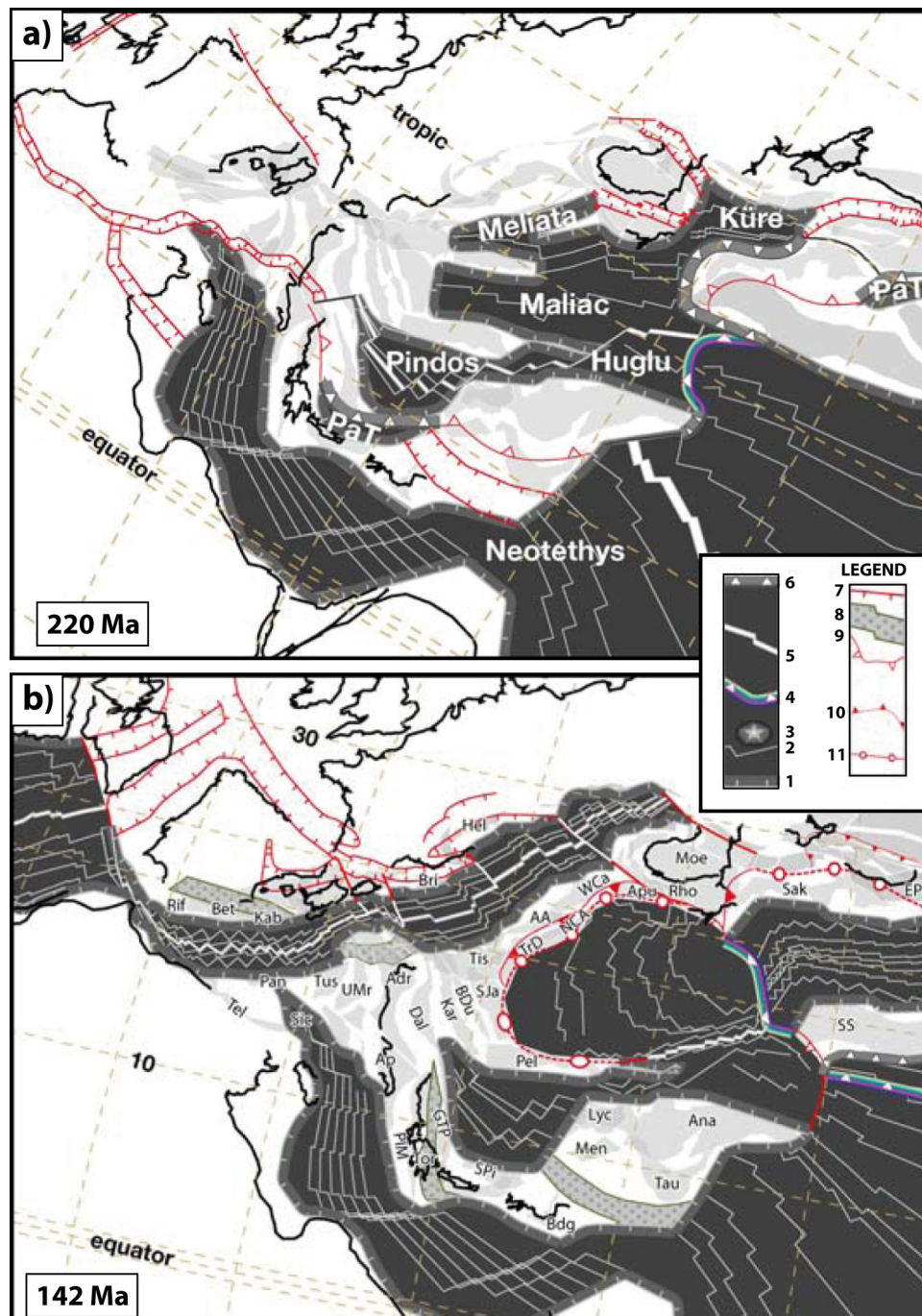


Figure I.16 : Plate tectonic reconstruction of the Alpine realm at (a) Late Triassic and (b) Late Jurassic stages. Symbols: 1: passive margin; 2: magnetic or synthetic anomalies; 3: seamount; 4: intra-oceanic subduction; 5: mid-ocean ridge; 6: active margin; 7: active rift; 8: inactive rift (basin); 9: collision zone; 10: thrust; 11: suture. Oceanic lithosphere in black. See Stampfli and Hochard (2009) for the meaning of abbreviations. From Stampfli and Hochard (2009).

The Alpine cycle

The geodynamic evolution during the Alpine cycle in the Pyrenees (i.e. Iberian/Ebro – European plate boundary) is a subject of debate since decades and a consensus is missing within the Earth Science community. From Late Jurassic to Late Santonian, the opening of southern North Atlantic and Bay of Biscay – Pyrenean systems occurred (Fig. I.16b). Numerous models have been proposed to explain the movement of the Iberian plate from Late Jurassic to Late Santonian but still a definitive model matching all data and observations is missing (See Barnett-Moore et al., 2016 and Nirrengarten et al., 2018 for an extended review and discussion).

The models proposed up to the moment can be grouped in three, despite minor differences in between them (Fig. I.17): 1) the strike-slip models, 2) the scissor-type models, and 3) the orthogonal rifting models.

1. The first strike-slip model implies more than 400km of left-lateral movement being accommodated along the North Pyrenean Fault from Aptian to Santonian time creating pull-apart basins in the Pyrenean system (e.g. Stampfli & Borel, 2002; Choukroune & Mattauer, 1978; Debross, 1987). This model is based mainly on paleomagnetic data, which have been recently questioned (Neres et al., 2013) and there is no field evidence supporting such strike-slip movement. Moreover, it also implies that no deformation occurred in the Iberia – European plate boundary from Jurassic to Aptian time, contrasting with the well constrained geological observations in the field (e.g. kilometre deep sedimentary basins such as Mauléon and Basque Cantabrian Basin (Masini et al., 2014; Quintana et al., 2015)).
2. The scissor-type model shows a 250km wide oceanic domain between Iberia and European plates that has been interpreted to close during Albian time resulting in a back-arc basin where the North Pyrenean basins are at present. The compression would have occurred from Late Santonian onwards (Advokaat, et al., 2014; Vissers et al., 2016; Sibuet et al., 2004). This model is supported basically on the interpretation of the magnetic anomalies (i.e. M-series) in the southern North Atlantic and Bay of Biscay as well as paleomagnetic data. However, the magnetic anomalies before the M3 (127Ma) have been reinterpreted as not being of oceanic origin and therefore not representing isochrons, which do not allow to use these magnetic anomalies for plate kinematic interpretations (Nirrengarten et al., 2017). Moreover this model would imply also a large subduction and collision in the Iberian range at Albian time, something not identified in the field (e.g. Rat et al., 2019).

3. The Orthogonal rifting model involve a first phase of strike slip deformation from Late Jurassic to Aptian followed by an orthogonal N-S direction of extension from Aptian to Cenomanian (Jammes et al., 2009; Tugend et al., 2015). Tavani et al. (2018) proposed an orthogonal extension from Late Jurassic to Late Cretaceous, implying limited lateral displacement between Iberia and Europe from Jurassic to Late Cretaceous. However, a strong and uniform Iberian plate would not fit with this model considering the E-W opening of the southern North Atlantic (Bernett-Moore, et al., 2016; Nirrengarten et al., 2018). But field evidence supporting the strike slip model proposed are not definitive and therefore further investigations need to be done.

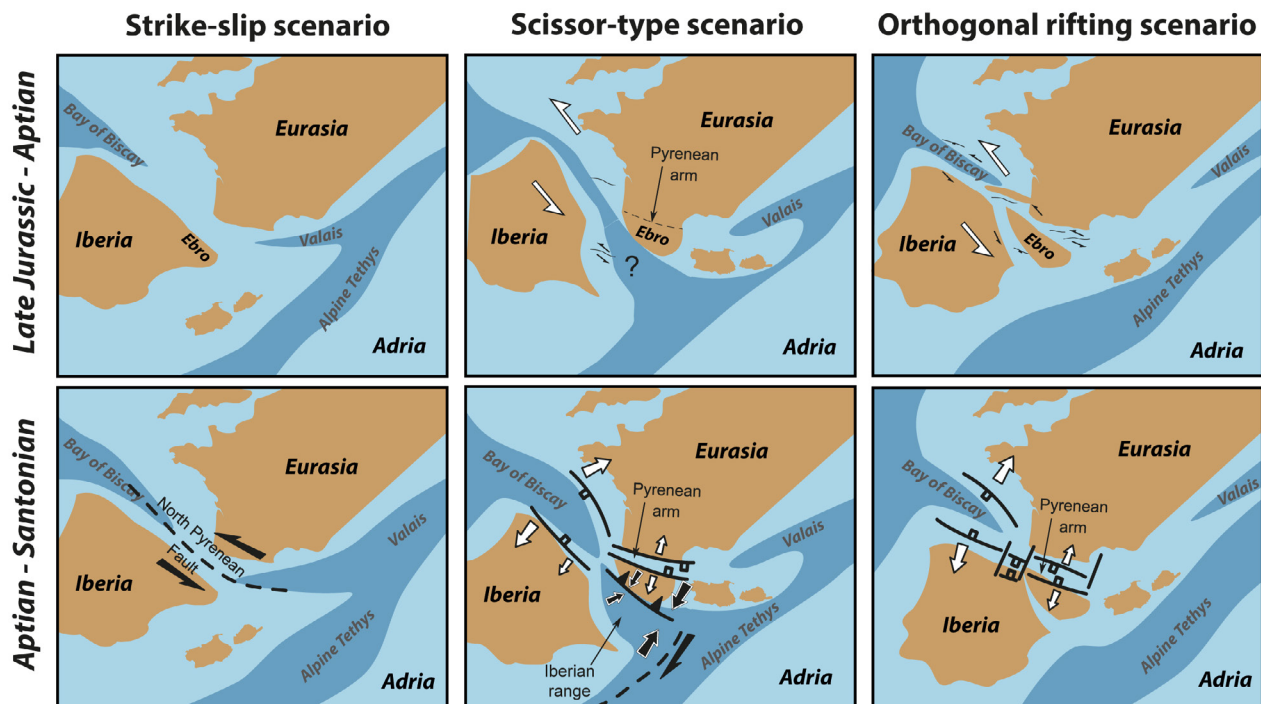


Figure I.17 : Different models proposed for the geodynamic evolution of the Iberia-Eurasia plate boundary at Late Jurassic-Aptian and at Aptian-Santonian times (modified after Tavani et al., 2018). Orthogonal rifting model after Tugend et al. (2015); Strike-slip model after Stampfli & Borel (2002); Scissor-type model after Sibuet et al. (2004). Modified after Lescoutre (2019).

On the other hand, what seems broadly accepted in the last years is that onset of compression would happen during Late Santonian (83 Ma) due to a change in the kinematics between Africa, Iberia and Eurasia. A compressional regime in the North Iberian margin from Late Santonian resulted in the formation of the Pyrenean orogenic system up to Miocene (Rosenbaum, et al., 2002; Macchiavelli et al., 2017) (Fig. I.18). Still, consistent field evidence supporting this idea needs to be found all along the orogen, as they are mainly in the central Pyrenees s.s. (Boillot and Capdevila, 1977; Teixell, 1996; Muñoz, 1992; McClay et al., 2004; Mencos et al., 2015).

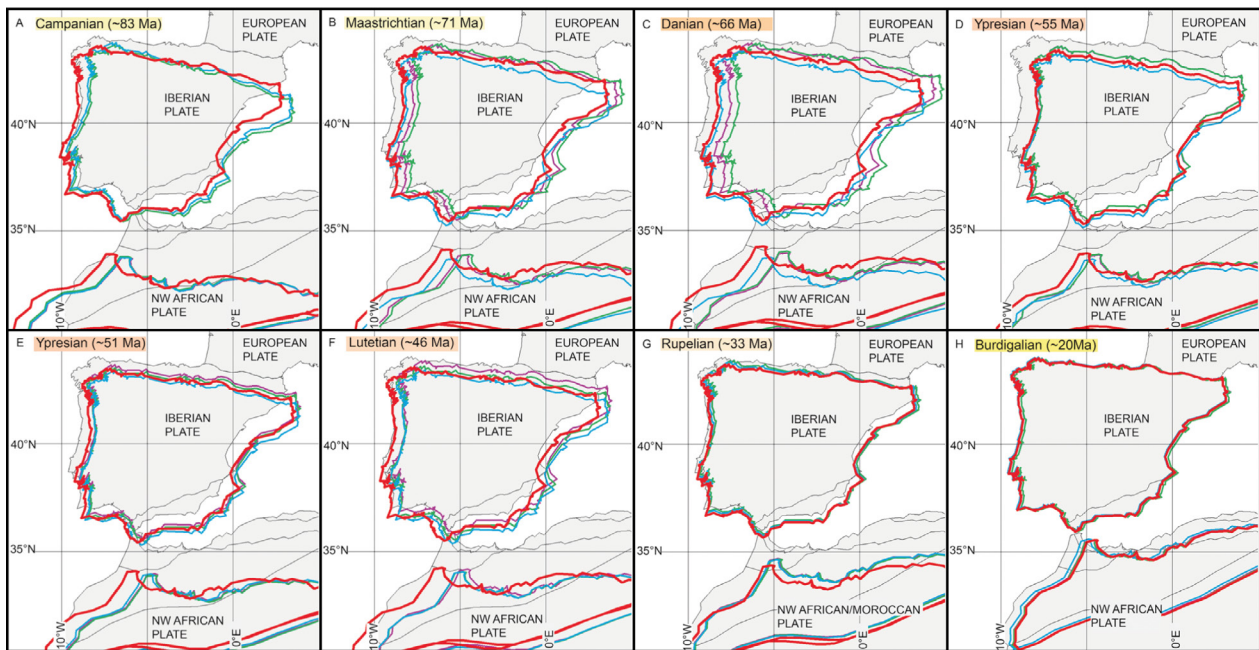


Figure I.18 : Different plate reconstructions for the Iberian and NW African/Moroccan plate. Red line: Macchiavelli et al., 2017; blue line: Vissers and Meijer (2012); green line: Rosenbaum et al. (2002); purple line: Srivastava et al. (1990). Present-day coastlines (grey areas) are shown for reference. From Macchiavelli et al. (2017).

D. OPEN DEBATES

D.1. MESOZOIC FRAMEWORK

As pointed out previously, an intense debate is occurring since decades on the kinematic evolution and plate restoration of Iberia and surrounding areas. The main issue is to fix the Iberian plate considering the opening of the southern North Atlantic (Bernett-Moore, et al., 2016; Nirrengarten et al., 2018; Angrand et al., 2020) but also the formation of the Mesozoic basins along the Iberian – European plate boundary (Tavani et al., 2018; Tugend et al., 2015) and the reorganization of the Alpine Tethys, and all the western Mediterranean at Mesozoic times (Angrand et al., 2020). Thus, regarding many proposals published during the last years, a solution reconciling all the observations and considerations have not been proposed and this debate seems far from a global solution.

Moreover, considering the uncertainties affecting the kinematics of Iberia and surrounding areas, and its implications for the plate tectonic restorations during Mesozoic, it has major implications for the interpretation of the Variscan. An extensive work is reported in the literature addressing the Variscan cycle with results such as the map of Fig. I.15 showing the present-day distribution of the main orogenic domains of the Variscan. However, as it has been summarized above, the plate reconstruction and kinematics of Iberia from Late Jurassic to Middle Santonian are not clear or at least, a consensus in

the Earth Science community is still missing. An evidence that seems irrefutable is the opening of the southern North Atlantic and therefore a lateral movement of Iberia of at least few hundreds of kilometres occurred at certain moment. Therefore, the present-day distribution of Variscan domains as presented in Fig. I.15 between Iberian and Europe should be discussed in the light of the Mesozoic kinematic framework.

D.2. PYRENEAN OROGEN: A CONTINUOUS OR SEGMENTED OROGEN?

The Pyrenean Orogen is the result of the Iberian/Ebro plate moving to the north and colliding with the European plate as explained before. Thus, the geographically speaking Pyrenees (i.e. mountain belt between Spain and France) are the result of such a collision. However, this would not explain the continuation of the mountain belt located westwards of the Pyrenees s.s. (i.e. Asturian Massif). But despite the E-W striking direction and continuity of the mountain belt as well as the major structures on map view (i.e. southern and northern frontal thrusts, Fig. I.13), the Pyrenean orogen results from the reactivation of a segmented rift system (Tugend et al., 2014a; Lescoutre & Manatschal, 2020). Moreover, whereas the connection between the Atlantic and Tethys was closed (Pyrenees s.s.), the Bay of Biscay remained open.

Therefore, questions can be formulated regarding the continuity of such orogenic system from the Pyrenees s.s. to the Asturian Massif, the role of the rift inheritance in the final orogenic architecture or the impact of rift segmentation for the subsequent reactivation and incorporation into the Pyrenean orogen.

E. DATA AND METHODOLOGY

This section summarizes the different methodologies and data used to develop this thesis. Four sub-sections structure the methodology and data part.

E.1. FIELD WORK

In order to understand the present-day architecture of the Basque – Cantabrian Pyrenees, two regional cross sections crossing the area from south to north were required. Therefore, a series of field campaigns were done to know the area, collect surface data (i.e. more than 1100 dip data) and take observations from facies distribution and complex areas not well resolved in maps. FieldMove App was used to support the field work with the orthophotographs, topographic and geological maps at 1:25.000 and 1:50.000 scales, when available. The surface data were not more distant than 1km from the trace of the cross section in most of the cases and only the wells and seismic lines closer to the trace

were projected and used for its construction. Move® software was the main tool used to construct the regional cross sections and treat with the field collected data.

A new thematic geological map at regional scale was also required and produced to support the new interpretation resulting from this thesis with the main goal of representing the tectono-stratigraphic evolution of the Basque – Cantabrian Pyrenees. In order to build the map, a combination of several geological maps (see Annex 2.3 for the reference list) from Instituto Geológico y Minero de España (IGME) but also from other thesis and publications as well as personal field observations were integrated (Fig. I.19) (Miró et al., 2020).

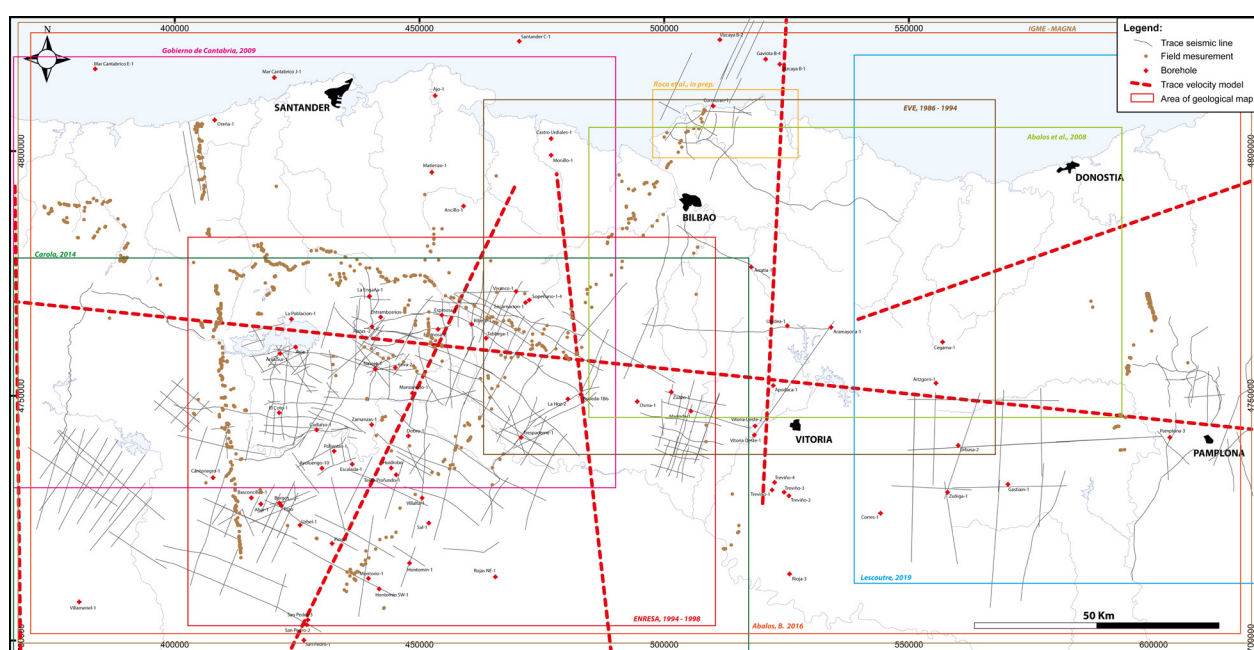


Figure I.19 : Hydrographical base map with the location of the main datasets used in this thesis.

E.2. SEISMIC DATA

To help the understanding of the present-day architecture of the Basque – Cantabrian Pyrenees and the construction of the regional cross sections, all the available seismic data was grouped in the same Move project to process and interpret. The seismic dataset used in this thesis is made of digital and printed seismic sections gently provided by IGME. All the seismic sections used and presented here were acquired during different campaigns between the early 70's and the 90's, when hydrocarbon exploration took place in the Basque – Cantabrian Pyrenees and surrounding areas. Therefore, the quality of such data is variable depending on the acquisition and processing methods they used, the filters they applied and technical limitations. For the development of this thesis, 324 seismic lines have been obtained and most of them interpreted (Fig. I.19). Seismic lines in paper format were scanned and converted at depth considering the borehole data but using an average time-depth conversion of 4,5 – 4,8 seconds (TWT) corresponding to 10.000 m. The surface geology

and boreholes were used to make a final adjustment of the seismic data considering the rest of datasets in order to build a consistent and coherent framework (Miró et al., 2020).

E.3. WELL DATA

Similar as the seismic data, all the wells available in the area were acquired (i.e. stratigraphic logs) and incorporated into the Move project to help the construction of the regional cross sections. The methodology used regarding the well data was similar to the one used for the seismic data. Most of the wells were drilled during the 40's to 80's and during a second phase of exploration in the 2000' by oil companies. The borehole data have been used to help the seismic interpretation as well as to complement the subsurface data. Such information was provided by the IGME using the lithological log to determine the different units established. A number of 79 boreholes have been obtained and projected to improve the results of this thesis (Fig. I.19).

The software used in this thesis for the homogenization of all the data in terms of projection and datum (UTM – Z30 – ETRS89) was Global Mapper®. The seismic interpretation and cross section performance were done with Move® as well as the displaying and visualization of all data in a 3D interface (Miró et al., 2020).

E.4. SANDBOX ANALOGUE MODELLING

An experimental program of sandbox analogue models was carried out at the Geomodels Analog Modeling Laboratory of the University of Barcelona (Fig. I.20). The models were inspired on the Basque – Cantabrian Pyrenean geology combining rigid blocks (i.e. made of wood) to simulate the basement inheritance, the silicon as an analogue material of Late Triassic salt, and dry silica sand to reproduce the sedimentary cover. The main goal was to investigate the role of a decoupling level overlapping basement faults during extension and subsequent reactivation of a segmented rift system. Furthermore, this experimental program helps to understand the formation of oblique structures developed in the transition of a thick- to thin-skinned domain under the same deformation direction. Further details on the development of the experimental programme are given in the Chapter 2 of this thesis.

The models were performed during the 2nd year of the thesis during my stay in Barcelona as the co-tutelle agreement established at the beginning of the project between the University of Strasbourg and University of Barcelona.



Figure I.20 : Geomodels Analogue Modelling Laboratory of the University of Barcelona where the experimental program was run.

F. SCIENTIFIC QUESTIONS

The objective of my PhD thesis is twofold: first, I aim to better understand the Basque – Cantabrian Pyrenees regarding the present-day architecture as well as to use the field example to investigate a hyperextended rift system involved into an orogen. Second, I seek to test and provide generic models that may help to understand worldwide analogues to the Pyrenees, the incorporation of rift systems into orogens and the strike variability governed by the presence of different decoupling levels.

This manuscript addresses three main problematics, which are organized in three research axes:

1. Formation and reactivation of a hyperextended rift system: The Basque – Cantabrian Pyrenees case:

Through the first research chapter of my thesis, I investigated how a hyperextended rift system may be characterized in the field and what is the influence of the rift inheritance on the final orogenic architecture and how it is involved in it. To do this, I performed a new thematic map representing the tectono-stratigraphy of the area considering the tectonic evolution. I analysed and integrated seismic data, well data and field data in order to construct two regional cross sections showing the present-day architecture as well as the rift template. This allowed me to get a picture of the Basque – Cantabrian Pyrenees along time and space and capture the importance of inheritance for subsequent integration of a hyperextended rift margin into an orogen. My approach was guided by the following questions:

- What is the present-day architecture of the Basque – Cantabrian Pyrenees?
- Which was the rift template and how did it influence the present-day architecture?
- How is a hyperextended rift margin reactivated?

2. Interplay between structural inheritance and pre-rift salt during formation and subsequent inversion of low- β rift systems

Through the second chapter of my thesis, I attempt to unravel the impact of inherited basement structures and a pre-rift salt unit partially overlapped on the formation and subsequent reactivation of proximal rift domains. Segmentation is presented in many rift systems and orogens worldwide, but it remains poorly understood how the thick to thin-skinned transitions evolve and how to explain oblique structures respect to the regional deformation direction (i.e. what controls their position and orientation). Considering the advantages offered by analogue models (i.e. control of input parameters, deformation rates, 3D structurally balanced solutions, among others), I used this technique to address the following questions:

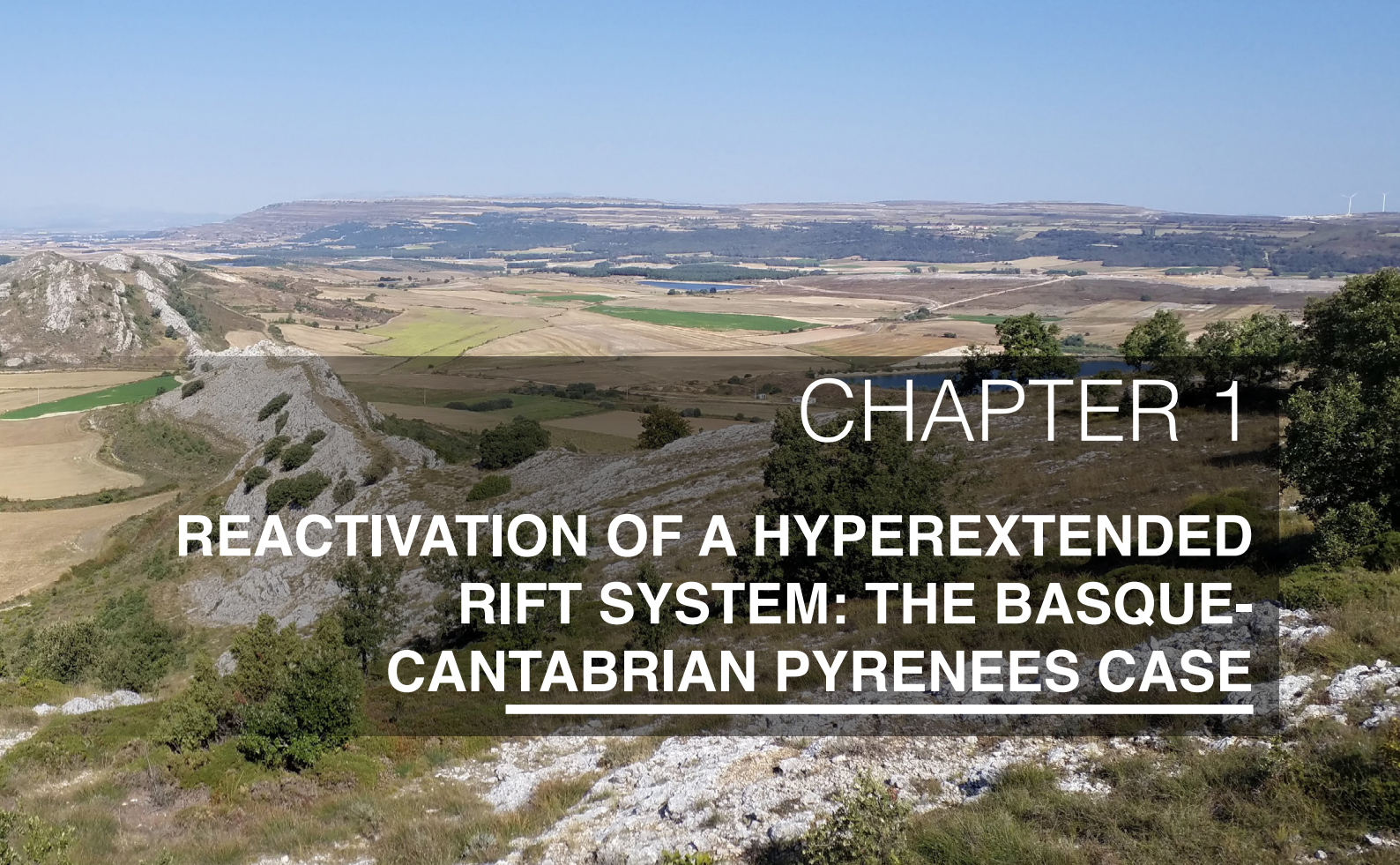
- How the transition of a thick- to thin-skinned domain evolve during extension and subsequent reactivation?
- What controls the formation of oblique structures respect to the deformation direction?
- How is the strain partitioning in the transitional domains?

3. Control of inheritance on the nucleation and growth of an orogen: insights from the Pyrenean Orogen:

Based on previous results as well as the integration of previous research done by colleagues of the project (Rodolphe Lescoutre in the Basque Massifs and Patricia Cadenas in the Offshore North Iberian Margin), the next step aims to understand at a large scale the inversion and incorporation of a segmented rift system into an orogen. Using the Pyrenean – Bay of Biscay example, where different scenarios have been recognized, a model is proposed driven by the following questions:

- What is the role of the main decoupling levels through time and space during the reactivation of a hyperextended rift system?
- How does spatial variability affect the incorporation of hyperextended rift systems into an orogen?
- When does a convergence change from subduction/accretion to collision phase?





CHAPTER 1

REACTIVATION OF A HYPEREXTENDED RIFT SYSTEM: THE BASQUE- CANTABRIAN PYRENEES CASE

The cover of Chapter 1 is composed by two photos: an upper one depicting the Tudanca Valley with the eastern termination of the Peña Sagra ridge made of Paleozoic basement (left) and the Jurassic to Lower Cretaceous succession unconformably overlying (right) (Cantabria); and a lower one illustrating the field expression of the Ubierna Fault in the Valdelucio Valley (Burgos province).

REACTIVATION OF A HYPEREXTENDED RIFT SYSTEM: THE BASQUE-CANTABRIAN PYRENEES CASE

Submitted to Basin Research

Jordi Miró^{1,2}, Patricia Cadenas³, Gianreto Manatschal¹ and
Josep Anton Muñoz²

¹ IPGS, EOST-CNRS, Université de Strasbourg, 1, rue Blessig, 67084 Strasbourg, France

² Institut de Recerca Geomodels, Departament de Dinàmica de la Terra i de l'Oceà, Facultat de Geologia, Universitat de Barcelona

³ BCSI, ICM, CSIC, 37 Passeig Marítim de la Barceloneta, 08003 Barcelona, Spain

ABSTRACT

This contribution aims the role of a multistage and polyphase rift system in the formation and reactivation of the Basque – Cantabrian Pyrenees. The understanding of the present-day architecture as well as the rift template, and the mechanisms of initial reactivation are addressed in this work. To carry out this study, two regional cross sections, integrating geological and geophysical information, across the central and western Basque – Cantabrian Pyrenees were constructed. Furthermore, a restoration to previous rift template at Cenomanian and Barremian ages is also presented. The two sections reveal different stages of the orogenic evolution. The Central section is governed by a thin-skinned structural style where the Upper Triassic salt decoupled the sedimentary cover and masks the basement architecture. In contrast, the Western section displays an interaction of both thin- and thick-skinned structural styles conditioned by the irregular distribution of the salt. Moreover, the Western section preserves the different rift stages at different positions due to the migration of deformation to the north (i.e. Bay of Biscay) preserving the rift architecture of distal parts slightly reactivated. These observations become fundamental to restore and understand the rift template in the distal parts of the Central section, where the extensional deformation was localized in the same basin, stacking the different rift events. We demonstrate the importance of rift inheritance (i.e. polyphase rifting) during the onset of convergence by reactivating the most distal and weak part of the rift systems (i.e. serpentinized mantle). However, whereas in the Central section two plates (i.e. Iberia and Europe) were involved during the compression resulting in the classical double wedge fold and thrust belt. In the Western section, an intraplate orogenic evolution is observed involving only the Iberian plate. Thus, the understanding of the nature and distribution of decoupling levels in the system is fundamental to reconstruct the structural evolution during the formation and reactivation of a hyperextended system.

Keywords: rift-inheritance, hyperextended rift system, multistage, polyphase, reactivation, Basque – Cantabrian Pyrenees, thin- vs thick-skin

1.1. INTRODUCTION

The Cantabrian-Pyrenean orogenic system has been used by the Earth Science community during decades as a natural laboratory. This is mainly thanks to the dense available data sets including geological, geophysical and geochemical data (Choukroune & ECORS Team 1989; Pous et al., 1995; Fernández-Viejo et al., 2000; Pedreira et al., 2003, 2007; Roca et al., 2011; Díaz et al., 2012; Carola et al., 2015; Chevrot et al., 2015; Fillon et al., 2016; Ruiz et al., 2017; Teixell et al., 2018; Wher et al., 2018; among many others) as well as the good outcrop conditions and easy accessibility. Ground-breaking studies focused on orogenic processes at the Pyrenees s.s. where the archetypal orogenic architecture of the fold and thrust belt has been defined (e.g. Choukroune & ECORS Team 1989; Muñoz, 1992; Beaumont et al., 2000; Campanyà et al., 2012, 2018; Mouthereau et al., 2014; Teixell et al., 2016; Chevrot et al., 2018; Muñoz et al., 2018). However, other studies addressed the orogenic architecture of the westward continuation of the Pyrenean belt to the Basque – Cantabrian Pyrenees (e.g. Quintana et al., 2015; Pedrera et al., 2017; García-Senz et al., 2019) and the Asturian Massif (e.g. Pulgar et al., 1996, 1999; Alonso et al., 1996, 2007; Teixell et al., 2018) (Fig. 1.1). More recent research, however, focused on the rift evolution preceding the Alpine orogeny and the inversion mechanisms (e.g. Jammes et al., 2009; Tugend et al., 2014a; Pedreira et al., 2015; Pedrera et al., 2017; DeFelipe et al., 2017, 2018; Gómez-Romeu et al., 2019; Ducoux et al., 2019; Lescoutre, 2019).

The Basque – Cantabrian Pyrenees, in between the Asturian Massif and the Pyrenees s.s. have been historically referred as the Basque – Cantabrian Basin or Basque-Cantabrian Zone in the literature (see Miró et al., 2020 for a revision of terminology). Here we use this term to refer to the Mesozoic extensional basin that was subsequently inverted and incorporated in the Basque – Cantabrian Pyrenees. The area has been intensively explored for hydrocarbon purposes from the 60's to the 90's, leading to the acquisition of a vast amount of commercial seismic reflection and drill hole data. Being one of the most imaged orogenic systems worldwide, this area becomes a valuable field example to study the evolution of a hyperextended rift system and the role of rift inheritance during the subsequent reactivation and incorporation into orogenic belts, as it has been addressed on the Pyrenees s.s. and on the Alps (Vergés & García-Senz, 2001; Mohn et al., 2012; Tugend et al., 2014a, 2015; Masini et al., 2014; Teixell et al., 2018). However, many questions remain concerning the role of the Mesozoic rift template during reactivation and formation of the

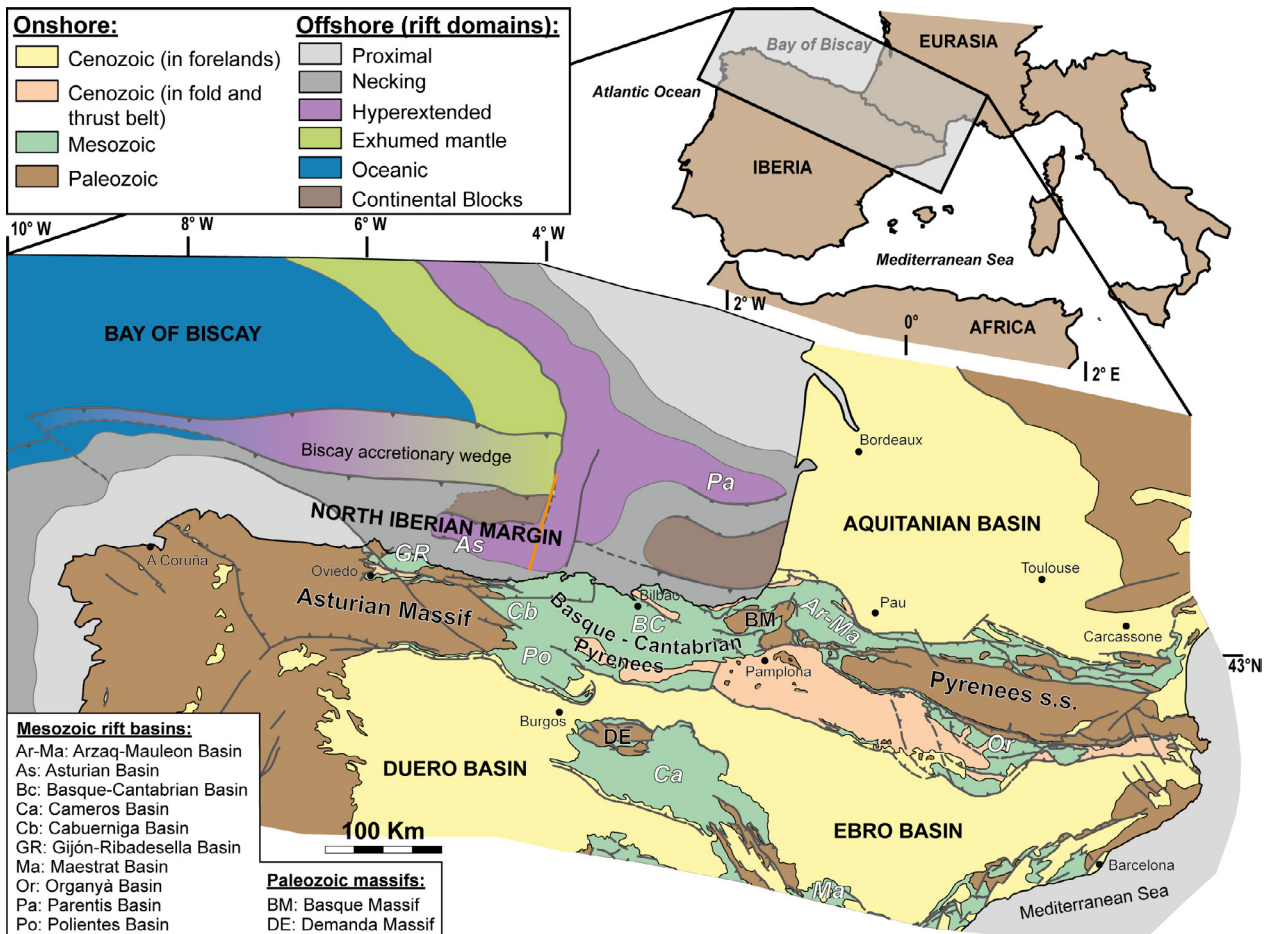


Figure 1.6 : Onshore a structural map of the Pyrenees and surrounding areas with the main terminology used in this work (modified from Carola et al., 2013). The offshore geology is represented by the rift domains (from Tugend et al., 2014 and Cadenas et al., 2018). Mesozoic rift basins are labelled in white and the orange line shows the position of the seismic line CS-146 modified in this work.

Basque – Cantabrian Pyrenees. Key questions are related to the nature and distribution of decoupling levels and buttresses inherited from the rift evolution and how they control the temporal and spatial evolution of deformation during reactivation.

Previous studies focused on a central geological cross-section to explain the evolution and architecture of the Basque – Cantabrian Pyrenees (e.g. Quintana et al., 2015; Pedrera et al., 2017). In this work we present a reinterpreted central cross-section integrating new and existing geological and geophysical data. Moreover, we introduce a new cross-section at the western termination of the Basque – Cantabrian Pyrenees that enables to characterize and discuss different style and stages of the formation and reactivation of a multistage rift system. The aim of the study is therefore twofold: 1) propose a new interpretation for the Basque – Cantabrian Pyrenees, and 2) decipher the role of the rift template and the mechanisms of the initial reactivation of a hyperextended domain.

1.1.1. FROM RIFT BASINS TO RIFT SYSTEMS: CONCEPTS AND TERMINOLOGY

In the literature, the Basque – Cantabrian Basin has been explained by using three different models of rift basins (Fig. 1.2a): 1) a strike slip transtensional basin model (Garcia-Mondejar 1989; Garcia-Mondejar et al., 1996), 2) a classical Low- β extensional basin model (Quintana, 2012; Quintana et al., 2015; Cámara, 2017), or 3) a hyperextension, high- β extensional basin model (Pedrera et al., 2017; Garcia-Senz et al., 2019). In this work we address the study of the inherited rift structures using the concept of multistage and polyphase rift systems, rather than using a monophasic basin model.

Each of the previous proposed rift basin models and its characteristic architecture and evolution have been defined in the North Iberian-Bay of Biscay rift system: 1) Low- β extensional rift basins, such as the Triassic Gijón-Ribadesella rift system (Fig. 1.1) (Cadenas et al. 2020), are bounded by listric or planar major extensional faults that control the creation of accommodation space (Fig. 1.2a). The syn-tectonic sequence usually thickens towards the bounding fault with the main depocenter remaining near the major fault. It develops a rollover anticline if the faults are listric. The footwall preserves the pre-rift sequence and may experience a flexural response generating some relief. Crustal thinning related to such classical extensional basins is explained by stretching and minor distributed ductile thinning but is, at the scale of the crust, low ($\beta < 1.5$). 2) Transtensional basins related to strike-slip faults (i.e. transtensional settings), such as the Late Jurassic-Early Cretaceous Asturian Basin (Fig. 1.1) (Cadenas et al. 2020), which are narrow, deep and lozenge shaped basins limited by subvertical faults. 3) Hyperextended (high- β) basins, floored by crust thinner than 10km and/or exhumed mantle (see Tugend et al., 2014b for detailed explanation). In such basins, the footwall is made of exhumed lower crust or mantle and the hanging wall consists of extensional allochthons and/or syn-kinematic sediments and the main depocenter is migrating in an opposite sense of exhumation, forming downward wedging sequences (e.g. Gillard et al. 2015). However, such basins evolve from initial stages of low- β basins.

In contrast to simple mono-phase basin models, recent studies revealed that rift systems evolve through either different phases and/or different stages (Fig. 1.2b). A polyphase rift system as used in this study is a concept developed by Lavier & Manatschal (2006), which has been extensively used in the rifting community. This concept is defined as a rift system that follows an evolution described by different phases, referred to as stretching, thinning, hyperextension, exhumation and sea-floor spreading (Péron-Pinvidic & Manatschal,

Reactivation of a hyperextended rift system: the Basque-Cantabrian Pyrenees case

2009). These phases result from a continuous strain localization following the same kinematic framework. In contrast, multistage rift systems result from the superposition of distinct rift systems generated at different time within a different kinematic framework (Cadenas et al., 2020). In a multistage rift system, the different rift events can be either mono or polyphase, but most important, they can be aborted and overprinted by new rift events. The complexity of multistage rift system, therefore, is minimal if the overprinting systems are monophasic, but can be significant if the overprinting systems are polyphase. In such cases, thick, earlier syn-rift sequences may be pre-rift to a later rift stage, creating complexities that are difficult to capture and argue when looking locally and not describing the systems at a larger scale. Thus, recognising and mapping different rift stages as well as defining the maturity of each of these rift systems is key to unravel complex rift systems as those observed in the Basque-Cantabrian Pyrenees.

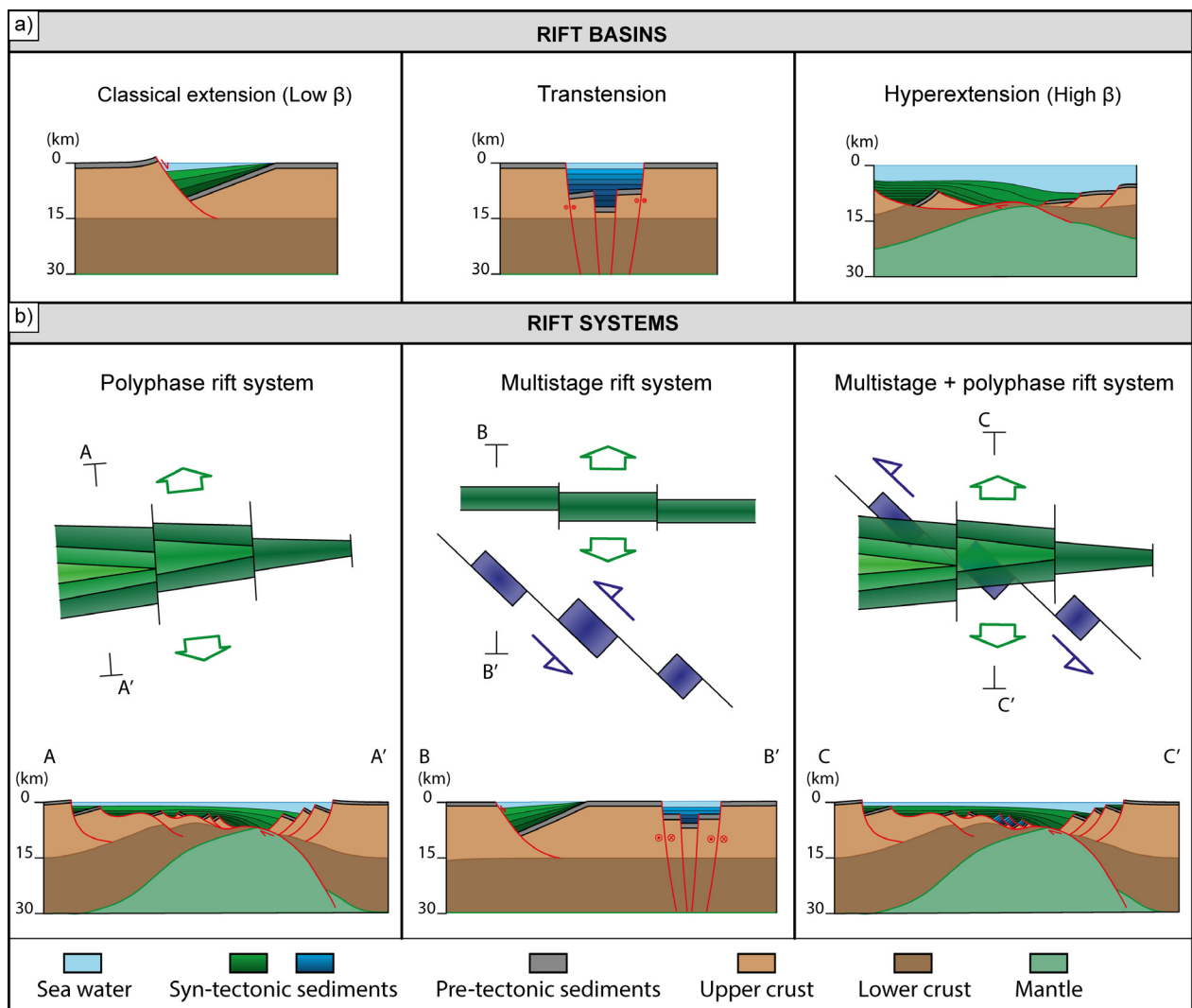


Figure 1.7 : a) Classification of extensional rift basins. b) Theoretical sketch showing the rift system variability (see the text for further details).

In this study we do not consider the Basque – Cantabrian Pyrenees as involving a single rift basin, but we define and map rift stages, define the kinematics and maturity of each stage and investigate the overprinting of later rift stages to previous ones. This approach enables to eventually define the rift template that is the result of the superposition of different rift stages and ultimately allow its role during reactivation to be investigated. In order to follow this new approach, we use the terminology introduced and developed by Sutra et al. (2013), Tugend et al. (2014a), and Cadenas et al. (2020) among others to explain the formation and evolution of the Mesozoic Basque – Cantabrian rift system.

1.2. GEOLOGICAL SETTING

The northern Iberian Peninsula experimented a complex tectonic evolution that started in the Paleozoic with the Variscan orogeny (Matte, 1991; Martínez-Catalán et al., 2007). From Permian to Cretaceous, the tectonic setting changed to a multistage extensional regime related to the opening of the Central and North Atlantic Ocean and the opening of the Bay of Biscay (Roest & Srivastava, 1991; Ziegler, 1988). After the Permian extensional collapse of the Variscan orogen, a first Triassic rift event resulted into rift basins surrounding the Paleozoic massifs (López-Gómez et al., 2019). The facies (i.e. shallow marine to subaerial) and thickness distribution of the Triassic succession suggest that during this event relatively minor accommodation space (i.e. crustal thinning) developed. It is important to note that the Late Jurassic – Early Cretaceous rift basins used partly the Triassic rift template (López-Gómez et al., 2019). However, as discussed below, the deposition of salt during the late stages of this Triassic event (i.e., Keuper) and its distribution, had a major control on the subsequent tectonic evolution of the study area (Carola et al., 2013; Muñoz, 2019). The second Late Jurassic to Early Cretaceous rift event resulted into the formation of NW- SE and W – E trending basins in the Pyrenean system (Tavani et al., 2018), and the development of NW – SE basins aligned along the southern limit of the Ebro Block (e.g. Cameros, Maestrat and Columbrets basins) (Salas et al., 2001). The third Aptian to Middle Cenomanian rift event led to the development of wide, E – W trending basins in the Pyrenean rift system (Jammes et al., 2009; Roca et al., 2011; Masini et al., 2014; Tugend et al., 2015; Lescoutre & Manatschal, 2020).

The Basque - Cantabrian Pyrenees include three Mesozoic basins (Figs. 1.1 and 1.3): (1) the Basque – Cantabrian Basin to the east, striking in a NW-SE direction for more than 100km and filled with a more than 12km thick Upper Jurassic to Middle Cenomanian succession (Brinkmann & Lögters, 1968). (2) The Polientes Basin to the south-west presents a more than 4km thick succession of Upper Jurassic to Middle Cenomanian sediments (Garcia de Cortazar & Pujalte, 1982; Pujalte, 1982). (3) The Cabuérniga Basin to the north-west includes

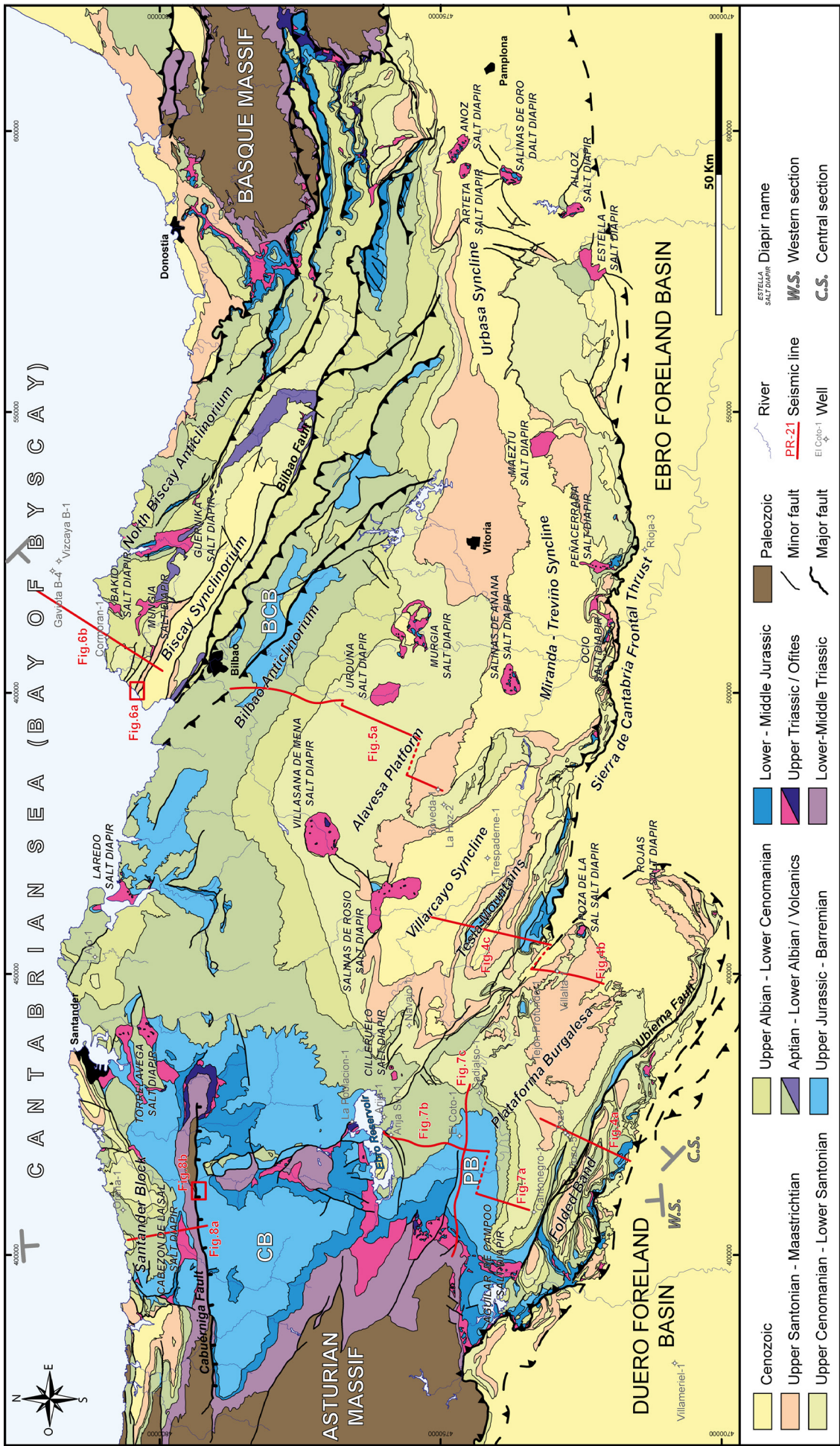


Figure 1.8 : Tectono-stratigraphic map of the Basque – Cantabrian Pyrenees and surroundings with the location of the different seismic line and wells shown in this work as well as the position of the Central and Western sections presented in this study (figures 11 and 12). BCB: Basque – Cantabrian Basin; CB: Cabuérniga Basin; PB: Polientes Basin.

an up to 3 km thick Upper Jurassic to Barremian succession and a thinner Aptian to Albian succession (Pujalte, 1979, 1981). The Cabuérniga Basin is bounded to the north by the so-called Santander Block (Robles et al., 2014). This block has been interpreted as a basement high during the Mesozoic evolution corroborated by the thin or even absent Jurassic to Lower Cretaceous sediments unconformably covered by a thin succession of Aptian to Oligocene sediments (Pujalte, 1979, 1981). Nevertheless, the southern Cabuérniga Basin was limited by the Reinosa/Ebro Reservoir area also interpreted as a high during Early Cretaceous between the Cabuérniga and the Polientes basins (Pujalte, 1982).

The lowermost Cretaceous successions in the previous basins are described by Pujalte (1989), Pujalte et al. (1996) and Robles et al. (1996). They consist of fluvio-lacustrine sediments with minor alluvial sediments interbedded. The Aptian-Albian succession is characterized by thick shallow carbonate platforms in the Cabuérniga Basin and surrounding the Basque-Cantabrian Basin, with facies changing to slope and deep marine sediments basinwards (García-Mondéjar & Robador, 1987; García-Mondéjar & Fernández-Mendiola, 1993). On the contrary, the Aptian-Albian facies observed in Polientes Basin to the south are mainly fluvial. In the Polientes and Cabuérniga basins, the Upper Jurassic to Lower Cretaceous infill progressively thins towards the W and NW and it unconformably overlies the Lower to Middle Jurassic rocks and the Triassic Bundsandstein sediments (García de Cortazar & Pujalte, 1982; Pujalte, 1982). The Paleozoic basement includes meta-sediments (Robles, 2004; Robles & Pujalte, 2004; Tavani et al., 2013) (Fig. 1.3). From the structural point of view, classical studies on the Cabuérniga – Polientes sector were done by Espina et al. (1994, 1996) interpreting a thick-skinned structural style with a N-S extension reactivating previous Variscan faults being subsequently used during compression. In the Basque – Cantabrian Basin, García-Mondéjar (1989) and García-Mondéjar et al. (1996) addressed the tectonic pattern during Middle Cretaceous times arguing for a strike slip evolution resulting in a transtensional basin. However, the most recent and complete studies addressing the entire Basque – Cantabrian Pyrenees and proposing a complete tectono-stratigraphic evolution for the area have been published by Quintana et al. (2015), Pedrera et al. (2017), García-Senz et al. (2019) and Cámara (2017) as referred in the introduction.

1.3. OBSERVATIONS IN THE BASQUE – CANTABRIAN PYRENEES: SEISMIC INTERPRETATIONS AND GEOLOGICAL CROSS SECTIONS

Field observations and the interpretation of commercial seismic reflection lines together with boreholes enable us to define the main stratigraphic and structural features of the

studied zone. We organize the description from south to north of the two regional sections: one first section crossing the central Basque – Cantabrian Pyrenees and a second crossing through the western termination of the area (Fig. 1.3).

1.3.1. CENTRAL BASQUE – CANTABRIAN PYRENEES

The SW – NE oriented Central section runs from the Duero foreland basin in the south to the offshore Landes High in the north (Fig. 1.3). The interpretation of this section resulted in long-lasting debates (e.g. Pedrera et al., 2017 and 2018; Pedreira et al., 2018; Muñoz, 2019) dealing with the rift architecture, high magnetic and gravimetric anomalies flooring the Bilbao Anticlinorium and the reactivation of the area. In this chapter, we present new observations including field, seismic reflection and borehole observations to propose a new interpretation of the Central section.

A south-directed frontal thrust delineates the southern limit of the Basque – Cantabrian Pyrenees. This structure is detached on the Triassic salt and thrust a thin Jurassic to Cretaceous succession on top of the flat Cenozoic sediments of the Duero foreland basin (Fig. 1.4a). Underlying this succession, a thin Upper Albian to Cenomanian detrital package is documented on top of the Palaeozoic basement drilled by the San Pedro borehole to the south (see Carola et al., 2015 for details). In the seismic sections, the contact between the Meso-Cenozoic sedimentary cover and the Paleozoic basement is determined by an interface between the strong reflections of the above sedimentary succession and the chaotic facies characteristic of the Paleozoic basement, which is slightly tilted to the north (Fig. 1.4a). The Villameriel-1 and the Rioja-3 wells (Fig. 1.3) drilled this contact supporting the interpretation.

The Folded Band, which spreads between the frontal thrust and the Ubierna Fault, presents a thin stratigraphic succession on top of a thick Upper Triassic salt unit and is affected by small imbricates resulting from the inversion of extensional faults (Figs. 1.3 and 1.4a). To the north, the so-called Burgalesa Platform is interpreted as an allochthonous unit where a thick Mesozoic succession is transported to the south-east over the Late Triassic salt, becoming a salt-detached domain oblique to the main Pyrenean trend, describing a salient (Fig. 1.3) (see Carola et al., 2015 for a detailed description of this domain). In the northern edge of this salient, a repetition of Lower Jurassic to Barremian shallow marine successions, which were drilled by the Tejón-Profundo-1 and the Villalta-1 boreholes, detaches on the Upper Triassic salt, overlaid by upper Albian detrital sediments (Fig. 1.4b). The link between the Burgalesa Platform and the Sierra de Cantabria Frontal Thrust (SCFT) is an area of debate due to the

Tertiary sediments outcropping in the field and limiting direct observations in the area and a different interpretation has been proposed (Hernaiz et al., 1994; Cañas et al., 1994).

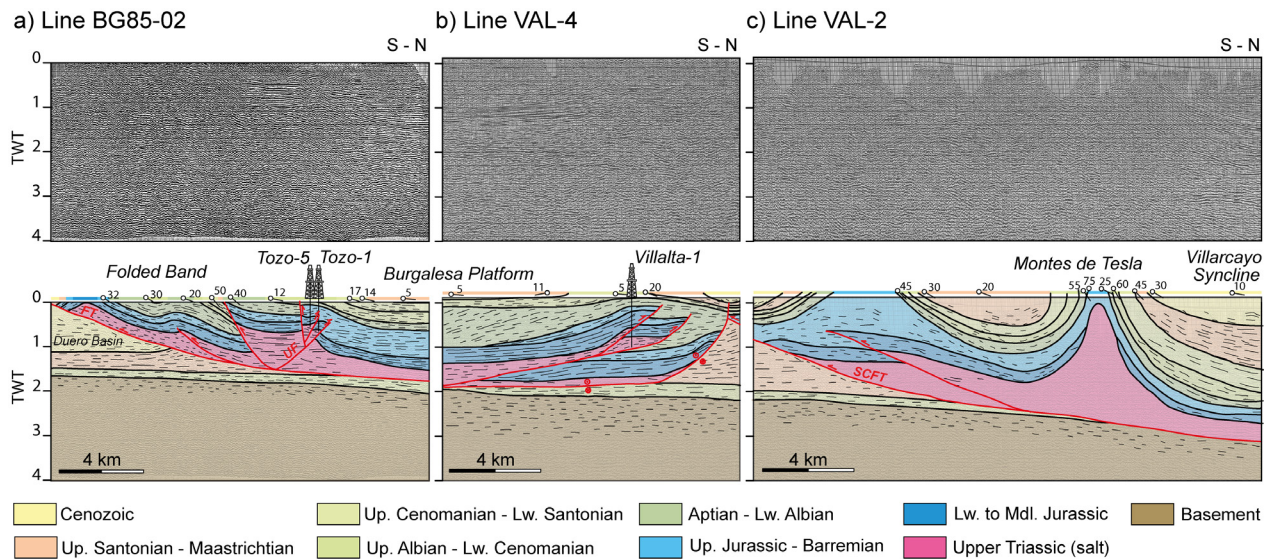


Figure 1.9 : N-S seismic sections in the (a) Folded Band, (b) Burgalesa Platform and (c) Sierra de Cantabria Frontal Thrusts - Montes de Tesla areas with the projection of Tozo and Villalta wells as well as the field data and outcropping units showing the structure of the southern Central section. FT: frontal thrust; UF: Ubierna Fault; SCFT: Sierra de Cantabria Frontal Thrust. See Fig. 3 for location.

However, the seismic section VAL-4 (Fig. 1.4b) shows the northern limit of the Burgalesa Platform unit with reflectors tilted to the south whereas right to the north the reflectors are flat. In between, a steeply dipping transpressional fault with a SE displacement of the hanging wall (i.e. Burgalesa Platform) is interpreted truncating the south directed SCFT, as documented in the next VAL-2 seismic line (Fig. 1.4c). The SCFT is a major feature continuous all along the southern border of the Basque – Cantabrian Pyrenees (Fig. 1.3). It is detached into the Upper Triassic salt, bringing the Mesozoic succession of the Basque – Cantabrian Basin on top of the Cenozoic sediments of Duero and Ebro foreland basins. The underlying basement is slightly tilted to the north beneath the SCFT, an inherent feature of foreland basins in front of thin-skinned fold and thrust belts [e.g. Canadian Rockies (Bally et al., 1966); Bolivian Andes (McQuarrie et al., 2005)] (Fig. 1.4c). Salt structures can be observed both to the south [i.e. Montes de Tesla area (Fig. 1.4c)] and to the north where diapirs developed (e.g. Salinas de Rosio, Fig. 1.3). The Navajo-1 well drilled more than 2.500 m of Late Triassic evaporites few kilometres to the west of Montes de Tesla structure before reaching top basement at 3.940m. The Montes de Tesla salt wall, fold the thin sedimentary succession on top up to vertical and even locally overturned positions and it constitutes the southern limb of the Villarcayo Syncline (Fig. 1.4c), which is cored by a thick synorogenic succession more than 2.600 m thick, drilled by the Trespaderne-1 borehole. The Villarcayo Syncline represents the western continuation of the Miranda – Treviño and Urbasa synclines, a continuous synform for more than hundred kilometres parallel to the SCFT

(Fig. 1.3). The northern limb of the Villarcayo Syncline is also determined by a salt inflated area represented at surface by the Salinas de Rosio and the Salinas de Añana salt diapir lineament (Fig. 1.3). The La Hoz-2 borehole drilled more than 1.600m of Upper Triassic evaporites in this position. A flatten area corresponding to the so-called Alavesa Platform, is observed following the section to the north between the previous diapir lineation and the salt wall described by Villasana de Mena – Orduña – Murgia salt diapirs at surface, which limit the Bilbao Anticlinorium to the south (Fig. 1.3).

The Bilbao Anticlinorium to the north, involves the thick sedimentary succession of the Basque – Cantabrian Basin. Fig. 1.5 shows the final distribution of depocenters corresponding to Upper Jurassic to Barremian, Aptian to Middle Albian and Upper Albian to Middle Cenomanian extensional phases, which are shifted progressively to the south-west (Fig. 1.5a). The Upper Jurassic to Barremian succession is made of more than 4.000m of shales and siliciclastic sandstones (Quintana, 2012), as the base of the unit is not cropping out, and it shows a narrow distribution near the Bilbao Fault along tens of kilometres in a NW – SE direction (Fig. 1.5b). The Aptian – Middle Albian is wider to the south, with thickness estimated about 6.000m (Quintana, 2012) but made of deep marine marls with few carbonate platforms isolated. The Upper Albian to Lower Cenomanian is the one reaching more southern latitudes and being thinner than the previous but with deep marine facies. Finally, the Upper Cenomanian to Lower Santonian sediments show a facies change in the Alavesa Platform from a bioclastic carbonate platform (prominent and characteristic in the landscape) distributed to the south into a slope facies and deep marine sediments to the north in the Bilbao Anticlinorium.

The northern limb of the Bilbao Anticlinorium corresponds to a highly deformed area and involves three main north vergent thrust sheets (Fig. 1.3), which are from south to north: the Villaro, the Mondragon and the Durango slices (see Abalos et al., 2008 for further details on this area). The northern limit of the Bilbao Anticlinorium is characterized by the Bilbao Fault, a NW – SE continuous structure all along the Basque – Cantabrian Basin poorly imaged in seismic data (Fig. 1.3). Immediately to the north of the Bilbao Fault, the tight Biscay Syncline includes a thick Late Cretaceous to Cenozoic syn-orogenic succession. At its northern edge, it shows a fault system characterized by steep faults and squeezed salt structures, as the one interpreted in the Sopela beach (Fig. 1.6a). Northward, the North Biscay Anticlinorium is observed at surface. It includes two stacks of Aptian to Cenomanian allochthonous units overlying a thin autochthonous succession of middle Cenomanian clastic sediments laying on top of the Palaeozoic basement at 3.300m, which were drilled by the borehole Cormorán-1. Offshore, the Gaviota B-4 and Vizcaya B-1 boreholes drilled

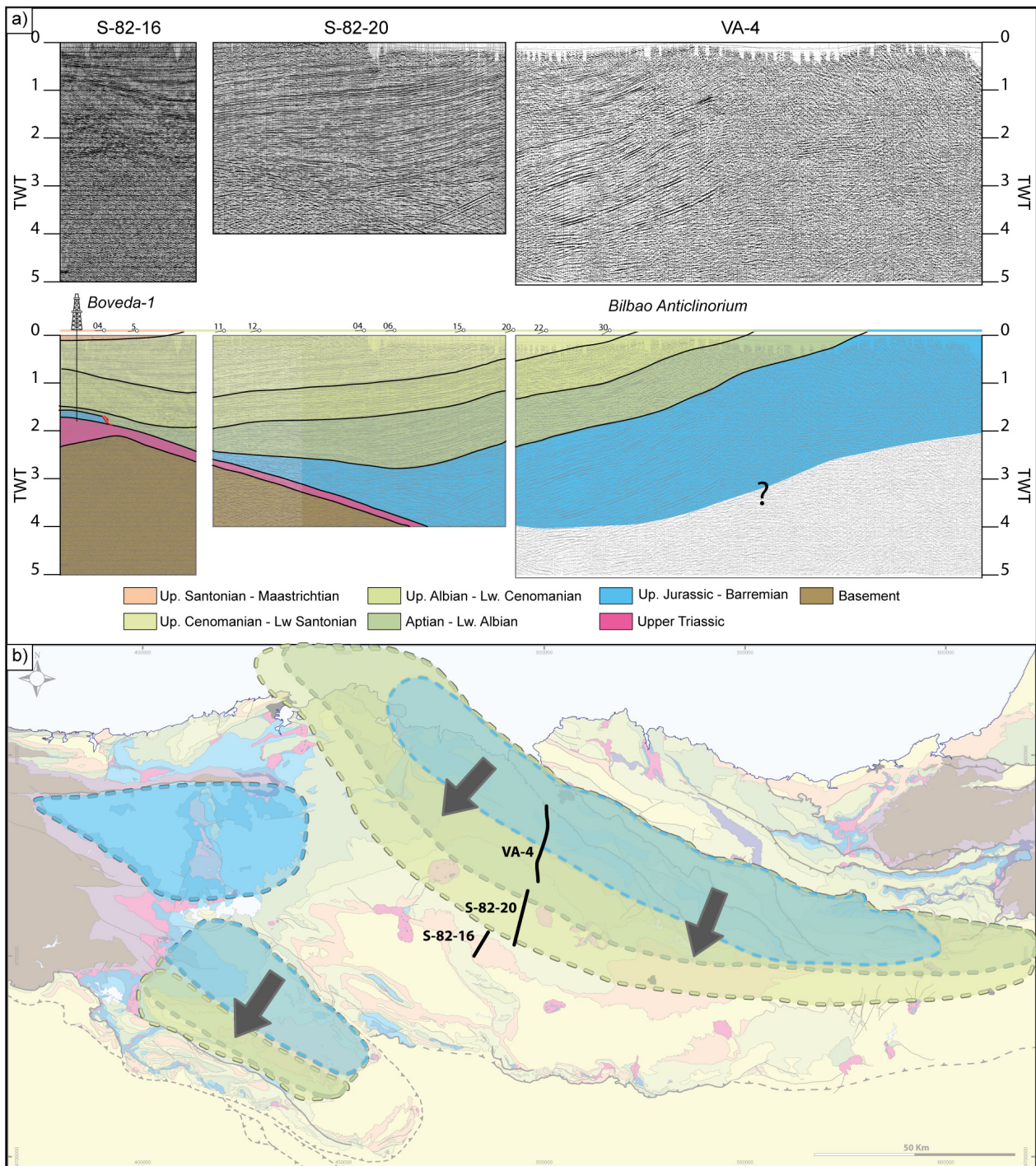


Figure 1.10 : a) N-S seismic section in the Alavesa Platform and Bilbao Anticlinorium areas showing the overlapping of Mesozoic syn-rift depocenters shifting to the south. See Fig. 3 and b) for location. b) Map of the different Mesozoic syn-rift depocenters of more than 2 km thick in the Basque – Cantabrian Pyrenees build from seismic interpretation and field observations. See colour legend in Fig. 5a

the basement at around 3.000m depth and an overlying sedimentary sequence including a thin Upper Albian to Middle Cenomanian syn-rift clastic succession and a thicker Upper Santonian to Oligocene syn-orogenic succession above (Fig. 1.6b).

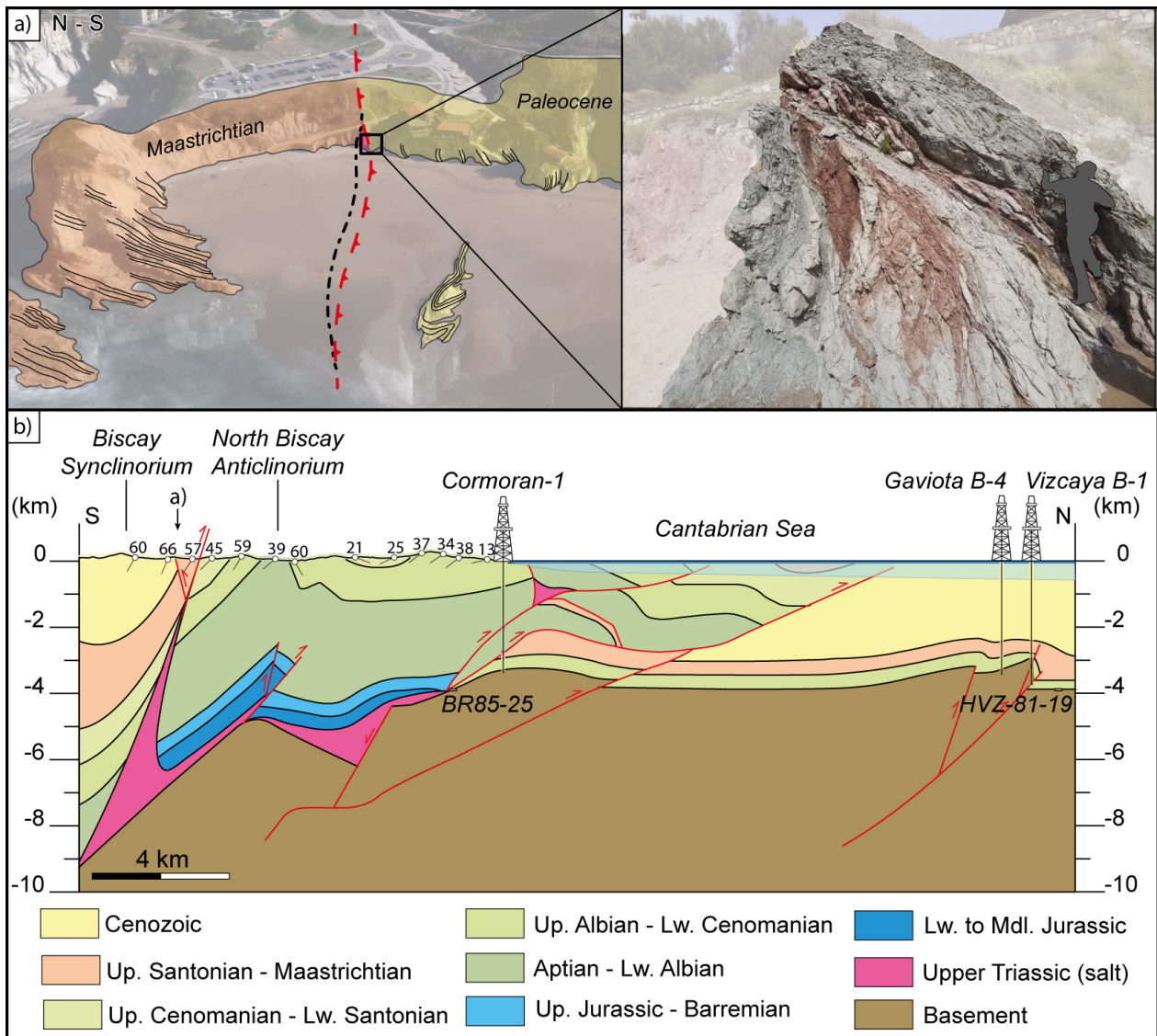


Figure 1.11 : a) Aerial photograph from the Sopela beach with the interpretation of the thrust weld and a field image of the detailed weld with the characteristic shear deformation. See location in Fig. 3 and b). b) Geological cross section in the northern Central section modified from Roca et al., subm. with the integration of field data, observations coming from BR85-25 and HZV-81-19 interpreted seismic lines and the projections of Cormoran-1, Gaviota B-a and Vizcaya B-1 boreholes.

1.3.2. WESTERN BASQUE – CANTABRIAN PYRENEES

The Western section runs from the onshore Duero foreland basin in the south to the Bay of Biscay in the north (Fig. 1.3). In this study we present a new interpretation of the onshore segment, whereas for the offshore segment we based on a depth conversion of the CS01-146 section described by Cadenas et al. (2020) (see location in Fig. 1.1).

The southern limit of the Basque – Cantabrian Pyrenees as well as the Folded Band area display a similar structure as the Central section and therefore it is not addressed in detail here. Nevertheless, from the Ubierna Fault to the north the structure changes significantly. The Western section shows the inverted Polientes Basin, where the Upper Jurassic to

Lower Albian sediments describe a migration of the depocenters towards the south. These sediments onlap a Lower to Middle Jurassic unit, which detaches on the Triassic salt and thickens slightly towards the north (Fig. 1.7a and b). These are typical characteristics of salt detached basins (Roma et al., 2018b).

The reactivation of the Polientes Basin is observed at surface as an anticline of the Upper Jurassic to Middle Albian sediments but cored at depth by basement rocks, as the E-W PR-21 seismic line shows where the Cadialso-1 well drilled this contact (Fig. 1.7c). In the southern Polientes Basin, a thin package of reflectors corresponding to the Upper Albian to Middle Cenomanian clastic sediments unconformably overlaying the Upper Jurassic to Middle Albian depocenters show an erosional unconformity (Figs. 1.3 and 1.7a). The northern limit of the Polientes Basin is an area where both reactivation of basement faults and salt structures are observed (Fig. 1.3). The Cilleruelo diapir crops out at surface (García-Mondéjar, 1982) and diapir contacts were drilled by the Arija-1 and La Poblacion-1 boreholes (Figs. 1.3 and 1.7b).

North of the Ebro Reservoir, the Cabuérniga Basin includes up to 900 m of Lower to Middle Jurassic carbonates and up to 3000 m of Upper Jurassic to Barremian fluvial and lacustrine sediments. Few small outcrops made of Aptian carbonate platforms are preserved to the east of the basin (Fig. 1.3). The Cabuérniga Basin is affected by gently

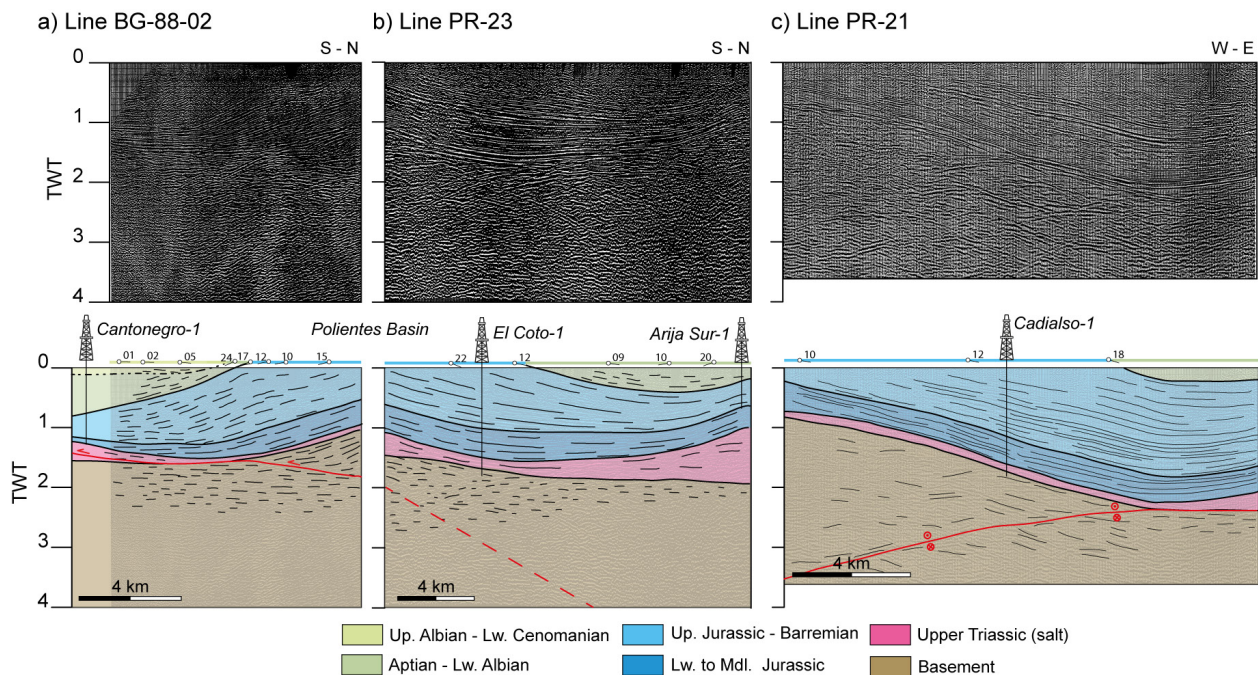


Figure 1.12 : N-S seismic sections (a and b) and E-W seismic section (c) in the Polientes Mesozoic Basin with the projection of the Cantenegro-1, El Coto-1 and Cadialso-1 boreholes and the surface data and geology. The E-W (c) section shows the thick- to thin-skin transition in the Western Basque – Cantabrian Pyrenees and the plunge observed in the sediments at surface controlled by the basement at depth. See Fig. 3 for location.

large-scale folds and no evidence of salt have been observed in the western Cabuérniga Basin. Still, some outcrops of evaporites next to the poorly understood N-S Besaya structure (also called Pas) are observed to the east of Cabuérniga Basin (Fig. 1.3).

The Cabuérniga Fault bounds the basin northwards. This fault trends in E-W direction and is a more than 50km continuous structure (Figs. 1.3 and 1.8). The hanging wall corresponds to the Lower Cretaceous succession described before whereas in the footwall, the Palaeozoic and Lower Triassic rocks crop out at the Sierra de Cabuérniga and the Santander Block (Fig. 1.8). This area, to the north, is characterized by a thin Mesozoic stratigraphic succession including Triassic evaporites to the east and an overlying Lower Jurassic to Cenozoic succession. Salt structures such as Cabezón de la Sal and Torrelavega salt diapirs but also thrusts and salt-core anticlines are observed in the Santander Block (Figs. 1.3 and 1.8a).

The area north of the Santander Block corresponds to the offshore part of the section, which has been modified from the interpretation done by Cadenas et al. (2020) (CS01-146 section). However, the seismic line interpreted by the previous authors is in time and therefore a depth conversion was applied by using $V_z = V_0 + k \cdot z$ where: V_0 is 1.75 Km/s (i.e. water velocity) and k is 0.4 according to reference values from Van Dalfsen et al. (2006).

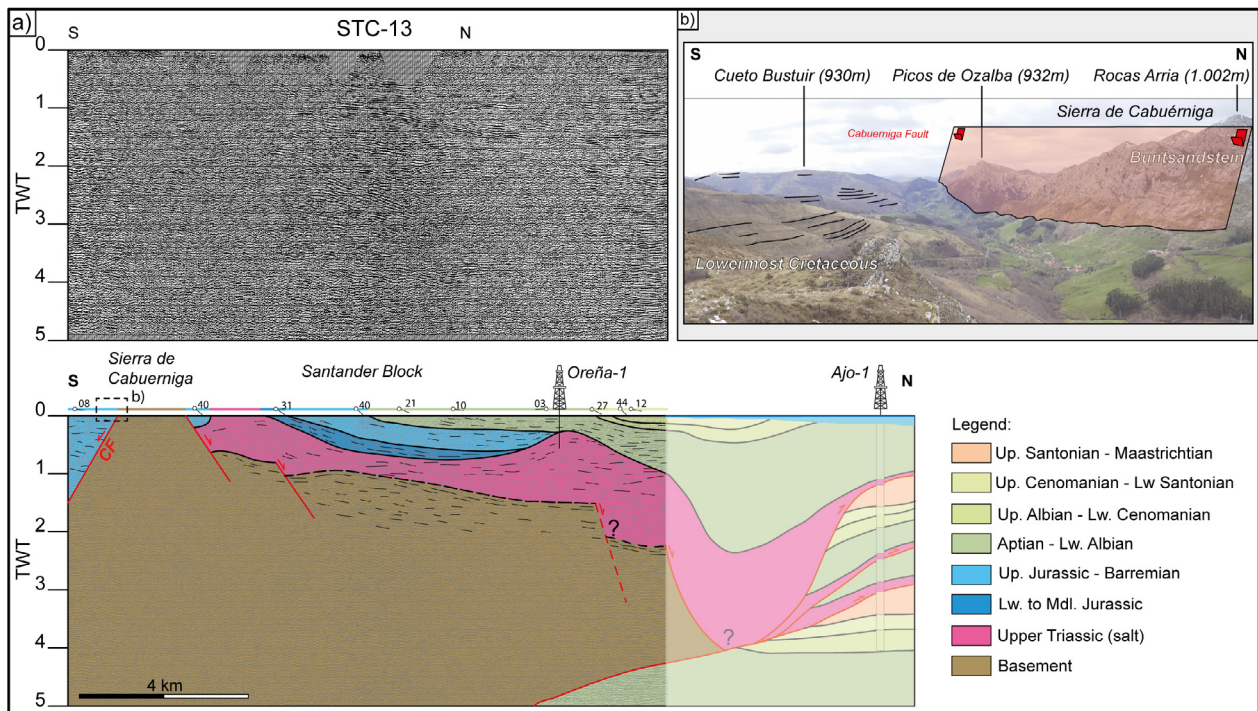


Figure 1.13 : a) N-S seismic section in the Santander Block area with the projection of the field data and surface geology as well as the Oreña-1 borehole and the Ajo-1 borehole to link the onshore with the offshore sections. CB: Cabuérniga Fault. b) Field image of the northern limit of the Cabuérniga Basin with the view to the Cabuérniga Fault. See location in Fig. 3.

Some onshore observations are fundamental for the onshore-offshore link. The Ajo-1 borehole, located near the Ajo Cape few kilometres to the east of the Western section (Fig. 1.3), drilled three repetitions of Aptian-Albian succession with Upper Triassic salt in between, and the basement was not reached at the base of that well (4.970m). Thus, an important omission of stratigraphy is recorded from Lower Jurassic to Barremian in this area. Onshore, a thin but complete Lower Cretaceous succession overlies Jurassic sediments. Offshore, more than 1.300 m thick succession of Aptian to Cenomanian sediments can be observed (Fig. 1.8a). Therefore, considering the previous observations and the thinning of the crust reported to the north in the Bay of Biscay where mantle was exhumed (Cadenas et al., 2020), a set of extensional faults dipping to the north is interpreted thinning the crust and showing tilted blocks towards the south (Fig. 1.9). Moreover, some north directed thrusts are interpreted cutting the extensional blocks.

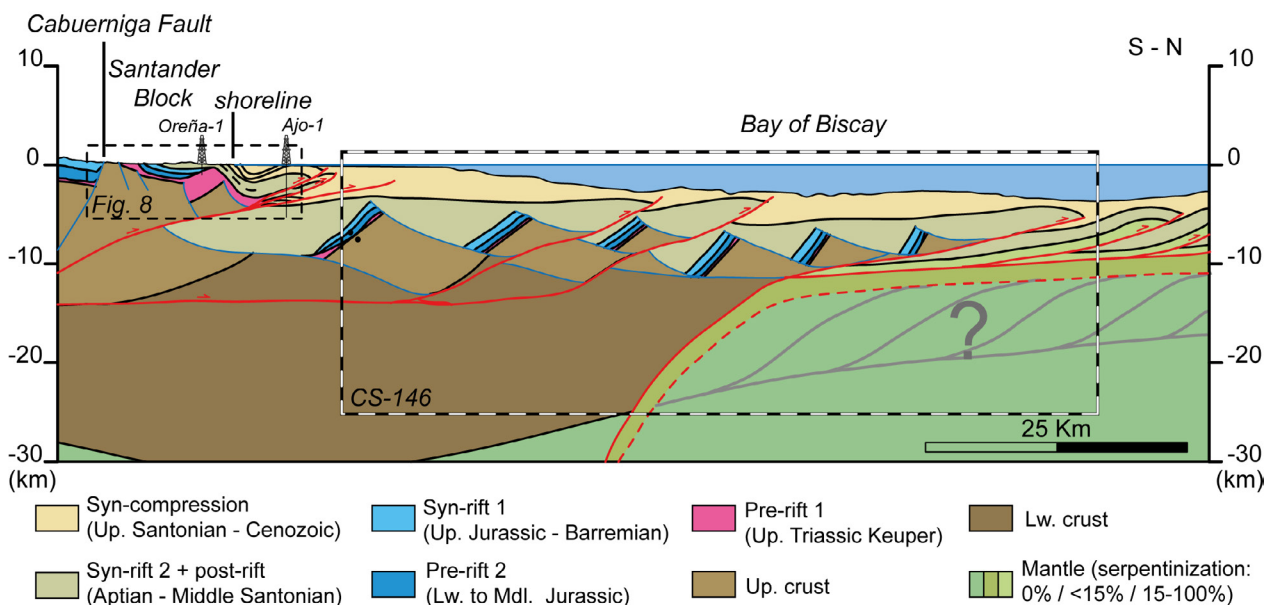


Figure 1.14 : Northern part of the Western section combining the STC-13 seismic line (Fig. 8) and a modified depth converted interpretation from the CS-146 seismic line of Cadenas et al. (2020). See Figs. 1 and 3 for location.

1.4. CRUSTAL ARCHITECTURE: GEOPHYSICAL CONSTRAINTS

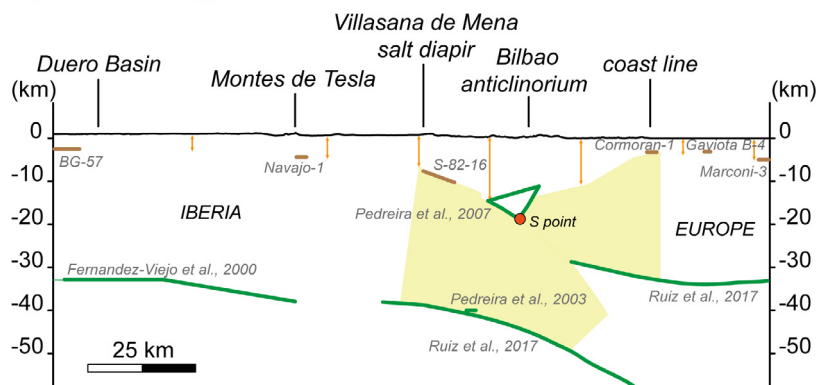
In this section we summarize the main geophysical constraints defining the crustal architecture of the area based on published seismic reflection data and velocity models (e.g. Fernández-Viejo et al., 2000; Pedreira et al., 2003 and Ruiz et al., 2017).

1.4.1. CENTRAL SECTION

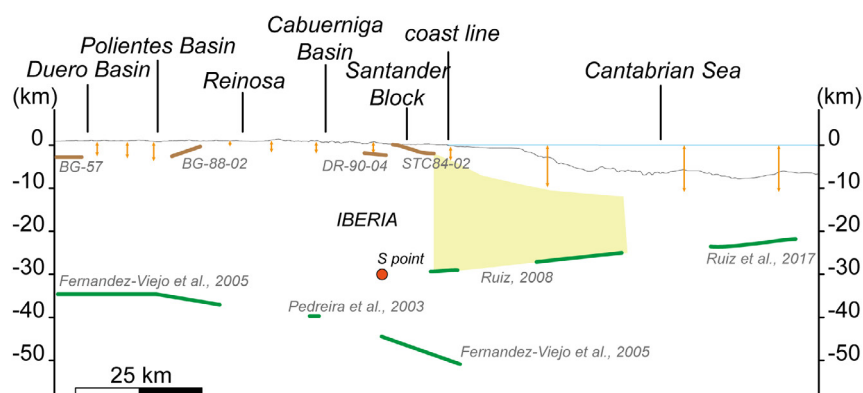
In the Central section (Fig. 1.10a), the Iberian crust to the south shows top basement slightly tilted to the north as described previously and a crustal thickness of about 30km

from the Duero basin until the lineament described by the Villasana de Mena – Urduña – Murgia salt diapirs (Fernández-Viejo et al., 2000) (Fig. 1.3). Further north, top basement is significantly tilted towards the north whereas the base of the crust follows a similar trend as southwards, indicating a thinning of the crust. To the north, two Moho surfaces have been interpreted showing the Iberian Moho beneath the European one (Ruiz et al., 2017). Although top basement cannot be imaged, the thickening of the sedimentary succession described in the Bilbao Anticlinorium implies that the remaining crust must be considerably thinned along the underthrust slab (i.e. necking domain). In contrast, the European crust shows its base at around 30km depth northward the Bilbao anticlinorium and continues to the north at a similar depth (Ruiz et al., 2017). The top basement in the European crust is reported by the Cormoran-1, Gaviota B-4, and Vizcaya B-1 boreholes between 3.000 and 3.500m depth. This defines a normal crustal thickness (i.e. 30km) to the north. Further south, the lack of evidence makes it difficult to locate the top basement beneath the Biscay Sinclinorium. However, the significant stratigraphic thickness reported in the literature (Meschede, 1987) also suggests a crustal thinning (i.e. necking domain).

a) Central segment



b) Western segment



Legend: — Moho / interpreted | Accomodation space
— Basement / interpreted ■ Necking domain

Figure 1.15 : Compiling of the published geophysical data along the central section (a) and Western section (b) coming from seismic, borehole and refraction data.

1.4.2. WESTERN SECTION

On the Western section (Fig. 1.10b), the southern part shows also a 30km thick Iberian crust beneath the Duero Basin. Both top basement and the base of the crust are slightly tilted to the north underneath the frontal structure and the Polientes Basin (Fernández-Viejo & Gallastegui., 2005). However, while the top basement is around 1 to 3 km depth in the Reinosa area as well as in Cabuérniga Basin, the base of the crust is going down to ~45km depth towards the north, beneath the Santander Block. Thus, a thickening of the crust from ~30km to more than 40km occurred in this area. On the contrary, in the Santander Block, the top basement is outcropping to the south and interpreted at 2km of depth to the north whereas the base of the crust is at 25km depth (Ruiz, 2007). Even a thinner Iberian crust is observed further north with a top basement interpreted down to 6 – 8 km depth (Fig. 1.9) whereas the base of the crust is depicted at almost 20km (Ruiz et al., 2017). Therefore, the present-day architecture of the northern Western section still preserves a crustal structure strongly inherited from the extensional period, despite the Alpine reactivation.

1.5. DISCUSSION

1.5.1. PRESENT-DAY ARCHITECTURE OF THE BASQUE – CANTABRIAN PYRENEES

Geological and geophysical observations presented above enable us to construct two complete crustal-scale sections and therefore to define the present-day crustal structure of the studied area. Substantial differences can be observed comparing both sections at a basin as well as at a crustal scale. While the Central section preserves a mature orogenic architecture, the Western section exhibits embryonic stages of the reactivation of a rifted margin. Comparing and understanding the link between the two sections is fundamental for the restoration of the Basque – Cantabrian rift template and its importance in controlling the reactivation.

Central section

In the Central section (Fig. 1.11a) two plates can be distinguished: the Iberian/Ebro plate to the south and the European plate to the north. A first order observation is the inter-wedging of the Iberian and the European Moho surfaces (Pedreira et al., 2007, 2015; Roca et al., 2011; Muñoz, 2019). The singular point [i.e. S-point corresponding to a point which delimits the pro-wedge to the south from the retro-wedge to the north (Willet et al., 1993; Jamieson & Beaumont, 2013)] is interpreted underneath the Bilbao Anticlinorium, at about 17km depth (Figs 1.10 and 1.11a). Southward of this point/line, south-vergent

structures predominate in the pro-wedge, whereas the retro-wedge is characterized by north-vergent structures. The European crust (i.e. retro-wedge crust) displays a thinning from north to south from a normal crustal thickness (i.e. 30km) beneath the Landes High to about 20 km to the south under the Biscay Synclinorium (Fig. 1.11). On the contrary, the Iberian crust (i.e. pro-wedge crust) thins from 30km beneath the Duero foreland basin to less than 10km in the underthrust slab (Fig. 1.11a). No intra-crustal contractional features are observed so far in the Iberian crust, whereas the European crust displays basement-involved contractional structures that have been interpreted to be decoupled in a mid-crustal detachment (Fig. 1.11a). On top, the allochthonous sedimentary cover is detached into the Upper Triassic salt level. We deduce, therefore, a relative displacement of the Basque – Cantabrian Basin of 35 km towards the south over the Duero foreland basin (Fig. 1.11a) showing well described faults and related fold structures (i.e. Bilbao Anticlinorium).

The salt structures corresponding to distal domains in the pro-wedge were transported passively with the sedimentary cover to the south. The preservation of the shape and morphology of diapirs at a map scale indicate minor or non-reactivation. In contrast, the salt structures located near the thrust front and the ones located in the retro-wedge were reactivated and squeezed during contractional deformation (e.g. weld observed in Sopela beach, Fig. 1.6a).

A high magnetic and gravimetric anomaly is observed beneath the Bilbao Anticlinorium, where the S-point is located, which has been interpreted as a body of intrusive rocks (Aller & Zeyen, 1996) or lower crustal rocks (Pedreira et al., 2007 and Quintana et al., 2015). Nevertheless, recent studies addressing the eastern Basque – Cantabrian Basin (DeFelipe et al., 2018; Ducoux et al., 2019; Lagabrielle et al., 2020) and surrounding basins such as Mauleón Basin (Jammes et al., 2009; Masini et al., 2014) have documented evidence of mantle exhumation in the distal parts of those basins. Therefore, and consistent with the previously mentioned studies, we suggest that this positive gravimetric anomaly results from a serpentinized mantle body exhumed during extension and captured during the first stages of reactivation and collision of the hyperextended rift system (for details see next chapter).

Relying on the presented observations, we interpret the Central section as a classical collisional-type section with a double-wedge geometry. The S-point defines the retro- vs. pro-wedge and delimits the position of the northward underthrusting of the Iberian Moho. Moreover, some observations need to be emphasized: (I) Both top basement and base of the crust (i.e. Moho) are observed but its internal architecture is ill defined in

seismic data and is therefore difficult to resolve and interpret. (II) The sedimentary cover is allochthonous due to the presence of Triassic salt, which acted as a decoupling level. Therefore, no direct correlation can be done between sedimentary cover and its pre-collisional basement, which makes that the description of the rift architecture is difficult in this section. Moreover, the distribution of more than 12 km thick Mesozoic sediments in the Basque – Cantabrian Basin argues for extreme crustal thinning and an extensional system flooring its southern margin, which is contradictory with a major south-dipping fault at the northern border. (III) There is a strong gravimetric anomaly underneath the Bilbao Anticlinorium, which is, according to more recent interpretations, linked to the presence of a serpentized mantle body.

Western section

The Western section, on the contrary, is going through one and the same plate, the Iberian plate. However, two underthrust slabs have been defined, a southward underthrust of exhumed mantle within the Biscay abyssal plain (Cadenas et al., 2020) and a northward underthrust of Iberian lower crust (Pedreira et al., 2003). We interpret the S-point at 15 km depth under the Cabuérniga Basin (Fig. 1.12a). Thus, a thickening of the crust is deduced from south to north in the pro-wedge, while a thinning of the crust is depicted from south to north in the retro-wedge. Regarding the sedimentary cover and due to the irregular distribution of Upper Triassic salt in the western termination of the Basque – Cantabrian Pyrenees (López-Gómez et al., 2019), the section combines both compressional decoupled and coupled domains. The frontal structure bringing the Mesozoic Polientes basin over the Duero foreland basin and the Santander Block are governed by a thin-skinned structural style, whereas, the Cabuérniga basin, and the offshore North Iberian Margin are mostly showing thick-skinned reactivation.

The structure observed across the Western section shows early stages of margin reactivation. Moreover, there is evidence for: (I) exhumation of mantle to the north (Cadenas, et al., 2018; Tugend et al., 2014a). (II) Salt is limited to some parts and primary contacts between sedimentary sequences and basement occurs where salt is absent. (III) Mid-crustal levels acting as decoupling levels and also rift-related crustal architecture preserved offshore can be observed (Cadenas et al., 2020). These observations contrast with those made in the Central section, where salt is present throughout the section and basement structures using the middle crust decoupling are not observed underneath. Thus, the early stages of reactivation, recognized in the Western section may be crucial for the understanding of the internal part of the Central section.

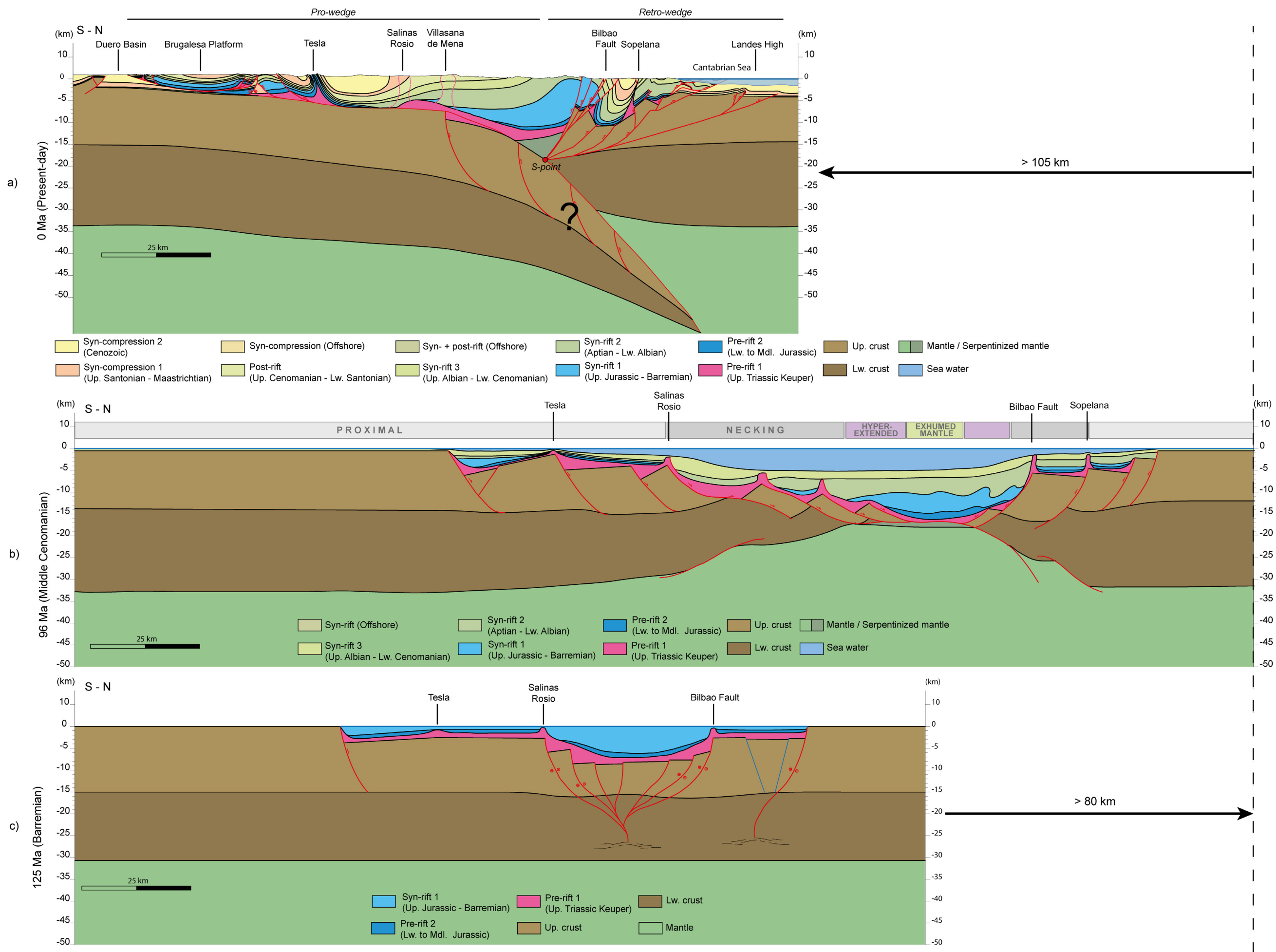


Figure 1.16 : a) Present-day crustal-scale cross section across the central Basque – Cantabrian Pyrenees (modified from Muñoz et al., 2019). See Fig. 3 for location. b) Restoration of the Central section at Middle Cenomanian times (end of multistage and polyphase extension) with the rift domains depicted on top. c) Restoration of the Central section at Barremian times (end of the first rift stage).

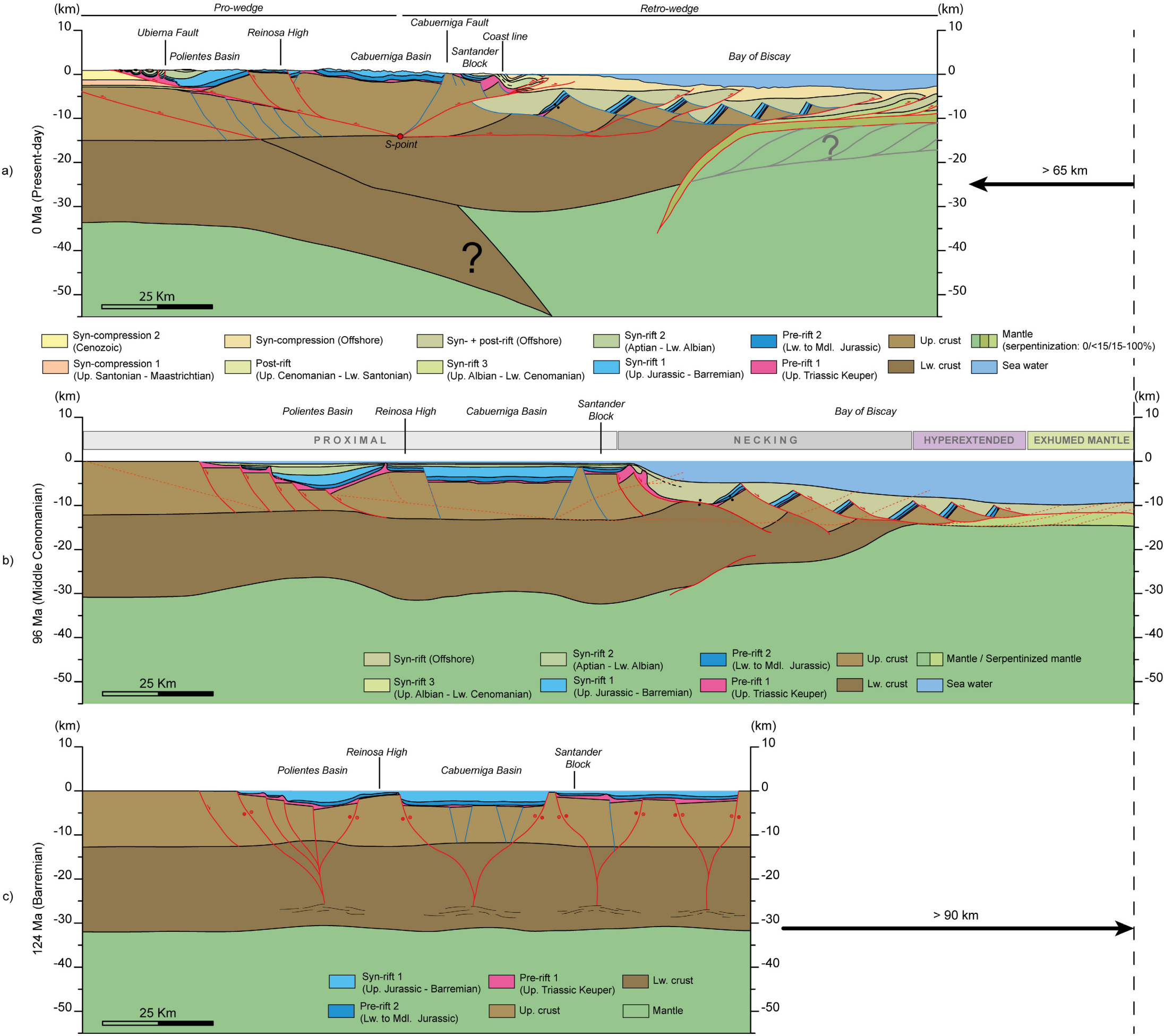


Figure 1.17: a) Present-day crustal-scale cross section across the western Basque – Cantabrian Pyrenees to the Bay of Biscay. See Fig. 3 for location. b) Restoration of the Western section at middle Cenomanian times (end of polyphase extensional event) with the rift domains depicted on top. Dashed lines show the future compressional structures. c) Restoration of the Western section at Barremian times (end of the first monopase rift stage).

1.5.2. BASQUE – CANTABRIAN RIFT TEMPLATE

In this chapter we discuss a kinematic restoration of the Western and Central sections back to the previous rift stages (i.e. Late Jurassic – Barremian and Aptian – Cenomanian). In our restoration we follow three fundamental concepts that are important to respect when restoring polyphase rift system. These three concepts are:

- (1) Areal crustal conservation: In 2D restorations of dip sections the initial and final crustal area need to be balanced assuming no movement out of the section and no or little erosion (Fig. 1.13a) (e.g. Sutra et al. 2013). Furthermore, the length of the initial top basement (top pre-rift) needs to be preserved, i.e. the initial length of the top crust must equal the final length. In contrast “new” top basement-sediment interfaces created through extensional exhumation surfaces need to be restored.
- (2) Bulk rheological evolution and implications for decoupling levels: During reactivation of hyperextended systems three potential decoupling levels can be activated, which are serpentized mantle (low friction), weak mid-crustal layers (thermal/compositional) and salt (low friction). Serpentized mantle is known to represent an efficient decoupling level (Sutra & Manatschal, 2012; Gillard et al. 2019; Lescoutre & Manatschal, 2020) (Fig. 1.13b). In contrast fresh mantle, when not serpentized, may remain coupled to the crust during deformation. A weak mid-crustal rheology not only controls extensional thinning (e.g. necking; Mohn et al. 2012) but can also localize deformation during thick-skin reactivation (Lescoutre & Manatschal 2020). The presence of a salt layer promotes decoupling of the sedimentary cover from the basement during both extension and contractional reactivation, disconnecting the final position of a sedimentary package from its initial position in the margin. Thus, the lateral continuity of salt, which may be an issue in hyperextended domains, is a key point (see discussion below).
- (3) Respect isostatic rules: In thermally equilibrated extensional settings there is an inverse proportional relation between crustal thickness and total accommodation space (Fig. 1.13c) (Tugend et al., 2014b). Thus, thick and/or deep syn- to post-rift sedimentary packages cannot overlie thick crust, or inversely, thin shallow marine syn- to post-rift sedimentary packages cannot overlie thin crust. Therefore, even in absence of direct observations of crustal thickness, the sedimentary sequence can provide vital information about the original thickness of the underlying crust prior to reactivation. This is particularly important for settings where the sedimentary section

is allochthonous and not sitting anymore on its initial pre-compressional basement as is the case in the Basque – Cantabrian Basin.

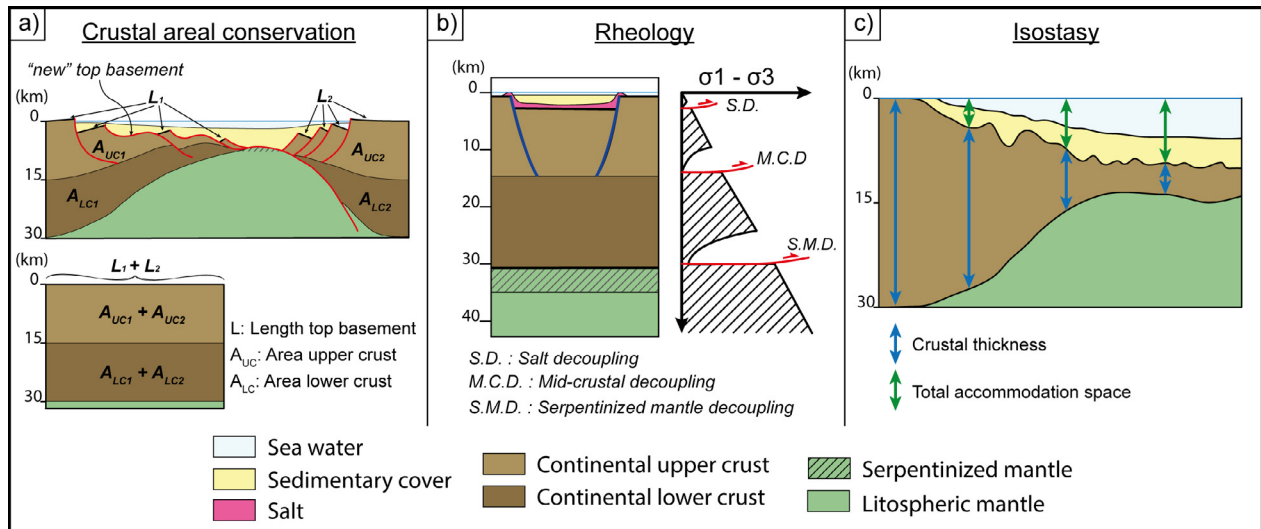


Figure 1.18 : The three basic concepts for a proper restoration of a hyperextended rifted margin. a) Crustal areal conservation and pre-rift length conservation. b) Rheological component by considering the different decoupling levels may influence such evolution. c) Isostasy, considering the crustal thickness vs total accommodation space relation.

Western section

The Aptian to Cenomanian rift stage accommodated, as previously proposed (e.g., Roca et al., 2011; Tugend et al., 2014a; Cadenas et al., 2020), most of the extension and rift-related accommodation space along this section. However, fluvial to deltaic sediments of Aptian-Albian age are observed in the Polientes basin and a thin Aptian-Albian shallow marine carbonate platform is observed in Cabuérniga basin, invoking a minor accommodation space created outside the Bay of Biscay, where kilometres thick depocenters with deep marine sediments support considerable thinning of the crust (Fig. 1.12b). The final architecture of the late Aptian to Cenomanian event resulted from a polyphase rift evolution, from stretching, thinning, mantle exhumation and finally oceanic accretion in the Bay of Biscay (Tugend et al., 2014a; Cadenas et al., 2018, accepted).

At the end of the Late Jurassic to Barremian rift stage, the Western section presented three basins (i.e. Polientes, Cabuerniga and future Bay of Biscay) filled by fluvial to lacustrine sediments with interbedded alluvial sediments (Pujalte, 1989 and Pujalte et al., 1996). These basins were separated by two basement highs (Fig. 1.12c): the so called Reinosa or Pantano del Ebro high between Polientes and Cabuérniga basins and the Santander Block between Cabuérniga Basin and the future Bay of Biscay. The limits of some of the previous basins such as Cabuérniga basin were established by sub-vertical faults (i.e. Cabuérniga

fault) that did not show a significant crustal thinning across the whole section. Therefore, we interpret these basins to have formed as more isolated and localized basins, showing probably similar characteristics and ages as the Asturian Basin (Cadenas et al., 2020) and other Late Jurassic to Barremian basins formed within a transtensional setting linked to the opening of the southern North Atlantic (Barnett-Moore et al., 2016; Nirrengarten et al., 2018; Angrand et al., 2020).

Thus, the Western section shows a re-organisation of the deformation through time and is characterised by a multi-stage rift system (Fig. 1.12) as it has been proposed offshore in the Bay of Biscay by Cadenas et al. (2020). We distinguish a first Triassic stage, relevant in terms of salt deposition and its irregular distribution (López-Gómez et al., 2019) for the subsequent evolution. A second Late Jurassic to Barremian and more distributed stage, which resulted into the development of localized basins, such as the Cabuérniga Basin (i.e. monophase rift stage) and did not show significant crustal thinning outside these basins. A third and most important Aptian to Cenomanian polyphase rift event that focused the main extension in the Bay of Biscay, resulting in a mantle exhumation in the most distal parts, as it has been proposed (Cadenas et al., 2020; García-Senz et al., 2019). As a result, the different rift stages were only slightly overlapped and therefore they can be identified and evaluated. Despite remarkable differences with the Central section regarding the sedimentary infill, the crustal architecture observed in the northern part of the Western section may represent a clue for what occurred in the Central section during the Cretaceous extensional evolution.

Central section

In contrast to the Western section, where the different rift events were formed next to each other and salt was not present throughout the section, the Central section shows three main differences: 1) the basins resulting from the multistage rift evolution are overlapped, resulting in the stacking of several depocenters; 2) the crust had to be extremely thin in order to allow for the deposition of more than 12km of sediments (see isostatic concept in Fig. 1.13c), which is also compatible with the occurrence of exhumed serpentinized mantle; and 3) thick salt was present across the whole section, as indicated by decoupling between the basement and post-salt sequences. As a consequence, extensional faults are difficult to recognize, and the former distal parts of the rift system are buried beneath thick sediments and/or underthrusts. Therefore, the understanding of the extensional evolution in the Western section, where different rift stages have been recognized separately, is fundamental to restore the Central section.

The Upper Jurassic to Barremian sediments of the Central section show the same depositional environments as those deposited in the basins reported from the Western section. Therefore, we propose that they formed in the same kinematic framework, i.e. in a transtensional setting controlled by steep faults rooting down into deep levels without thinning remarkably the crust (Fig. 1.11c). However, the presence of thick Late Triassic salt masks the direct link between surface and deep structures and make it difficult to interpret the link between the Triassic and Late Jurassic structures.

During the Aptian to Cenomanian extension localized over the locus of earlier extension, depositing a more than 8km thick succession of shallow to deep marine sediments over a previously deposited Late Jurassic to Barremian succession. Thus, in the Central section, an earlier crustal thinning during the second rift event was followed and overprinted by a polyphase rift event which led to necking, crustal thinning, and, locally, mantle exhumation (Fig. 1.11b). The Upper Jurassic to Barremian depocenter acted as a pre-rift unit during the subsequent Late Aptian to Cenomanian rift event but due to the presence of salt acting as a decoupling level, a continuous depocenter recorded the complete extensional evolution. In fact, the presence of a thick pre-rift salt layer kept the sedimentary cover decoupled during the extensional process, enabling the preservation of salt into the new real state rift domains, including exhumed mantle (e.g. Jammes et al. 2010).

At the same time, salt structures started to growth, triggered by the first stages of extension, being more significant the ones located in the necking domains. Prominent salt diapirs are located at the upward projection of the necking zone (i.e. Alavesa Platform, Fig. 1.11). During subsequent stages of compression, these diapirs were transported passively to the south, preserving their former geometry (e.g. Villasana de Mena and Salinas de Rosio salt dapirs) (Figs. 1.3 and 1.11). This is also consistent with the field observations showing that the leading edge of the post-rift Coniacian platform and its change to slope and deep marine facies occurred in the Alavesa Platform, suggesting a basin deepening within a necking domain, i.e. the location where the crust thinned from 30km to ≤ 10 km (Mohn et al., 2012; Tugend et al., 2014a).

Regarding the conjugate European margin, it is narrower and steeper, which is compatible with an upper plate geometry. Thus, we interpret the northern European margin as an upper plate and the southern Iberia margin as a lower plate, following the architecture characteristics of asymmetric hyperextended rift systems (Hauptert et al., 2016).

1.5.3. THE ROLE OF DECOUPLING LEVELS DURING THE REACTIVATION OF A HYPEREXTENDED RIFT SYSTEM

The role of decoupling levels is fundamental to understand the final architecture of the orogenic system. In the hyperextended Basque-Cantabrian rift system, up to three main decoupling levels have been identified and can be reactivated during convergence, which are : (1) the serpentinized mantle, (2) the ductile middle crust, and (3) weak horizons within the sedimentary succession (i.e. salt) (see rheological concept when restoring hyperextended rift systems explained above and Fig. 1.14).

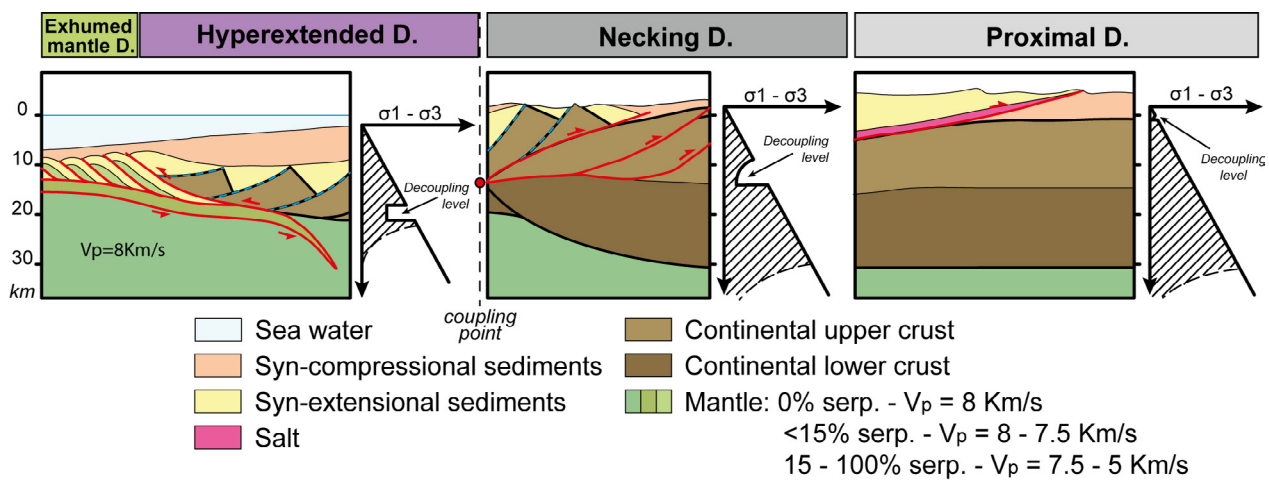


Figure 1.19 : Theoretical distribution of decoupling levels at the end of extension that will control the reactivation of a hyperextended margin. From the reactivation of the serpentinized mantle occurring at first in the more distal domains initiating the underthrusting, to the reactivation of a mid-crustal decoupling in the necking domain to the final decoupling of the sedimentary cover in the salt where it is available.

In the Western and Central sections presented in this study, similarities and differences can be observed. The onset of compression is difficult to constrain due to the overprint in the Central section and the lack of drill hole data in the Western section. Moreover, in contrast to collisional systems, that are tightly linked to the creation of topography and well documented in the Pyrenees s.s. (e.g. Boillot & Capdevila, 1977; McClay et al., 2004; Mencos et al., 2015), the initial subduction remains difficult to date. Commonly, it has been suggested that the first decoupling level being used during the reactivation was the serpentinized mantle and that serpentinized mantle has been underthrust beneath stronger and denser fresh mantle (Péron-Pinvidic et al., 2008; Lundin & Doré, 2011). This stage has been interpreted in the most distal part of the Western section (Cadenas et al., 2020). Although not well imaged, part of the distal domain is interpreted to be underthrust and reworked. We suggest that this event had few or non-response in the proximal domains outcropping in the area. The exact structure of the reactivated zone is not understood in detail, but based on velocity models (Ruiz et al., 2017) and analogies from

field observations in the Alps (Epin et al., 2017), we suggest that the strong serpentinitized upper mantle acted as a decoupling/shear zone, while the less serpentinitized underlying mantle, characterised by higher densities and velocities and lower frictional coefficients, formed duplexes over the subducting, strong, unserpentinitized mantle.

The subsequent evolution is different in the two sections. In the Western section, the main decoupling level used during the subsequent stage was the mid-crustal level allowing the reactivation of previous extensional shear zones and, eventually, creating new thrusts ramping up through the crust and resulting in crustal thickening (Cadenas et al. 2020). However, in the proximal domain (i.e. Polientes Basin and Folded Band) as well as in the necking domain, where salt was present, compressional structures detached on the Late Triassic horizon. Thus, a complex interplay between thick and thin skin reactivation can be observed (Fig. 1.12). In contrast, the Central section preserved a continuous salt layer at the end of extension allowing the accommodation of most of the deformation by transporting the sedimentary infill relatively to the south on top of the foreland basins. No evidence of contractional structures is observed in the Iberian crust in the Central part of the Basque – Cantabrian Pyrenees and just few reactivated normal faults are interpreted in the asymmetric European margin (Fig. 1.11).

1.6. CONCLUSION

Two main questions guided this work. The first regarding the present-day structure and architecture of the Basque – Cantabrian Pyrenees and the second about the role of the rift template and more precisely the former hyperextended system during the subsequent reactivation as well as the mechanisms leading the reactivation. Based on geological and geophysical observations, we developed two cross-sections through the central and western Basque – Cantabrian Pyrenees. The Central section shows a classical double wedge orogenic architecture with two tectonic plates implicated and sedimentary cover deformed in a thin-skinned structural style. On the contrary, the Western section shows an intraplate compressional architecture where both thin-skinned and thick-skinned structural styles controlled the final architecture.

Moreover, while both sections may have undergone a similar initial reactivation during which the exhumed serpentinitized mantle was used as main decoupling level, the subsequent evolution shows substantial differences between the two sections. In the Central section, salt controlled the reactivation and resulted in a decoupling of the sedimentary cover from the underlying basement. Thus, this section represents a classical thin-skinned architecture in which the basement structures played a minor role during compression. On

the contrary, the Western section shows an intraplate orogenic architecture in which only the Iberian plate is involved and, unlike the Central section, collision with the conjugate margin did not occur. Thus, the final architecture of the Western section is governed by two distinct underthrusts that are separated in space and likely also in time. To the north, the section is limited by the southward underthrust of exhumed mantle (i.e. Bay of Biscay) whereas to the south, a northward underthrust of the Iberian lower crust resulting in an indentation and thickening of the Iberian crust. On top, a combination of thick- and thin-skinned structural styles is co-existing considering the uneven distribution of salt.

Despite locale results, this study is among the first in integrating the three fundamental concepts developed in hyperextended systems, which are: the concepts of restoration (Fig. 1.13), rheology (Fig. 1.14) and polyphase vs multistage rifting (Fig. 1.2), all of which have fundamental implications in analysing and restoring collisional orogens and deciphering the underlying processes.

The Basque – Cantabrian Pyrenees offer the possibility to propose complete kinematic reconstructions of an orogenic system back to its initial hyperextended state. However, it is not a unique place. Most collisional orogens may have gone through similar stages, that may have been obliterated by the complexity of an orogenic overprint. Unravelling the rift inheritance is not a detail, but necessary to understand orogenic processes. This study is a first step, others are necessary to further improve our understanding of the growth of orogenic systems. Thus, the major conclusion of this paper is that the recognition and understanding of the nature and distribution of decoupling levels, during extension and subsequent reactivation, is among the most fundamental steps to reconstruct the structural evolution occurring in the formation and reactivation of a hyperextended rift systems or rifted margins.

ACKNOWLEDGEMENTS

This work is supported by the OROGEN project (TOTAL – CNRS – BRGM partnership). The seismic and borehole data have been provided by the Instituto Geológico y Minero de España (IGME) and Midland Valley is also thanked for providing the Move software. We thank Nick Kusznir for helping in the depth conversion process and Rodolphe Lescoutre and the Orogen community for fruitful geological discussions.





CHAPTER 2

**ROLE OF INHERITANCE IN A THICK-
TO THIN-SKIN TRANSITION: INSIGHTS
FROM ANALOGUE MODELLING AND
BASQUE – CANTABRIAN PYRENEES**

The cover of Chapter 2 depicts a detail of the link between the thick-skinned domain and the transitional domain in Model 1 of the experimental program.

ROLE OF INHERITANCE IN A THICK- TO THIN-SKIN TRANSITION: INSIGHTS FROM ANALOGUE MODELLING AND BASQUE – CANTABRIAN PYRENEES

Tectonophysics, in prep.

Miró, J.^{1, 2}; Ferrer, O.²; Muñoz, J. A.²; Manatschal, G.¹

¹ Institut de Physique du Globe de Strasbourg, CNRS-UMR 7516, EOST, Université de Strasbourg, 1, rue Blessig, 67084 Strasbourg, France

² Institut de Recerca GEOMODELS, Departament de Dinàmica de la Terra i de l'Oceà, Facultat de Ciències de la Terra, Universitat de Barcelona, C/ Martí i Franquès s/n 08028, Barcelona, Spain.

ABSTRACT

Transitions from thick- to thin-skin structural domains are poorly investigated using analogue models and frequently misunderstood in the field. This contribution aims to address the linkage between basement-controlled domains and salt decoupled domains where a transitional domain overlaps the pre-rift salt over the basement inherited structures. An experimental program using physical models is designed with a setup inspired on the transition from the thin-skinned Basque – Cantabrian Pyrenees to the thick-skinned Asturian Massif to the west. The experimental results show that oblique structures forms in the transitional domain, which position and orientation depends on the linkage of the active structures occurring in both surrounding thick- and thin-skinned domains. The deformation in the thick-skinned domain results in significant topography but narrow deformation area whereas in the thin-skinned domain deformation is more distributed due to the decoupling, resulting in a wider deformation area of less topography. As a result, syn-contractional sedimentation is occurring mainly in the foreland basin in the thick-skinned domain whereas it is more distributed in the foreland but also within the deformation area in the thin-skinned domain. Syntectonic sedimentation delays forward propagation of the thrust front, controlling the orientation and kinematics of the structures along the transfer zone.

2.1. INTRODUCTION

The presence of inherited structures and weak horizons at different structural levels are among the most important factors controlling the structural evolution of orogenic systems (Beaumont et al., 2000; Butler et al., 2006; Amilibia et al., 2008; Miro et al., *subm.*). Most mountain belts have reactivated former rift systems and passive margins. As a result, reactivation of inherited extensional systems has been widely recognized as a fundamental feature for the understanding of the structure of fold and thrust belts (Tugend et al., 2014a;

Chenin et al., 2017; Muñoz, 1992). In addition, the uneven distribution of weak decollement levels plays also a significant role in the along-strike variation of the structural style of fold-and-thrust belts [e.g. Zagros (Molinaro et al., 2005), Andes (Kley et al., 1999), Apennines (Tozer et al., 2002), Pyrenees (Carola et al., 2013)]. Such variation is expressed by differences in the structural style and final topography, changes on the vergence, and presence of oblique and transverse structures connecting different segments of the fold and thrust belt.

The formation of fold and thrust belts involving rift systems (i.e. inversion tectonics) is widely recognized in thick-skinned structural styles, as basement is usually involved during the reactivation of extensional faults [e.g. Asturian Massif (Pulgar et al., 1999), Andes (Carrera et al., 2006; Iaffa et al., 2011)]. On the contrary, the presence of weak horizons in the cover succession, such as evaporitic formations, results into decoupling and thin-skinned structural styles [e.g. Pyrenees (Carola et al., 2015; Muñoz et al., 2018), Alps (Granado et al., 2018)]. Many studies have focused on the characterization of inversion tectonics from field case studies and modelling approaches, both by numerical and analogue techniques (McClay, 1989; McClay & Buchanan, 1992; Pinto et al., 2010; Bonini et al., 2012; Granado et al., 2017; Granado & Ruh, 2019). Also, many modelling studies have focused on the understanding of the effect of the variation of the mechanical properties of the weak horizons on the structure of inverted salt-bearing rift systems incorporated into fold and thrust belts (Bahroudi & Koyi, 2003, Vidal et al. 2013, Ferrer et al., 2014, 2016; Roma et al., 2018a, 2018b; Pla et al., 2019; Dooley & Hudec, 2020). However, few modelling studies deal with the superposition of basement-inherited features and decoupled systems (Ferrer et al., 2016; Roma et al., 2018a, 2018b; Dooley & Hudec, 2020).

Regardless the timing of salt deposition (pre-, syn-), the distribution of salt in rift systems and passive margins, is usually controlled by the geometry of the basement-involved extensional system (Rowan, 2014). Nevertheless, such distribution has a strong control on the understanding of along-strike differences in the structural style during the tectonic inversion of rift systems and passive margins. As such, the final distribution of pre-rift salt depends on factors as the initial thickness, the amount of extensional deformation, and the erosion in the uplifted footwalls. If the salt is syn-rift, thickness and facies distribution depend on the geometry of the fault system and the interplay between fault through, sedimentation rate, and environmental depositional conditions (Rowan, 2014). To our knowledge, a 3D modelling approach to address this issue has not yet been performed, regardless it is a quite common structural problem in fold and thrust belts that have resulted from the inversion of extensional systems involving salt, such as the Zagros, Pyrenees, Hellenids, among many other contractional systems. Instead, sandbox analogue

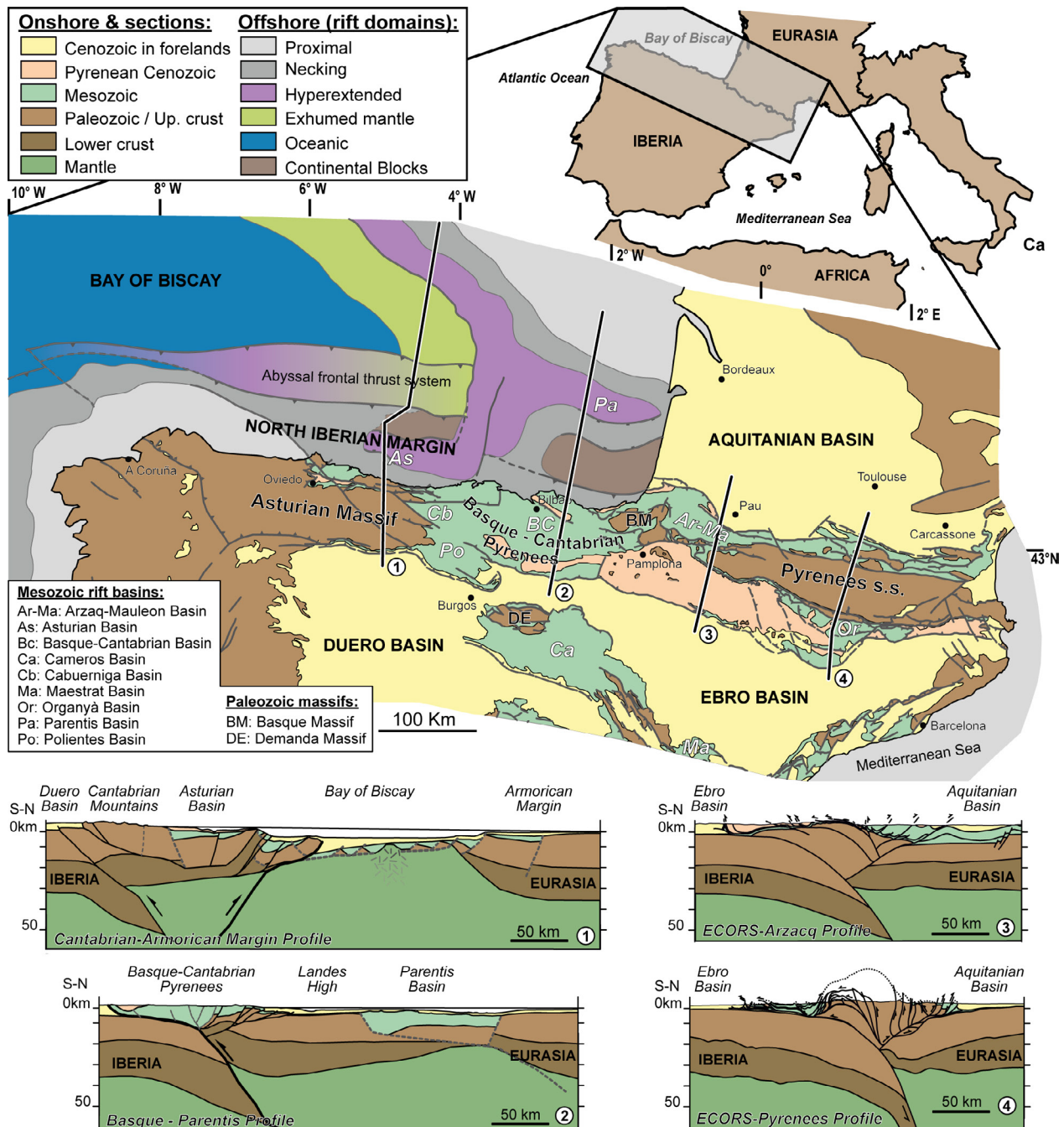
models have been used in multiple structural problems such as: structural inheritance in extensional oblique rift systems (e.g. McClay & White, 1995; Amilibia et al., 2005); basement-controlled transfer zones (e.g. Acocella et al., 1999; Wu et al., 2009); contractional reactivation of inherited normal faults with (e.g. Bonini et al., 2012; Ferrer et al. 2012; Roma et al., 2018b; Dooley & Hudec, 2020) and without evaporites (e.g. Pinto et al., 2010; Granado et al., 2017); distribution and impact of salt in thin-skinned extensional setting (e.g. Vendeville & Jackson, 1992; Jackson & Vendeville, 1994), and the role of basement faults beneath decoupling horizons (e.g. Withjack & Callaway et al., 2000; Dooley et al., 2005; Ferrer et al., 2016; Roma et al., 2018a, 2018b).

Our modelling approach has been inspired for the understanding of the thick- to thin-skinned deformation transition between the Asturian Massif and the Basque-Cantabrian Pyrenees, which is an area of debate since years. While it is accepted that Asturian Massif results from a thick-skinned evolution due to the lack of weak horizons (Alonso et al., 1996; Pulgar et al., 1999), some authors argue that the Basque – Cantabrian Pyrenees is also governed by a thick-skinned structural style with minor influence of salt tectonics (Quintana et al., 2015; García-Senz et al., 2019). However, it is well characterized the presence of a salt unit underlaying the Mesozoic rift basins (López-Gómez et al., 2019) as well as the significant thickness and overall distribution of salt through the area (Cámara, 2017). Therefore, an alternative interpretation considering a thin-skinned deformation at the Basque – Cantabrian Pyrenees is also well documented (e.g. Tavani et al., 2013; Carola et al., 2013, 2015; Cámara & Flinch., 2017, 2020; Muñoz, 2019; Miró et al. subm.). In this sense, the present work aims to address such controversy by using physical models dealing the interplay between inherited basement structures (i.e. rigid blocks) and the lateral overlapping of a weak horizon (i.e. salt). The experimental program allowed (1) to understand the thick- to thin-skinned transition, (2) how deformation links both domains, and (3) to improve the understanding of the Asturian Massif – Basque-Cantabrian Pyrenees transition.

2.2. GEOLOGICAL SETTING

The Pyrenean orogenic system is a doubly verging fold and thrust belt that limits the Eurasian and Iberian plates resulting from the inversion of the multistage and polyphase rift evolution occurred in the northern Iberia from Late Jurassic to Early Cretaceous times (Muñoz, 1992; Roca et al., 2011; Tugend et al., 2014a, Tavani et al., 2018; Cadenas et al., 2020; Lescoutre et al., subm.; Miró et al., subm.). Its present-day architecture changes significantly along strike due to the different tectono-sedimentary evolution and structural

style (Fig. 2.1) which resulted in a wide terminology, used here as: a) the Pyrenees *s.s.* for the eastern portion of the orogen where Mesozoic basins are located north and south of an Axial zone made of Paleozoic rocks and the higher topography of the mountain belt; b) the Basque – Cantabrian Pyrenees in the central portion of the orogen characterized by the inversion of the Basque – Cantabrian Basin where Mesozoic rocks outcrops resulting in smoother topography; and c) the Asturian Massif to the west characterized by Paleozoic rocks with almost no Mesozoic successions and also significant topography (Fig. 2.1) [see Miró et al. (2020) for a terminology review].



The present work focuses on the reactivated proximal rift domain observed in the southern link between the Basque – Cantabrian Pyrenees and the Asturian Massif, referring to those areas that never suffered a crustal thinning to less than 25 km thick but have been later involved in the Alpine orogeny (Tugend, et al., 2014a, Cadenas et al., 2018; Miró et al., subm.) (Fig. 2.2). The Basque – Cantabrian Pyrenees are the result of the inversion of the western North Iberian Rift System, which developed a complex multistage and polyphase evolution reaching the most evolved phase during middle Cretaceous with exhumation of mantle in the most distal domains (Miró et al., subm.). However, due to the amount of salt present in the system since the Late Triassic rift event (López-Gómez et al., 2019, Lagabriele et al., 2020), the reactivation of the Basque – Cantabrian Pyrenees occurred in a thin-skinned structural style, starting during the Late Cretaceous up to the Oligocene (Riba & Jurado, 1992; Carola et al., 2015; Muñoz, 2019; Miró et al., subm.). Thus, the Mesozoic sedimentary succession of the southern Basque – Cantabrian Pyrenees have been relatively transported more than 30 km tens of kilometres to the south over the foreland basin (Muñoz, 2019; Miró et al., subm.) (Fig. 2.2). As a result, whereas salt structures developed in the proximal domains have been reactivated and squeezed during the inversion, the ones located to the north (i.e. Alavesa Platform) and developed in more distal domains are still preserved showing non, or only slightly, contractional reactivation (e.g. Salinas del Rosio and Villasana de Mena salt diapirs). The underlying basement is flat in the foreland Duero and Ebro basins whereas slightly dipping towards the hinterland beneath the frontal thin-skinned thrust (Carola et al., 2015; Muñoz, 2019; Miró et al. subm.).

The Asturian Massif, on the contrary, is the result of a thick-skinned contractional deformation controlled by the reactivation of previous Variscan faults (Alonso et al., 1996; Gallastegui, 2000). Triassic salt was not deposited in this area or it was completely eroded (López-Gómez et al., 2019) conditioning the contractional thick-skinned structural style in comparison to the Basque – Cantabrian Pyrenees to the east. The interpretations of the Asturian Massif (e.g. Alonso et al., 1996, Pulgar et al., 1999) shows a major mid-crustal sole thrust dipping to the north and being flat at about 20km depth acting as an intracrustal decoupling for the structures depicted in the hanging wall (Fig. 2.2). The fault propagation fold observed in the sediments located in the northern limit of the Duero Basin represent the field expression of this major sole thrust (Pulgar et al., 1999).

In fact, a coupled system is observed to the west (i.e. Asturian Massif) and a decoupled system is observed to the east (i.e. Basque – Cantabrian Pyrenees) conditioned by the distribution of the Late Triassic salt. This leads to a transitional domain in between where

the accommodation of deformation during the extension and subsequent reactivation has been the focus of debates (e.g. Tavani et al., 2013; Carola et al., 2013).

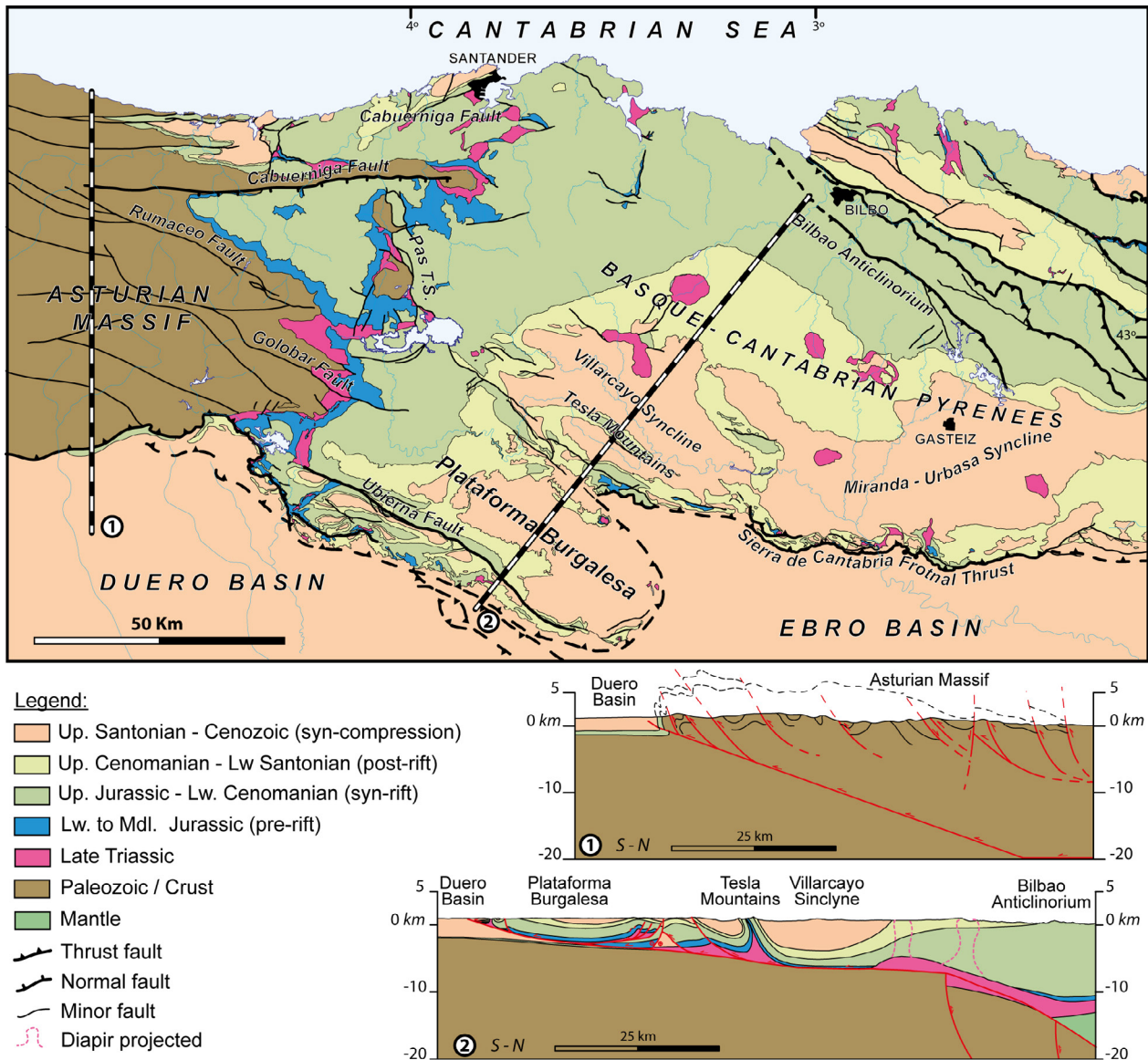


Figure 2.2 : Tectonostratigraphic map of the Basque – Cantabrian Pyrenees – Asturian Massif junction and geological cross section showing the along strike variability of the structural style, thick-skinned to the west and thin-skinned to the east. Cross section 1 from Alonso et al. (1996).

2.3. ANALOGUE MODELLING

The experimental methodology, analogue material's properties, scaling and the different analytical techniques used in this study are described in the following sections.

2.3.1. EXPERIMENTAL METHODOLOGY

Set-up

The analogue experiments were carried out in a 75 cm-long, 70 cm-wide, and 35 cm-deep glass-sided deformation box (Fig. 2.3a and b). Two mobile walls orthogonal to the glass-sided walls made the experiment a closed system. Both glass-walls were fixed whereas the two metallic walls were moved by servomotors during the experiment. Two rigid wooden blocks attached to the mobile walls were used to simulate the inherited basement structures (Fig. 2.3a and b). Both blocks thinned progressively eastwards from 22 to 2 mm along 410 mm. The northern block had a rectangular planview shape whereas the southern one was trapezoidal (Fig. 2.3a and b). In both cases, a surface dipping 60 degrees towards the inner part of the model simulated inherited basement extensional faults (Fig. 2.3a, b and e). The space between the two blocks was filled with white silica sand keeping the eastwards regional dip. The rigid blocks and the white sand were overlaid by a purple sand layer wedging eastward as the previous materials. In contrast, the eastern side of the rig was filled by a 19 mm-thick polymer layer pinching out to the west on top of the basement sand-wedge (Fig. 2.3c and d). According to the polymer distribution, three domains have been defined: a) a coupled domain without polymer; b) a transitional domain where the polymer overlaps the basement blocks; and c) a decoupled domain where the thickness of the polymer is constant (Fig. 2.3d). A 10 mm-thick blue sand layer overlaid the polymer layer covering the decoupled and transitional domains, and pinching-out westwards on the coupled domain (Fig. 2.3c).

Analogue materials and scaling

The models were built using materials suitable to carry out simulations of upper crustal deformation (see Weijermars & Schmeling, 1986; Dell'Ertale & Schellart, 2013). Well-sorted and rounded dry silica sand was the material used as analogue for brittle rocks in the upper continental crust (Schellart, 2000). A polydimethylsiloxane (PDMS) polymer was used as analogue of viscous salt in nature (Weijermars, 1986; Dell'Ertale & Schellart, 2013). The silica sand (white or colored) with an average grain size of 199 μm obeys a Mohr-Coulomb criterion of failure (Hubbert, 1951; Mandl et al., 1977). The mechanical properties of the poured sand were determined by Roma et al. (2018a) by means a shear

box test, resulting in 34.6° of internal friction, $1500 \text{ Kg}\cdot\text{m}^{-3}$ bulk density, 0.69 of internal friction coefficient and a low apparent cohesive strength of 55Pa. The polymer is a near-Newtonian viscous fluid with a density of $972 \text{ Kg}\cdot\text{m}^{-3}$, a viscosity of $1.6\times 10^{-4} \text{ Pa}$ and a strain ranges of $1.83\times 10^{-4} \text{ cm}\cdot\text{s}^{-1}$ at 20°C (Dell'Ertolo & Schellart, 2013). The properties of the materials used, and the scaling factors of the experimental programme are summarised on Table 1.

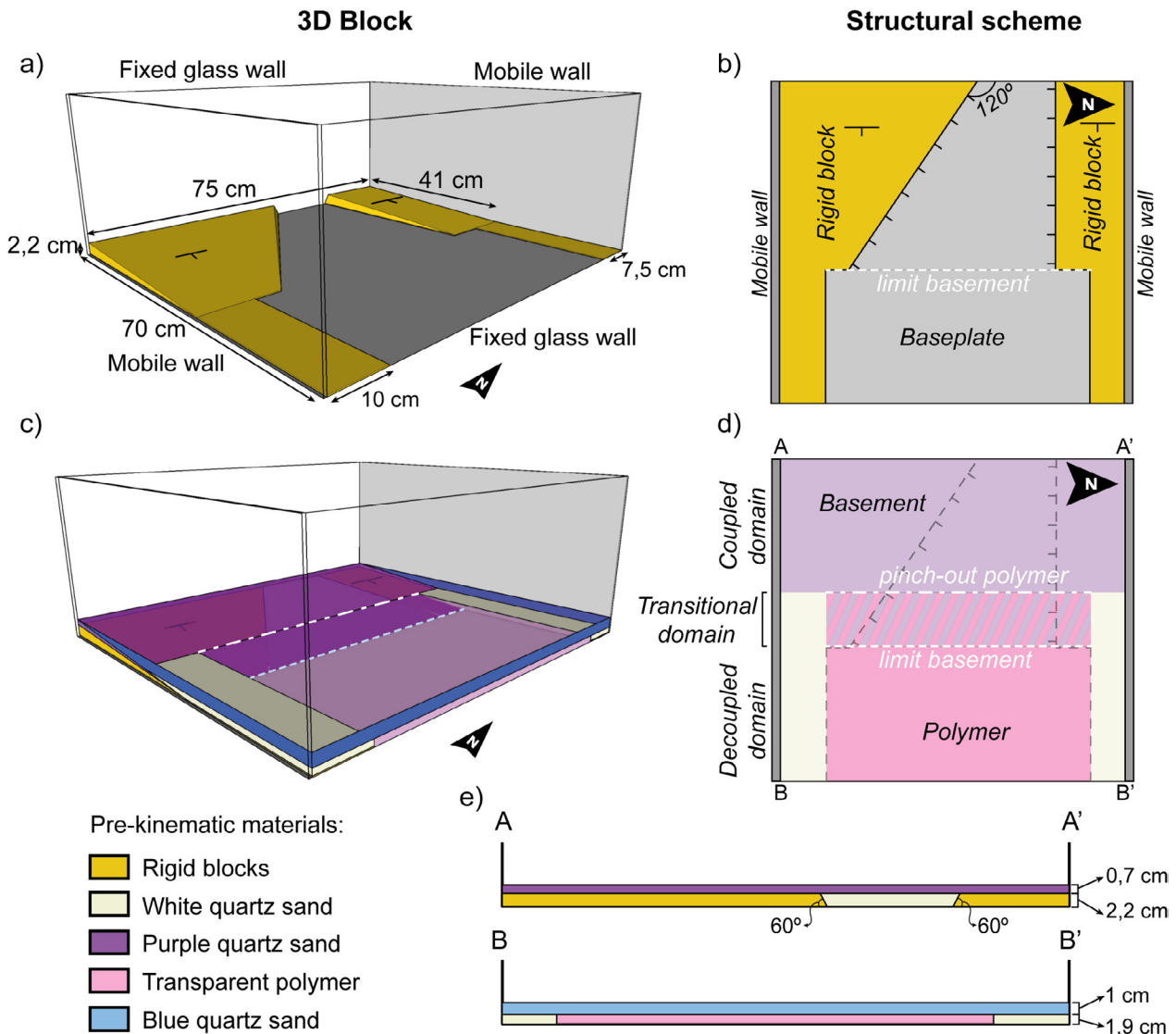


Figure 2.3 : 3D (left) and top view (right) schemes of the experimental setup. A) 3D diagram showing the disposition of the rigid blocks at the base of the model. B) top view of the previous 3D diagram. C) final organization of the setup with transparency of various sand-layers. Note the limit of basement and pinch-out of the polymer as indicated in d). D) top view of model with basement sand and polymer to show the overlapping area and the limits of both units which defines the different structural domains. E) section view of the coupled and decoupled domains located in d).

Table 1 : Scaling parameters used in the experimental program

Parameter	Experiment	Nature	Ratio
Length (m)	0.01	1000	10^{-5}
Density sand ($\text{Kg}\cdot\text{m}^{-3}$)	1500	2700	0.55
Gravity acceleration ($\text{m}\cdot\text{s}^{-2}$)	9.81	9.81	1
Density polymer ($\text{Kg}\cdot\text{m}^{-3}$)	972	2200	0.44
Viscosity polymer ($\text{Pa}\cdot\text{s}$)	$1.6\cdot 10^4$	$10^{18} - 10^{19}$	$1.6 \times 10^{-14/-15}$

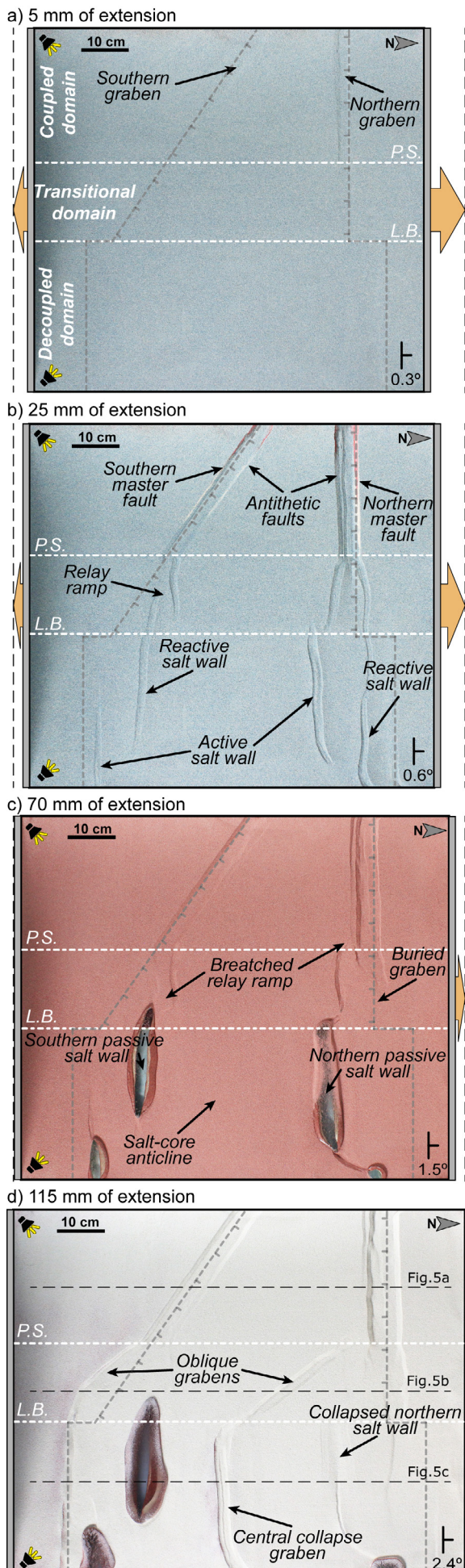
Procedure

The extensional deformation was achieved by moving the two end walls by a motor-driven worm-screw controlled by a computer. In order to produce more accommodation space to the north, where the main depocenter was located in the Basque-Cantabrian Basin, the northern wall moved at a higher velocity (3mm/h) than the southern one (2mm/h). To favour the early development of salt structures, the first syn-extensional sand layer was poured after 5 hours. All subsequent sand layers were settled every 3 hours. Before the sedimentation of each syn-extensional layer (white and red sand), the rig was tilted 0.35° northwards to simulate the progressive tilting of an extensional rifted margin. At the end of the Model-1 the total extension was 127mm (Table 2), (75mm for the northern end wall and 52mm for the southern one), the syn-kinematic sand pack comprised 8 syn-extensional sand layers, and the total tilting was 2.8° .

Table 2 : Experimental program

Experiment	Total extension (mm)	Extension rate (mm/h)	Total shortening (mm)	Shortening rate (mm/h)	Syn-comp. sedimentation	Time (hours)
Model - 1	127	3 (N wall) 2 (S wall)	-	-	-	31
Model - 2	127	3 (N wall) 2 (S wall)	200	6 from N 0 from S	-	64
Model - 3	127	3 (N wall) 2 (S wall)	200	6 from N 0 from S	Yes	68

After the extensional episode, a 5mm-thick yellow sand layer was added on top of the Model-2 and Model-3 simulating a post-extensional unit. Both models were subsequently shortened by moving the northern end wall at a velocity of 6mm/h during 38 hours reaching 200 mm of total shortening. In contrast, the southern end wall was kept fixed. Syn-compressional sedimentation in Model-3 (Table 2) was simulated by alternating green and white sand layers every 3 hours. In addition, after the deposition of each syn-compressional sand layer the rig was tilted 0.2° to the north up to additional 2.2° to simulate the orogenic flexure (e.g. Basque – Cantabrian Pyrenees, Fig. 2.2).



2.4. EXPERIMENTAL RESULTS

This chapter describes the experimental results of the three models pointing out on the kinematics of each deformation phase. Thus, Model-1 zooms in on the extensional evolution and allows to understand the role of compositional and structural inheritance during the rift phase. Model-2 and Model-3 were similar to Model-1 but shortening was subsequently applied to understand how the inversion tectonics of the pre-existing extensional structures is. In addition, Model-3 explores the role of syn-compressional sedimentation during inversion. The description of each model has been addressed according to the style of deformation of the three structural domains previously described (Fig. 2.3c and d).

2.4.1. MODEL-1

Model-1 is the baseline experiment performed to understand the main structural elements developed during the extensional episode. During the initial stages of extension, the experiment shows a strong control of the basal plates configuration in the coupled domain,

Figure 2.4 : Top view evolution of Model-1. Illumination comes from the left. Shadowed areas are surface-breaching faults dipping to right (north) and illuminated areas are surface-breaching faults dipping to left (south). The position of the basement rigid blocks is showed in grey dotted lines and the pinch-out of the salt (P.S.) and the limit of basement blocks (L.B.) in white dotted lines. A) top view after 5 mm of extension. B) top view after 25 mm of extension. C) top view after 70 mm of extension. D) top view after 115 mm of extension. See text for details.

where an E-W trending graben develops over the edge of the northern basal plate, and a NW – SE trending graben over the southern one (Fig. 2.4a). On the contrary, any structure developed in the decoupled and the transitional domains. As extension increases, the northern E-W graben of the coupled domain widens controlled by a major normal fault rooted at the edge of the basal plate to the north, and a set of two antithetic faults developed to the south (Fig. 2.4b). Similarly, the southern oblique graben also widens but only a single antithetic fault developed due to a lower extension rate than in the northern graben (Fig. 2.4b). In contrast, twice of grabens have developed in the decoupled domain all of them trending perpendicular to the deformation axis, i.e. E-W. Thin-skinned extension triggered the development of reactive salt walls below these grabens that evolved to active in the grabens where the overburden was more stretched (Fig. 2.4b). In the transitional domain, extension is accommodated in two grabens connecting the northern graben of the coupled domain with the two salt walls of the decoupled domain. This syncline sinks because of the polymer expulsion towards the bounding graben feeding salt walls. Two stepping E-W grabens develop southwards connecting the oblique graben of the coupled domain with the reactive salt wall of the decoupled domain (Fig. 2.4b).

Despite syn-kinematic sedimentation, further extension widens the two grabens at the coupled domain by generating new antithetic normal faults (Fig. 2.4c). Northwards regional tilting triggered gravitational gliding in the decoupled and transitional domains, where the symmetric bounding graben becomes progressively asymmetric evolving to half-graben controlled by the down-dip faults. With increasing of extension, reactive salt walls evolved locally to active and finally to passive state piercing the overburden (Vendeville & Jackson, 1992; Jackson et al, 1994; Rowan & Giles, 2020) (Fig. 2.4c). A wide salt-core anticline started to grow in an intermediate position between the two salt walls, being progressively overlapped by the syn-kinematic sand layers (Fig. 2.4c). At the meantime in the transitional domain, the northernmost graben was buried. Extensional deformation concentrates in the north-dipping faults of the following grabens, that as extension increases, are progressively hard-linked by footwall breached relay ramps. Similarly, the westwards propagation of the southern graben controlling the growth of the passive salt wall becomes an inactive, and a footwall breached relay ramp links with the southernmost graben of the transitional domain (Fig. 2.4c).

In further stages of extension, the evolution of the coupled domain is governed by widening the grabens and the formation of new antithetic faults (Fig. 2.4d). In the decoupled domain, polymer extrusion continues until 80 mm of extension when the source layer is depleted, and primary welds develop flanking the two major salt walls. Welding interrupts the

polymer flow towards the northern salt wall that becomes progressively buried by syn-kinematic sedimentation. Subsequent extension produces the fall of this salt wall with the development of collapse structures (Figs. 2.4d, 2.5c).

In the meantime, a crestal collapse graben develops in a salt-cored anticline between the two salt walls (Fig. 2.5c). The extensional structures related to the southern salt wall become also inactive and were buried. In this area, extensional deformation shifts to the southern edge of the decoupled domain where a new basinwards dipping fault develops. During this last stage, previous E-W grabens of the transitional domain were abandoned, and two new NW – SE oblique transtensional graben developed. These new structures link the major grabens of the coupled domain with the central graben and the last basinward dipping fault developed at the southern edge of the decoupled domain (Fig. 2.4d).

Fig. 2.5 shows the structural style at the end of extension in the three characterized domains. The coupled domain is characterised by two major grabens, whose development is constrained by the rigid blocks: a master fault nucleates at the edge of the rigid blocks, and a set of antithetic faults that become younger towards the master fault develop as extension increases (Fig. 2.5a). Whereas deformation in the coupled domain concentrates in the two main grabens separated by an undeformed plateau, in the transitional and the decoupled domains it is distributed along the salt basin.

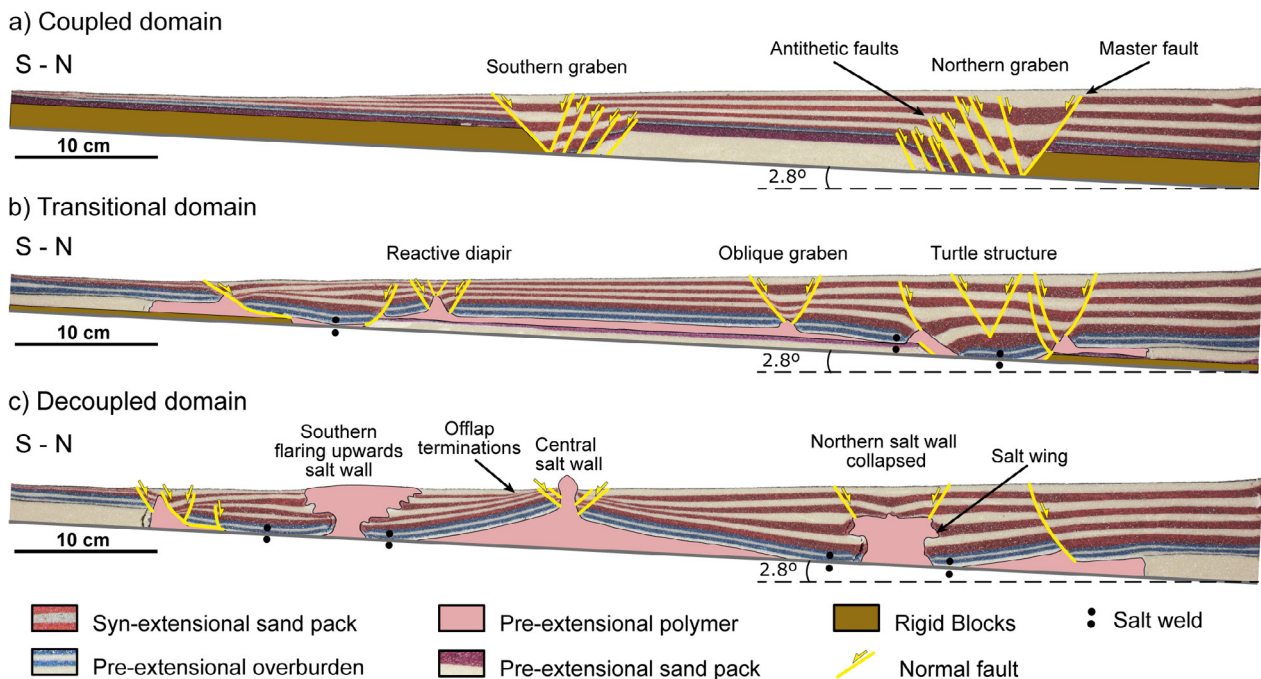


Figure 2.5 : Cross sections at the end of the extensional deformation (127 mm). A) coupled domain; B) transitional domain; C) decoupled domain. See Fig. 4d for location of sections.

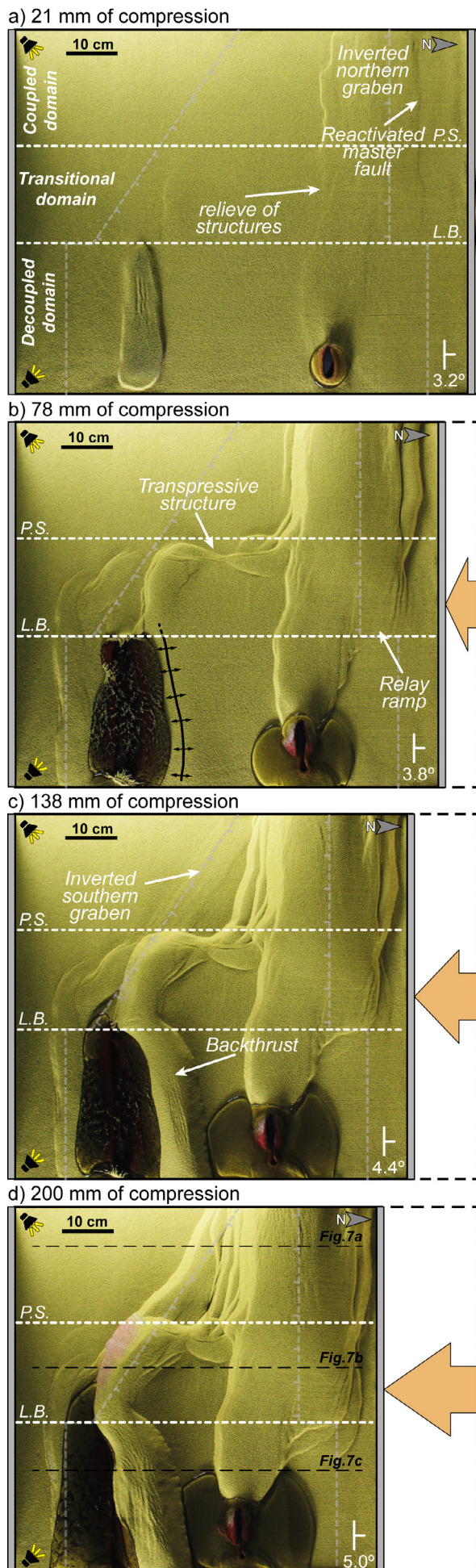
In the transitional domain the location of early structures was also controlled by the coupled domain. Thus, a basinwards dipping fault controlled the development of half-graben in the northern sector whereas in the southern sector a counter-regional fault constrained the growth of half-graben (Fig. 2.5b). Whereas the early sand layers thicken towards these faults, a change of the location of depocenters occurred when the hanging wall of these faults touched down forming a salt weld indicating flip-flop tectonics (Quirk et al., 2003; Quirk & Pilcher, 2012) (Fig. 2.5b). It is at this point when the counter-regional fault develops in the northern part of the transitional domain and the basinwards dipping fault in the southern one. Furthermore, two grabens with reactive diapirs stand out in the central part of this domain, the southern one is the lateral termination of the southern salt wall of the decoupled domain and the northern one is the oblique graben developed during late extension that links the northern graben of the decoupled domain with the central salt wall of the decoupled domain (Figs. 2.4d and 2.5b). Another oblique structure is the southernmost listric fault linking, during late stages of extension, the southern graben of the coupled domain with the extensional faults developed at the southern salt pinch-out of the decoupled domain.

Finally, the structure of the decoupled domain is characterized by a fully decoupled deformation controlled by the polymer flow during extension. Whereas the southern salt wall was a flaring upwards geometry, the northern one was buried after source layer depletion (Fig. 2.5c). Further extension widens the diapir and its roof collapsed developing a graben (diapir fail according to Vendeville & Jackson, 1992). A wide salt-cored anticline develops at the central part of the section triggered by polymer inflation as indicated by the different offlaps in the syn-kinematic sand layers. A crestal graben was generated during late extension allowing the piercement of a new passive salt wall. Two extensional listric faults accommodate late extension at the southern pinch-out of the polymer layer and northwards of the northern salt wall (Fig. 2.5c).

2.4.2. MODEL-2

Since the extensional evolution of Model-2 followed the same steps as Model 1, but it was subsequently shortened without syn-contractional sedimentation (Table 1), this section will focus on the description of the results related to the contractional episode of this model.

During onset of shortening, deformation concentrates at the closest structures to the moving wall in the coupled domain. The northern graben arches and uplifts by the inversion of the northern master fault and the formation of a foreland-directed thrust (Figs.



2.6a and 2.7). In the decoupled domain, shortening squeezes both the northern and southern salt walls arching and uplifting its roof during diapir rejuvenation (Fig. 2.6a). Salt extrusion rate enhances by shortening, especially at the eastern termination of the buried diapir located northwards of the decoupled domain (Fig. 2.6a). In the transitional domain, the northern master fault extended from the coupled domain is also inverted, and a foreland-directed thrust nucleates at the apex of the reactive diapir located at the southern edge of the southern inherited E-W graben (Fig. 2.4c). After 21 cm of shortening, the graben located at the south of the transitional domain (Fig. 2.5b) is slightly reactivated by a foreland-directed thrust nucleated at the apex of the reactive diapir (Fig. 2.6a). During early inversion, the thrust front evidences a strong control of the pre-existing extensional and salt structures, being rectilinear trending W-E in the coupled domain and slightly shifted southwards and arched in the decoupled domain. At the transitional domain both thrust fronts overlap in a soft linkage relieving thick- and thin-skinned domains respectively (Fig. 2.6a).

Figure 2.6 : Top view evolution of Model-2. Illumination comes from the left. The position of the basement rigid blocks is showed in grey dotted lines and the pinch-out of the salt (P.S.) and the limit of basement blocks (L.B.) in white dotted lines. A) top view after 21 mm of compression. B) top view after 78 mm of compression. C) top view after 138 mm of compression. D) top view at the end of compression (200 mm). See text for details.

In further stages of shortening, the height of the northern inverted graben at the coupled domain increases by the emplacement of south-verging thrusts in a piggy-back sequence, but also by the footwall shortcut that develops at the northern edge of the graben (Figs 2.6b, 2.7a). In the decoupled domain, the buried northern salt wall narrows, increasing the uplifting and folding of its roof (Fig. 2.7c). At the eastern termination, the extruding polymer forms a salt sheet that flows down the limbs of the resulting anticline (Fig. 2.6b). Contractional deformation reaches the southern pinch-out of the salt basin where an E-W trending foreland-verging thrust developed. The southern salt wall increased the extrusion rate resulting in a large salt sheet at surface (Fig. 2.6b). The salt-cored anticline located between the two salt walls is progressively amplified as shortening increases. The structural complexity of the transitional domain increases as deformation evolved. The northern E-W trending thrust front becomes rectilinear, linking the foreland-verging thrust of the coupled domain with the foreland-directed thrust nucleated at the top of the buried northern salt wall (Fig. 2.6b). More to the south, the structural style of the transitional domain is strongly controlled by salt thicknesses (Stewart, 1999). The E-W trend of the decoupled domain structures progressively curves in a NW-SE trend (Fig. 2.6b). Tear faults develop at the edge of the salt basin accommodating differential shortening between domains and segmenting the thrust sheets (Fig. 2.6b).

This tear fault links the deformation front of the decoupled domain with the deformation front of the coupled. Southwards of the tear fault, the E-W trending thrust at the pinch-out of the salt basin takes a NW-SE trend in the transitional domain.

Increasing shortening forced the rise of a prominent topography in most structures. The southern salt wall of the decoupled domain becomes progressively squeezed until to develop a secondary weld around 80 mm shortening (Figs. 2.6c and 2.7c). After welding, contractional deformation shifts from the southern thrust front towards the anticline northwards of the southern salt wall. This structure is progressively amplified first by bucking and then by the development of a thrust in its southern limb (Figs. 2.6c and 2.7c). Shortening reactivates the secondary weld as a fault weld causing the counterclockwise rotation of the anticline's frontal limb. Once it is near vertical, buttressing triggers the nucleation of a back thrust (Figs. 2.6c and 2.7c). After 138 mm shortening begins the reactivation of the oblique southern graben at the coupled domain, that is coeval to a vertical axis rotation of the structures at the transitional domain and an increase in the thrusts curvature (compare Figs. 2.6b and 2.6c). New tear faults trending parallel to the shortening direction develop close to the polymer lateral pinch-out in the transitional domain.

From this point until the end of the experiment, shortening amplifies previous structures. In the coupled domain, the orogenic wedge favours the propagation of contractional deformation towards the foreland with the initial inversion of the southern oblique graben which is subsequently cut by a foreland-directed thrust (Fig. 2.6d and 2.7a). In the decoupled domain, shortening concentrates at the salt-cored anticline located northwards of the southern salt wall, which is amplified developing a crestal collapse graben (Fig. 2.6d and 2.7a). Only during the last stages of deformation, the frontal thrust is reactivated (Fig. 2.6d). In the transitional domain, contractional deformation is accommodated by the thrust that nucleates at the apex of the reactive diapir inherited from the previous extensional episode (Fig. 2.4b). This structure links the salt-cored anticline of the decoupled domain with the frontal thrust of the coupled domain (Fig. 2.6d). At the northwards sector of the transitional domain, there is also a significant uplift of the graben because of the pre-salt impinging into the overburden (coupled deformation). Part of the deformation is absorbed by the reactivation of the inherited primary weld as a thrust weld.

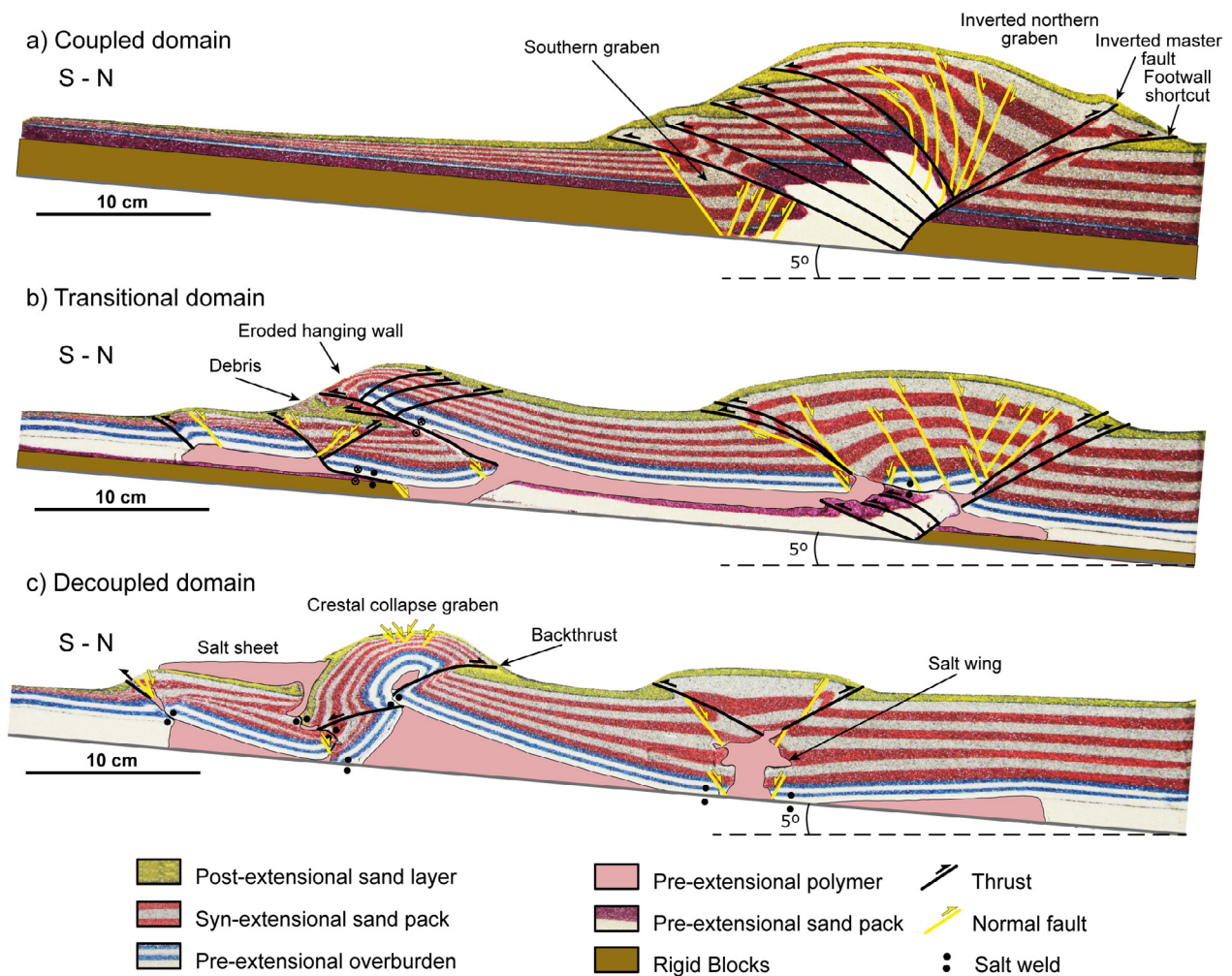


Figure 2.7 : Cross sections at the end of the compressional deformation (200 mm). A) coupled domain; B) transitional domain; C) decoupled domain. See Fig. 6d for location of sections.

2.4.3. MODEL-3

Model-3 followed the same kinematic evolution than Model-1 and Model-2, but in this case syn-contractional sedimentation was introduced (Table 1). Thus, due to the similar evolution of this model with Model-2, this section will only address the most remarkable differences due to syn-contractional sedimentation.

Despite syn-kinematic sedimentation, the contractional evolution of the three structural domains during early shortening is considerably similar to Model 2 (compare Figs. 2.6a and 2.8a). The most outstanding differences take place after 70 mm shortening when syn-contractional sedimentation inhibits the propagation of the deformation at the southern salt pinch-out. As a result, shortening is accommodated by the salt-scored anticline northwards of the southern salt wall (Fig. 2.8b), which for a similar shortening rate reaches a higher topographic relief (Figs. 2.6b and 2.8b). The buttressing produced by the secondary weld together with the syn-kinematic sedimentation, force that most of the deformation was absorbed by the back-thrust developing an asymmetric anticline (Fig. 2.9c). A new diapir pierces the

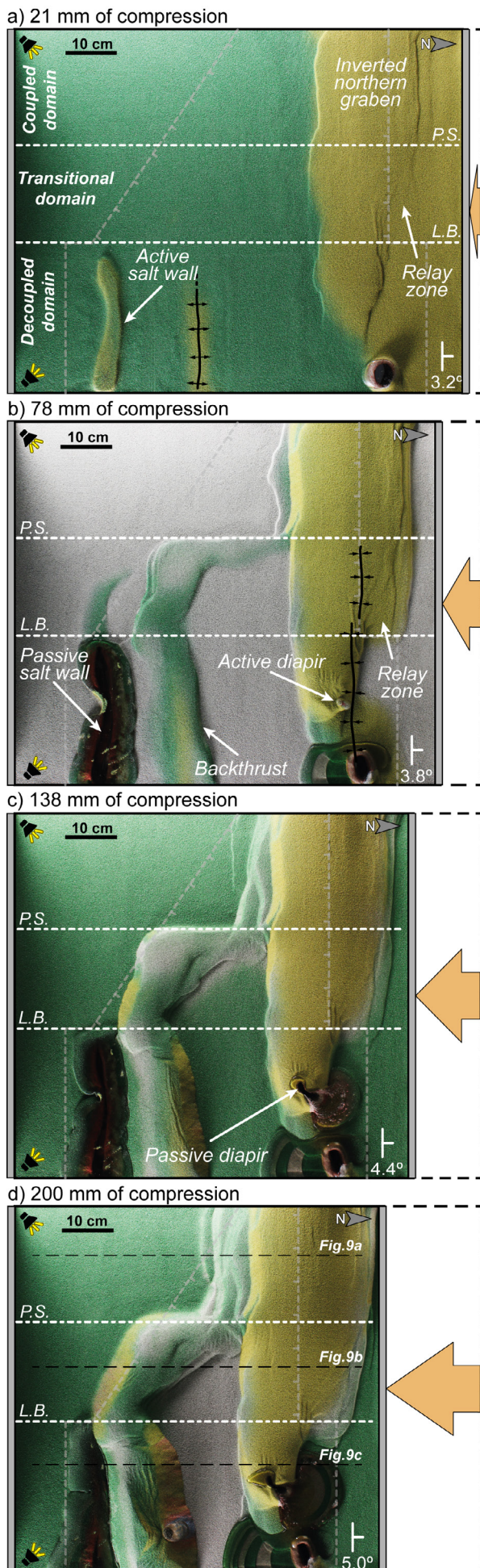


Figure 2.8 : Top view evolution of Model-3. Illumination comes from the left. The position of the basement rigid blocks is showed in grey dotted lines and the pinch-out of the salt (P.S.) and the limit of basement blocks (L.B.) in white dotted lines. A) top view after 21 mm of compression. B) top view after 78 mm of compression. C) top view after 138 mm of compression. D) top view at the end of compression (200 mm). See text for details.

overburden of the northern salt wall that progressively thins by crestal extension as fold growths. In the translational domain, the geometry of the structures is also slightly different from that of Model 2. In this case, just a N-S trending tear fault accommodates deformation throughout the experiment (Fig. 2.8b). In the coupled domain the oblique southern graben and its continuation towards the transitional domain is slightly folded and uplifted during this episode but is rapidly fossilized by subsequent syn-kinematic sedimentation (Fig. 2.9a).

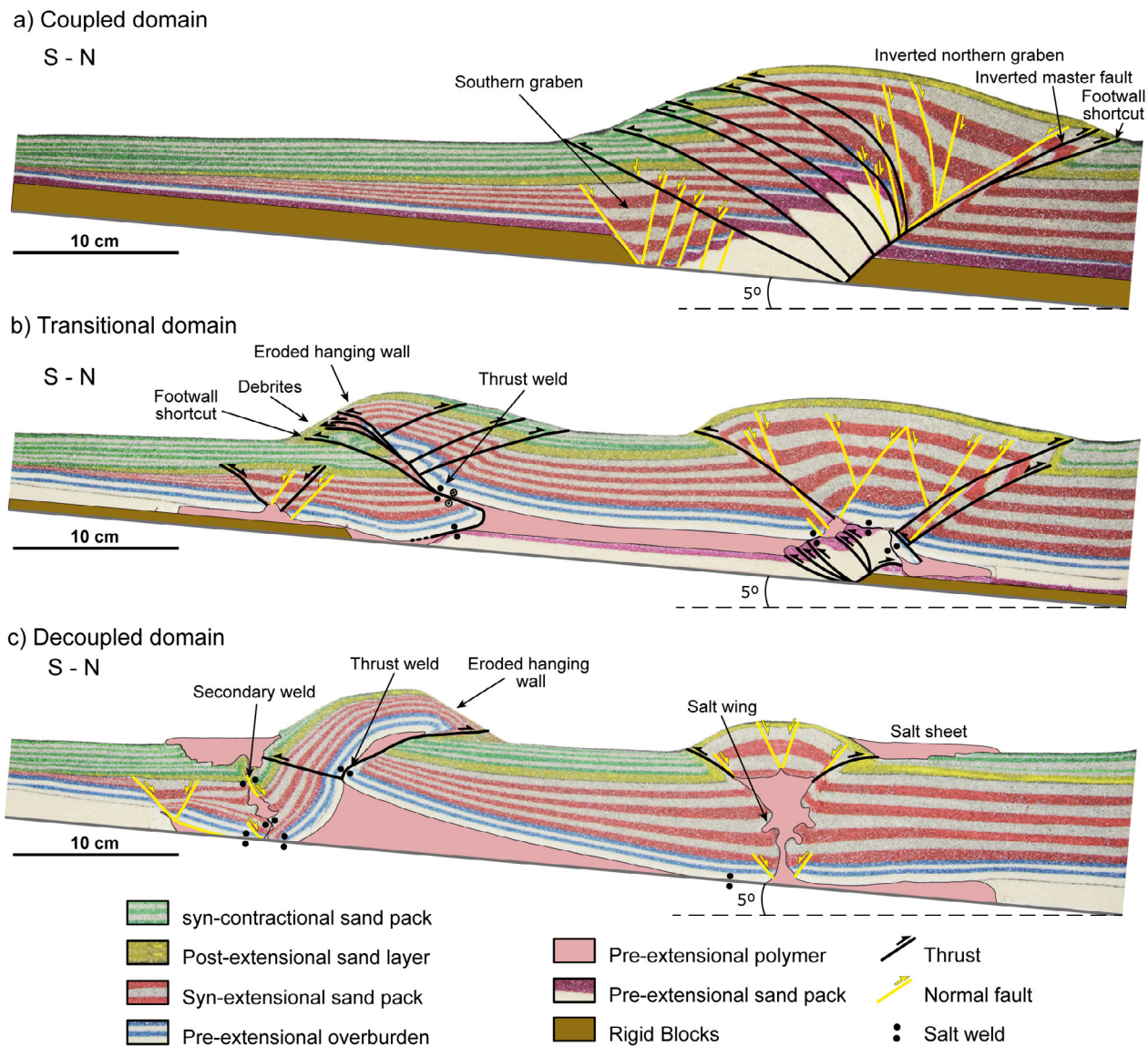


Figure 2.9 : Cross sections at the end of the compressional deformation (200 mm). A) coupled domain; B) transitional domain; C) decoupled domain. See Fig. 8d for location of sections.

During the subsequent stages of compression, the major structures of the model are barely amplified. A crestal collapse graben develops in the salt-cored anticline of the decoupled domain (Figs. 2.8c and d). Likewise, the volume of polymer at the salt sheets at the end of the experiment is less than in model 2. The final section of the decoupled domain (Fig. 2.9c) shows that the northern salt wall is practically welded at the end of the experiment.

This fact triggered a greater upwards polymer flow raising and folding the roof where an incipient crestal collapse graben developed (Fig. 2.9c). Notice the oblique southern graben of the coupled domain is inactive due to the syn-kinematic sedimentation that inhibit the forward propagation of the deformation until the end of the model (Figs. 2.8d and 2.9a).

2.5. DISCUSSIONS

2.5.1. THICK-TO THIN-SKINNED TRANSITION

The coupled domain presents a final thick-skinned architecture controlled by the reactivation of the edges of the rigid blocks, aiming to represent basement-involved faults, oriented E-W and NE-SW respectively, as observed in the studied field area (e.g. Cabuérniga, Rumaceo and Golobar faults, Fig. 2.1). On the contrary, the decoupled domain, as imposed by the presence of a silicon (salt) layer underneath the brittle succession, shows a thin-skinned architecture characterized by structures trending E-W, perpendicular to the main deformation axis, either in extension or contraction. Such evolution is consistent with the setup proposed (Fig. 2.3), however, what becomes relevant of these models is the transitional domain where the structures of both domains are linked.

During extension, the structures developed in the transitional domain at the early stages of deformation are located at the intersection between the edges of the rigid blocks and the pinch out of the silicon (Fig. 2.4b). However, their orientation follows the structural trend of the decoupled domain. This result confirms that even a thin layer of a weak horizon may promote decoupling from the underlying basement inherited features, regardless they may control the location of the suprasalt structures. The grabens developed in the transitional domain are overstepped with respect the ones formed above the decoupling domain, as the location of the latter depends on the thickness of the brittle overburden and the distance from the salt pinch out, and eventually from the salt walls. As a result of the non-collinearity between the extensional faults, relay ramps developed in the transitional domain connecting the parallelly-oriented grabens (Figs. 2.4b and 2.4c). In addition, the thickness of the salt controls the salt structures that developed in each domain. Thus, in the transitional domain, where the silicon progressively thins westwards, reactive diapirs form, whereas in the decoupled domain, where silicon is thicker, salt structures progressed to develop salt walls.

The formation of primary welds by salt evacuation in the decoupled domain has a significant impact on the location of new structures as deformation progressed, and, as a consequence, has also an impact on the trending of the younger extensional faults in the transitional domain, as their orientation depends on the linkage between the active

structures of the decoupled and coupled domains (Fig. 2.4d). Welding of the basins adjacent to the salt wall of the decoupled domain has promoted the migration of the deformation toward the pinch out of the salt layer as well as the collapse of the central salt pillow and related salt wall (Fig. 2.4d). These new formed extensional faults, which are located in a different position with respect the former ones, tend to connect with the reactivated basement-involved fault at the coupled domain, which remain in a fixed position. As a result, new extensional faults with an oblique trend form in the transitional domain. Such oblique grabens in the transitional domain could be interpreted without information of the modelling set up as the result of a dextral displacement of a subsalt N-S trending strike-slip faults.

During the contractional deformation, the transitional domain is also the area where oblique and transverse structures develop. However, and differently with respect to the extensional event, a hard linkage developed characterized by N-S strike-slip faults and thrusts connecting the frontal structures that develop in the decoupled and coupled domains (Figs. 2.6, 2.8 and 2.10). Salt structures developed during the extension in the decoupled domain are the first ones that experienced contractional deformation at the early stages of compression. Diapirs are squeezed and their overburden folded (Figs. 2.6 and 2.8). Syn-tectonic sedimentation localizes the deformation and delays or inhibits the activation of the southern (forward) pinch out of the silicon layer (Figs. 2.9-2.11). In the coupled domain, where silicon is absent, the contractional deformation localized in the northern graben. As a result, it has a significant impact on the structures that develop in the transitional domain as they connect through time the active structures in the coupled and decoupled domains. Thus, is the combination of the location of the salt structures, that developed during the extensional deformation, and the syn-compressional sedimentation, that controls the location of the active structures in the decoupled domain, which consequently determine the orientation and location of the structures in the transitional domain.

A change of vergence occurs in the thrust related to the central salt-core anticline. While a north-directed thrust affecting the northern limb is observed in the decoupled domain (Fig. 2.11a and b), due to the buttressing effect generated by the squeezed southern salt wall and the rotated southern limb, a south directed thrust is observed in the transitional domain where the southern salt wall is not present anymore and there is no buttressing forcing the deformation going northwards (Fig. 2.11d). In between a transition is observed in Figure 2.11c where both south directed and north directed thrust coexist. Eastwards, the south directed thrust links with a N-S strike slip fault developed during initial stages of

compression in the pinch out of the salt, connecting the deformation front of coupled and decoupled domains (Fig. 2.10). During contractional evolution, a vertical axis rotation is occurring in the frontal salt-detached structure, as the deformation in the couple domain remains to the north whereas in the transitional domain evolve southwards. As a result, the northern strike slip fault is observed in section view as a positive flower structure (Fig. 2.10f), controlled by the salt termination and bringing the decoupled and transitional domains to the south. The southern edge of the structure is described as a lateral ramp of a south-directed thrust linked to the central structure of the decouple domain (Fig. 2.10g).

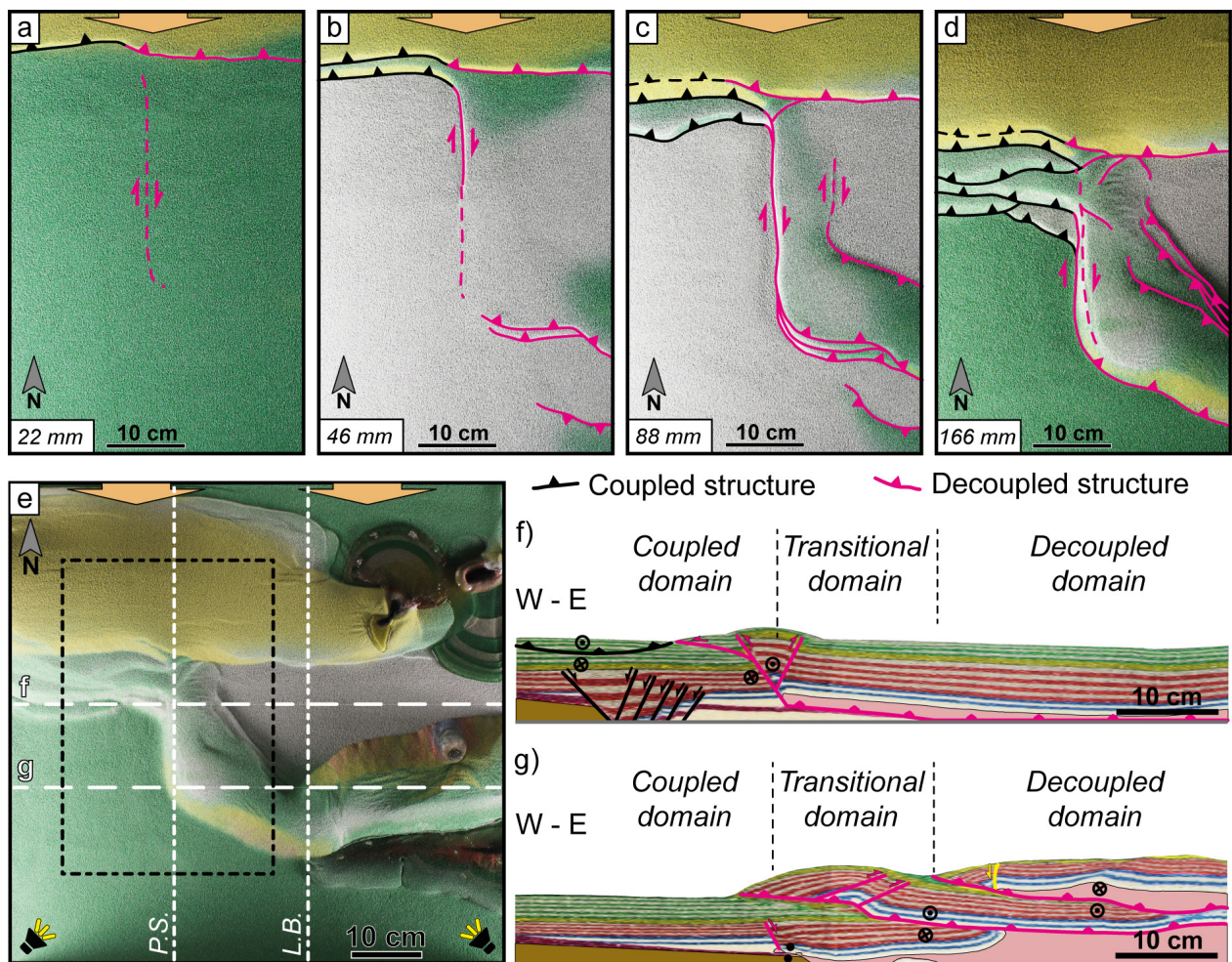


Figure 2.10 : The upper part shows a top view evolution of the transitional domains: a) after 22mm of compression, b) after 46 mm of compression, c) after 88 mm of compression, d) after 166mm of compression. E) top view at the end of compression (200 mm) with the location of the detailed evolution in black square (a to d). f) W-E cross section to the north (see location in e). G) W-E cross section to the south (see location in e).

The impact of the syn-compressional sedimentation on the transitional domain and associated structures is also notably. Whereas in the Model-2 structures striking NW-SE are developed during early stages of contraction being later crosscut by N-S strike slip faults (Fig. 2.6), in the Model-3 the active structures in both surrounding domains are in a different position resulting in a simpler evolution as explained above governed by N-S orientations.

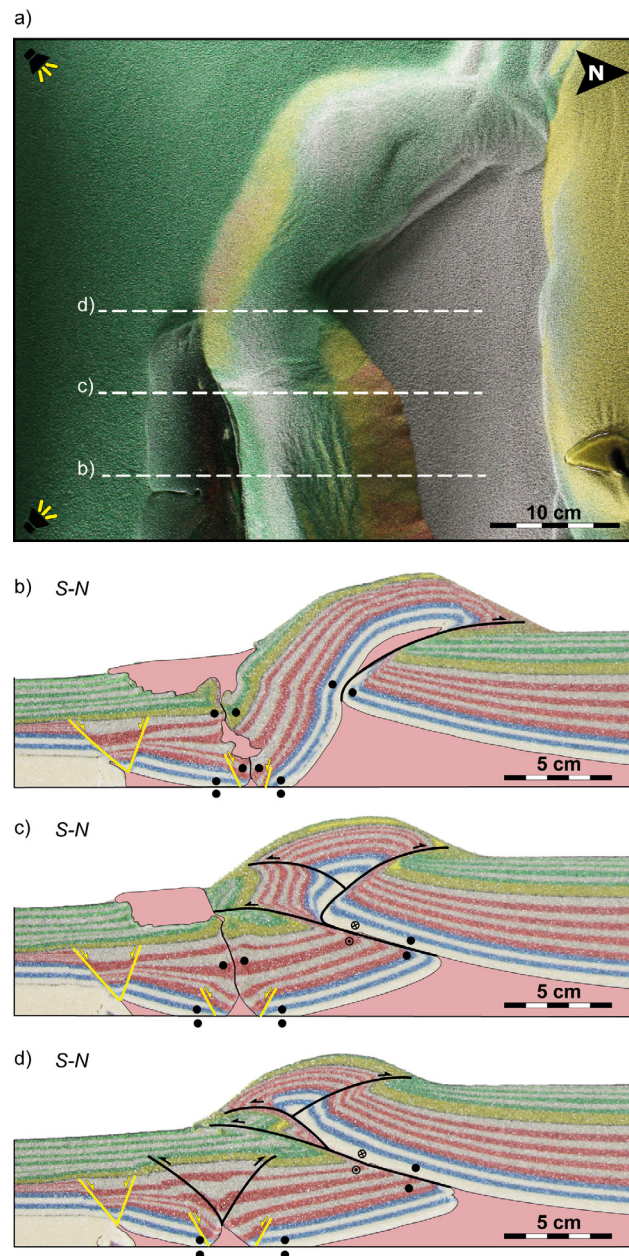


Figure 2.11 : a) top view at the end of compressional deformation with the location of detailed sections displayed below. B) to D) detailed cross sections from east (b) to west (d) showing the changing of vergence in structures from the decoupled to transitional domains. In section c) structures with both vergence coexist.

2.5.2. COMPARISON TO THE ASTURIAN MASSIF AND BASQUE – CANTABRIAN PYRENEES

A first general correlation of the models presented in this work and the transition between the Asturian Massif and the Basque – Cantabrian Pyrenees is the regional plunge to the east observed in both cases. The Asturian Massif presents higher topography and a narrower deformation zone, whereas the Basque – Cantabrian Pyrenees presents a lower topography and a wider area of deformation (Fig. 2.1). This work shows such correlation, as the Asturian Massif, consistently with the coupled domain, is controlled by the reactivation of basement structures following a thick-skinned structural style (Fig. 2.12c

and d). This domain is governed by the Coulomb-wedge theory, and because of the higher basal friction due to the lack of an efficient decoupling, more relief is supported before to create a new thrust in front, and as a result the area of deformation is narrow but high. On the contrary, the Basque – Cantabrian Pyrenees shows a final architecture similar to the one observed in the decoupled domain with a significantly different behaviour due to the presence of an efficient decoupling (i.e. salt) at the base. As such, the deformation tends to be transferred to the front creating large transport thrusts (Fig. 2.12e and f) and squeeze the salt structures favouring the extrusion of salt (i.e. salt glacier of Salinas de Rosio, Fig. 2.12b) resulting in a much wider deformation zone but less topography due to the major distribution of deformation. However, the contractional deformation applied in both coupled and decoupled domains in the models is the same, confirming the impact of the presence of a decoupling level for the final architecture of an orogen (Fig. 2.12a) which explains the regional plunge observed in the field as well as the distribution of deformation.

The transitional domain between the thick-skinned Asturian massif and the thin-skinned Basque Cantabrian Pyrenees is characterized by the presence of numerous oblique and

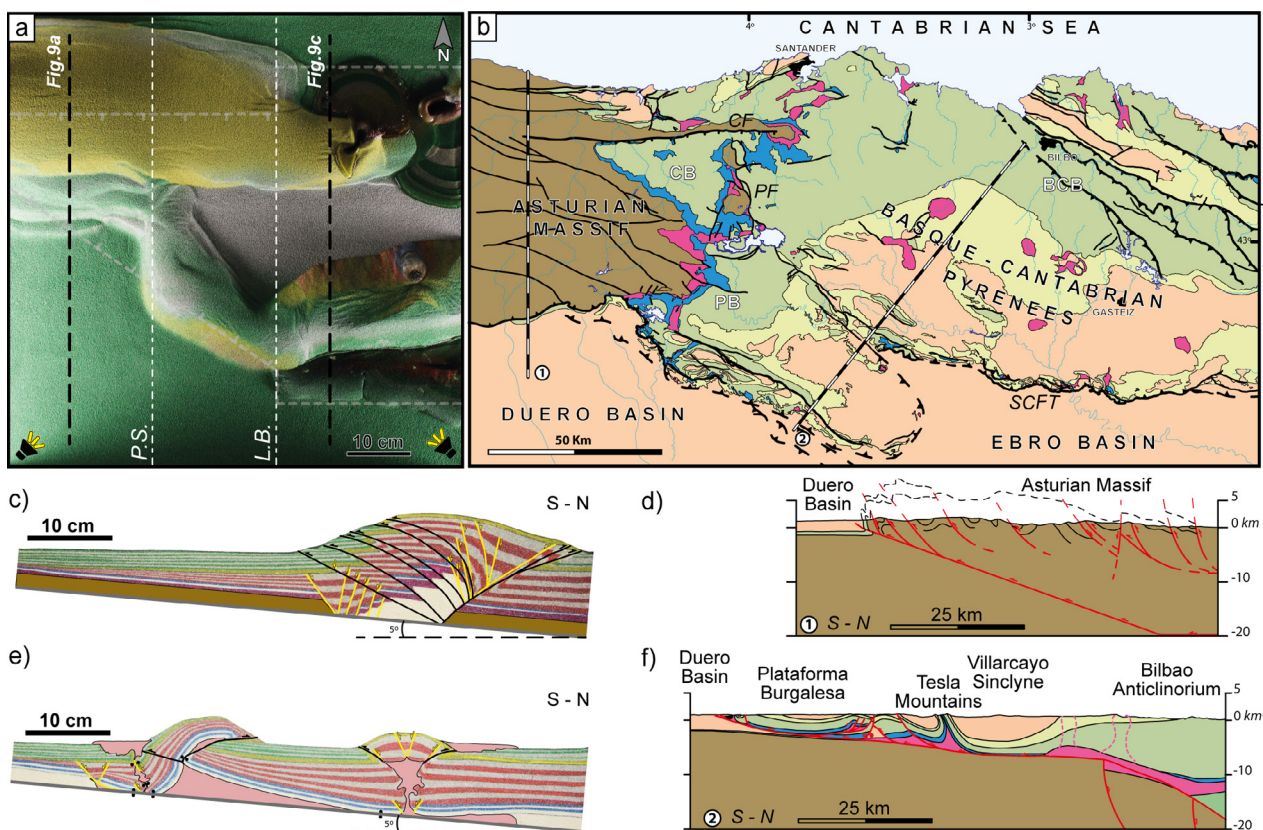


Figure 2.12 : a) top view of Model-3 at the end of compression. B) tectonostratigraphic map of the Basque – Cantabrian Pyrenees – Asturian Massif junction. C) cross section of the coupled domain showing the thick-skinned architecture in Model-3. D) cross section through the Asturian Massif showing the thick-skinned architecture similar to what observed in the model. E) section through the decoupled domain in Model-3. F) geological cross section across the southern Basque – Cantabrian Pyrenees showing the thin-skinned character.

transversal structures, as revealed in our models. The main structures in this transitional domain trend mostly N-S to NW-SE and are not consistent with a transpressive inversion model with a NW-SE shortening direction (Tavani et al., 2013) or with the reactivation of a regional basement transfer feature. In detail, the structures observed in the transitional domain between the Asturian Massif and Basque Cantabrian Pyrenees are more complicated than the ones reproduced in our models, mainly resulting from the intricate geometry of the Triassic and Late Jurassic-Early Cretaceous rifts systems that developed in the area and controlled the distribution of the Triassic salt (López-Gómez et al., 2019, Miró et al., *subm.*).

However, some striking similarities are observed. The Pas thrust system, oriented NW-SE to N-S, connects the western edge of the salt inflated area located north of the Plataforma Burgalesa with the inverted Cabuérniga extensional fault system, where the basement is involved. The hanging wall of the Pas thrust shows a pop-up structure as also revealed by our models (Figs. 2.9b and 2.10f). It involves the basement of the transitional domain that has been thrust on top of the coupled domain as partially shown in our models (Fig. 2.9b). In the section of Fig. 2.10f the Pas thrust would correspond with the western thrust of the pop-up at the boundary between the transitional and coupled domain. Regardless that in this section it is not the main thrust, it may change along strike bringing the subsalt succession on top of the salt layer as observed in other sections (Fig. 2.9b). Along strike changes of vergence in the transitional and decoupled domains is another feature reproduced in the models and observed also in the field case study (Figs. 2.9, 2.11 and 2.12). Other oblique features are observed further south in the transitional domain between the Asturian Massif and the Basque-Cantabrian Pyrenees (Fig. 2.2). They also connect the former salt walls or salt inflated areas located along the southern edge of the Plataforma Burgalesa and the present thrust front with the inverted basement-involved faults of the Asturian massif.

A second aspect related to the previous one is the distribution of syn-contractual sedimentation. Whereas in the Asturian Massif (*i.e.* coupled domain) the syn-contractual sedimentation occurred exclusively in the foreland Duero Basin due to the orogenic wedge developed to the north (Fig. 2.11c and d) (Pulgar et al., 1999; Alonso, 2007), in the Basque – Cantabrian Pyrenees (*i.e.* decoupled domain) the distribution of deformation favoured a more distributed topography and therefore a more distributed syn-contractual deformation both in the foreland basin but also in the piggyback basins between the main salt structures (Miró et al. *subm.*) (Fig. 11e and f). In between, minor basins with triangular shapes partially controlled by thick-skinned and thin-skinned structures are located (*e.g.* Cabuérniga and Polientes Basins).

2.6. CONCLUSIONS

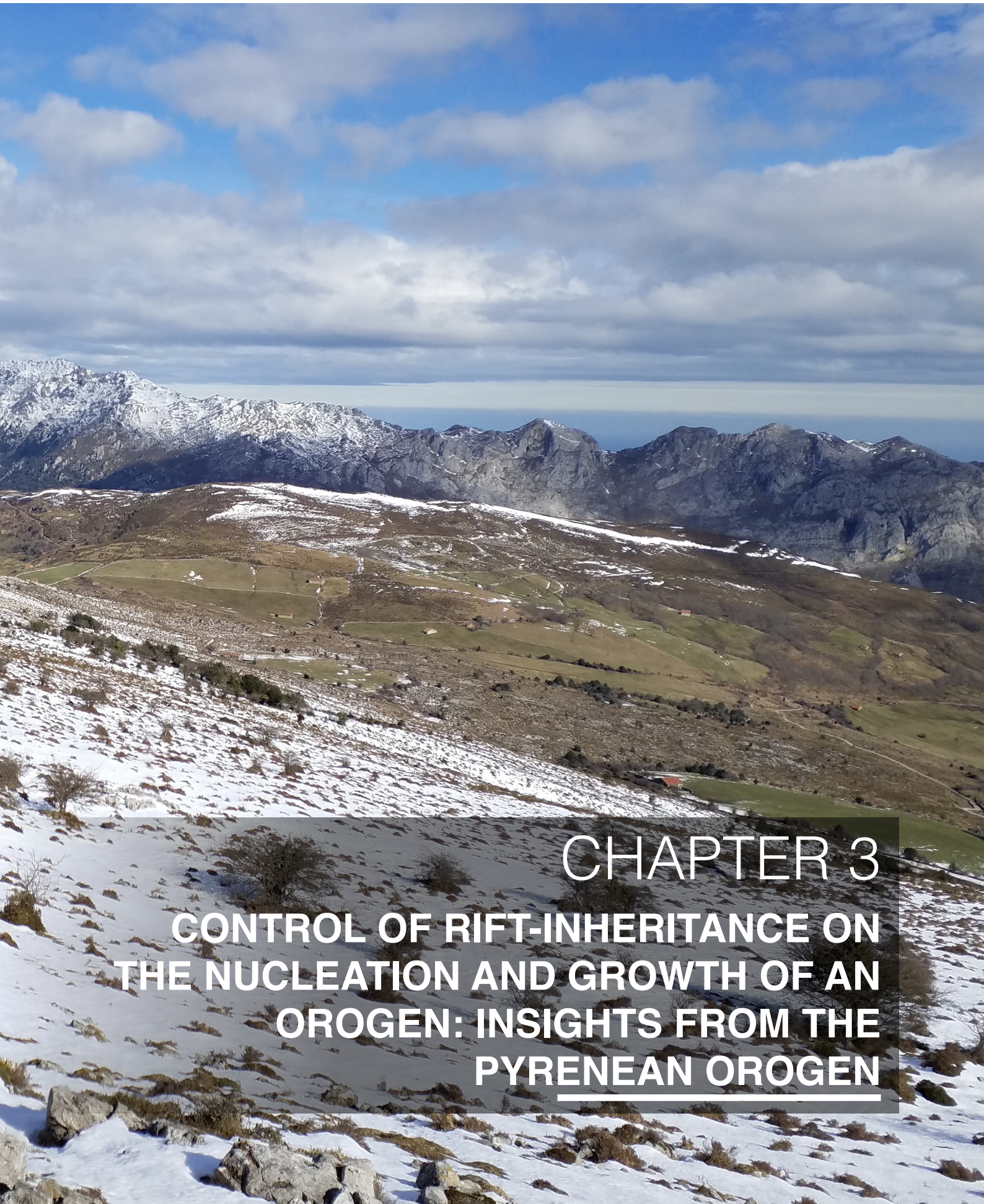
The aim of this study is to understand how deformation is distributed along thick- to thin-skinned transitions in order to better understand the link between the Asturian Massif and Basque – Cantabrian Pyrenees. The experimental program presented here demonstrates that in transitional areas between domains with and without salt, oblique structures are generated in which orientation and kinematics depends on the evolution of active structures in the surrounding thick- and thin-skinned domains. Thus, the distribution of salt, which depends on the geometry and distribution of the previous basement-involved rift system, will have a fundamental impact determining the position and distribution of structures in transitional domains.

Moreover, it is reinforced the thin-skinned structural deformation interpreted in the Basque – Cantabrian Pyrenees by presenting significant analogies with the models presented. Domains with presence of salt results in a wider distribution of deformation and less topography in comparison to the thick-skin domains. The syn-tectonic sedimentation is distributed both in foreland basins but also within the deformed areas between salt structures, whereas in thick-skinned dominated areas syn-contractional sedimentation is mostly restricted to foreland basins.

ACKNOWLEDGEMENTS

This work was funded by the Orogen project, a consortium for research between CNRS, TOTAL and BRGM. The experiments were carried out in the GEOMODELS Analog Modeling Laboratory at the University of Barcelona.





CHAPTER 3

CONTROL OF RIFT-INHERITANCE ON THE NUCLEATION AND GROWTH OF AN OROGEN: INSIGHTS FROM THE PYRENEAN OROGEN

The cover of Chapter 3 depicts the western termination of the Cabuérniga Basin with the Asturian Massif in the background (Lamasón Valley, Cantabria).

CONTROL OF RIFT-INHERITANCE ON THE NUCLEATION AND GROWTH OF AN OROGEN: INSIGHTS FROM THE PYRENEAN OROGEN

Geology, in prep.

J. Miró^{1,2}; R. Lescoutre³, P. Cadenas⁴, G. Manatschal¹, J.A. Muñoz²

¹ IPGS, CNRS-UMR 7516, Université de Strasbourg, 1 rue Blessig, 67084 Strasbourg, France

² IRG, DDTO, Universitat de Barcelona, Martí i Franquès s/n, 08028 Barcelona, Spain

³ Department of Earth Sciences, Uppsala University, Villavägen 16, 75236 Uppsala, Sweden

⁴ BCSI, ICM, CSIC, Passeig Marítim de la Barceloneta 37, 08003 Barcelona, Spain

ABSTRACT

This work aims to investigate the influence of rift-inheritance and related decoupling levels during the reactivation of segmented hyperextended rift systems and subsequent orogenic evolution by using the Pyrenean Orogen as a natural laboratory. Three crustal sections show different orogenic architectures that reflect the temporal and spatial reactivation of a complex 3D rift template. Embryonic, local subductions nucleated in the exhumed mantle domain along the strongly segmented rift system, using serpentinized mantle as a decoupling level. Collision initiated in the east, where exhumed mantle and hyperextended domains were first consumed resulting in the transfer of the locus of deformation to mid-crustal levels. Collision occurred across the whole domain, even where mantle remained available for subduction (e.g. Western section). In salt dominated parts (e.g. Central section), shortening was accommodated by thin-skin tectonics, resulting in a decoupling of the sedimentary section from the underlying basement. Thus, while initial stages of reactivation and collision are mainly controlled by rift-inheritance, more advanced stages of collision are likely dominated by orogenic growth controlled by the Coulomb-wedge theory.

3.1. INTRODUCTION

Numerous studies investigated subduction zones and collisional orogens (e.g. Jamieson & Beaumont, 2013), however, little is known about how the structures nucleated and grew in time and space and how far the inherited rift template controlled this evolution. This subject has been handled in few studies [e.g. Caledonides (Andersen et al., 2012), Alps (Beltrando et al., 2014) and Pyrenees (Tugend et al., 2014a)], however, the main problem is the lack of good analogues and the fact that modelling the onset of convergence and testing realistic initial conditions remain challenging.

Previous studies described the importance of decoupling levels such as serpentinized mantle, ductile mid-crustal levels, and intra-sedimentary low frictional layers (e.g. salt or clays) inherited from the rift phase for the subsequent contractional reactivation (e.g. Peron-Pinvidic et al., 2008; Lundin & Doré, 2011; Erdos et al., 2014; Lescoutre & Manatschal, 2020; Miró et al., *subm.*). While the importance of such levels has been investigated in 2D sections, their along-strike variability and their control on the nucleation and along strike architecture of orogenic systems is yet little understood.

In this study, the 3D aspect of such decoupling horizons and their role during incipient reactivation of a segmented rift system is discussed. The study is using a unique natural laboratory, the Bay of Biscay – Pyrenean system, partially integrated in the Pyrenean Orogen (Fig. 3.1) resulting from the inversion of the North Iberian Rift System (NIRS). The Mesozoic NIRS developed as a result of a multistage and polyphase rift evolution (Tugend et al., 2014a; Cadenas et al., 2020; Miró et al., *subm.*) and displays a significant along-strike segmentation of the rift system. Reactivation and inversion of the NIRS occurred during the northward displacement of Iberia and Africa relative to Europe that was in the order of 140 ± 30 km (Macchiavelli et al., 2017).

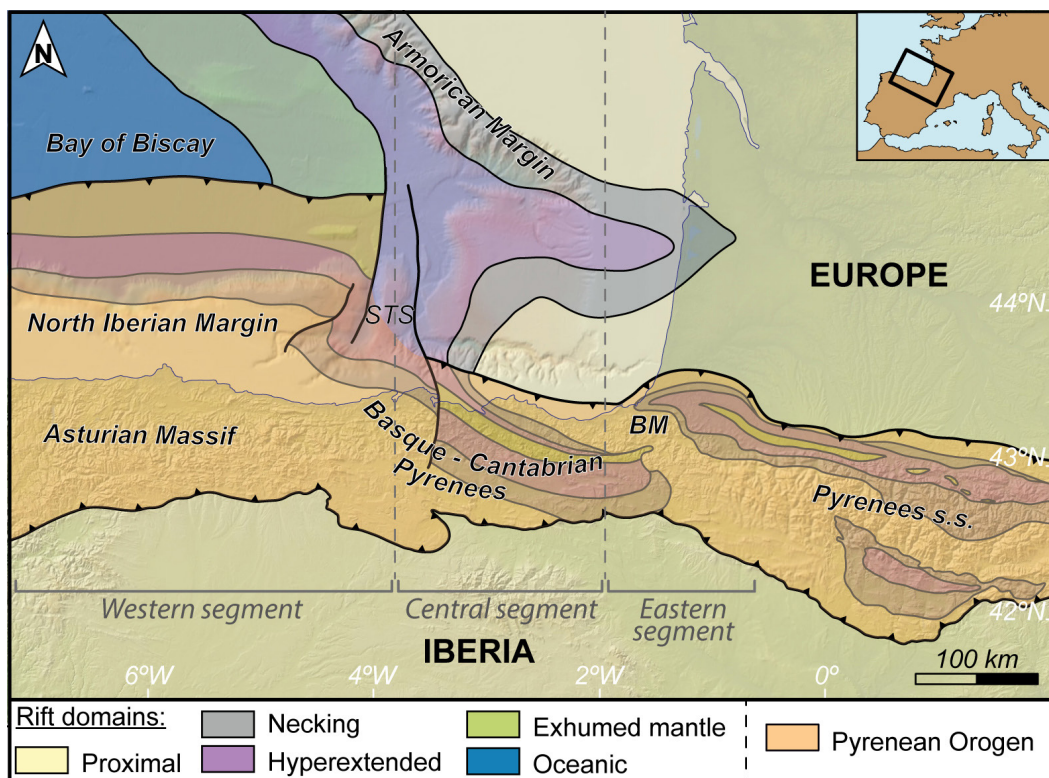


Figure 3.1 : Rift domain map of the Pyrenean – BoB area. STS: Santander Transfer System, W: Western section, C: Central section; E: Eastern section. Modified from Tugend et al., 2014 and Cadenas et al., 2018

The present-day orogenic architecture of the Pyrenean Orogen, extending from the Asturian Massif in the west to the easternmost Pyrenees s.s. to the east, has been intensively studied over the last decades by using geophysical (Chevrot, et al. 2018; Pedreira et al., 2007; Ruiz et al. 2017) and geological (Roca et al., 2011; Muñoz et al., 2018; Quintana et al., 2015; Teixell et al., 2018) approaches, ranking it among the most investigated and best imaged orogenic systems worldwide. The structure of the Pyrenees s.s. can be described as a north-dipping slab rooting a double asymmetric crustal wedge (Chevrot et al., 2018; Muñoz, 1992) while the Asturian Massif to the westernmost mountain belt, shows a more complex and immature orogenic architecture bounded to the north by a partly reactivated passive margin along the North Iberian Margin (Fernández-Viejo & Gallastegui, 2005). As a result, incipient stages of reactivation are preserved along strike, allowing to assess the influence of inheritance during the reactivation of a rifted margin in the west and a hyperextended rift system in the east, today preserved in the Pyrenean Orogen.

3.2. THE BASQUE – CANTABRIAN PYRENEES (BCP)

The BCP can be represented by three regional cross sections, referred to as the Western, Central and Eastern sections, representing three different final orogenic architectures showing the along strike variability of the system (Fig. 3.2). The N-S trending Western section shows, to the north, a south-dipping embryonic subduction of exhumed mantle (Cadenas et al., 2020) and, to the south, a north-dipping intra-Iberian slab (Fig. 3.2, 0 Ma stage) thrust under the Palaeozoic rocks of the Asturian massif (thick-skinned deformation). However, the sedimentary cover is detached over the Upper Triassic salt in the southern and central part of the section (thin-skinned deformation) leading to a hybrid structural style. (2) The Central section strikes SW – NE and is interpreted as a thin-skinned dominated section where the folded sedimentary cover is detached along the Upper Triassic salt. Nevertheless, the Iberian crust is thrust under the European crust in a thick-skinned manner (Muñoz, 2019; Miro et al., *subm.*) (Fig. 3.2, 0 Ma stage).

Finally, the SW-NE oriented Eastern section is characterised by two main thrusts of opposite vergence underthrusting the European and Iberian crusts beneath a crustal wedge (thick-skinned deformation) corresponding to the Basque Massifs (Fig. 3.2, 0 Ma stage). North and south of the Basque Massifs, the two former rift basins have been detached in the Upper Triassic evaporites (thin-skinned deformation), along which serpentized mantle rocks have been recognized, and inverted as a pop-up structure (Lescoutre & Manatschal, 2020).

3.3. THE NORTH IBERIAN RIFT SYSTEM

Here, an attempt to establish the NIRS template at the end of the last Aptian to Middle Cenomanian rift event corresponding to the pre-orogenic state is presented. The NIRS is slightly reactivated to the west but strongly inverted to the east. Remnants of the former rift system including exhumed subcontinental mantle, rift structures and the pre- to syn-rift stratigraphic record, allow to restore the area back to the end of extension. The restoration of the system used the three fundamental concepts of restoration of rift systems which include: 1) crustal areal conservation, 2) use of rheological interfaces, and 3) respecting isostasy (see Miro et al. *subm.* for details).

The NIRS is characterized by a set of E-W trending basins along the Iberia – Europe plate boundary (e.g. Bay of Biscay (BoB), Basque – Cantabrian Basin and Mauléon Basin). The three sections in Fig. 3.2 (95Ma stage) show three different rift architectures along the system: (1) to the west, rifting lead to mantle exhumation and eventually oceanic accretion in the BoB forming a mature passive margin (Fig. 3.1); (2) in the Central section extreme crustal thinning and mantle exhumation are suggested by the occurrence of mantle and granulite rocks, syn-rift High Temperature/Low Pressure (HT/LP) metamorphism and thick (>15 km) syn- to post-rift sediments; and (3) in the Eastern section two overlapping hyperextended rift segments north and south of the Basque Massifs, locally associated with mantle exhumation and HT/LP metamorphism and terminating as V-shaped basins, have been evidenced based on restored cross-sections (Lescoutre et al. *subm.*). As a result, a complex distribution of segmented V-shape rift basins at different stages of maturity characterize the NIRS at the end of the rifting phase (Fig. 3.2, 95Ma stage).

3.4. THE INVERSION OF THE NORTH IBERIAN RIFT SYSTEM

Although indirectly supported by plate kinematic models (Macchiavelli et al. 2017; Nirrengarten et al., 2018), the onset of reactivation of the NIRS at Late Santonian remains poorly recorded and is mostly suggested based on local field observations in the Pyrenees s.s. (Boillot & Capdevila, 1977; Teixell, 1996; Muñoz, 1992; Mencos et al., 2015) and in the Basque-Cantabrian Pyrenees (Razin, 1989; Ferrer et al., 2008). In contrast, thermochronological data from the Palaeozoic massifs of the Pyrenean Orogen and the syn-orogenic sedimentary record in the foreland basins broadly suggest crustal thickening and onset of collision at Eocene until Miocene (e.g. DeFelipe et al., 2019; Bosch et al., 2016; Fillon et al., 2016). Thus, the timing and the mode of deformation at the onset of reactivation remain ill defined. Yet, by comparing the distribution of the three main decoupling levels in the present-day and restored cross-sections across the 3 segments along the NIRS, a consistent model for reactivation can be proposed.

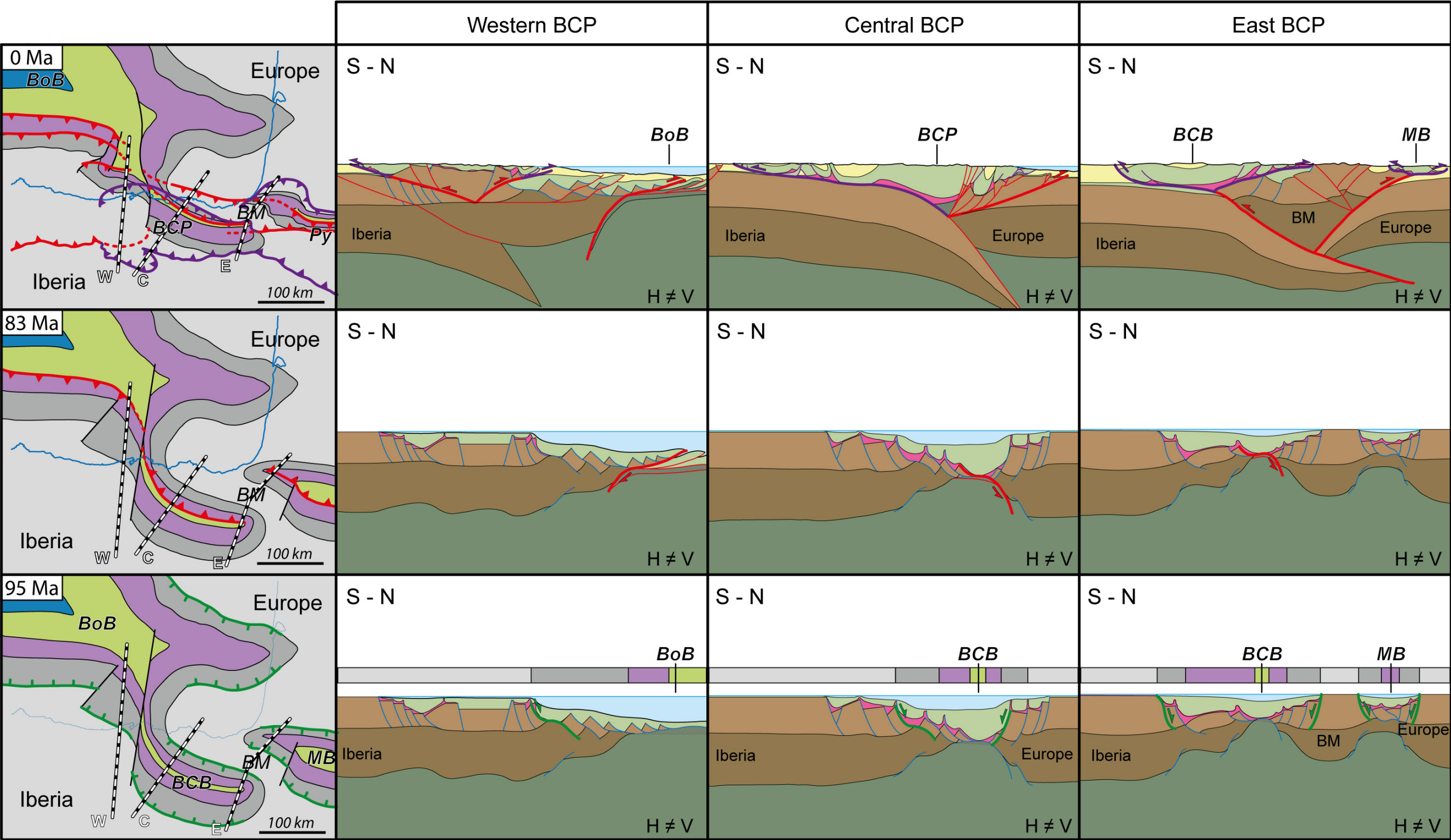


Figure 3.2: Present-day and restoration to onset of compression and end of extension of the BoB - BCP represented by rift domain maps to the left and three representative sections to the right showing three different scenarios. Sections modified from Miró et al., subm. and Lescoutre et al. subm.

In the Western section, the most distal parts of the hyperextended rift system are partially preserved and correspond to the exhumed mantle domain (Cadenas et al., 2020; Miró et al., *subm.*). During exhumation, the uppermost mantle was serpentized due to the interaction with seawater. Serpentinization at rifted margins rarely affects levels deeper than 6 km (Gillard et al., 2019) and represents, due to its low friction, an important decoupling level that can be reactivated during the initial stages of convergence (Peron-Pinvidic et al., 2008). Since serpentization may have occurred beneath the hyperextended crust, the fresh and stronger mantle was pushed back into the mantle while the overlying serpentized mantle and hyperextended crust were accreted in the embryonic accretionary wedge (Miró et al., *subm.*, Fig. 3.2, 83Ma stage). It is important to note that during this proto-subduction of mantle beneath the hyperextended crust no major crustal thickening is expected.

In the Central section, and similarly to the Western section, the serpentized exhumed mantle was used as a decoupling level and accommodated shortening by allowing subduction of the dense, not serpentized mantle. However, the occurrence of salt throughout the section explains the role of salt since early stages during reactivation. This favoured the thrusting of the salt overburden over the forelands already during early stages and the reactivation of salt structures, allowing to form locally syn-contractual sediments (Fig. 3.2, 83Ma) (Pujalte et al., 2000; Robles et al., 2014).

In the Eastern section, a proto-subduction started in both V-shaped rift basins governed by serpentized mantle. However, the presence of the Basque Massif crustal block in between the two hyperextended basins conditioned the co-existence of thick and thin-skinned structures along strike. While the sedimentary basins were detached in the Upper Triassic salt and passively inverted as pop-up structures, new thick-skinned shortcuts connected the termination of hyperextended domains (i.e. tip of subduction) of both segments through the Basque Massif.

Our observations suggest that reactivation of the NIRS initiated in the exhumed mantle domain, being strongly controlled by the rift template. While subduction was in the BoB towards the south, in the adjacent BCP it was north dipping. Such along-strike change of subduction direction required a transfer system between the two basins (i.e. STS, Fig. 3.1). In contrast, in the eastern section two subduction of opposite direction initiated north and south of the Basque massifs, leading to the formation of thick-skinned short-cutting structures at the termination of the two overlapping rift segments. Such shortcutting structures of opposite vergence were responsible for the formation of a pro-orogenic wedge already in the early stages of convergence.

When the necking domain entered subduction, a major change in the evolution of the orogenic occurred. These zones are made by >10 km continental crust not allowing the serpentinization of the underlying mantle. As a consequence, these zones are coupled to the mantle and acted as a buttress leading to start the main collisional phase, coinciding with the growth of topography. In the Eastern section, the Basque massif was uplifted as a pop-up structure and finally resulted in the subduction of Iberia beneath Europe as observed in the Pyrenees s.s. (Fig. 3.2, 0 Ma stage). In the Central section Iberia subducted beneath Europe reactivating basement structures of the overriding plate (i.e. Europe). The subducting plate was however only slightly reactivated due to the high amount and efficiency of the salt in decoupling the deep, thick-skinned basement structures from the overlaying sedimentary cover.

A major re-organisation of the orogenic system in the western section occurred once “subductable” domains were consumed in the sections further to the east during Eocene time. The deformation front was transferred southward by creating a northward intra Iberian thrust domain. It is interesting to note that the new, intraplate fault system, is not related to any recognisable syn-rift structure, but it is located in the along-strike continuation of the thin-skinned South Pyrenean Frontal Thrust in the sections further to the east. From that moment onwards, a continuous E-W striking fold and thrust belt formed along the Pyrenean Orogen.

3.5. FROM A HYPEREXTENDED SYSTEM TO A COLLISIONAL OROGEN

Based on our study of the Pyrenean Orogen natural laboratory, we can establish a generic model for the reactivation of hyperextended rift systems and their incorporation in orogens. In both section and map views, the presence and distribution of three rift-inherited decollement levels are fundamental.

The first reactivation phase occurring in hyperextended rift system is the subduction/accretion, occurring in the most distal domains where the mantle is exhumed and serpentinized. These domains compose the weakest part of the system, host the most efficient decoupling (i.e. serpentinized mantle) and they present dense material (i.e. fresh mantle) that can be subducted beneath hyperextended crust. Since the hyperextended rift system and the related decoupling system is segmented, during onset of convergence reactivation initiates in each basin independently (Fig. 3.3a). Furthermore, the subduction of mantle beneath hyperextended crust does not create significant topography and, as a result, syn-contractional sediments are difficult to identify. The hyperextended domain composed

of very thin crust is likely to subduct following the fresh mantle or being incorporated in the subsequent early collisional phase explained hereafter. Subsequently, the early collisional phase starts when the exhumed mantle domains are subducted, and the necking domains of both conjugate margins collide. The mid-crustal decollement is reactivated, previous basement extensional faults are reactivated, and the crust starts to thicken by accretion (Fig. 3.3b). Consequently, topography starts to grow, and syn-compressional sediments form and can record this process in the foreland basins. Finally, the late collisional phase, is characterized by the main stacking of crust in the hinterland resulting in a prominent topography. This is the most favourable moment to reactivate the uppermost decollement, thrusting the sedimentary succession to the forelands using sedimentary features (e.g. salt or clays) (Fig. 3.3c). However, the stratigraphic architecture, including possible salt or clay levels, strongly controlled by the rift evolution, will significantly influence the reactivation as well as the final architecture of the orogen. As such, if the salt is pre-rift and thick enough to be continuously present at the end of extension, this decoupling will be reactivated during early stages of contraction resulting in wider and less high orogens.

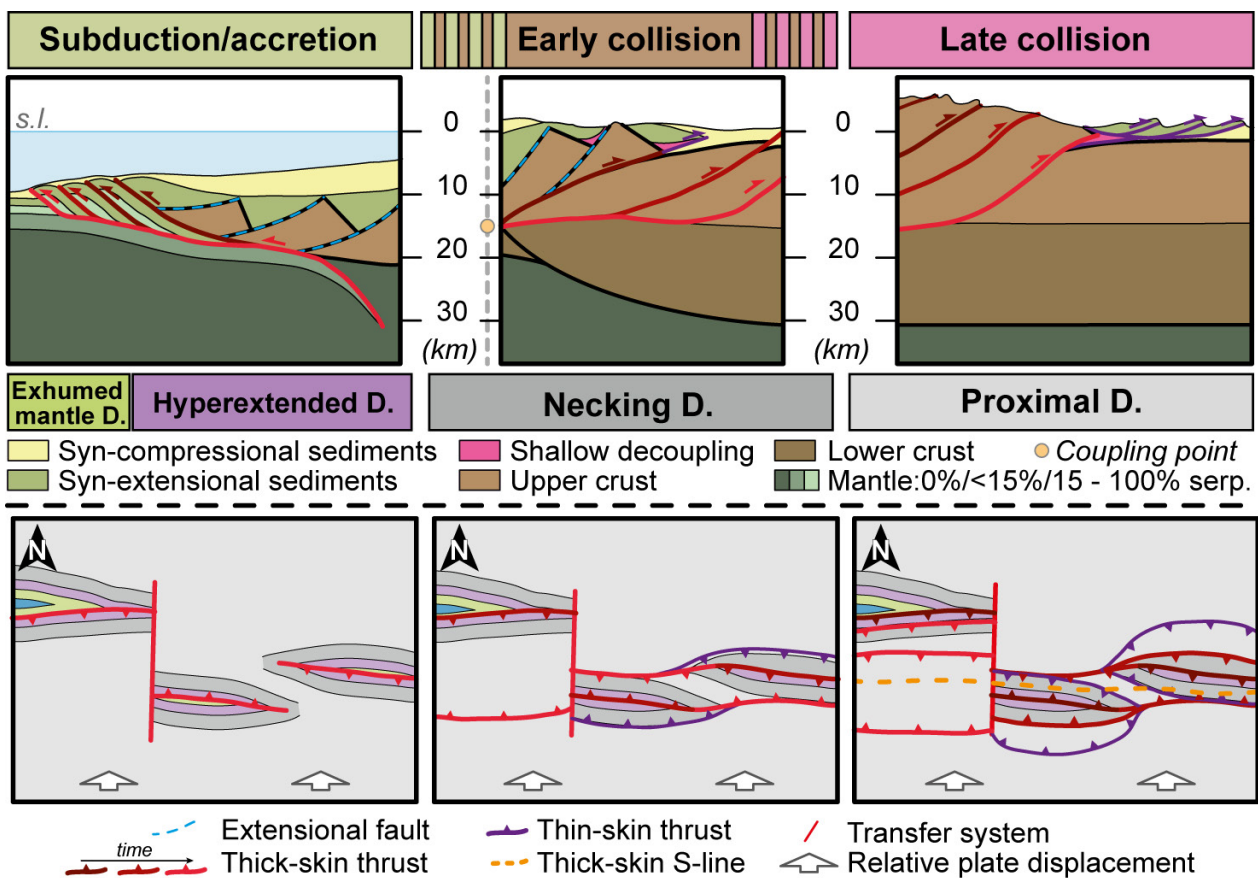


Figure 3.3 : Reactivation of a hyperextended rift margin model in section view (top) and map view (bottom). Note the distribution of the main decollements and the link between rift domains and evolution (i.e. timing) of an orogen.


3.6. CONCLUSIONS

This work attempted to investigate the role of rift-inheritance during the reactivation of a segmented and hyperextended rift system. A key factor resulted in the understanding of the rift template and the distribution of decoupling levels that can be potentially used during subsequent reactivation in time and space which is controlled by the rift template. Thus, although a cylindrical orogenic structure is predicted for the formation of an accretionary wedge in layer-cake models (Davis et al., 1983), in reality a diachronous and complex orogenic evolution appears to be controlled during initial stages by rift inheritance (early subduction and collision phase) while the later stages may be approximated by the classical Coulomb wedge-theory.

ACKNOWLEDGEMENTS

This study was funded by the Orogen project (consortium of CNRS, Total and BRGM).



A full-page background image showing a rugged coastline. Dark, jagged rock formations protrude from the sea. White, frothy waves are crashing against the rocks, creating large splashes and spray. The sky is overcast with grey clouds. The overall mood is powerful and dramatic.

GENERAL SYNTHESIS AND DISCUSSION

The cover photo of the General Synthesis & Discussion depicts a steeply dipping bedding of turbidites with nicely preserved pillow lavas (Armintzako Portua, Bizkaia).

GENERAL SYNTHESIS AND DISCUSSION

The main purpose of this project was to focus on the role of inheritance and segmentation during the formation and subsequent reactivation of hyperextended rift systems and their incorporation into collisional orogens. The Basque – Cantabrian Pyrenees are the perfect case study to develop such investigations with the final goal of understanding this area as well as obtaining new ideas and concepts to export and help the study of other analogue systems worldwide. The Basque – Cantabrian Pyrenees link the Pyrenees s.s. to the east with the Asturian Massif to the west and the Bay of Biscay to the north, and define a triple junction between the Iberia – Ebro – European plates (see Introduction, Fig. I.17 and Chapter 1). However, the extensional evolution of this domain appears to be more complex than what has been proposed previously (i.e. García-Mondéjar, 1989; Quintana et al., 2015; Pedrera et al., 2017; García-Senz et al., 2019) resulting from a multistage and polyphase evolution leading the formation of a segmented rift system (see Chapter 1). Both during extension and reactivation, the distribution of Upper Triassic salt subdivided the area into different structural domains (thin- vs thick-skin), which are linked by the so-called transitional domains where oblique structures predominate increasing the structural complexity of the system (see Chapter 2). Segmentation resulting from the multistage and polyphase rift evolution combined with the presence and distribution of main decoupling levels (serpentinized mantle, mid-crustal levels and salt) had a strong impact on the subsequent reactivation and formation of the Pyrenean Orogen (see Chapter 3). In this synthesis, the main questions established in the introduction are discussed and the main ideas and learnings are emphasized.

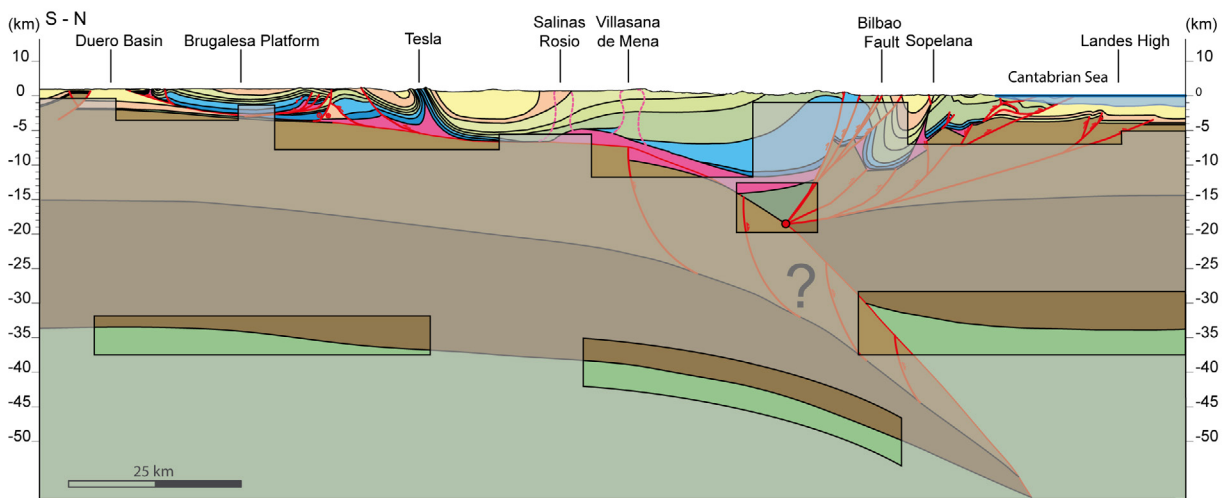
INTEGRATION OF DATASETS TO BUILD A COHERENT FRAMEWORK AND A CONSISTENT INTERPRETATION OF THE BASQUE – CANTABRIAN PYRENEES.

This thesis offered the opportunity to work with a wide range of datasets including field data, seismic reflection and refraction, borehole, gravity, and magnetic data bridging a wide range of scales. Existing datasets have been integrated, together with new data/observations in a coherent framework (i.e. 3D workspace in Move) to build a consistent interpretation of the Basque – Cantabrian Pyrenees shown in Chapter 1. Fig. D.1 illustrates, using the example of the Central and Western sections, the areas covered by direct (field) and indirect (geophysical) observations that allowed to construct the whole sections.

Refraction seismic data and the resulting velocity models were used to determine Moho depth. This type of data provides a good approximation and imaging of deep crustal levels

while potential field techniques are non-unique and only allow to test interpretations (e.g. gravity models used by Pedrera et al., 2017; García-Senz et al., 2019). The interpretation of most of the seismic reflection data available in the area combined with the projection of borehole data made possible to interpret the upper part of the crust defining the top basement, which seems to be almost flat or slightly dipping to the north beneath the southern limb of the Bilbao Anticlinorium and Alavesa Platform (see Chapter 1). This interpretation contrasts with previous interpretations where top basement shows reactivated blocks controlling the present-day architecture of the sedimentary succession (e.g. Quintana et al., 2015). The combination of previous datasets enabled also to determine the thickness variation of the crust and the architecture of the underthrust slabs (see Chapter 1).

a) Central Basque - Cantabrian section



b) Western Basque - Cantabrian section

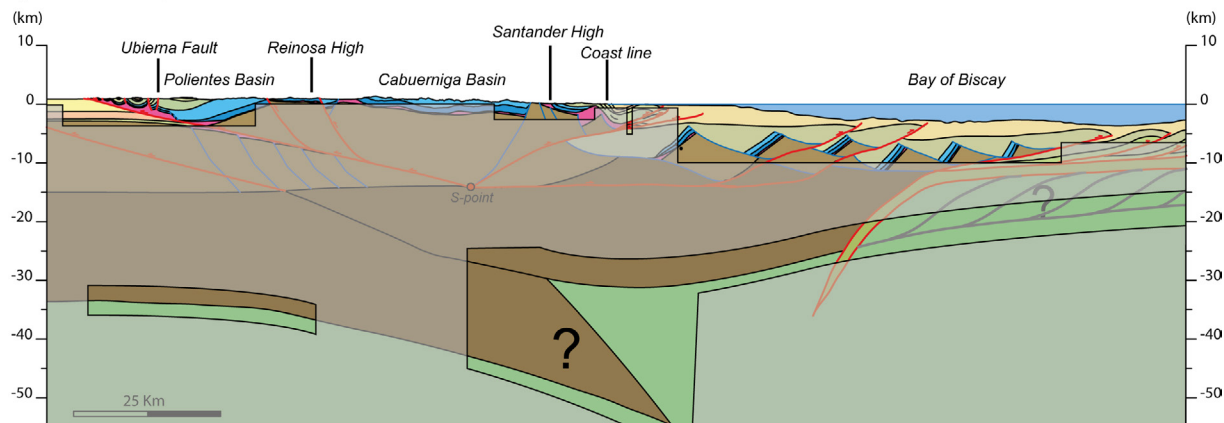


Figure D.1 : a) Central Basque – Cantabrian section and b) Western Basque – Cantabrian section with the geological and geophysical observations highlighted.

The correlation of reflexion seismic data, boreholes and field observations in a 3D workspace enabled to establish a consistent tectono-stratigraphic framework. Contrary to what have been proposed previously by Quintana et al. (2015), Pedrera et al. (2017) and García-Senz et al. (2019) among others, several indicators revealed in this work argues for

a thin-skin structural style in the Basque – Cantabrian Pyrenees: the preservation of diapirs in the southern limb of the Bilbao Anticlinorium while squeezed salt structures in the deformation front, the amount of salt drilled by boreholes (e.g. > 1500 m in Navajo-1 and La Hoz-2), the interpreted seismic data, and the comparison between the crustal thickness and sedimentary thickness considering fundamental isostatic concepts. Moreover, the understanding of the generic model of a polyphase rift system (hyperextension concept) widely developed in the literature (e.g. Perón-Pinvidic & Manaschal, 2009; Sutra & Manaschal, 2012; Perón-Pinvidic et al., 2013) combined with the tectono-stratigraphic framework and the analysis of along strike sections (Western and Central sections) presented in this thesis, enabled to argue for a multistage and polyphase rift evolution occurring in the area by showing the migration of deformation through time, contrary to what is argued in previous studies as a monophase rift model, difficult to explain the mantle exhumation with a major fault (e.g. Quintana et al., 2015).

Finally, the understanding and application of the fundamental concepts when restoring hyperextended rift systems [i.e. crustal area conservation, bulk rheology composition and isostasy rules (see Chapter 1 for detailed explanation)] made possible to restore the proposed crustal scale cross sections, testing its viability, whereas previous works do not accomplish such systematic and coherent restorations (e.g. Pedrera et al., 2017 and García – Senz et al., 2019). Thus, the combination of concepts with different datasets providing access to different observation scales with different targets is fundamental to build a consistent crustal-scale interpretation, as exemplified in this thesis.

The construction of both the Central and Western sections considering all datasets allowed to restore the area to pre-orogenic stages and to reconstruct part of the extensional Wilson Cycle recognized in the Basque – Cantabrian Pyrenees. Rifting initiated in Triassic and terminated in Cenomanian, going through three stages. Later, reactivation of the North-Iberian Rift System occurred during Late Cretaceous incorporating the previous extensional basins into the Pyrenean orogen until Miocene. In contrast to an idealized Wilson Cycle, in the Basque – Cantabrian Pyrenees neither a mature spreading nor a subduction system have been reported, suggesting an incomplete cycle (Chenin et al. 2017 and 2018). Thus, the drifting phase in the Basque – Cantabrian domain never developed going directly from rifting to proto-subduction (Fig. D.2). Instead, in the Bay of Biscay to the west, the maturity of the extensional system reached the formation of oceanic crust, whereas in the eastern Pyrenees s.s. the system remained immature reaching the mantle exhumation, showing an along strike evolution.

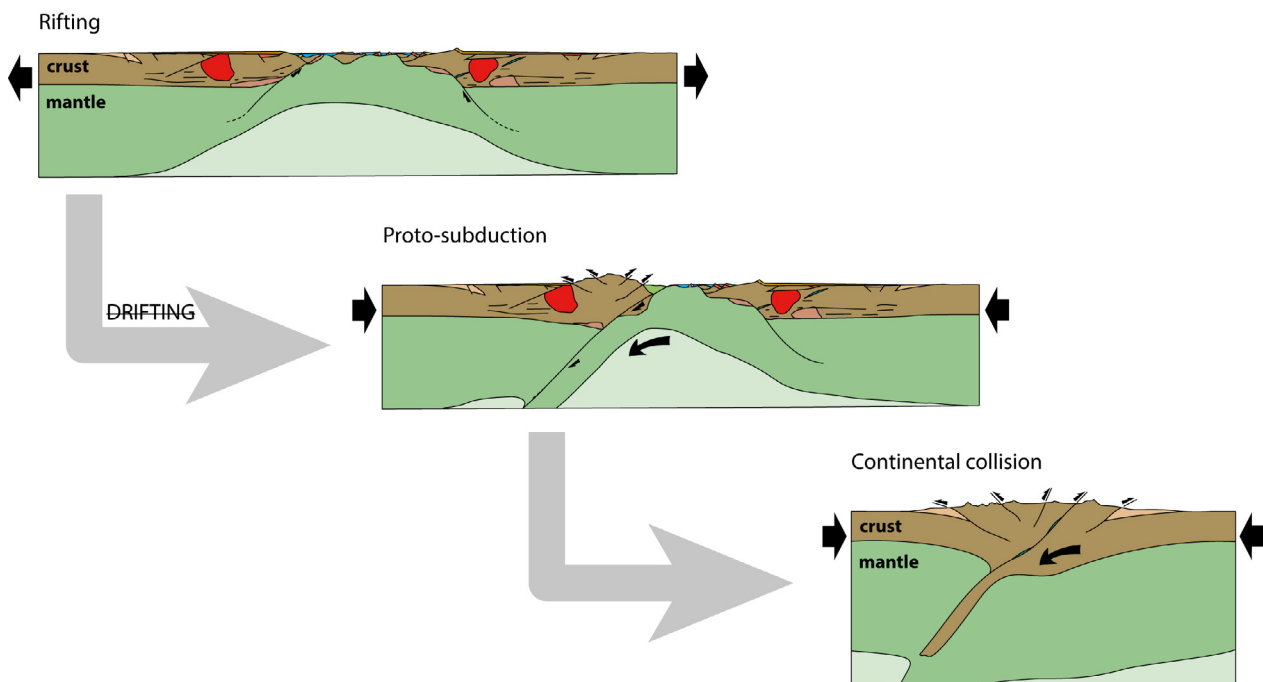


Figure D.2 : Evolution of the Wilson Cycle interpreted in the Basque – Cantabrian Pyrenees. Note that drifting phase is missing evolving directly from rifting to proto-subduction.

THE BASQUE – CANTABRIAN BASIN: AN EVOLVING PERSPECTIVE

Classically, the Basque – Cantabrian Basin has been explained by using the Central section (Fig. 1.11). As summarized in Chapter 1, most authors who interpreted the area in the last years argued for classical low- β rift systems or monophase rift models (García Mondéjar, 1989; Quintana et al., 2015; Pedrera et al., 2017; García-Senz et al., 2019). However, the integration of all existing datasets, the characterization of tectono-stratigraphic units through the entire area (i.e. distribution of depocenters of different age) and the construction of more sections along strike, enabled to propose a new extensional evolution arguing for a multistage and polyphase rift system.

A first event occurred during Late Triassic resulting in rift basins with deposition of evaporites, which distribution and extension remains poorly understood. However, the facies (shallow to sub-areal) and thickness (< 2 – 3 km) observed, reveals that extension was unlikely linked to high- β values and did not significantly affect the crustal thickness (Fig. D.3a). A second event during Late Jurassic to Barremian, overprinted and reactivated some of the Late Triassic basins as suggested by the occurrence of Late Triassic rocks beneath all the thick Upper Jurassic – Barremian sedimentary sequences in these basins and surrounding areas (e.g. Asturias Basin). Basins resulting from this event present mainly fluvial to lacustrine facies with interbedded alluvial deposits, are of moderate size and of lozenge shape (few tens of km long) and relatively thick (3-4 km), aligned along

NW – SE corridors (Fig. D.3b). Recent interpretations as the one suggested in this thesis propose a genesis resulting from a transtensional kinematics (i.e. monophasic rift). Finally, a third event occurred from Aptian to Cenomanian resulted in E-W oriented wide and deep basins, which experimented a significant crustal thinning leading the mantle exhumation at the floor of the basins during late extension. Thus, the last stage has been interpreted as a polyphase event resulting in necking, hyperextended and exhumed mantle domains (Fig. D.3c). As a result, the extensional evolution of the area is considered as a multistage and polyphase rift system (see Introduction and Chapter 1 for details).

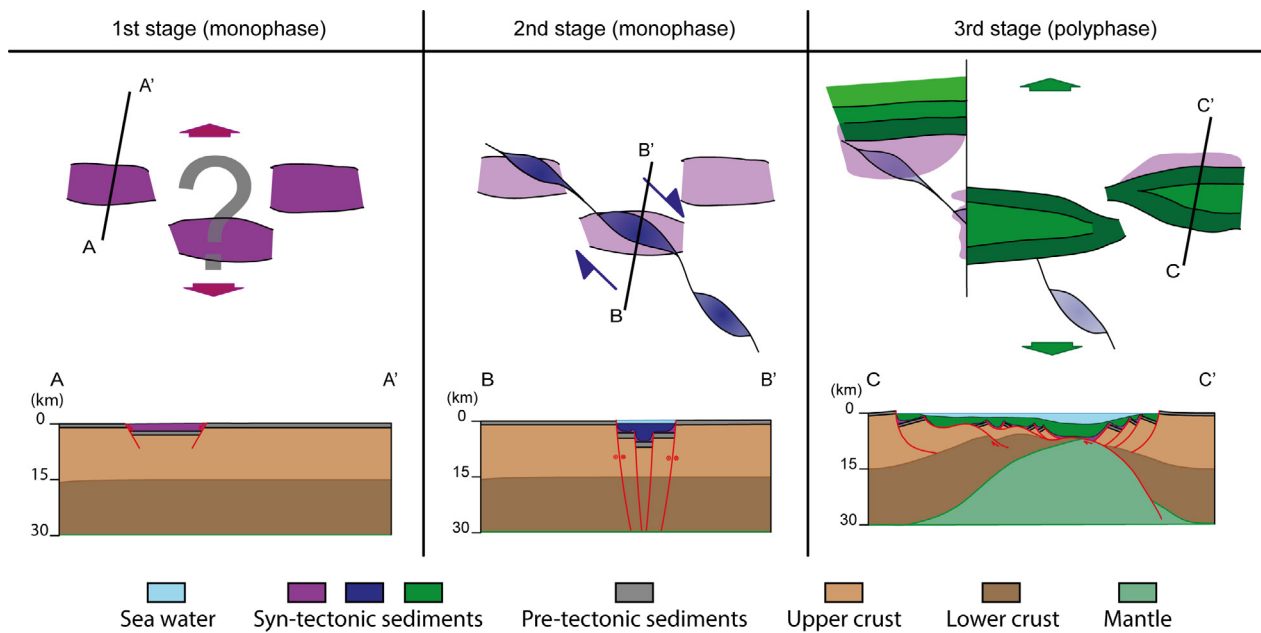


Figure D.3 : Multistage evolution interpreted in the Basque – Cantabrian Pyrenees in a map view (upper part) and section view (lower part). 1st stage corresponds to Late Triassic; 2nd stage corresponds to Late Jurassic – Barremian; and 3rd stage correspond to Aptian to Cenomanian.

The fact that Central section presents the three rift events overprinted may lead to wrong interpretations and misinterpreting the importance of inheritance as summarized before. Therefore, the along strike variation and characterization of different depocenters and its characteristics is a key factor to establish a consistent model through the area. This asks for a re-evaluation of former studies and the integration of these new concepts in the interpretation of orogenic systems

FROM 2D TO 3D: THE IMPORTANCE OF INHERITANCE

In the last decades, the classical way to study orogens has been the construction of geological cross sections parallel to the shortening direction (e.g. Pyrenees: Muñoz, 1992; Alps: Schmid et al., 2004; Andes: Carrera et al., 2006), but less understood remain the along strike variations due to the segmented nature of tectonic systems. A relevant aspect resultant from this thesis is the along strike observations and its integration in a common framework in order to understand the reorganization of deformation through time and space. Some key factors controlling the reactivation of an orogen, in a 3D perspective, are analysed in this work:

- Presence and distribution of decoupling levels such as serpentized mantle, mid-crustal levels, and salt and clay-rich intra-sedimentary horizons.
- Along strike segmentation of the rift system determining the location of initial reactivation.
- The results of this study suggest that in distal domains the onset of reactivation is controlled by the occurrence of serpentized mantle that can act as a decoupling level during initial convergence as proposed previously (Perón-Pinvidic et al., 2008; Lundin & Doré, 2011; Erdos et al., 2014; Lescoutre, 2019). As a result, if the extensional system is segmented, reactivation starts in each segment independently considering the distribution and location of the weakest and most favourable positioned decoupling level. In subsequent stages, once the first decoupling is consumed or becomes less efficient, the mid-crustal levels can be reactivated starting the continental collision. At this point, crustal thickening occurs and hence major topography will be created. However, focusing the intra-sedimentary decollement, often represented by evaporites or clays, its reactivation will depend on its distribution and thickness (i.e. only if such horizon is continuous and thick enough, it will be used as a decoupling horizon).

The experimental program carried out in this thesis (see Chapter 2 for details) addressed the transition from thick to thin-skinned tectonics and how deformation is linked between both domains, referring to the intra-sedimentary decollement. The well characterized field example (i.e. Basque – Cantabrian Pyrenees and its junction to the Asturian Massif) inspired the setup of analogue models. Such experimental program is among the few ones playing with an interplay of structural and compositional inheritance during both extension and compressional reactivation. Some major learnings can be emphasized:

High vs width of fold and thrust belts is a function of the distribution of decoupling levels: the presence of an efficient decoupling level (i.e. salt) results in a wide deformation area with a more distributed deformation and less topographic response. On the contrary, areas without efficient decollements are narrower but with high topographic response (Chapter 2, Fig. 2.12) compatible with the predictions of the Coulombe-wedge theory.

- Importance of overlapping between inherited basement structures and decoupling horizons: active structures in surrounding domains (both basement-involved and salt decoupled) controlled the position of oblique structures in transitional domains. However, its orientation does not follow the structural trend of the basement structures, being controlled by the thickness and distribution of the weak layer and its overburden, commonly with a minor wavelength than in the decoupled domain.
- Previous studies proposed a thick-skinned structural style in the Basque – Cantabrian Pyrenees with a strong continuity of the Asturian Massif basement structures (e.g. Quintana et al., 2015), which determine the present-day architecture. However, the numerous similarities between the field and the analogue models support the geological interpretation proposed in this thesis (Chapter 1) contrasting the previous interpretations: (1) narrow area of deformation and high topography response in the Asturian Massif similar to the coupled domain of the models, (2) oblique structures observed in the Western Basque – Cantabrian Pyrenees (e.g. Zamanzas, and Pas) with a minor wavelength and a general structural plunge to the east similar to the transitional domain of the models, and (3) wider area of deformation with low structural relief and salt structures with bigger wavelength in the decoupled domain similar to what is observed in the Basque – Cantabrian Pyrenees. Moreover, the models presented in this study also discuss the NW – SE transpressive reactivation proposed by Tavani et al. (2013) in the transition from the Asturian Massif to the Basque – Cantabrian Pyrenees, as it would be incompatible with such compressional structures in a N-S direction.



A full-page background image showing a sunset or sunrise over a mountain range. The sky is filled with soft, colorful clouds in shades of orange, yellow, and blue. A bright light source, likely the sun, is partially obscured by a dark cloud, creating a lens flare effect. A thin, horizontal streak, possibly a satellite or aircraft, is visible in the upper middle part of the sky. The foreground shows the dark silhouettes of mountain peaks.

CONCLUSIONS

The cover photo of the Conclusions depicts a spectacular sunset behind the Peña Labra ridge, after a long day of fieldwork. Photo captured from Reinosa village (Cantabria).

CONCLUSIONS

The aim of this PhD is to investigate: (1) the present-day architecture of the Basque – Cantabrian Pyrenees, (2) the former rift template, (3) the link with the western Asturian Massif and the transition from thick to thin-skinned domains by using physical models, and (4) the reactivation of the segmented North Iberian rift system and its incorporation into the Pyrenean Orogen. The main learnings of this thesis can be summarized as follow:

1. PRESENT-DAY ARCHITECTURE OF THE BASQUE – CANTABRIAN PYRENEES

The Basque – Cantabrian Pyrenees (BCP) are the result of the inversion and incorporation of a multistage and polyphase rift system into the Pyrenean Orogen. Such complexity is captured by two regional crustal scale cross sections through the Central and Western BCP.

- In the Central BCP, the Iberian plate underthrust the European plate. The folded sedimentary cover is allochthonous, detached on the Upper Triassic salt relatively transported by more than 45km to the south.
- In the Western BCP, one and the same plate (Iberian plate) is involved in the present-day orogenic architecture. A southward proto-subduction of exhumed mantle is observed to the north in the Bay of Biscay whereas a northward underthrust of the Iberian plate beneath the same Iberian crust is interpreted to the south. Distribution of salt is more irregular resulting in a combination of thick- and thin-skinned structural styles deforming the sedimentary cover.

2. THE NORTH IBERIAN RIFT SYSTEM

A multistage evolution is characterized in this thesis involving three rift events:

- Late Triassic event: Considering the facies (mainly evaporitic) and thicknesses (less than 2-3km) observed, the crustal thickness is little affected arguing for a monophasic low- β rift event.
- Late Jurassic – Barremian event: considering the NW – SE aligned basins (i.e. Cabuérniga, Polientes, Basque – Cantabrian Basin) filled up by lacustrine to fluvial sediments and controlled by steep faults when observed (e.g. Cabuérniga Fault), this event has been interpreted as monophasic resulting from a trans-tensional period.

- Aptian to Middle Cenomanian: E – W aligned wide basins with facies changing from carbonate platforms in proximal areas to deep marine sediments in distal parts. Facies and thickness (more than 8km) but also the presence of mantle rocks related to such depocenters calls for a significant crustal thinning resulting from a hyperextension and mantle exhumation during such event. As a result, a polyphase event from stretching, necking, hyperextension and mantle exhumation occurred in the area.

3. WESTERN TERMINATION OF THE BASQUE – CANTABRIAN PYRENEES AND LINK TO THE ASTURIAN MASSIF. HOW DEFORMATION IS ACCOMMODATED IN A THICK-TO THIN-SKIN TRANSITION

Oblique structures are observed in the Western Basque – Cantabrian Pyrenees composing a transitional domain between the thick-skinned Asturian Massif and the thin-skinned central Basque – Cantabrian Pyrenees. Major learnings from this thesis are:

- Transitional domains are formed where different inherited components are overlapped during both extensional and compressional evolution. Such evolution resulted in oblique structures to the deformation axis. The position of such structures depends on the active structures in the surrounding domains, but its orientation does not follow the orientation of basement structures. Instead, its evolution is related to the salt flow, the thickness of the weak horizon and its overburden.
- The involvement of syn-contractional sedimentation evidence the structural style controlling the orogenic architecture. Thick-skinned domains results in narrow areas of deformation building significant topography and syn-contractional sedimentation is mainly located in the forelands. On the contrary, thin-skinned domains shows a wider area of deformation with lower topographies and more distributed syn-contractional sedimentation both in the forelands but also in piggy-back basins within the thrust wedge. As a result, the transitional domain shows a regional structural plunge to the east from the thick- to the thin-skinned domain.

4. REACTIVATION AND INCORPORATION OF THE NORTH IBERIAN RIFT SYSTEM INTO THE PYRENEAN OROGEN

Presence and distribution of potential decoupling levels within the former rift template are crucial elements controlling the reactivation of a hyperextended rift system and the formation of an orogenic system. The sequence/pattern of reactivation proposed here is:

- Reactivation initiates in the most distal rift domains where exhumed mantle is serpentinized being an efficient decoupling level. The fresh and strong mantle is pulled down beneath the hyperextended crust. This early reactivation does not thicken the crust and therefore it may not be well recorded in the sedimentary succession. Hyperextended crust and serpentinized mantle may be deformed and incorporated into the accretionary wedge.
- A second phase is described by continental collision, when exhumed mantle and hyperextended domains are consumed and necking domains face each other. In that moment, the mid-crustal decollement is the one accommodating most of the deformation by reactivating previous extensional faults or generating new thrusts. As a result, crust will be thickened, and relief created leading to important sedimentation in the forelands.
- A last phase may reactivate the intra-sedimentary decoupling (e.g. salt or clays) to propagate the deformation even further. However, this phase will be conditioned to the presence of a possible decollement and in that case on its distribution in function of the depositional setting, either syn-extensional or syn-compressional.

In the central Basque – Cantabrian Pyrenees, the presence of the Upper Triassic salt throughout the area, favoured the reactivation since the initial stages. Therefore, two decoupling horizons were active during early stages (i.e. serpentinized mantle and salt). However, in the Asturian Massif due to the lack of salt throughout the area, early stages of reactivation were controlled by the serpentinized mantle decoupling. The subsequent collisional phase occurring in the central Basque – Cantabrian Pyrenees as well as in the Pyrenees s.s. forced a reorganization of deformation to the west, which resulted in the northward underthrusting of Iberian crust beneath the same Iberian crust showing an intraplate orogenic architecture. Thus, the early stages were more localized and characterized by a segmented reactivation in function of the position of decoupling domains, whereas the later stages were more distributed and in line with the Mohr-Coulomb wedge theory, being influenced by the along strike evolution.





OUTLOOKS

The cover photo of the Outlooks corresponds to a panoramic view to the Ojo Guareña Natural Monument with the Coniacian carbonate platform (post-rift) drawing the skyline of the ridges (Burgos province).

OUTLOOKS

This section aims to open the discussion to remaining and new questions that result from this study as well as to put the results of this study in a more global perspective including the definition of diagnostic elements or transferable knowledge to consider for future applications in orogenic systems.

REMAINING DEBATES

KINEMATIC EVOLUTION OF THE IBERIA AND SURROUNDING PLATES

The study of the Basque – Cantabrian Pyrenees presented in this thesis proposed a complex rift evolution and subsequent reactivation providing kinematic constraints for the plate organization between Iberia, Ebro and Europe. It is argued that contractional reactivation occurred in a roughly N-S direction, similar to the last rift event (Aptian to Cenomanian polyphase extension) resulting in E-W aligned basins in the Pyrenees s.s.. However, the previous rift event (Upper Jurassic to Barremian) is interpreted of being the result of a transitional period, being mainly recorded in NW – SE aligned trans-tensional basins along the diffuse Iberian – Ebro plate boundary. Therefore, these results suggest a complex evolution considering not only the main plate boundary (Iberia/Europe) but also micro-plates or intra-plate (Ebro/Iberia boundary) corridors. Despite the multiple models proposed to explain such evolution (see Introduction for details and references), the Mesozoic kinematic evolution of the Iberia plate is still unresolved. The results of this study have been integrated in a new, plate kinematic model (Frasca et al. subm. in Annex 3). Still further studies corroborating this model are necessary. A key question raised by this study is linked to the question about the value of kinematic indicators measured in the field and how can they be upscaled to a plate kinematic scale. Moreover, how far the local kinematic indicators can record the kinematics of plates is a question that is of particular importance in settings where the cover sequences are decoupled from the underlying basement.

LINK BETWEEN INHERITANCE AND CRUSTAL ROOTS ALONG THE PYRENEAN OROGEN

In the last decades, many studies investigated the crustal roots of the Pyrenees s.s. and the Basque Massif (e.g. Campanyà et al., 2012, 2018; Chevrot et al., 2015, 2018; Wang et al., 2016). However, less investigated is the westwards continuation beneath the Basque – Cantabrian Pyrenees and the Asturian Massif (Pulgar et al., 1996; Fernández-Viejo et

al., 2000; Pedreira et al., 2007, 2015; Fernández-Viejo, et al. 2020). Interpretations have been proposed arguing that the link in origin and morphology between the Pyrenean s.s. crustal root and the Asturian Massif crustal root should be different as the Basque – Cantabrian in between did not form an important thickening during collision (Fernández-Viejo et al., 2020).

In this thesis we show the linkage of the previous domains and how deformation is reorganized to the west due to the collision occurring to the Pyrenees s.s.. In fact, two main factors play a significant role during the formation of the orogen: (1) the inherited rift template, which determined the location of the proto-subduction and location of the mountain belt, and (2) the Upper Triassic salt, which played a crucial role during subsequent stages. In the Basque – Cantabrian Pyrenees the abundance and efficiency of such decoupling inhibits a significant reactivation of mid-crustal detachment of the Iberian plate, resulting in a northward underthrust of Iberia beneath Europe, thickening the crust to the north in the European plate. However, to the west in the Asturian Massif, due to the lack of a shallow decoupling, the mid-crustal decoupling accommodated the contractional deformation by thickening the crust. where the deformation was lately localized (frontal thrust within the Iberian plate). Therefore, a shifting in where the crust is thickened is observed along strike from the Asturian Massif to the Basque – Cantabrian Pyrenees and Pyrenees s.s. The results of this study suggest that rift inheritance (i.e. rift template and distribution of salt) are among the controlling factors responsible for this orogen-lateral change in the rooting level. More investigations regarding this topic including further geological evidence and the imaging of E-W crustal cross sections are necessary to resolve this problem.

TRANSFERABLE KNOWLEDGE

This section aims to synthesize the main learnings and transferable knowledge of this thesis, i.e. to define the main learnings that can be considered to be generic and therefore can be applied in other orogenic systems worldwide. Such transferable knowledge is, by definition, limited to first order elements.

Subduction systems occur in the most distal parts of the former extensional system by pulling down the denser and likely also stronger oceanic crust beneath the continental crust. On the other hand, fold and thrust belts usually form continent-ward of the necking zone by affecting the previously little thinned continental crust (25 – 30 km thick crust) and sedimentary succession is relatively thin. Therefore, rift inheritance is of minor importance in these two domains, even though possible intra-sedimentary decoupling horizons may lead to thin-skin reactivation (see Chapter 2). However, in between the proximal margin and the oceanic crust, the crust thins from ~30 km to 0 km in the so-called necking and hyperextended rift domains, where the coupling point is located. Oceanward of the coupling point, fluids penetrate the mantle resulting in serpentinisation and creation of an efficient decoupling horizon for the subsequent reactivation. Towards the continent, instead, mid crustal levels characterized by ductile material are preserved and they can be also reactivated during contraction. As a consequence of the crustal thinning, the total accommodation space (which is inverse proportional to the crustal thickness) increases being filled either by thick sediments or water, resulting in deep-water, often rich in clays and shales oceanwards. In such areas, the rift inheritance becomes fundamental during reactivation and formation of orogens since the deforming domain is not a simple layer cake. One of the main outcomes of this project is, therefore, to show the importance of rift inheritance in the evolution and architecture of orogens.

A first learning of this thesis is the analysis of the syn-rift stratigraphy and its link to rift domains incorporated into the orogenic belt in terms of thickness and facies variations, distribution, and limits to make proper restorations considering the fundamental concepts explained in Chapter 1 (i.e., crustal areal conservation, crustal rheological weaknesses and intra-basin weak horizons, Fig. 1.13). Thus, diagnostic elements allow to recognize the rift template in an orogenic system, such as (1) significantly thickening (more than 3-4 km) of sedimentary succession and/or deepening of the facies indicating an increasing total accommodation space, and therefore the necking domain; (2) the S-point, closely related to the coupling point of the former rift system (see Chapter 1 and 3); and (3) presence of serpentinized mantle rocks and/or ophiolites indicative of the existence of hyperextended

or exhumed mantle domains in the former rift system; or in a large scale. However, in this thesis it is emphasized the relevance of recognizing those elements not only in a section view but also in a map view, in order to construct rift domain maps with S-lines along strike in an orogenic system to understand the distribution of the rift template incorporated.

A crucial learning become also the distribution of decoupling levels resulting from the extensional evolution: (1) serpentized mantle, in most distal domains of the rift system where the crust is extremely thin (basinwards of the coupling point, Fig. 1.14); (2) mid-crustal rheological weakness, mostly in the necking domain; and (3) the intra-sediment decoupling levels (e.g. salt or clays), which distribution and connectivity to other decoupling levels depend on timing of deposition and thickness (Fig. 1.14).

In addition to 2D considerations, this work emphasizes also the along strike variability within a rift segment, having the classical polyphase rift section in the central rift segment, which may be completely reactivated, whereas at segment edges the system needs to reorganize creating short cuts and pre-existing structures may be preserved.

The combination of above presented elements allows to understand the present-day architecture of an orogenic system and its evolution from the former rifted system (see Chapter 3). Segmentation of the former rift system occurring during extension will result in transfer systems during reactivation and therefore the recognition of inherited elements may help the understanding of along strike variations in a contractional system. It is common to address the study of the internal parts of orogens by using analytical techniques (e.g. thermochronology, P-T conditions analysis, petrology) dealing with detailed scale, but sometimes the first order is underestimated, ignored, or not taken into account. Therefore, an approach is proposed in this work to deal with orogenic systems by recognizing first order diagnostic elements (e.g. rift domains, S-line, nature and distribution of decoupling horizons) in order to better understand its evolution and final architecture.





REFERENCES

The cover photo of the References depicts the steeply dipping bedding of the Paleocene sediments in Itzurun hondartza (Zumaya village, Gipuzkoa).

A

- Ábalos, B., Alkorta, A., & Iríbar, V. (2008). Geological and isotopic constraints on the structure of the Bilbao anticlinorium (Basque–Cantabrian basin, North Spain). *Journal of Structural Geology*, 30(11), 1354–1367. DOI: 10.1016/j.jsg.2008.07.008
- Ábalos, B. (2016). Geologic map of the Basque-Cantabrian Basin and a new tectonic interpretation of the Basque Arc. *International Journal of Earth Sciences*, 105(8), 2327–2354. Doi: 10.1007/s00531-016-1291-6
- Acocella, V., Salvini, F., Funiciello, R., & Faccenna, C. (1999). The role of transfer structures on volcanic activity at Campi Flegrei (Southern Italy). *Journal of Volcanology and Geothermal Research*, 91(2-4), 123-139. DOI: 10.1016/S0377-0273(99)00032-3
- Advokaat, E. L., van Hinsbergen, D. J., Maffione, M., Langereis, C. G., Vissers, R. L., Chierchi, A., Schroeder, R., Madani, H., & Columbu, S. (2014). Eocene rotation of Sardinia, and the paleogeography of the western Mediterranean region. *Earth and Planetary Science Letters*, 401, 183-195. DOI: 10.1016/j.epsl.2014.06.012
- Aller, J., & Zeyen, H. J. (1996). A 2.5-D interpretation of the Basque country magnetic anomaly (northern Spain): geodynamical implications. *Geologische Rundschau*, 85(2), 303-309.
- Allmendinger, R. W., Jordan, T. E., Kay, S. M., & Isacks, B. L. (1997). The evolution of the Altiplano-Puna plateau of the Central Andes. *Annual review of earth and planetary sciences*, 25(1), 139-174.
- Alonso, J. L., Pulgar, J. A., García-Ramos, J. C., & Barba, P. (1996). Tertiary basins and alpine tectonics in the Cantabrian Mountains, NW Spain. In P. F. Friend & C. J. Dabrio (Eds.), *Tertiary basins of Spain: The stratigraphic record of crustal kinematics* (pp. 214–227). Cambridge: Cambridge University Press.
- Alonso, J. L., Pulgar, F. J. Á., & Pedreira, D. (2007). El relieve de la Cordillera Cantábrica. *Enseñanza de las Ciencias de la Tierra*, 15(2), 151-163.
- Amilibia, A., McClay, K. R., Sàbat, F., Muñoz, J. A., & Roca, E. (2005). Analogue modelling of inverted oblique rift systems. *Geologica Acta*, 3(3), 0251-271. DOI: 10.1344/105.000001395
- Amilibia, A., Sàbat, F., McClay, K. R., Muñoz, J. A., Roca, E., & Chong, G. (2008). The role of inherited tectono-sedimentary architecture in the development of the central Andean mountain belt: Insights from the Cordillera de Domeyko. *Journal of Structural Geology*, 30(12), 1520-1539. DOI: 10.1016/j.jsg.2008.08.005
- Andersen, T. B., Corfu, F., Labrousse, L., & Osmundsen, P. T. (2012). Evidence for hyperextension along the pre-Caledonian margin of Baltica. *Journal of the Geological Society*, 169(5), 601-612. DOI: 10.1144/0016-76492012-011
- Angrand, P., Mouthereau, F., Masini, E., & Asti, R. (2020). A reconstruction of Iberia accounting for W-Tethys/N-Atlantic kinematics since the late Permian-Triassic. *Solid Earth Discussions*, 1-24. DOI: 10.5194/se-11-1313-2020
- Argand, E. (1916). *Sur l'arc des Alpes occidentales*. G. Bridel.

- Arthaud, F., & Matte, P. (1977). Late Paleozoic strike-slip faulting in southern Europe and northern Africa: Result of a right-lateral shear zone between the Appalachians and the Urals. *GSA Bulletin*, 88(9), 1305–1320. DOI: 10.1130/0016-7606(1977)88<1305:LPS-FIS>2.0.CO;2
- Aurell, M., Robles, S., Bádenas, B., Rosales, I., Quesada, S., Meléndez, G., & García-Ramos, J. C. (2003). Transgressive–regressive cycles and Jurassic paleogeography of northeast Iberia. *Sedimentary Geology*, 162(3–4), 239–271. DOI: 10.1016/S0037-0738(03)00154-4

B

- Ballèvre, M., Catalán, J. R. M., López-Carmona, A., Pitra, P., Abati, J., Fernández, R. D., Ducassou, C., Arenas, R., Bosse, V., Castiñeiras, P., Fernández-Suárez, J., Gómez, J., Paquette, J. L., Peucat, J. J., Poujol, M., Ruffet, G., & Sánchez, S. (2014). Correlation of the nappe stack in the Ibero-Armorican arc across the Bay of Biscay: a joint French–Spanish project. *Geological Society, London, Special Publications*, 405(1), 77–113. DOI: 10.1144/SP405.13
- Bahroudi, A., & Koyi, H. (2003). Effect of spatial distribution of Hormuz salt on deformation style in the Zagros fold and thrust belt: an analogue modelling approach. *Journal of the Geological Society*, 160(5), 719–733. DOI: 10.1144/0016-764902-135
- Bally, A. W., Gordy, P. L., & Stewart, G. A. (1966). Structure, seismic data, and orogenic evolution of southern Canadian Rocky Mountains. *Bulletin of Canadian Petroleum Geology*, 14(3), 337–381.
- Barnett-Moore, N., Hosseinpour, M., & Maus, S. (2016). Assessing discrepancies between previous plate kinematic models of Mesozoic Iberia and their constraints. *Tectonics*, 35(8), 1843–1862. DOI: 10.1002/2015TC004019
- Barnolas, A., & Pujalte, V. (2004). La Cordillera Pirenaica. *Geología de España*, 233–241.
- Beaumont, C., Ellis, S., Hamilton, J., & Fullsack, P. (1996). Mechanical model for subduction-collision tectonics of Alpine-type compressional orogens. *Geology*, 24(8), 675–678.
- Beaumont, C., Muñoz, J. A., Hamilton, J., & Fullsack, P. (2000). Factors controlling the Alpine evolution of the central Pyrenees inferred from a comparison of observations and geodynamical models. *Journal of Geophysical Research: Solid Earth*, 105(B4), 8121–8145. DOI: 10.1029/1999JB900390
- Beaumont, C., Jamieson, R. A., Nguyen, M. H., & Medvedev, S. (2004). Crustal channel flows: 1. Numerical models with applications to the tectonics of the Himalayan-Tibetan orogen. *Journal of Geophysical Research: Solid Earth*, 109(B6). DOI: 10.1029/2003JB002809
- Belousov, V. V. (1962). Basic problems in geotectonics. *MacGraw Hill*, NY.
- Belousov, V. V., & Milanovsky, Y. Y. (1977). On tectonics and tectonic position of Iceland. *Tectonophysics*, 37(1–3), 25–40.
- Beltrando, M., Manatschal, G., Mohn, G., Dal Piaz, G. V., Brovarone, A. V., & Masini, E. (2014). Recognizing remnants of magma-poor rifted margins in high-pressure orogenic belts: The Alpine case study. *Earth-Science Reviews*, 131, 88–115. DOI: 10.1016/j.earscirev.2014.01.001

- Bernoulli, D. (1964). *Zur Geologie des Monte Generoso (Lombardische Alpen): ein Beitrag zur Kenntnis der südalpinen Sedimente*. na.
- Bixel, F., & Lucas, C. (1987). Approche géodynamique du Permien et du Trias des Pyrénées dans le cadre du Sud-Ouest Européen. *Cuadernos de Geología Ibérica= Journal of Iberian Geology: An International Publication of Earth Sciences*, (11), 57–82.
- Bodego, A., Iriarte, E., Agirrezabala, L. M., García-Mondéjar, J., & López-Horgue, M. A. (2015). Synextensional mid-Cretaceous stratigraphic architecture of the eastern Basque–Cantabrian basin margin (western Pyrenees). *Cretaceous Research*, 55, 229–261. DOI: 10.1016/j.cretres.2015.01.006
- Boillot, G., & Capdevila, R. (1977). The Pyrenees: Subduction and collision?. *Earth and Planetary Science Letters*, 121(5):151–160
- Boillot, G., Recq, M., Winterer, E. L., Meyer, A. W., Applegate, J., Baltuck, M., Bergen, J. A., Comas, M. C., Davies, T. A., Dunham, K., Evans, C. A., Girardeau, J., Goldberg, G., Haggerty, J., Jansa, L. F., Johnson, J. A., Kasahara, J., Loreau, J. P., Luna-Sierra, E., Moullade, M., Ogg, J., Sarti, M., Thürow, J., & Williamson, M. (1987). Tectonic denudation of the upper mantle along passive margins: a model based on drilling results (ODP leg 103, western Galicia margin, Spain). *Tectonophysics*, 132(4), 335–342. DOI: 10.1016/0040-1951(87)90352-0
- Bonini, M., Sani, F., & Antonielli, B. (2012). Basin inversion and contractional reactivation of inherited normal faults: A review based on previous and new experimental models. *Tectonophysics*, 522, 55–88. DOI: 10.1016/j.tecto.2011.11.014
- Bosch, G. V., Teixell, A., Jolivet, M., Labaume, P., Stockli, D., Domènech, M., & Monié, P. (2016). Timing of Eocene–Miocene thrust activity in the Western Axial Zone and Chaînons Béarnais (west-central Pyrenees) revealed by multi-method thermochronology. *Comptes Rendus Geoscience*, 348(3–4), 246–256. DOI: 10.1016/j.crte.2016.01.001
- Brinkmann, R., & Logters, H. (1968). Diapirs in western Pyrenees and foreland, Spain. *Diapirism Diapirs, AAPG Spec. Vol. Tulsa, Oklahoma A153*: 275–292
- Buiter, S. J. (2012). A review of brittle compressional wedge models. *Tectonophysics*, 530, 1–17. DOI: 10.1016/j.tecto.2011.12.018
- Butler, R. W., Tavarnelli, E., & Grasso, M. (2006). Structural inheritance in mountain belts: an Alpine–Apennine perspective. *Journal of Structural Geology*, 28(11), 1893–1908. DOI: 10.1016/j.jsg.2006.09.006
- Burke, K. (2011). Plate tectonics, the Wilson Cycle, and mantle plumes: geodynamics from the top. *Annual Review of Earth and Planetary Sciences*, 39, 1–29. DOI: 10.1146/annurev-earth-040809-152521

C

- Cadenas, P., Fernández-Viejo, G., Pulgar, J. A., Tugend, J., Manatschal, G., & Minshull, T. A. (2018). Constraints Imposed by Rift Inheritance on the Compressional Reactivation of a Hyperextended Margin: Mapping Rift Domains in the North Iberian Margin and in the Cantabrian Mountains: Rift domains in the North Iberian margin. *Tectonics*, 37(3), 758–785. DOI: 10.1002/2016TC004454

References

- Cadenas, P., Manatschal, G., & Fernández-Viejo, G. (2020). Unravelling the Architecture and evolution of the multi-stage North Iberian/Bay of Biscay rift. *Gondwana Research*. DOI: 10.1016/j.gr.2020.06.0261342-937/2020
- Cámara, P. (1997). The Basque-Cantabrian basin's Mesozoic tectono-sedimentary evolution. *Mémoires de la Société Géologique de France*, 171, 187-191.
- Cámara, P. (2017). Salt and Strike-Slip Tectonics as Main Drivers in the Structural Evolution of the Basque-Cantabrian Basin, Spain. In *Permo-Triassic Salt Provinces of Europe, North Africa and the Atlantic Margins* (pp. 371–393). Elsevier. DOI: 10.1016/B978-0-12-809417-4.00018-5
- Cámara, P., & Flinch, J. F. (2017). The southern Pyrenees: a salt-based fold-and-thrust belt. In *Permo-Triassic Salt Provinces of Europe, North Africa and the Atlantic Margins* (pp. 395-415). Elsevier. DOI: 10.1016/B978-0-12-809417-4.00019-7
- Cámara, P. (2020). Inverted turtle salt anticlines in the eastern Basque-Cantabrian basin, Spain. *Marine and Petroleum Geology*, 104358. DOI: 10.1016/j.marpetgeo.2020.104358
- Camilleri, P. A., & Chamberlain, K. R. (1997). Mesozoic tectonics and metamorphism in the Pequop Mountains and Wood Hills region, northeast Nevada: Implications for the architecture and evolution of the Sevier orogen. *Geological Society of America Bulletin*, 109(1), 74-94.
- Campanyà, J., Ledo, J., Queralt, P., Marcuello, A., Liesa, M., & Muñoz, J. A. (2012). New geoelectrical characterisation of a continental collision zone in the West-Central Pyrenees: Constraints from long period and broadband magnetotellurics. *Earth and Planetary Science Letters*, 333, 112-121. DOI: 10.1016/j.epsl.2012.04.018
- Campanyà, J., Ledo, J., Queralt, P., Marcuello, A., Muñoz, J. A., Liesa, M., & Jones, A. G. (2018). New geoelectrical characterization of a continental collision zone in the Central–Eastern Pyrenees: Constraints from 3-D joint inversion of electromagnetic data. *Tectonophysics*, 742, 168-179. DOI: 10.1016/j.tecto.2018.05.024
- Cañas, C. R., Hernaiz, P. P., Malagón, J., & Serrano, A. (1994). Notas sobre la estructura cabalgante de Rojas-Santa Casilda. *Geogaceta*, 15, 135–138.
- Carey, S. W. (1975). *Paleomagnetism and Earth Expansion*. University of Tasmania, Department of Geology.
- Carey, S. W. (1978). A philosophy of the earth and universe. In *Papers and Proceedings of the Royal Society of Tasmania* (Vol. 112, pp. 5-19).
- Carola, E., Tavani, S., Ferrer, O., Granado, P., Quintà, A., Butillé, M., & Muñoz, J. A. (2013). Along-strike extrusion at the transition between thin- and thick-skinned domains in the Pyrenean Orogen (northern Spain). *Geological Society, London, Special Publications*, 377(1), 119-140. DOI: 10.1144/SP377.3
- Carola, E. (2014). The transition between thin- to thick-skinned styles of deformation in the Western Pyrenean Belt. Ph. D. Thesis. Universitat de Barcelona, Spain.
- Carola, E., Muñoz, J. A., & Roca, E. (2015). The transition from thick-skinned to thin-skinned tectonics in the Basque-Cantabrian Pyrenees: the Burgalesa Platform and surroundings. *International Journal of Earth Sciences*, 104(8), 2215–2239. DOI: 10.1007/s00531-015-1177-z

- Carrera, N., Muñoz, J. A., Sàbat, F., Mon, R., & Roca, E. (2006). The role of inversion tectonics in the structure of the Cordillera Oriental (NW Argentinean Andes). *Journal of Structural Geology*, 28(11), 1921-1932. DOI: 10.1016/j.jsg.2006.07.006
- Casas, A., Kearey, P., Rivero, L., & Adam, C. R. (1997). Gravity anomaly map of the Pyrenean region and a comparison of the deep geological structure of the western and eastern Pyrenees. *Earth and Planetary Science Letters*, 150(1-2), 65-78. DOI: 10.1016/S0012-821X(97)00087-3
- Castañares, L. M., Robles, S., Gimeno, D., & Vicente Bravo, J. C. (2001). The Submarine Volcanic System of the Errigoiti Formation (Albian-Santonian of the Basque-Cantabrian Basin, Northern Spain): Stratigraphic Framework, Facies, and Sequences. *Journal of Sedimentary Research*, 71(2), 318-333. DOI: 10.1306/080700710318
- Catalán, J. M., Arenas, R., García, F. D., Cuadra, P. G., Gómez-Barreiro, J., Abati, J., Castiñeiras, P., Ferández-Suárez, J., Sánchez, S., Andonegui, P., González, E., Díez, A., Rubio, F., & Valle, B. (2007). Space and time in the tectonic evolution of the northwestern Iberian Massif: Implications for the Variscan belt. In *4-D framework of continental crust* (Vol. 200, pp. 403-423). Geological Society of America Memoir Boulder, Colorado.
- Chalmers, J. A., & Pulvertaft, T. C. R. (2001). Development of the continental margins of the Labrador Sea: a review. *Geological Society, London, Special Publications*, 187(1), 77-105. DOI: 10.1144/GSL.SP.2001.187.01.05
- Chapple, W. M. (1978). Mechanics of thin-skinned fold-and-thrust belts. *Geological Society of America Bulletin*, 89(8), 1189-1198.
- Chenin, P., Manatschal, G., Lavier, L. L., & Erratt, D. (2015). Assessing the impact of orogenic inheritance on the architecture, timing and magmatic budget of the North Atlantic rift system: a mapping approach. *Journal of the Geological Society*, 172(6), 711-720. DOI: 10.1144/jgs2014-139
- Chenin, P., Manatschal, G., Picazo, S., Müntener, O., Karner, G., Johnson, C., & Ulrich, M. (2017). Influence of the architecture of magma-poor hyperextended rifted margins on orogens produced by the closure of narrow versus wide oceans. *Geosphere*, 13(2), 559-576. DOI: 10.1130/GES01363.1
- Chenin, P., Schmalholz, S. M., Manatschal, G., & Karner, G. D. (2018). Necking of the lithosphere: A reappraisal of basic concepts with thermo-mechanical numerical modeling. *Journal of Geophysical Research: Solid Earth*, 123(6), 5279-5299. DOI: 10.1029/2017JB014155
- Chenin, P., Picazo, S., Jammes, S., Manatschal, G., Müntener, O., & Karner, G. (2019). Potential role of lithospheric mantle composition in the Wilson cycle: a North Atlantic perspective. *Geological Society, London, Special Publications*, 470(1), 157-172. DOI: 10.1144/SP470.10
- Chenin, P., Schmalholz, S. M., Manatschal, G., & Duretz, T. (2020). Impact of crust-mantle mechanical coupling on the topographic and thermal evolutions during the necking phase of 'magma-poor' and 'sediment-starved' rift systems: A numerical modeling study. *Tectonophysics*, 228472. DOI: 10.1016/j.tecto.2020.228472

References

- Chevrot, S., Sylvander, M., Diaz, J., Ruiz, M., Paul, A., & PYROPE Working Group. (2015). The Pyrenean architecture as revealed by teleseismic P-to-S converted waves recorded along two dense transects. *Geophysical Journal International*, 200(2), 1096-1107. DOI: 10.1093/gji/ggu400
- Chevrot, S., Sylvander, M., Diaz, J., Martin, R., Mouthereau, F., Manatschal, G., Masini, E., Calassou, S., Grimaud, F. Pauchet, H., & Ruiz, M. (2018). The non-cylindrical crustal architecture of the Pyrenees. *Scientific Reports*, 8(1), 9591. DOI: 10.1038/s41598-018-27889-x
- Choukroune, P., & Mattauer, M. (1978). Tectonique des plaques et Pyrenees; sur le fonctionnement de la faille transformante nord-pyreneenne; comparaisons avec des modeles actuels. *Bulletin de La Societe Geologique de France*, S7-XX(5), 689-700. DOI : 10.2113/gssgfbull.S7-XX.5.689
- Choukroune, P., & ECORS Team (1989). The ECORS Pyrenean deep seismic profile reflection data and the overall structure of an orogenic belt. *Tectonics*, 8(1):23-39. DOI: 10.1029/tc008i001p00023
- Choukroune, P. (1989). Etude Continentale et Océanique par Reflexion et Refraction Sismique (ECORS) Team, The ECORS Pyrenean deep seismic profiles reflection data and the overall structure of an orogenic belt. *Tectonics*, 8, 23-39.
- Cohen, C. R. (1982). Model for a passive to active continental margin transition: implications for hydrocarbon exploration. *AAPG Bulletin*, 66(6), 708-718.
- Cochelin, (2016). Champ de déformation du socle paléozoïque des Pyrénées. Ph. D. Thesis. Université de Toulouse, France.
- Contrucci, I., Matias, L., Moulin, M., Géli, L., Klingelhofer, F., Nouzé, H., Aslanian, D., Olivet, J., Réhault, J. P. & Sibuet, J. C. (2004). Deep structure of the West African continental margin (Congo, Zaïre, Angola), between 5 S and 8 S, from reflection/refraction seismics and gravity data. *Geophysical Journal International*, 158(2), 529-553. DOI: 10.1111/j.1365-246X.2004.02303.x

D

- Dahlen, F. A., Suppe, J., & Davis, D. (1984). Mechanics of fold-and-thrust belts and accretionary wedges: Cohesive Coulomb theory. *Journal of Geophysical Research: Solid Earth*, 89(B12), 10087-10101.
- Dahlen, F. A. (1984). Noncohesive critical Coulomb wedges: An exact solution. *Journal of Geophysical Research: Solid Earth*, 89(B12), 10125-10133.
- Dahlen, F. A. (1990). Critical taper model of fold-and-thrust belts and accretionary wedges. *Annual Review of Earth and Planetary Sciences*, 18(1), 55-99.
- Dahlstrom, C. D. (1970). Structural geology in the eastern margin of the Canadian Rocky Mountains. *Bulletin of Canadian Petroleum Geology*, 18(3), 332-406.
- Davis, D., Suppe, J., & Dahlen, F. A. (1983). Mechanics of fold-and-thrust belts and accretionary wedges. *Journal of Geophysical Research: Solid Earth*, 88(B2), 1153-1172. DOI:10.1029/JB088iB02p01153

- Debroas, E. J. (1987). Modele de bassin triangulaire a l'intersection de décrochements divergents pour le fosse albo-cenomanien de la Ballongue (zone nord-pyreneenne, France). *Bulletin de La Societe Geologique de France*, III(5), 887. DOI: 10.2113/gssgfbull.III.5.887
- De Charpal, O., Guennoc, P., Montadert, L., & Roberts, D. G. (1978). Rifting, crustal attenuation and subsidence in the Bay of Biscay. *Nature*, 275(5682), 706-711.
- DeFelipe, I., Pedreira, D., Pulgar, J. A., Iriarte, E., & Mendia, M. (2017). Mantle exhumation and metamorphism in the Basque-Cantabrian Basin (NS pain): Stable and clumped isotope analysis in carbonates and comparison with ophicalcites in the North-Pyrenean Zone (Urdach and Lherz). *Geochemistry, Geophysics, Geosystems*, 18(2), 631-652. DOI: 10.1002/2016GC006690
- DeFelipe, I., Álvarez Pulgar, F. J., & Pedreira Rodríguez, D. (2018). Crustal structure of the Eastern Basque-Cantabrian Zone-western Pyrenees: from the Cretaceous hyperextension to the Cenozoic inversion. *Revista de la Sociedad Geológica de España*, 31 (2).
- DeFelipe, I., Pedreira, D., Pulgar, J. A., Van der Beek, P. A., Bernet, M., & Pik, R. (2019). Unraveling the Mesozoic and Cenozoic tectonothermal evolution of the eastern Basque-Cantabrian zone-western Pyrenees by low-temperature thermochronology. *Tectonics*, 38(9), 3436-3461. DOI: 10.1029/2019TC005532
- Dell'Ertale, D., & Schellart, W. P. (2013). The development of sheath folds in viscously stratified materials in simple shear conditions: An analogue approach. *Journal of Structural Geology*, 56, 129-141. DOI: 10.1016/j.jsg.2013.09.002
- Dewey, J. F., & Bird, J. M. (1970). Mountain belts and the new global tectonics. *Journal of Geophysical Research*, 75(14), 2625-2647.
- Dewey, J. F., & Burke, K. (1974). The Wilson cycle. *Nature*, 294, 313-316.
- Diaz, J., Pedreira, D., Ruiz, M., Pulgar, J. A., & Gallart, J. (2012). Mapping the indentation between the Iberian and Eurasian plates beneath the Western Pyrenees/Eastern Cantabrian Mountains from receiver function analysis. *Tectonophysics*, 570, 114-122. DOI: 10.1016/j.tecto.2012.07.005
- Dietrich, R., & Witherspoon, W. (1978). Palinspastic map of east Tennessee. *American Journal of Science*, 278(4), 543-550.
- Dooley, T., McClay, K. R., Hempton, M., & Smit, D. (2005). Salt tectonics above complex basement extensional fault systems: results from analogue modelling. In *Geological Society, London, Petroleum Geology Conference series* (Vol. 6, No. 1, pp. 1631-1648). Geological Society of London. DOI: 10.1144/0061631
- Dooley, T. P., Hudcok, M. R., Pichel, L. M., & Jackson, M. P. (2020). The impact of base-salt relief on salt flow and suprasalt deformation patterns at the autochthonous, paraautochthonous and allochthonous level: insights from physical models. *Geological Society, London, Special Publications*, 476(1), 287-315. DOI: 10.1144/SP476.13
- Doré, A. G., Lundin, E. R., Jensen, L. N., Birkeland, Ø., Eliassen, P. E., & Fichler, C. (1999). Principal tectonic events in the evolution of the northwest European Atlantic margin. In *Petroleum Geology of Northwest Europe: Proceedings of the 5th Conference* (pp. 41-61). Geological Society of London. DOI: 10.1144/0050041

- Ducoux, M., Jolivet, L., Callot, J. P., Aubourg, C., Masini, E., Lahfid, A., Homonnay, E., Cagnard, F., Gumiaux, C., & Baudin, T. (2019). The Nappe des Marbres Unit of the Basque-Cantabrian Basin: The Tectono-thermal Evolution of a Fossil Hyperextended Rift Basin. *Tectonics*, 38(11), 3881–3915. DOI: 10.1029/2018TC005348

E

- Ellis, S., Beaumont, C., Jamieson, R. A., & Quinlan, G. (1998). Continental collision including a weak zone: the vise model and its application to the Newfoundland Appalachians. *Canadian Journal of Earth Sciences*, 35(11), 1323–1346.
- Ellis, S., Schreurs, G., & Panien, M. (2004). Comparisons between analogue and numerical models of thrust wedge development. *Journal of Structural Geology*, 26(9), 1659–1675. DOI: 10.1016/j.jsg.2004.02.012
- Epin, M.-E., Manatschal, G., & Amann, M. (2017). Defining diagnostic criteria to describe the role of rift inheritance in collisional orogens: the case of the Err-Platta nappes (Switzerland). *Swiss Journal of Geosciences*, 110(2), 419–438. DOI: 10.1007/s00015-017-0271-6
- Erdős, Z., van der Beek, P., & Huisman, R. S. (2014). Evaluating balanced section restoration with thermochronology data: A case study from the Central Pyrenees. *Tectonics*, 33(5), 617–634. DOI: 10.1002/2013TC003481
- Erslev, E. A., Kellogg, K. S., Bryant, B., Ehrlich, T. K., Holdaway, S. M., & Naeser, C. W. (1999). Laramide to Holocene structural development of the northern Colorado Front Range.
- Espina, R.G. (1994). Mesozoic extension and Alpine compression in the western border of the Vasco-Cantabrian basin. *Cuad. Lab. Xeol. Laxe*, Vol. 19, 137–150.
- Espina, R. G. (1996). Tectónica extensional en el borde occidental de la Cuenca Vasco-Cantábrica (Cordillera Cantábrica, NO de España). *Geogaceta*, 20 (4), 890 - 892.

F

- Fernández-Viejo, G., Gallart, J., Pulgar, J. A., Córdoba, D., & Dañobeitia, J. J. (2000). Seismic signature of Variscan and Alpine tectonics in NW Iberia: Crustal structure of the Cantabrian Mountains and Duero basin. *Journal of Geophysical Research: Solid Earth*, 105(B2), 3001–3018. DOI: 10.1029/1999JB900321
- Fernández-Viejo, G., & Gallastegui, J. (2005). The ESCI-N Project after a decade: A síntesis of the results and open questions. *Trabajos de geología*, 25(25), 9–27. DOI: 10.17811/tdg.25.2005.9-27
- Fernández-Viejo, G., Cadenas, P., Acevedo, J., & Llana-Funez, S. (2020). Assessment of the continuity of the orogenic root beneath the Cantabrian-Pyrenean orogen. EGU General Assembly 2020. DOI: 10.5194/egusphere-egu2020-13772
- Ferrer, O., Roca, E., Benjumea, B., Muñoz, J. A., Ellouz, N., & Marconi Team. (2008). The deep seismic reflection MARCONI-3 profile: Role of extensional Mesozoic structure during the Pyrenean contractional deformation at the eastern part of the Bay of Biscay. *Marine and Petroleum Geology*, 25(8), 714–730. DOI: 10.1016/j.marpet-geo.2008.06.002

- Ferrer, O., Jackson, M.P.A., Roca, E., & Rubinat, M. (2012). Evolution of salt structures during extension and inversion of the Offshore Parentis Basin (Eastern Bay of Biscay). In *Alsop, G.I., Archer, S.G., Hartley, A.J., Grant, N.T., Hodgkinson, R. (Eds.), Salt Tectonics, Sediments and Prospectivity*. 363. Geological Society, London, Special Publications, pp. 361–380. DOI: 10.1144/SP363.16.
- Ferrer, O., Roca, E., & Vendeville, B.C. (2014). The role of salt layers in the hangingwall deformation of kinked-planar extensional faults: Insights from 3D analogue models and comparison with the Parentis Basin. *Tectonophysics*, 636, 338-350.
- Ferrer, O., McClay, K.R., & Sellier, N.C. (2016). Influence of fault geometries and mechanical anisotropies on the growth and inversion of hanging-wall synclinal basins: insights from sandbox models and natural examples. In: Child, C., Holdsworth, R.E., Jackson, C.A.L., Manzocchi, T., Walsh, J.J., Yieldings, G. (Eds.), *The Geometry and Growth of Normal Faults*. 439 Geological Society, London, Special Publications. DOI: 10.1144/SP439.8.
- Fillon, C., Pedreira, D., Van der Beek, P. A., Huisman, R. S., Barbero, L., & Pulgar, J. A. (2016). Alpine exhumation of the central Cantabrian Mountains, Northwest Spain. *Tectonics*, 35(2), 339–356. DOI: 10.1002/2015TC004050
- Fletcher, R., Kusznir, N., & Cheadle, M. (2009). Melt initiation and mantle exhumation at the Iberian rifted margin: Comparison of pure-shear and upwelling-divergent flow models of continental breakup. *Comptes Rendus Geoscience*, 341(5), 394-405. DOI: 10.1016/j.crte.2008.12.008
- Frisch, W., Meschede, M., & Blakey, R. C. (2010). *Plate tectonics: continental drift and mountain building*. Springer Science & Business Media.
- Floquet, M. (2004). El Cretácico superior de la Cuenca Vasco-Cantábrica y áreas adyacentes. In: Vera J.A. (ed) *Geología de España*. Sociedad Geológica de España – Instituto Geológico y Minero de España, Madrid, pp. 299-306.

G

- Gallastegui, J. (2000). Estructura cortical de la cordillera y margen continental cantábricos: perfiles ESCI-N. *Trabajos de Geología*, 22(22), 3-234.
- García de Cortázar, A., & Pujalte, V. (1982). Litoestratigrafía y facies del grupo Cabuerniga (Malm-Valangienense inferior?) al sur de Cantabria, NE de Palencia. *Cuadernos de Geología Ibérica*, 8, 5-21.
- García-Mondéjar, J. (1982). Tectónica sinsedimentaria en el Aptiense y Albiense de la región vasco-cantábrica occidental. *Cuadernos de Geología Ibérica*, 8, 23-26.
- García-Mondéjar, J., & García-Pascual, I. (1982). Estudio geológico del anticlinorio de Bilbao entre los ríos Nervión y Cadagua. *Kobie*, 12, 101-137.
- García-Mondéjar, J., Pujalte, V., & Robles, S. (1986). Características sedimentológicas secuenciales y tectonoestratigráficas del triásico de la Cantabria y norte de Palencia. *Cuadernos de Geología Ibérica*, 10, 151–172.
- García-Mondéjar, J., & Robador, A. (1987). Sedimentación y paleografía del Complejo Urgoniano (Aptiense-Albiense) en el área de Bermeo (región Vasco-Cantábrica septentrional). *Acta geológica hispánica*, 21(1), 411-418.

- García-Mondéjar, J. (1989). Strike-slip Subsidence of the Basque-Cantabrian Basin of Northern Spain and its Relationship to Aptian-Albian Opening of Bay of Biscay. In: Tankard AJ, Balkwill HR (eds) *Extensional Tectonics and Stratigraphy of the North Atlantic Margins. American Association of Petroleum Geologist, Memoir 46*, pp. 395–409.
- García-Mondéjar, J., & Fernández-Mendiola, P. A. (1993). Sequence stratigraphy and systems tracts of a mixed carbonate and siliciclastic platform-basin setting: the Albian of Lunada and Soba, northern Spain. *AAPG bulletin*, 77(2), 245–275.
- García-Mondéjar, J., Agirrezabala, L.M., Aranburu, A., Fernández-Mendiola, P.A., Gomez-Perez, I., López-Horgue, M.A., & Rosales, I. (1996). The Aptian–Albian tectonic pattern of the Basque Cantabrian Basin (Northern Spain). *Geological Journal*, 31, 13–45.
- García-Mondéjar, J., López-Horgue, M., Aranburu, A., Fernández-Mendiola, P. (2005). Pulsating subsidence during a rift episode: stratigraphic and tectonic consequences (Aptian–Albian, northern Spain). *Terra Nova*, 2005, 17, 6, 517–525. DOI: 10.1111/j.1365-3121.2005.00644.x
- García-Mondéjar, J., Carracedo-Sánchez, M., Owen, H., Fernández-Mendiola, P. (2018). The Early Aptian volcanic episode of Gutíolo (N Spain): Expression of the Bilbao Rift Fault Zone. *Geological Journal*, 54, 6, 3509–3526. DOI: 10.1002/gj.3342
- García-Senz, J., Pedrera, A., Ayala, C., Ruiz-Constán, A., Robador, A., & Rodríguez-Fernández, L. R. (2019). Inversion of the north Iberian hyperextended margin: the role of exhumed mantle indentation during continental collision. *Geological Society, London, Special Publications*, SP490–2019–112. DOI: 10.1144/SP490-2019-112
- Gerya, T., & Stöckhert, B. (2006). Two-dimensional numerical modeling of tectonic and metamorphic histories at active continental margins. *International Journal of Earth Sciences*, 95(2), 250–274. DOI: 10.1007/s00531-005-0035-9
- Gillard, M., Autin, J., Manatschal, G., Sauter, D., Munschy, M., & Schaming, M. (2015). Tectonomagmatic evolution of the final stages of rifting along the deep conjugate Australian-Antarctic magma-poor rifted margins: Constraints from seismic observations: Australian-Antarctic margins evolution. *Tectonics*, 34(4), 753–783. DOI: 10.1002/2015TC003850
- Gillard, M., Tugend, J., Müntener, O., Manatschal, G., Karner, G. D., Autin, J., Sauter, D., Figueredo, P., & Ulrich, M. (2019). The role of serpentinization and magmatism in the formation of decoupling interfaces at magma-poor rifted margins. *Earth-Science Reviews*, 196, 102882. DOI: 10.1016/j.earscirev.2019.102882
- Gómez, J. J., Goy, A., & Barrón, E. (2007). Events around the Triassic–Jurassic boundary in northern and eastern Spain: A review. *Palaeogeography, Palaeoclimatology, Palaeoecology*, 244(1–4), 89–110. DOI: 10.1016/j.palaeo.2006.06.025
- Gómez-Romeu, J., Masini, E., Tugend, J., Ducoux, M., & Kusznir, N. (2019). Role of rift structural inheritance in orogeny highlighted by the Western Pyrenees case-study. *Tectonophysics*, 766, 131–150. DOI: 10.1016/j.tecto.2019.05.022
- Granado, P., Ferrer, O., Muñoz, J. A., Thöny, W., & Strauss, P. (2017). Basin inversion in tectonic wedges: Insights from analogue modelling and the Alpine-Carpathian fold-and-thrust belt. *Tectonophysics*, 703, 50–68. DOI: 10.1016/j.tecto.2017.02.022

- Granado, P., Roca, E., Strauss, P., Pelz, K., & Munoz, J. A. (2018). Structural styles in fold-and-thrust belts involving early salt structures: The Northern Calcareous Alps (Austria). *Geology*, 47(1), 51–54. DOI: 10.1130/G45281.1
- Granado, P., & Ruh, J. B. (2019). Numerical modelling of inversion tectonics in fold-and-thrust belts. *Tectonophysics*, 763, 14–29. DOI: 10.1016/j.tecto.2019.04.033
- Graveleau, F., Malavieille, J., & Dominguez, S. (2012). Experimental modelling of orogenic wedges: A review. *Tectonophysics*, 538, 1–66. DOI: 10.1016/j.tecto.2012.01.027

H

- Hamilton, W. B. (1988). Laramide crustal shortening. *Interaction of the Rocky Mountain foreland and the Cordilleran thrust belt: Geological Society of America Memoir*, 171, 27–39.
- Hauptert, I., Manatschal, G., Decarlis, A., & Unternehr, P. (2016). Upper-plate magma-poor rifted margins: Stratigraphic architecture and structural evolution. *Marine and Petroleum Geology*, 69, 241–261. DOI: 10.1016/j.marpetgeo.2015.10.020
- Hernaiz, P.P. (1994). La Falla de Ubierna (margen SO de la cuenca Cantábrica). *Geogaceta*, 16, 39–42.
- Hernaiz, P. P., Serrano, A., Malagón, J., & Rodríguez Cañas, C. (1994). Evolución estructural del margen SO de la cuenca Vasco-Cantábrica. *Geogaceta*, 15(7994), 743–746.
- Hernández, J.M^a, Pujalte, V., Robles, S., & Martín-Closas, C. (1999). División estratigráfica genética del grupo Campóo (Malm-Cretácico interior, SW cuenca Vasco-cantábrica). *Rev. Soc. Geol. España*, 12 (3–4), 377–396.
- Hopper, J. R., Mutter, J. C., Larson, R. L., & Mutter, C. Z. (1992). Magmatism and rift margin evolution: Evidence from northwest Australia. *Geology*, 20(9), 853–857. DOI: 10.1130/0091-7613(1992)020<0853:MARMEE>2.3.CO;2
- Hubbert, M.K. (1951). Mechanical basis for certain familiar geologic structures. *Geological Society of America Bulletin*, 62(4), 355–372.

I

- Iaffa, D. N., Sàbat, F., Muñoz, J. A., Mon, R., & Gutierrez, A. A. (2011). The role of inherited structures in a foreland basin evolution. The Metán Basin in NW Argentina. *Journal of Structural Geology*, 33(12), 1816–1828. DOI: 10.1016/j.jsg.2011.09.005
- InfoIGME. Aplicación de consulta de información de hidrocarburos. Instituto Geológico y Minero de España. Available from <http://info.igme.es/Hidrocarburos/> (last consult: 2020/15/05)
- Izquierdo-Llavall, E., Roca, E., Xie, H., Pla, O., Muñoz, J. A., Rowan, M. G., Yuan, N., & Huang, S. (2018). Influence of overlapping décollements, syntectonic sedimentation, and structural inheritance in the evolution of a contractional system: The central Kuqa fold-and-thrust belt (Tian Shan Mountains, NW China). *Tectonics*, 37(8), 2608–2632. DOI: 10.1029/2017TC004928

J

- Jackson, J. A. (1980). Reactivation of basement faults and crustal shortening in orogenic belts. *Nature*, 283(5745), 343-346.
- Jackson, M. P., Vendeville, B. C., & Schultz-Ela, D. D. (1994). Structural dynamics of salt systems. *Annual Review of Earth and Planetary Sciences*, 22(1), 93-117. DOI: 10.1146/annurev.earth.22.050194.000521
- Jamieson, R. A., & Beaumont, C. (2013). On the origin of orogens. *Geological Society of America Bulletin*, 125(11-12), 1671-1702. DOI: 10.1130/B30855.1
- Jammes, S., Manatschal, G., Lavier, L., & Masini, E. (2009). Tectonosedimentary evolution related to extreme crustal thinning ahead of a propagating ocean: Example of the western Pyrenees. *Tectonics*, 28(4). DOI: 10.1029/2008TC002406
- Jammes, S., Lavier, L., & Manatschal, G. (2010). Extreme crustal thinning in the Bay of Biscay and the Western Pyrenees: From observations to modeling. *Geochemistry, Geophysics, Geosystems*, 11(10). DOI: 10.1029/2010GC003218
- Jammes, S., & Lavier, L. L. (2019). Effect of contrasting strength from inherited crustal fabrics on the development of rifting margins. *Geosphere*, 15(2), 407-422. DOI: 10.1130/GES01686.1

K

- Kley, J., Monaldi, C. R., & Salfity, J. A. (1999). Along-strike segmentation of the Andean foreland: causes and consequences. *Tectonophysics*, 301(1-2), 75-94. DOI: 10.1016/S0040-1951(98)90223-2
- Krabbendam, M., & Barr, T. D. (2000). Proterozoic orogens and the break-up of Gondwana: why did some orogens not rift?. *Journal of African Earth Sciences*, 31(1), 35-49.
- Kusznir, N. J., & Matthews, D. H. (1988). Deep seismic reflections and the deformational mechanics of the continental lithosphere. *Journal of Petrology*, (1), 63-87.

L

- Lagabriele, Y., Labaume, P., & de Saint Blanquat, M. (2010). Mantle exhumation, crustal denudation, and gravity tectonics during Cretaceous rifting in the Pyrenean realm (SW Europe): Insights from the geological setting of the lherzolite bodies. *Tectonics*, 29(4). DOI: 10.1029/2009TC002588
- Lagabriele, Y., Asti, R., Duretz, T., Clerc, C., Fourcade, S., Teixell, A., Labaume, P., Corre, B., & Saspiturry, N. (2020). A review of cretaceous smooth-slopes extensional basins along the Iberia-Eurasia plate boundary: How pre-rift salt controls the modes of continental rifting and mantle exhumation. *Earth-Science Reviews*, 201, 103071. DOI: 10.1016/j.earscirev.2019.103071
- Lavier, L. L., & Manatschal, G. (2006). A mechanism to thin the continental lithosphere at magma-poor margins. *Nature*, 440(7082), 324-328. DOI: 10.1038/nature04608
- Lemoine, M., Tricart, P., & Boillot, G. (1987). Ultramafic and gabbroic ocean floor of the Ligurian Tethys (Alps, Corsica, Apennines): In search of a genetic model. *Geology*, 15(7), 622-625.

- Lescoutre, R. (2019). Formation and reactivation of the Pyrenean-Cantabrian rift system: inheritance, segmentation and thermal evolution. Ph. D. Thesis. Université de Strasbourg, France.
- Lescoutre et al. subm.
- Lescoutre, R., & Manatschal, G. (2020). Role of rift-inheritance and segmentation for orogenic evolution: example from the Pyrenean-Cantabrian system. *BSGF-Earth Sciences Bulletin*, 191, 18. DOI: 10.1051/bsgf/2020021
- Lindholm, R. C. (1978). Triassic-Jurassic faulting in eastern North America—A model based on pre-Triassic structures. *Geology*, 6(6), 365-368.
- López-Gómez, J., Alonso-Azcárate, J., Arche, A., Arribas, J., Barrenechea, J. F., Borruel-Abadía, V., ... & Díez, J. B. (2019). Permian-Triassic Rifting Stage. In *The Geology of Iberia: A Geodynamic Approach* (pp. 29-112). Springer, Cham. DOI: 10.1007/978-3-030-11295-0_3
- López-Gómez, J., Martín-González, F., Heredia, N., de la Horra, R., Barrenechea, J. F., Cadenas, P., Juncal, M., Díez, J., Borruel-Abadía, V., Pedreira, D., García-Sansegundo, J., Farias, P., Galé, C., Lago, M., Ubide, T., Fernández-Viejo, G., & Gand, G. (2019). New lithostratigraphy for the Cantabrian Mountains: A common tectono-stratigraphic evolution for the onset of the Alpine cycle in the W Pyrenean realm, N Spain. *Earth-Science Reviews*, 188, 249–271. DOI: 10.1016/j.earscirev.2018.11.008
- López-Horgue, M. A., Poyato-Ariza, F. J., Cavin, L., & Bermudez-Rochas, D. D. (2014). Cenomanian transgression in the Basque-Cantabrian Basin (northern Spain) and associated faunal replacement. *Journal of Iberian Geology*, 40(3), 489–506. DOI: 10.5209/rev_JIGE.2014.v40.n3.42819
- Lotze, F. (1960). Zur Gliederung der Oberkreide in der Baskischen Depression (Nordspanien). *N. Jb. Geol. Palaönt. Abh.*, 3: 132-144.
- Lowell, J. D. (1995). Mechanics of basin inversion from worldwide examples. *Geological Society, London, Special Publications*, 88(1), 39-57.
- Lundin, E.R., & Doré, A.G. (2011). Hyperextension, serpentinization, and weakening: A new paradigm for rifted margin compressional deformation. *Geology* 39(4): 347–350. DOI: 10.1130/G31499.1.

M

- Macchiavelli, C., Vergés, J., Schettino, A., Fernández, M., Turco, E., Casciello, E., Torne, M., Pierantoni, P. P., & Tunini, L. (2017). A new southern North Atlantic isochron map: Insights into the drift of the Iberian plate since the Late Cretaceous. *Journal of Geophysical Research: Solid Earth*, 122(12), 9603-9626. DOI: 10.1002/2017JB014769
- Malavieille, J. (1984). Modelisation experimentale des chevauchements imbriques; application aux chaines de montagnes. *Bulletin de la Société géologique de France*, 7(1), 129-138.
- Malavieille, J. (2010). Impact of erosion, sedimentation, and structural heritage on the structure and kinematics of orogenic wedges: Analog models and case studies. *Gsa Today*, 20(1), 4-10.

- Manatschal, G., Froitzheim, N., Rubenach, M., & Turrin, B. D. (2001). The role of detachment faulting in the formation of an ocean-continent transition: insights from the Iberia Abyssal Plain. *Geological Society, London, Special Publications*, 187(1), 405-428. DOI: 10.1144/GSL.SP.2001.187.01.20
- Manatschal, G. (2004). New models for evolution of magma-poor rifted margins based on a review of data and concepts from West Iberia and the Alps. *International Journal of Earth Sciences*, 93(3), 432-466. DOI: <https://doi.org/10.1007/s00531-004-0394-7>
- Manatschal, G., & Müntener, O. (2009). A type sequence across an ancient magma-poor ocean-continent transition: the example of the western Alpine Tethys ophiolites. *Tectonophysics*, 473(1-2), 4-19. DOI: 10.1016/j.tecto.2008.07.021
- Manatschal, G., Lavier, L., & Chenin, P. (2015). The role of inheritance in structuring hyperextended rift systems: Some considerations based on observations and numerical modeling. *Gondwana Research*, 27(1), 140-164. DOI: 10.1016/j.gr.2014.08.006
- Mandl, G., De Jong, L. N. J., & Maltha, A. (1977). Shear zones in granular material. *Rock mechanics*, 9(2-3), 95-144.
- Martín-Chivelet, J., Floquet, M., García-Senz, J., Callapez, P. M., López-Mir, B., Muñoz, J. A., Barroso-Barcenilla, F., Segura, M., Soares, A. F., Dinis, P. M., Marques, J. F., & Arbués, P. (2019). Late Cretaceous Post-Rift to Convergence in Iberia. In: *The Geology of Iberia: A Geodynamic Approach*, Springer, Cham., pp. 285-376. DOI: https://doi.org/10.1007/978-3-030-11295-0_7
- Martínez Catalán, J., Arenas, R., García, F. D., Cuadra, P. G., Gómez-Barreiro, J., Abati, J., Castiñeiras, P., Fernández-Suárez, J., Sánchez, S., Andonaegui, P., Clavijo, E., Díez, A., Rubio, F., & Valle, B. (2007). Space and time in the tectonic evolution of the northwestern Iberian Massif: Implications for the Variscan belt. In *4-D framework of continental crust* (Vol. 200, pp. 403-423). Geological Society of America Memoir Boulder, Colorado. DOI: 10.1130/2007.1200(21)
- Masini, E., Manatschal, G., Mohn, G., & Unternehr, P. (2012). Anatomy and tectono-sedimentary evolution of a rift-related detachment system: The example of the Err detachment (central Alps, SE Switzerland). *Bulletin*, 124(9-10), 1535-1551. DOI: 10.1130/B30557.1
- Masini, E., Manatschal, G., Tugend, J., Mohn, G., & Flament, J. M. (2014). The tectono-sedimentary evolution of a hyper-extended rift basin: the example of the Arzacq-Mauléon rift system (Western Pyrenees, SW France). *International Journal of Earth Sciences*, 103(6), 1569-1596. DOI: 10.1007/s00531-014-1023-8
- Matte, P. (1991). Accretionary history and crustal evolution of the Variscan belt in Western Europe. *Tectonophysics*, 196(3-4), 309-337. DOI: 10.1016/0040-1951(91)90328-P
- Matte, P. (2001). The Variscan collage and orogeny (480–290 Ma) and the tectonic definition of the Armorica microplate: a review. *Terra nova*, 13(2), 122-128. DOI: 10.1046/j.1365-3121.2001.00327.x
- McClay, K. R. (1989). Analogue models of inversion tectonics. *Geological Society London, Special Publications*, 44, 1, 41-59.
- McClay, K. R., & Buchanan, P. G. (1992). Thrust faults in inverted extensional basins. In: *Thrust tectonics*. Springer, Dordrecht, 93-104.

- McClay, K. R., & White, M. J. (1995). Analogue modelling of orthogonal and oblique rifting. *Marine and Petroleum Geology*, 12(2), 137-151. DOI: 10.1016/0264-8172(95)92835-K
- McClay, K., Muñoz, J. A., & García-Senz, J. (2004). Extensional salt tectonics in a contractional orogen: A newly identified tectonic event in the Spanish Pyrenees. *Geology*, 32(9), 737-740. DOI: 10.1130/G20565.1
- McClay, K. R., Whitehouse, P. S., Dooley, T., & Richards, M. (2004). 3D evolution of fold and thrust belts formed by oblique convergence. *Marine and Petroleum Geology*, 21(7), 857-877.
- McKenzie, D. (1978). Some remarks on the development of sedimentary basins. *Earth and Planetary science letters*, 40(1), 25-32.
- McQuarrie, N., & DeCelles, P. (2001). Geometry and structural evolution of the central Andean backthrust belt, Bolivia. *Tectonics*, 20(5), 669-692. DOI: 10.1029/2000TC001232
- McQuarrie, N., Horton, B. K., Zandt, G., Beck, S., & DeCelles, P. G. (2005). Lithospheric evolution of the Andean fold-thrust belt, Bolivia, and the origin of the central Andean plateau. *Tectonophysics*, 399(1-4), 15-37. DOI: 10.1016/j.tecto.2004.12.013
- Mencos, J., Carrera, N., & Muñoz, J. A. (2015). Influence of rift basin geometry on the subsequent postrift sedimentation and basin inversion: The Organyà Basin and the Bóixols thrust sheet (south central Pyrenees). *Tectonics*, 34(7), 1452-1474. DOI: 10.1002/2014TC003692
- Meschede, M. (1987). The tectonic and sedimentary development of the Biscay synclinorium in northern Spain. *Geologische Rundschau*, 76(2), 567-577.
- Minshull, T. A., Dean, S. M., White, R. S., & Whitmarsh, R. B. (2001). Anomalous melt production after continental break-up in the southern Iberia Abyssal Plain. *Geological Society, London, Special Publications*, 187(1), 537-550. DOI: 10.1144/GSL.SP.2001.187.01.26
- Minshull, T. A. (2009). Geophysical characterisation of the ocean-continent transition at magma-poor rifted margins. *Comptes Rendus Geoscience*, 341(5), 382-393. DOI: 10.1016/j.crte.2008.09.003
- Miró, J., Muñoz, J.A., Manatschal, G., & Roca, E. (2020). The Basque – Cantabrian Pyrenees: report of data analysis, *BSGF – Earth Sciences Bulletin* Vol: 200005
- Miró et al. Subm. (See chapter 1)
- Mohn, G., Manatschal, G., Beltrando, M., Masini, E., & Kuszniir, N. (2012). Necking of continental crust in magma-poor rifted margins: Evidence from the fossil Alpine Tethys margins. *Tectonics*, 31(1). DOI: 10.1029/2011TC002961
- Molinaro, M., Leturmy, P., Guezou, J. C., Frizon de Lamotte, D., & Eshraghi, S. A. (2005). The structure and kinematics of the southeastern Zagros fold-thrust belt, Iran: From thin-skinned to thick-skinned tectonics. *Tectonics*, 24(3). DOI: 10.1029/2004TC001633
- Mouthereau, F., Filleaudeau, P. Y., Vacherat, A., Pik, R., Lacombe, O., Fellin, M. G., Castelltort, S., Christophoul, F., & Masini, E. (2014). Placing limits to shortening evolution in the Pyrenees: Role of margin architecture and implications for the Iberia/Europe convergence. *Tectonics*, 33(12), 2283-2314. DOI: 10.1002/2014TC003663

References

- Muñoz, J. A. (1992). Evolution of a continental collision belt: ECORS-Pyrenees crustal balanced cross-section. In *Thrust tectonics* (pp. 235-246). Springer, Dordrecht. DOI: 10.1007/978-94-011-3066-0_21
- Muñoz, J.A. (2002). The Pyrenees. In: Gibbons W., Moreno T. Eeds. *The Geology of Spain. Geological Society London*, London, 370–385.
- Muñoz, J. A., Beamud, E., Fernández, O., Arbués, P., Dinarès-Turell, J., & Poblet, J. (2013). The Ainsa Fold and thrust oblique zone of the central Pyrenees: Kinematics of a curved contractional system from paleomagnetic and structural data. *Tectonics*, 32(5), 1142-1175. DOI: 10.1002/tect.20070
- Muñoz, J. A., Mencos, J., Roca, E., Carrera, N., Gratacós, O., Ferrer, O., & Fernández, O. (2018). The structure of the South-Central-Pyrenean fold and thrust belt as constrained by subsurface data. *Geologica Acta*, 16(4), 439-460. DOI: 10.1344/GeologicaActa2018.16.4.7
- Muñoz, J. A. (2019). Alpine Orogeny: Deformation and Structure in the Northern Iberian Margin (Pyrenees sl). In *The Geology of Iberia: A Geodynamic Approach* (pp. 433-451). Springer, Cham. DOI: 10.1007/978-3-030-11295-0_9
- Muñoz, J.A. (2019). L'orògen Pirinenc: estructura i inversió del Marge Nord-Ibèric. *Memòries de la Reial Acadèmia de Ciències i Arts de Barcelona*. Tercera època, num. 1058, Vol. LXVIII, num.1

N

- Neres, M., Miranda, J. M., & Font, E. (2013). Testing Iberian kinematics at Jurassic-Cretaceous times. *Tectonics*, 32(5), 1312–1319. DOI: 10.1002/tect.20074
- Nemčok, M., Mora, A., & Cosgrove, J. (2013). Thick-skin-dominated orogens; from initial inversion to full accretion: an introduction. *Geological Society, London, Special Publications*, 377(1), 1-17. DOI: 10.1144/SP377.17
- Nirrengarten, M., Manatschal, G., Tugend, J., Kusznir, N. J., & Sauter, D. (2017). Nature and origin of the J-magnetic anomaly offshore Iberia–Newfoundland: implications for plate reconstructions. *Terra Nova*, 29(1), 20-28. DOI: 10.1111/ter.12240
- Nirrengarten, M., Manatschal, G., Tugend, J., Kusznir, N., & Sauter, D. (2018). Kinematic evolution of the southern North Atlantic: Implications for the formation of hyper-extended rift systems. *Tectonics*, 37(1), 89-118. DOI: 10.1002/2017TC004495

O

- Osmundsen, P. T., & Ebbing, J. (2008). Styles of extension offshore mid-Norway and implications for mechanisms of crustal thinning at passive margins. *Tectonics*, 27(6). DOI: 10.1029/2007TC002242

P

- Pedreira, D., Pulgar, J. A., Gallart, J., & Díaz, J. (2003). Seismic evidence of Alpine crustal thickening and wedging from the western Pyrenees to the Cantabrian Mountains (north Iberia). *Journal of Geophysical Research: Solid Earth*, 108(B4). DOI: 10.1029/2001jb001667

- Pedreira, D., Pulgar, J. A., Gallart, J., & Torné, M. (2007). Three-dimensional gravity and magnetic modeling of crustal indentation and wedging in the western Pyrenees-Cantabrian Mountains. *Journal of Geophysical Research*, 112(B12), B12405. DOI: 10.1029/2007JB005021
- Pedreira, D., Afonso, J. C., Pulgar, J. A., Gallastegui, J., Carballo, A., Fernández, M., García-Castellanos, D., Jiménez-Munt, I., Semprich, J., & García-Moreno, O. (2015). Geophysical-petrological modeling of the lithosphere beneath the Cantabrian Mountains and the North-Iberian margin: Geodynamic implications. *Lithos*, 230, 46–68. DOI: 10.1016/j.lithos.2015.04.018
- Pedreira, D., Pulgar, J. A., Díaz, J., Alonso, J. L., Gallastegui, J., & Teixell, A. (2018). Comment on “Reconstruction of the Exhumed Mantle Across the North Iberian Margin by Crustal-Scale 3-D Gravity Inversion and Geological Cross Section” by Pedrera et al. *Tectonics*, 37(11), 4338–4345. DOI: 10.1029/2018TC005129
- Pedrera, A., García-Senz, J., Ayala, C., Ruiz-Constán, A., Rodríguez-Fernández, L. R., Robador, A., & González Menéndez, L. (2017). Reconstruction of the Exhumed Mantle Across the North Iberian Margin by Crustal-Scale 3-D Gravity Inversion and Geological Cross Section: Mantle Along the Basque-Cantabrian Basin. *Tectonics*, 36(12), 3155–3177. DOI: 10.1002/2017TC004716
- Pedrera, A., García-Senz, J., Ayala, C., Ruiz-Constán, A., Rodríguez-Fernández, L. R., Robador, A., & González Menéndez, L. (2018). Reply to Comment by Pedreira et al. on “Reconstruction of the Exhumed Mantle Across the North Iberian Margin by Crustal-Scale 3-D Gravity Inversion and Geological Cross Section.” *Tectonics*, 37(11), 4346–4356. DOI: 10.1029/2018TC005222
- Péron-Pinvidic, G., Manatschal, G., Dean, S.M., & Minshull, T.A. (2008). Compressional structures on the West Iberia rifted margin: controls on their distribution. *Geological Society, London, Special Publications* 306(1): 169–183. DOI: 10.1144/SP306.8.
- Péron-Pinvidic, G., & Manatschal, G. (2009). The final rifting evolution at deep magma-poor passive margins from Iberia-Newfoundland: a new point of view. *International Journal of Earth Sciences*, 98(7), 1581-1597. DOI: 10.1007/s00531-008-0337-9
- Péron-Pinvidic, G., Manatschal, G., & Osmundsen, P.T. (2013). Structural comparison of archetypal Atlantic rifted margins: A review of observations and concepts. *Marine and Petroleum Geology*, 43, 21-47. DOI: 10.1016/j.marpetgeo.2013.02.002
- Péron-Pinvidic, G., Manatschal, G., & the “IMAGinING RIFTING” Workshop Participants (2019). Rifted margins: State of the art and future challenges. *Frontiers in Earth Science*, 7, 218. DOI: 10.3389/feart.2019.00218
- Peropadre, C., Mediato, J. F., Hernaiz, P. P., Robador, A., Solé, F. X., & Sarrionandía, F. (2012). La discordancia de La Mesa (base de las Facies Utrillas) en el sinclinal de Polientes (Cretácico, Cuenca Vasco-Cantábrica): implicaciones tectónicas. *Geotemas*, 13, 85.
- Petri, B. (2014). Formation et exhumation des granulites permienes. Établir les conditions pré-rift et déterminer l’histoire de l’exhumation syn-rift. Ph. D. Thesis. Université de
- Pfiffner, O. A. (2006). Thick-skinned and thin-skinned styles of continental contraction. *Special Papers-Geological Society of America*, 414, 153. DOI: 10.1130/2006.2414(09)

References

- Pfiffner, O. A. (2016). Basement-involved thin-skinned and thick-skinned tectonics in the Alps. *Geological Magazine*, 153(5-6), 1085-1109. DOI: 10.1017/S0016756815001090
- Pinto, L., Muñoz, C., Nalpas, T., & Charrier, R. (2010). Role of sedimentation during basin inversion in analogue modelling. *Journal of Structural Geology*, 32(4), 554-565. DOI: 10.1016/j.jsg.2010.03.001
- Pla, O., Roca, E., Xie, H., Izquierdo-Llavall, E., Muñoz, J. A., Rowan, M. G., Ferrer, O., Gratacós, O., Yuan, N., & Huang, S. (2019). Influence of Syntectonic Sedimentation and Décollement Rheology on the Geometry and Evolution of Orogenic Wedges: Analog Modeling of the Kuqa Fold-and-Thrust Belt (NW China). *Tectonics*, 38(8), 2727-2755. DOI: 10.1029/2018TC005386
- Pous, J., Muñoz, J., Ledo, J., & Liesa, M. (1995). Partial melting of subducted continental lower crust in the Pyrenees. *Journal of the Geological Society*, 152(2), 217-220.
- Price, R. A. (1971). Gravitational sliding and the foreland thrust and fold belt of the North American Cordillera: Discussion. *Geological Society of America Bulletin*, 82(4), 1133-1138.
- Price, R. A. (1973). Large-scale gravitational flow of supracrustal rocks, southern Canadian Rockies. *Gravity and tectonics*, 491-502.
- Puigdefàbregas, C., Muñoz, J. A., & Vergés, J. (1992). Thrusting and foreland basin evolution in the Southern Pyrenees. In: McClay, K. R. (Ed.), *Thrust Tectonics*, pp. 247-254. Doi: 10.1007/978-94-011-3066-0_22
- Pujalte, V. (1979). Control tectónico de la sedimentación “purbeck-weald” en las provincias de Santander y N. de Burgos. *Acta Geológica Hispánica*, 14, 216- 222.
- Pujalte, V. (1981). Sedimentary succession and palaeoenvironments within fault-controlled basin: the “Wealden” of the Santander area, Northern Spain. *Sedimentary Geology*, 28, 293-325.
- Pujalte, V. (1982). La evolución paleogeográfica de la cuenca ‘Wealdense’de Cantabria. *Cuadernos de Geología Ibérica*, 8, 65-83.
- Pujalte, V. (1989). Ensayo de correlación de las sucesiones del Oxfordiense-Barremiense de la Región Vasco-Cantábrica basado en macrosecuencias deposicionales: implicaciones paleogeográficas. *Cuadernos de Geología Ibérica*, 13, 199-215.
- Pujalte, V., Robles, S., Orue-etxebarria, X., Zapata, M., & García-Portero, J. (1989). Influencia del eustatismo y la tectónica en la génesis de secuencias y macrosecuencias deposicionales del Maastrichtiense superior-Eoceno inferior de la Cuenca Vasca. In: *Congreso Español de Sedimentología*. 12. Simposios, pp. 147-156.
- Pujalte, V., Robles, S., & Hernández, J. M. (1996). La sedimentación continental del Grupo Campóo (Malm-Cretácico basal de Cantabria, Burgos y Palencia): testimonio de un reajuste hidrográfico al inicio de una fase rift. *Cuad. Geol. Ibérica*, 21, 227-251.
- Pujalte, V., Robles, S., Orue-Etxebarria, X., Baceta, J. I., Payros, A., & Larruzea, I. F. (2000). Uppermost Cretaceous-Middle Eocene strata of the Basque-Cantabrian Region and western Pyrenees: a sequence stratigraphic perspective. *Revista de la Sociedad Geológica de España*, 13(2), 191-211.

Pulgar, J., Gallart, J., Fernández-Viejo, G., Pérez-Estaún, A., Álvarez-Marrón, J., & ESCIN Group (1996). Seismic image of the Cantabrian Mountains in the western extension of the Pyrenees from integrated ESCIN reflection and refraction data. *Tectonophysics*, 264, 1–19.

Pulgar, J. A., Alonso, J. L., Espina, R. G., & Marín, J. A. (1999). La deformación alpina en el basamento varisco de la Zona Cantábrica. *Trabajos De Geología*, 21(21), 283–295. DOI: 10.17811/tdg.21.1999.283-295

Q

Quesada, S., Robles, S., & Pujalte, V. (1991). Correlación secuencial y sedimentológica entre registros de sondeos y series de superficie del Jurásico Marino de la Cuenca de Santander (Cantabria, Palencia y Burgos). *Geogaceta*, 10, 3-6.

Quesada, S., Robles, S., & Pujalte, V. (1993). El Jurásico Marino del margen suroccidental de la Cuenca Vasco-Cantábrica y su relación con la exploración de hidrocarburos. *Geogaceta*, 13, 92–96.

Quesada, S., Robles, S., & Rosales, I. (2005). Depositional architecture and transgressive–regressive cycles within Liassic backstepping carbonate ramps in the Basque–Cantabrian basin, northern Spain. *Journal of the Geological Society*, 162(3), 531–548. DOI: 10.1144/0016-764903-041

Quintà, A., & Tavani, S. (2012). The foreland deformation in the south-western Basque–Cantabrian Belt (Spain). *Tectonophysics*, 576–577, 4–19. DOI: 10.1016/j.tecto.2012.02.015

Quintana, L., (2012). Extensión e Inversión Tectónica en el sector central de la Región Vasco-Cantábrica (Cantabria-Vizcaya, norte de España). Ph. D. Thesis. Universidad de Oviedo, Spain.

Quintana, L., Pulgar, J. A., & Alonso, J. L. (2015). Displacement transfer from borders to interior of a plate: A crustal transect of Iberia. *Tectonophysics*, 663, 378–398. DOI: 10.1016/j.tecto.2015.08.046

Quirk, D. G., Barragan, R., Boucher, J., Clemson, J., Tsire, J., Minko, G. B., ... & Leveille, J. (2003). Salt tectonics in Gabon: generic model for pre-salt and post-salt structures in West Africa. *Africa – New Plays, New Perspectives, PESGB/HGS Conference*, Houston, 3–4 Sep., Extended Abstracts (CD).

Quirk, D. G., & Pilcher, R. S. (2012). Flip-flop salt tectonics. *Geological Society, London, Special Publications*, 363(1), 245-264. DOI: 10.1144/SP363.11

R

Rat, P. (1988). The Basque-Cantabrian Basin between the Iberian and European plates. Some facts but still many problems. *Revista de la Sociedad Geológica de España*, 1, 327–348.

Rat, J., Mouthereau, F., Brichau, S., Crémades, A., Bernet, M., Balvay, M., Ganne, J., Lahfid, A., & Gautheron, C. (2019). Tectonothermal evolution of the Cameros basin: Implications for tectonics of North Iberia. *Tectonics*, 38(2), 440-469. DOI: 10.1029/2018TC005294

References

- Razin, P. (1989). Evolution tecto-sédimentaire alpine des Pyrénées Basques à l'Ouest de la transformante de Pamplona (province du Labourd) (Doctoral dissertation).
- Reston, T. J., & Pérez-Gussinyé, M. (2007). Lithospheric extension from rifting to continental breakup at magma-poor margins: rheology, serpentinisation and symmetry. *International Journal of Earth Sciences*, 96(6), 1033-1046. DOI: 10.1007/s00531-006-0161-z
- Reston, T. J. (2009). The extension discrepancy and syn-rift subsidence deficit at rifted margins. *Petroleum Geoscience*, 15(3), 217-237. DOI: 10.1144/1354-079309-845
- Reston, T., & Manatschal, G. (2011). Rifted margins: Building blocks of later collision. In *Arc-continent collision* (pp. 3-21). Springer, Berlin, Heidelberg. DOI: 10.1007/978-3-540-88558-0_1
- Riba, O., & Jurado, M.J. (1992). Reflexiones sobre la geología de la parte occidental de la Depresión del Ebro. *Acta Geológica Hispánica*, Libro Homenaje a Oriol Riba Arderiu, 27(1/2):177-193
- Ribes, C., Manatschal, G., Ghienne, J. F., Karner, G. D., Johnson, C. A., Figueredo, P. H., Incerpi, N., & Epín, M. E. (2019). The syn-rift stratigraphic record across a fossil hyper-extended rifted margin: the example of the northwestern Adriatic margin exposed in the Central Alps. *International Journal of Earth Sciences*, 108(6), 2071-2095. DOI: 10.1007/s00531-019-01750-6
- Robles, S., Pujalte, V., & García-Mondéjar, J. (1988). Evolución de los sistemas sedimentarios del margen continental cantábrico durante el Albiense y Cenomaniense, en la transversal del litoral vizcaino. *Revista de la Sociedad Geológica de España*, 1, 409-441.
- Robles, S., Pujalte, V., Hernández, J.M., & Quesada, S. (1996). La sedimentación aluvio-lacustre de la Cuenca de Cires (Jurásico sup.-Berriasiense de Cantabria): un modelo evolutivo de las cuencas lacustres ligadas a la etapa temprana del rift noribérico. *Cuadernos de Geología Ibérica*, 21, 253-275.
- Robles, S. (2004). El Pérmico de la Cuenca Vasco-Cantábrica. In: Vera J.A. (ed) *Geología de España. Sociedad Geológica de España – Instituto Geológico y Minero de España*, Madrid, pp. 269-271.
- Robles, S., & Pujalte, V. (2004). El Triásico de la Cordillera Cantábrica. In: Vera J.A. (ed) *Geología de España. Sociedad Geológica de España – Instituto Geológico y Minero de España*, Madrid, pp. 274-276.
- Robles, S., Aranburu, A., & Apraiz, A. (2014). La Cuenca Vasco-Cantábrica: génesis y evolución tectonosedimentaria. *Enseñanza de las Ciencias de la Tierra*, 22(2), 99.
- Roca, E., Muñoz, J. A., Ferrer, O., & Ellouz, N. (2011). The role of the Bay of Biscay Mesozoic extensional structure in the configuration of the Pyrenean orogen: Constraints from the MARCONI deep seismic reflection survey. *Tectonics*, 30(2). DOI: 10.1029/2010TC002735
- Rodríguez-Lázaro, J., Pascual, A., & Elorza, J. (1998). Cenomanian events in the deep western Basque Basin: the Leioa section. *Cretaceous Research*, 19(6), 673-700.
- Roeder, D., & Witherspoon, W. (1978). Palinspastic map of east Tennessee. *American Journal of Science*, 278(4), 543-550.

- Roeder, D., Roberts, D. G., & Bally, A. W. (2013). Convergent margins and orogenic belts. *Regional Geology and Tectonics: Principles of Geologic Analysis A, 1*, 114-177. DOI: 10.1016/B978-0-444-53042-4.00006-6
- Roest, W. R., & Srivastava, S. P. (1991). Kinematics of the plate boundaries between Eurasia, Iberia, and Africa in the North Atlantic from the Late Cretaceous to the present. *Geology*, 19(6), 613-616. DOI: 10.1130/0091-7613(1991)019<0613:KOTPB>2.3.CO;2
- Roma, M., Vidal-Royo, O., McClay, K., Ferrer, O., & Muñoz, J. A. (2018a). Tectonic inversion of salt-detached ramp-syncline basins as illustrated by analog modeling and kinematic restoration. *Interpretation*, 6(1), T127-T144. DOI: 10.1190/INT-2017-0073.1
- Roma, M., Ferrer, O., Roca, E., Pla, O., Escosa, F. O., & Butillé, M. (2018b). Formation and inversion of salt-detached ramp-syncline basins. Results from analog modeling and application to the Columbrets Basin (Western Mediterranean). *Tectonophysics*, 745, 214-228. DOI: 10.1016/j.tecto.2018.08.012
- Rosenbaum, G., Lister, G. S., & Duboz, C. (2002). Relative motions of Africa, Iberia and Europe during Alpine orogeny. *Tectonophysics*, 359(1-2), 117-129. DOI: 10.1016/S0040-1951(02)00442-0
- Rowan, M. G. (2014). Passive-margin salt basins: Hyperextension, evaporite deposition, and salt tectonics. *Basin Research*, 26(1), 154-182. DOI: 10.1111/bre.12043
- Rowan, M. G., & Giles, K. A. (2020). Passive versus active salt diapirism. *AAPG Bulletin*, (20,200,622). DOI: 10.1306/05212020001
- Ruiz, M. (2007). Caracterizació estructural i sismotectònica de la litosfera en el domini Pirenaico-Cantàbric a partir de mètodes de sísmica activa i pasiva. Ph. D. Thesis, Universitat de Barcelona, Spain.
- Ruiz, M., Díaz, J., Pedreira, D., Gallart, J., & Pulgar, J. A. (2017). Crustal structure of the North Iberian continental margin from seismic refraction/wide-angle reflection profiles. *Tectonophysics*, 717, 65-82. DOI: 10.1016/j.tecto.2017.07.008

S

- Salas, R., Guimerà, J., Mas, R., Martín-Closas, C., Meléndez, A., & Alonso, A. (2001). Evolution of the Mesozoic central Iberian Rift System and its Cainozoic inversion (Iberian chain). *Peri-Tethys Memoir*, 6, 145-185.
- Schellart, W. P. (2000). Shear test results for cohesion and friction coefficients for different granular materials: scaling implications for their usage in analogue modelling. *Tectonophysics*, 324(1-2), 1-16. DOI: 10.1016/S0040-1951(00)00111-6
- Schmid, S.M., Fügenschuh, B., Kissling, R. & Schuster, R. (2004): TRANSMED Transects IV, V and VI: Three lithospheric transects across the Alps and their forelands. In: Cavazza W, Roure F, Spakman W, Stampfli GM, and Ziegler PA (eds) *The TRANSMED Atlas: the Mediterranean Region from Crust to Mantle*. Springer Verlag, in press.
- Serrano, A., Hernaiz, P.P., Malagón, J., Rodríguez Cañas, C. (1994). Tectónica distensiva y halocinesis en el margen SO de la cuenca Vasco-Cantábrica. *Geogaceta*, 15, 131-134

References

- Serrano, A., & Martínez del Olmo, W. (2004). Estructuras diapíricas de la zona meridional de la Cuenca Vasco-Cantábrica. In: Vera J.A. (ed) *Geología de España*. Sociedad Geológica de España – Instituto Geológico y Minero de España, Madrid, pp. 334-338.
- Sibuet, J. C., Srivastava, S. P., & Spakman, W. (2004). Pyrenean orogeny and plate kinematics. *Journal of Geophysical Research: Solid Earth*, 109(B8). DOI: 10.1029/2003JB002514
- Sibuet, J. C., Srivastava, S., & Manatschal, G. (2007). Exhumed mantle-forming transitional crust in the Newfoundland-Iberia rift and associated magnetic anomalies. *Journal of Geophysical Research: Solid Earth*, 112(B6). DOI: 10.1029/2005JB003856
- Srivastava, S. P., Roest, W. R., Kovacs, L. C., Oakey, G., Levesque, S., Verhoef, J., & Macnab, R. (1990). Motion of Iberia since the Late Jurassic: results from detailed aeromagnetic measurements in the Newfoundland Basin. *Tectonophysics*, 184(3-4), 229-260. DOI: 10.1016/0040-1951(90)90442-B
- Soto, R., Casas-Sainz, A. M., Villalaín, J. J., & Oliva-Urcia, B. (2007). Mesozoic extension in the Basque–Cantabrian basin (N Spain): Contributions from AMS and brittle mesostructures. *Tectonophysics*, 445(3-4), 373–394. Doi: 10.1016/j.tecto.2007.09.007
- Soto, R., Casas-Sainz, A. M., Villalaín, J. J., Gil-Imaz, A., Fernández-González, G., Del Río, P., Calvo, M., & Mochales, T. (2008). Characterizing the Mesozoic extension direction in the northern Iberian plate margin by anisotropy of magnetic susceptibility (AMS). *Journal of the Geological Society*, 165(6), 1007–1018. Doi: 10.1144/0016-76492007-163
- Stampfli, G. M., & Borel, G. D. (2002). A plate tectonic model for the Paleozoic and Mesozoic constrained by dynamic plate boundaries and restored synthetic oceanic isochrons. *Earth and Planetary Science Letters*, 196(1-2), 17-33. DOI: 10.1016/S0012-821X(01)00588-X
- Stampfli, G. M., & Hochard, C. (2009). Plate tectonics of the Alpine realm. *Geological Society, London, Special Publications*, 327(1), 89-111. DOI: 10.1144/SP327.6
- Stevaux, J., & Winnock, E. (1974). Les bassins du Trias et du Lias inferieur d'Aquitaine et leurs episodes evaporitiques. *Bulletin de La Societe Geologique de France*, S7-XVI(6), 679–695. DOI: 10.2113/gssgfbull.S7-XVI.6.679
- Stewart, S. A. (1999). Geometry of thin-skinned tectonic systems in relation to detachment layer thickness in sedimentary basins. *Tectonics*, 18(4), 719-732. DOI: 10.1029/1999TC900018
- Suppe, J. (2007). Absolute fault and crustal strength from wedge tapers. *Geology*, 35(12), 1127-1130. DOI: 10.1130/G24053A.1
- Sutra, E., & Manatschal, G. (2012). How does the continental crust thin in a hyperextended rifted margin? Insights from the Iberia margin. *Geology*, 40(2), 139–142. DOI: 10.1130/G32786.1
- Sutra, E., Manatschal, G., Mohn, G., & Unternehr, P. (2013). Quantification and restoration of extensional deformation along the Western Iberia and Newfoundland rifted margins. *Geochemistry, Geophysics, Geosystems*, 14(8), 2575-2597. DOI: 10.1002/ggge.20135

T

- Tavani, Stefano, Carola, E., Granado, P., Quintà, A., & Muñoz, J. A. (2013). Transpressive inversion of a Mesozoic extensional forced fold system with an intermediate décollement level in the Basque-Cantabrian Basin (Spain). *Tectonics*, 32(2), 146–158. DOI: 10.1002/tect.20019
- Tavani, S., Bertok, C., Granado, P., Piana, F., Salas, R., Vigna, B., & Muñoz, J. A. (2018). The Iberia-Eurasia plate boundary east of the Pyrenees. *Earth-Science Reviews*, 187, 314–337. DOI: 10.1016/j.earscirev.2018.10.008
- Teixell, A. (1996). The Ansó transect of the southern Pyrenees: basement and cover thrust geometries. *Journal of the Geological Society*, 153(2), 301–310. DOI: 10.1144/gsjgs.153.2.0301
- Teixell, A., Labaume, P., & Lagabriele, Y. (2016). The crustal evolution of the west-central Pyrenees revisited: inferences from a new kinematic scenario. *Comptes Rendus Geoscience*, 348(3–4), 257–267. DOI: 10.1016/j.crte.2015.10.010
- Teixell, A., Labaume, P., Ayarza, P., Espurt, N., de Saint Blanquat, M., & Lagabriele, Y. (2018). Crustal structure and evolution of the Pyrenean-Cantabrian belt: A review and new interpretations from recent concepts and data. *Tectonophysics*, 724–725, 146–170. DOI: 10.1016/j.tecto.2018.01.009
- Tozer, R. S. J., Butler, R. W. H., & Corrado, S. (2002). Comparing thin-and thick-skinned thrust tectonic models of the Central Apennines, Italy. *EGU Stephan Mueller Special Publication Series*, 1, 181–194.
- Tugend, J. (2013). Rôle de l’hyper-extension lors de la formation de systèmes de rift et implications pour les processus de réactivation et de formation des orogènes : l’exemple du Golfe de Gascogne et des Pyrénées. Ph. D. Thesis. Université de Strasbourg, France.
- Tugend, J., Manatschal, G., Kusznir, N. J., Masini, E., Mohn, G., & Thion, I. (2014a). Formation and deformation of hyperextended rift systems: Insights from rift domain mapping in the Bay of Biscay-Pyrenees. *Tectonics*, 33(7), 1239–1276. DOI: 10.1002/2014TC003529
- Tugend, J., Manatschal, G., Kusznir, N. J., & Masini, E. (2014b). Characterizing and identifying structural domains at rifted continental margins: application to the Bay of Biscay margins and its Western Pyrenean fossil remnants. *Geological Society, London, Special Publications*, 413(1), 171–203. DOI: 10.1144/SP413.3
- Tugend, J., Manatschal, G., & Kusznir, N. J. (2015). Spatial and temporal evolution of hyperextended rift systems: Implication for the nature, kinematics, and timing of the Iberian-European plate boundary. *Geology*, 43(1), 15–18. DOI: 10.1130/G36072.1

V

- Van Dalssen, W., Doornenbal, J. C., Dortland, S., & Gunnink, J. L. (2006). A comprehensive seismic velocity model for the Netherlands based on lithostratigraphic layers. *Netherlands Journal of Geosciences*, 85(4), 277–292.

References

- Vanderhaeghe, O. (2012). The thermal–mechanical evolution of crustal orogenic belts at convergent plate boundaries: A reappraisal of the orogenic cycle. *Journal of Geodynamics*, 56, 124-145. DOI: 10.1016/j.jog.2011.10.004
- Vendeville, B. C., & Jackson, M. P. (1992). The rise of diapirs during thin-skinned extension. *Marine and Petroleum Geology*, 9(4), 331-354. DOI: 10.1016/0264-8172(92)90047-I
- Vergés, J., & García-Senz, J. (2001). Mesozoic evolution and Cainozoic inversion of the Pyrenean rift. *Mémoires du Muséum national d'histoire naturelle* (1993), 186, 187-212.
- Vergés, J., Fernández, M., & Martínez, A. (2002). The Pyrenean orogen: pre-, syn-, and post-collisional evolution. *Journal of the Virtual Explorer*, 8, 57-76. Doi: 10.3809/jvirtex.2002.00058
- Vidal-Royo, O., Muñoz, J. A., Hardy, S., Koyi, H., & Cardozo, N. (2013). Structural evolution of the Pico del Águila anticline (External Sierras, southern Pyrenees) derived from sandbox, numerical and 3D structural modelling techniques. *Geologica Acta: an international earth science journal*, 11(1), 1-23.
- Vissers, R. L. M., & Meijer, P. T. (2012). Iberian plate kinematics and Alpine collision in the Pyrenees. *Earth-Science Reviews*, 114(1-2), 61-83. DOI: 10.1016/j.earscirev.2012.05.001
- Vissers, R. L., van Hinsbergen, D. J., van der Meer, D. G., & Spakman, W. (2016). Cretaceous slab break-off in the Pyrenees: Iberian plate kinematics in paleomagnetic and mantle reference frames. *Gondwana Research*, 34, 49-59. DOI: 10.1016/j.gr.2016.03.006

W

- Wang, Yi, Chevrot, S., Monteiller, S., Komatitsch, D., Mouthereau, F., Manatschal, G., Sylvander, S., Diaz, J., Ruiz, M., Grimaud, F., Benahmed, S., Pauchet, H., & Martin, R. (2016). The deep roots of the western Pyrenees revealed by full waveform inversion of teleseismic P waves. *Geology*, 44, 6, 475-478. DOI: 10.1130/G37812.1
- Wehr, H., Chevrot, S., Courrioux, G., & Guillen, A. (2018). A three-dimensional model of the Pyrenees and their foreland basins from geological and gravimetric data. *Tectonophysics*, 734, 16-32. DOI: 10.1016/j.tecto.2018.03.017
- Weijermars, R., & Schmeling, H. (1986). Scaling of Newtonian and non-Newtonian fluid dynamics without inertia for quantitative modelling of rock flow due to gravity (including the concept of rheological similarity). *Physics of the Earth and Planetary Interiors*, 43(4), 316-330. DOI: 10.1016/0031-9201(86)90021-X
- Weijermars, R. (1986). Flow behaviour and physical chemistry of bouncing putties and related polymers in view of tectonic laboratory applications. *Tectonophysics*, 124(3-4), 325-358. DOI: 10.1016/0040-1951(86)90208-8
- Wernicke, B. (1981). Low-angle normal faults in the Basin and Range Province: nappe tectonics in an extending orogen. *Nature*, 291(5817), 645-648.
- Wernicke, B. (1985). Uniform-sense normal simple shear of the continental lithosphere. *Canadian Journal of Earth Sciences*, 22(1), 108-125. DOI: 10.1139/e85-009
- Whitmarsh, R. B., Manatschal, G., & Minshull, T. A. (2001). Evolution of magma-poor continental margins from rifting to seafloor spreading. *Nature*, 413, 150.

- Whitmarsh, R. B., Minshull, T. A., Russell, S. M., Dean, S. M., Loudon, K. E., & Chian, D. (2001). The role of syn-rift magmatism in the rift-to-drift evolution of the West Iberia continental margin: geophysical observations. *Geological Society, London, Special Publications*, 187(1), 107-124. DOI: 10.1144/GSL.SP.2001.187.01.06
- Willett, S., Beaumont, C., & Fullsack, P. (1993). Mechanical model for the tectonics of doubly vergent compressional orogens. *Geology*, 21(4), 371-374.
- Wilson, J. T. (1966). Are the structures of the Caribbean and Scotia arc regions analogous to ice rafting?. *Earth and Planetary Science Letters*, 1(5), 335-338.
- Wilson, J. T. (1968). Static or mobile earth: the current scientific revolution. *Proceedings of the American Philosophical Society*, 112(5), 309-320.
- Withjack, M. O., & Callaway, S. (2000). Active normal faulting beneath a salt layer: an experimental study of deformation patterns in the cover sequence. *AAPG bulletin*, 84(5), 627-651. DOI: 10.1306/C9EBCE73-1735-11D7-8645000102C1865D
- Wu, J. E., McClay, K., Whitehouse, P., & Dooley, T. (2009). 4D analogue modelling of transtensional pull-apart basins. *Marine and Petroleum Geology*, 26(8), 1608-1623. DOI: 10.1016/j.marpetgeo.2008.06.007
- Wyoming State Geological Survey (2020, July 22): Geologic history of Wyoming. Retrieved from <https://www.wsgs.wyo.gov/wyoming-geology/geologic-history.aspx>

Z

- Ziegler, P. A. (1988). Post-Hercynian plate reorganization in the Tethys and Arctic-North Atlantic domains. In *Developments in Geotectonics* (Vol. 22, pp. 711-755). Elsevier. DOI: 10.1016/B978-0-444-42903-2.50035-X





ANNEXES

The cover photo of the Annexes is taken from the Doniene Gaztelugatxeko hermitage, facing the Cantabrian Sea (Bizkaia province) to the west.

ANNEX 1: THE BASQUE - CANTABRIAN PYRENEES: REPORT OF DATA ANALYSIS

Accepted in BSGF – Earth Science Bulletin

Jordi Miró^{1,2}, Josep A. Muñoz², Gianreto Manatschal¹, Eduard Roca²

1 Institut de Physique du Globe de Strasbourg, CNRS-UMR 7516, EOST, Université de Strasbourg, 1 rue Blessig, F-67084 Strasbourg Cedex, France

2 Institut de Recerca Geomodels, Departament de Dinàmica de la Terra i de l'Oceà, Facultat de Ciències de la Terra, Universitat de Barcelona, Barcelona 08028, Spain

Corresponding author: jmiropadrisa@unistra.fr

Key Words: Basque – Cantabrian Pyrenees, tectono-stratigraphy, seismic data, drill hole data

Mots-clés : Pyrénées Basque – Cantabriques, tectono-stratigraphie, sismique de réflexion, données de forage

ABSTRACT

This contribution presents the analysis of a data set that was put together in the PhD thesis of Jordi Miró which is part of the OROGEN Project. The Basque – Cantabrian Pyrenees, that are the focus of this report, have been extensively studied over the last years. Several open debates in the Earth Science community aroused from this realm regarding the formation and reactivation of rift domains and formation of fold and thrust belts. This report summarizes the main tectonic models proposed to explain both the extension and reactivation history over this area and compile a series of data to consider for further discussions and interpretations. This report includes a thematic map of the Basque – Cantabrian Pyrenees showing an analysis of the tectono-stratigraphic evolution of the area. The map covers an area of more than 33.000 km² and is a graphic representation of the geology of the region based on a large geodatabase including previous published maps and field observations. A composite reflection seismic line crossing the entire Basque – Cantabrian Pyrenees from the Ebro foreland basin to the offshore Landes High is also presented. This section enables to present a continuous dataset along the entire area with the projection of few drill holes, which are presented with the stratigraphic logs following the same tectono-stratigraphic legend obtained from the previous analysis.

The main goal of this data report is to provide a coherent and complete dataset to the community, which enables to propose, discuss and test some of the new concepts related to the formation and reactivation of rifted margins. This data report is complementary to the contributions of Lescoutre & Manatschal (2020) and Cadenas et al. 2020 that are part of the same special volume.

RÉSUMÉ

Cette contribution présente l'analyse d'une compilation de données acquises par Jordi Miró lors de sa thèse de doctorat qui s'inscrit dans le projet OROGEN. Les Pyrénées Basco-Cantabriques, qui sont l'objet de ce rapport, ont été largement étudiées au cours de ces dernières années. Cette chaîne orogénique a alimenté de nombreuses discussions concernant la formation et la réactivation des domaines de rift ainsi que la formation des chaînes d'avant-pays (« fold-and-thrust belt »). Ce rapport résume les principaux modèles proposés dans la zone d'étude pour expliquer l'évolution tectonique de l'extension à la réactivation, et compile une série de données à prendre en considération pour les discussions et interprétations futures. Il comprend notamment une carte thématique des Pyrénées Basco-Cantabriques montrant les différentes unités tectono-stratigraphiques de la zone. La carte, qui couvre une superficie de plus de 33000 km², est une représentation graphique de la géologie régionale s'appuyant sur une large quantité de données comprenant des cartes publiées précédemment ainsi que de nouvelles observations de terrain. Un profile de réflexion sismique composite traversant la totalité des Pyrénées Basco-Cantabriques (du bassin d'avant-pays de l'Ebre au Haut des Landes) est également présentée. Cette section permet de présenter un ensemble de données continu sur toute la zone via notamment la projection des informations extraites des puits de forage tels que les logs stratigraphiques.

L'objectif principal de ce rapport est de fournir à la communauté scientifique un ensemble de données cohérent et complet permettant de proposer, discuter et tester certains des nouveaux concepts liés à la formation et à la réactivation des marges hyper-étirées. Ce rapport de données fournit des informations complémentaires aux études disponibles dans cette publication spéciale du projet OROGEN.

1.1. INTRODUCTION

This report presents the analysis of a data set used in the PhD thesis of J. Miró to propose and test new extensional concepts for the Basque – Cantabrian Pyrenees [e.g. multistage and polyphase (Cadenas et al., 2020; Péron-Pinvidic & Manatschal, 2009)] and their role on the subsequent inversion of these basins. This report is part of a PhD that is in the framework of the OROGEN Project (www.rogen-project.com). The aim of the OROGEN Project is to make all data sets used and produced available for the community, the reason why this report is part of this special volume.

Datasets are fundamental to propose, discuss, improve, and test new tectonic concepts and models. In the case of the Basque – Cantabrian Pyrenees, many datasets have been published during the last decades supporting the most recent interpretations. These datasets include: magnetic data (Pedreira et al., 2007); gravity data (Pedrera et al., 2017; García-Senz et al., 2019); velocity models (Pedreira et al., 2003); seismic refraction (Ruiz et al., 2017); thermochronology data (Fillon et al., 2016), and magnetic susceptibility data (Soto et al., 2007; Soto et al., 2008). Some studies using reflection seismic data have been published recently (e.g. Carola et al., 2015; Pedrera et al., 2017) but a continuous seismic line crossing the entire Basque – Cantabrian Pyrenees has not been assembled and published yet. In this report we present a composite reflection seismic line crossing the whole Basque – Cantabrian Pyrenees from the Ebro Basin in the south to the offshore Landes High in the north. This composite line combined with available drill hole data from the area and tomographic data provides a dataset that forms the foundation for new interpretations and models of the area as well as for their calibration. To localize and help the understanding of the data presented (i.e. seismic lines and drill holes) a thematic map of the Basque – Cantabrian Pyrenees has been compiled based on the revision of previous geological maps, as well as field observations. The aim is to analyse the tectono-sedimentary evolution of the area in order to propose a new, simple and clear legend to understand the tectono-stratigraphic evolution of the area. Although this map is mainly built on existing data and does not pretend to be new, the compilation as presented in the map defines and describes the distribution of tectono-stratigraphic units in a new way and forms the foundation to support a new set of models and ideas presented in this volume and other upcoming publications.

The Pyrenees, geologically speaking, constitute the westernmost branch of the Alpine orogenic system that connects from the Pyrenees through the Alps and the Carpathians to the Himalayas (Carola, 2014). Within the Pyrenees, the stratigraphic record and the

structural style changes significantly along strike (Carola et al., 2013) and as a result, different physiographic units can be identified along the mountain belt. This fact has been captured in the literature with a wide range of names, both geographical and geological, being used to refer to the same areas (Fig. A1.1) (see Barnolas & Pujalte, 2004 for an extended revision of terminology). In this work, the area located between the Pamplona System [(Lescoutre & Manatschal 2020 (in this volume)] to the east and the Asturian Massif (also referred to as Cantabrian Mountains) to the west, will be named as the Basque – Cantabrian Pyrenees (Fig. A1.1). The traditional term Basque – Cantabrian Basin will be used to refer to the Mesozoic extensional basins that were formed between the Iberia, Ebro and Eurasian plate boundaries in this domain.

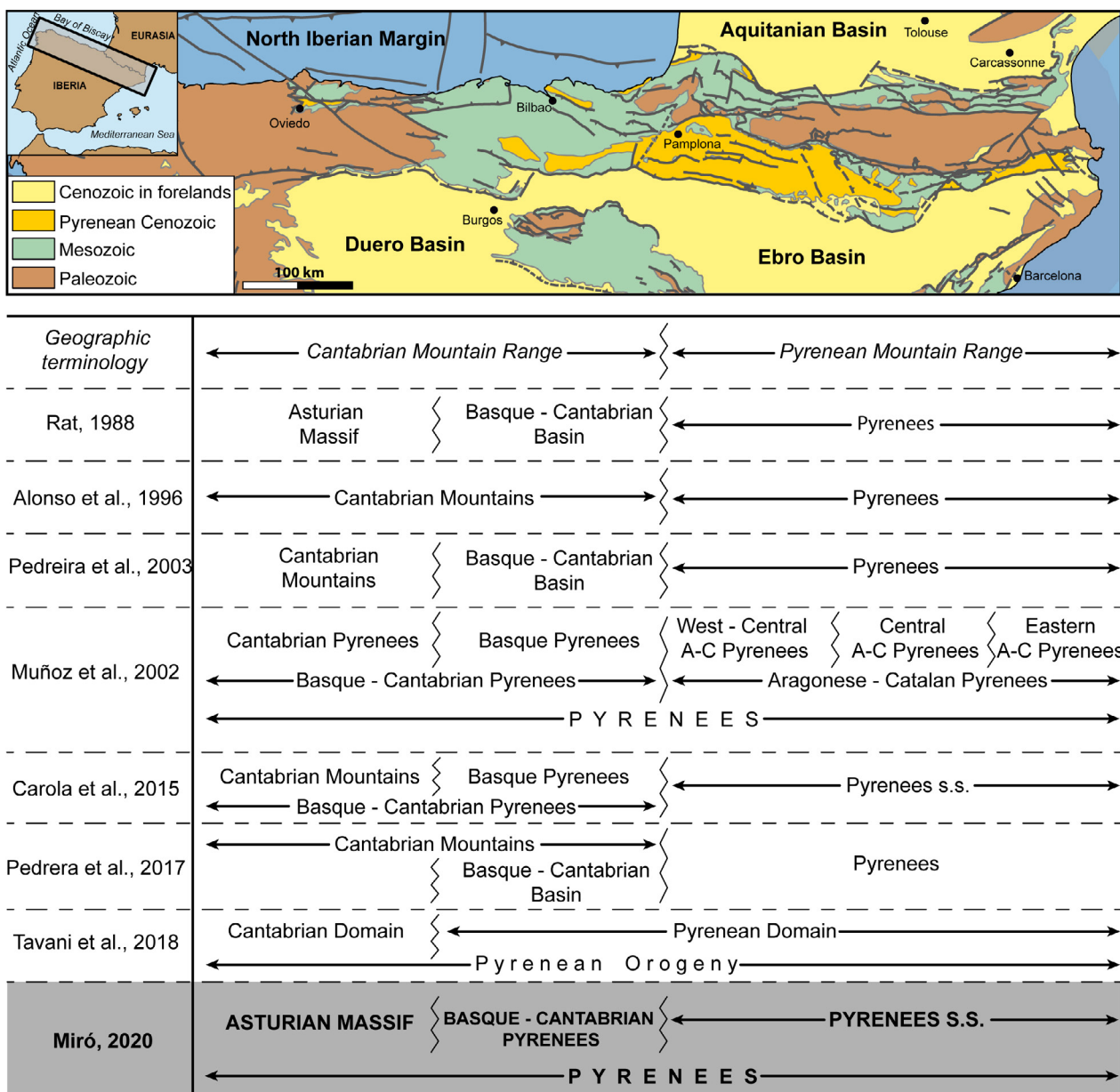


Figure A1.1 : Geographic terminology and some examples of geological terminology used in the Pyrenees. Modified from Barnolas and Pujalte (2004) and Carola et al. (2013).

1.2. GEOLOGICAL FRAMEWORK

The Basque – Cantabrian Pyrenees are part of the doubly verging Pyrenean Orogen, which resulted from the Late Cretaceous to Cenozoic collision between the Iberia and Eurasian plates (Puigdefàbregas et al., 1992; Muñoz, 2002; Vergés et al., 2002) (Fig. A1.2a). The Alpine orogeny inverted the Mesozoic basins developed in the Bay of Biscay – Pyrenean realm, where a segmented hyperextended system formed the limit between the Iberian and European plates during the Late Jurassic to the Early Cretaceous. The transtensional and extensional evolution led to extreme crustal thinning (< 10km) and locally to mantle exhumation in some of those basins (e.g. Basque – Cantabrian Basin and Mauleón Basin), whereas the Bay of Biscay further to the west reached the formation of oceanic crust (Sibuet et al., 2004; Tavani et al., 2018). However, the so-called Basque – Cantabrian Basin comprises, in fact, up to three Mesozoic sub-basins (Fig. A1.2a): (1) the Basque Cantabrian Basin *sensu strictu*, a NW - SE elongated basin with a more than 12km thick succession of Upper Jurassic to Cenomanian sediments forming, at present, the Bilbao Anticlinorium (Lotze, 1960; Brinkmann & Lögters, 1968; Pujalte, 1989; García-Mondéjar et al., 1996; Barnolas & Pujalte, 2004; García-Mondéjar et al., 2005); (2) the Cabuerniga Basin, a triangular shape basin with at least 3km of Upper Jurassic to Lower Cretaceous sediments located to the north-west of the Basque – Cantabrian Pyrenees (Pujalte, 1979, 1981; García-Mondéjar & García-Pascual, 1982; Espina, 1994) ; and (3) the Polientes Basin, located to the south-west of the area with a sedimentary succession of more than 4km of sediments, Upper Jurassic to Lower Cretaceous in age (García de Cortazar & Pujalte, 1982; Pujalte, 1982; Espina, 1996). The formation and reactivation of the Basque – Cantabrian Basin is the subject of a long debate between different schools, as detailed below.

1.2.1. EXTENSIONAL BASIN MODELS PROPOSED IN THE BASQUE – CANTABRIAN PYRENEES

Three main extensional rift basin models can be invoked to explain the formation of the North Iberian rift system: the classical low- β basin (i.e. North Sea – type basins), the strike-slip trans-tensional basin (i.e. San Andreas system) and the high- β basin model (i.e. hyperextended Iberia margin type system) (Fig. A1.2b).

In the Basque-Cantabrian Pyrenees all the previous models have been proposed to explain the formation and evolution of the extensional system. Quintana et al. (2015), Pedrera et al. (2017) and García-Senz et al. (2019) proposed that the basins were controlled by a main south-dipping normal fault located to the north. Consequently, they interpreted the Mesozoic succession in the Bilbao Anticlinorium area as the result of an extensional

rollover related to the major fault. A second group of authors (e.g. García-Mondéjar, 1989; García-Mondéjar et al., 1996, 2018) suggested a trans-tensional strike-slip model to explain the Mesozoic depocenter of the Basque – Cantabrian Basin. Moreover, Cámara (1997, 2017) introduced salt tectonics in the same kinematic model to explain the presence of diapirs and salt-walls. The latter model proposed a sort of salt-controlled mini-basins instead of basement-controlled half-graben basins. A third interpretation, inspired by the recent publications addressing the Newfoundland and West Iberia margins (Péron-Pinvidic & Manatschal, 2009) and the Arzacq-Mauleon Basin (Jammes et al., 2009; Lagabriele et al., 2010), explains the Mesozoic evolution of the Bay of Biscay by a combination of the classical extensional model and the hyperextended model (Roca et al., 2011). Following this interpretation, high-angle normal faults controlled the deformation in the brittle parts of the crust and mantle, while deformation was distributed and decoupled in the ductile levels. In areas where crust was notably thinner due to high lithospheric extension, the basin structure was asymmetric and controlled by extensional detachment faults dipping to the north and cutting the entire residual <10km thick brittle crust (e.g. Basque – Cantabrian Basin).

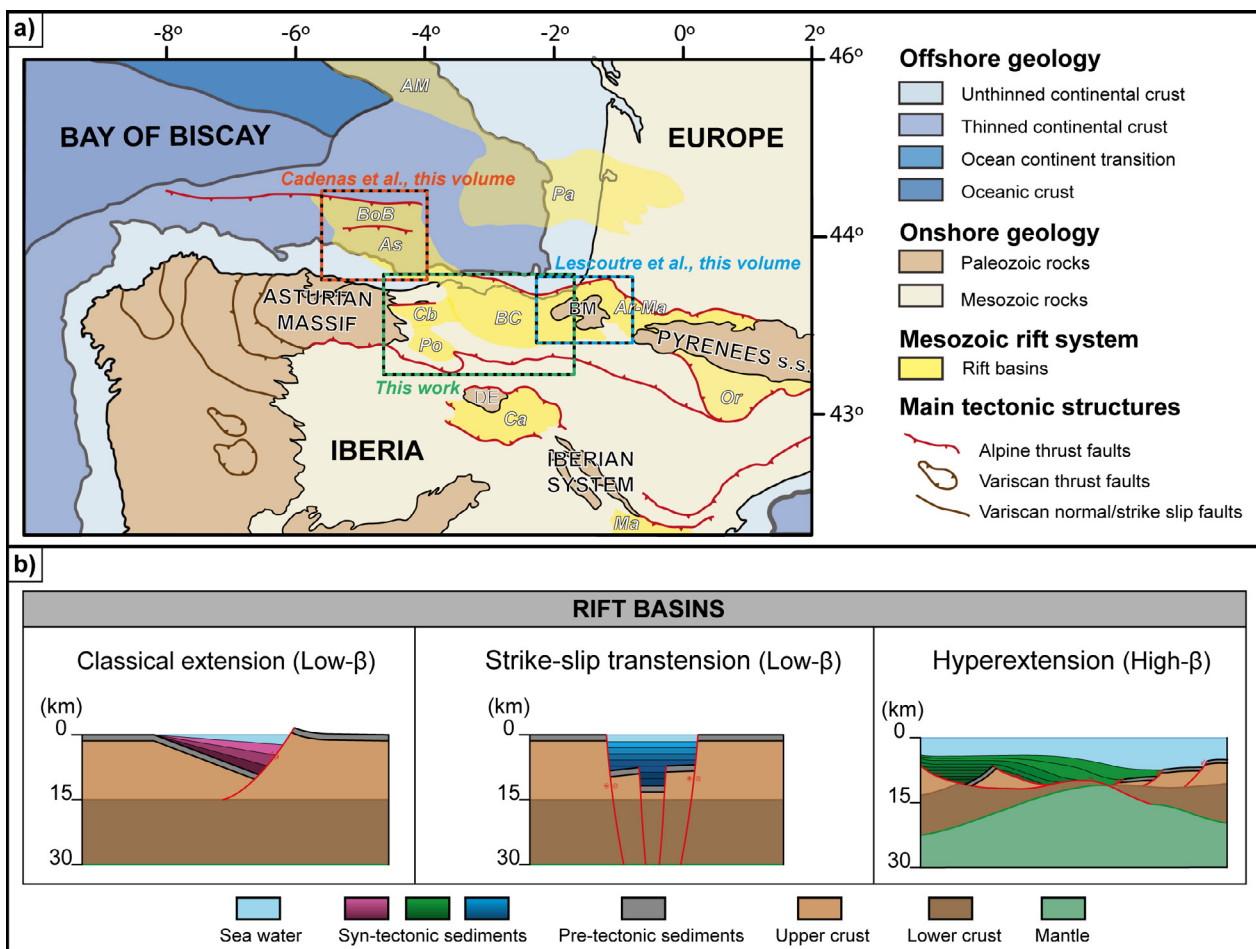


Figure A1.2 : a) Tectonic map of the Pyrenean – Bay of Biscay realm with the main structural features resulted from the Alpine orogeny and the presence of the main Mesozoic basins labelled in white: AM: Armorican Margin Basin, Ar-Ma: Arzaq-Mauleon Basin, As: Asturian Basin, BC: Basque – Cantabrian Basin s.s., BoB: Bay of Biscay Basin, Ca: Cameros Basin, Cb: Cabuerniga Basin, Po: Polientes Basin, Or: Organyà Bain, Ma: Maestrat Basin, Pa: Parentis Basin. Labelled in black Paleozoic Massifa: BM: Basque Massif, DE: Demanda Massif. Modified after Masini *et al.* (2014). b) Rift basin models described in the literature.

1.2.2. COMPRESSIONAL MODELS APPLIED TO THE BASQUE – CANTABRIAN PYRENEES

For the subsequent reactivation of the depocenters located in the Basque – Cantabrian Basin, different models have been proposed, being grouped in: (1) thin-skinned models, (2) basement-involved thin-skinned models and (3) thick-skinned strike-slip models.

The first thin-skinned model (Hernaiz et al, 1994 and reference therein; Serrano et al., 1994) was inspired on the south-western part of the Basque – Cantabrian Pyrenees related to the frontal imbricates (Folded Band) and the Burgalesa Platform (Fig. A1.3). This model argued for Jurassic to Lower Cretaceous sediments detached from the Paleozoic basement along the Triassic evaporites and transported several kilometres to the south. A more recent study proposed a thin-skin reactivation for the entire Basque – Cantabrian Basin, suggesting a large transport of the Mesozoic succession to the south on top of the Upper Triassic evaporites (Muñoz, 2019).

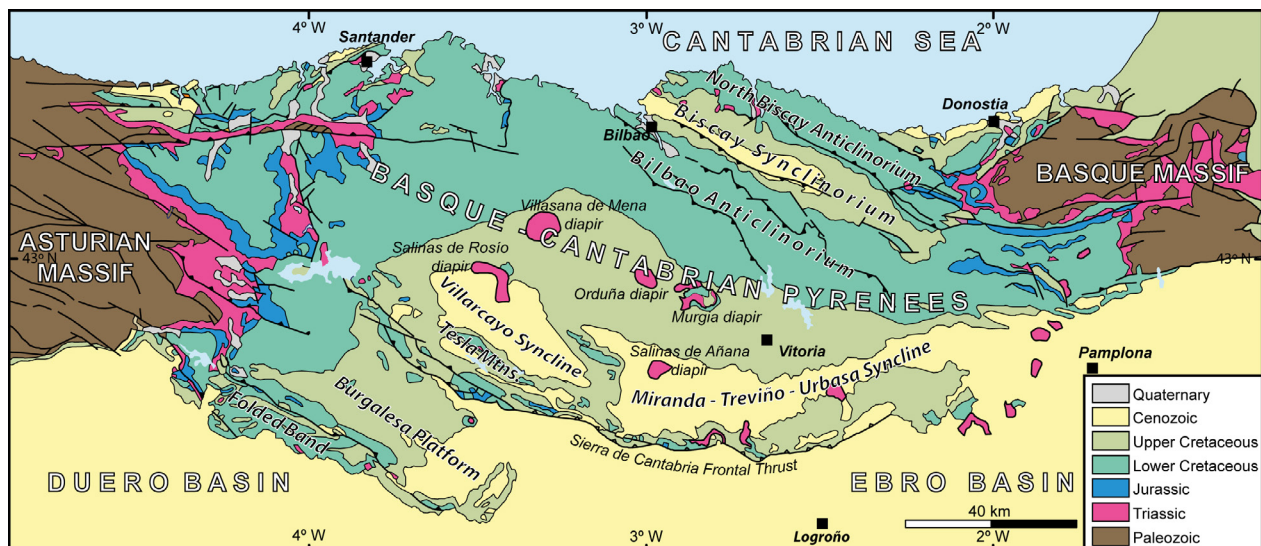


Figure A1.3 : Simplified geological map of the Basque – Cantabrian Pyrenees with the main domains labelled in capital letters and minor domains labelled in black. Modified after Ábalos et al. (2008).

The second group of models assumed the involvement of the basement even in the frontal imbricates. Some authors argued for relatively thin basement thrust sheets, suggesting a basement-involved thin-skinned deformation (Espina, 1996; Quintana et al., 2015). These

authors recognized the presence of Triassic evaporites, which formed salt accumulations, such as diapirs, and acting as a partial decoupling horizon. Opposed to this interpretation, Pedrera et al. (2017) and García-Senz et al. (2019) suggested the classical thick-skinned deformation style, where thrusts are cutting the entire upper crust and some of them even the lower crust, implying a minor role of the salt during compressional reactivation. These models assumed that the compressional phase was controlled by the reactivation of inherited extensional structures describing a complex set of basement blocks, defining the architecture observed on the sedimentary cover.

The third set of models explained the contractional evolution of the Basque – Cantabrian Pyrenees as a reactivation of the extensional faults bounding the half-grabens with a significant component of strike-slip deformation, either with an important role of the Upper Triassic salt (Tavani et al., 2013; Cámara, 2017) or a minor influence of salt (García-Mondéjar et al., 1996; García-Mondéjar et al., 2018).

1.3. DATA

The composite seismic line presented in this report includes nine seismic lines provided by the Spanish Geological Survey (IGME) (see Annex 2.1 for details): BB-1, PR-42, PR-42-P, S-82-14, VA-4, BR-9, BR-61, BR85-25 and 615. They were acquired between the 70's and the 90's during different hydrocarbon exploration campaigns after the first oil discoveries in the Basque – Cantabrian Pyrenees, such as the Ayoluengo oil field in 1963. Nine drill holes drilled during the same period for hydrocarbon exploration purposes and also provided by IGME have been projected to the composite seismic line (see Annex 2.2 for more information): Rojas NE-1, Navajo-1, Trespaderne-1, La Hoz-2, Zuazo-1, Ubidea-1, Arratia-1, Cormoran-1 and Vizcaya B-1. In order to project the boreholes that are in depth in a seismic line that is in time, a simple time-depth conversion to the seismic section has been done by using a generic velocity of 4800 m/s.

A compilation of several geological maps as well as maps from other thesis and publications have been compiled to present a new global thematic map of the entire Basque – Cantabrian Pyrenees (see Annex 2.3 for the references of all the maps used). The simple but consistent organization of the units allows to document the tectono-stratigraphic evolution of the area from Triassic to present-day. The Fig. A1.4 shows the polygons of the areas covered by the maps compiled in this report and the location of the drill hole data as well as seismic data presented.

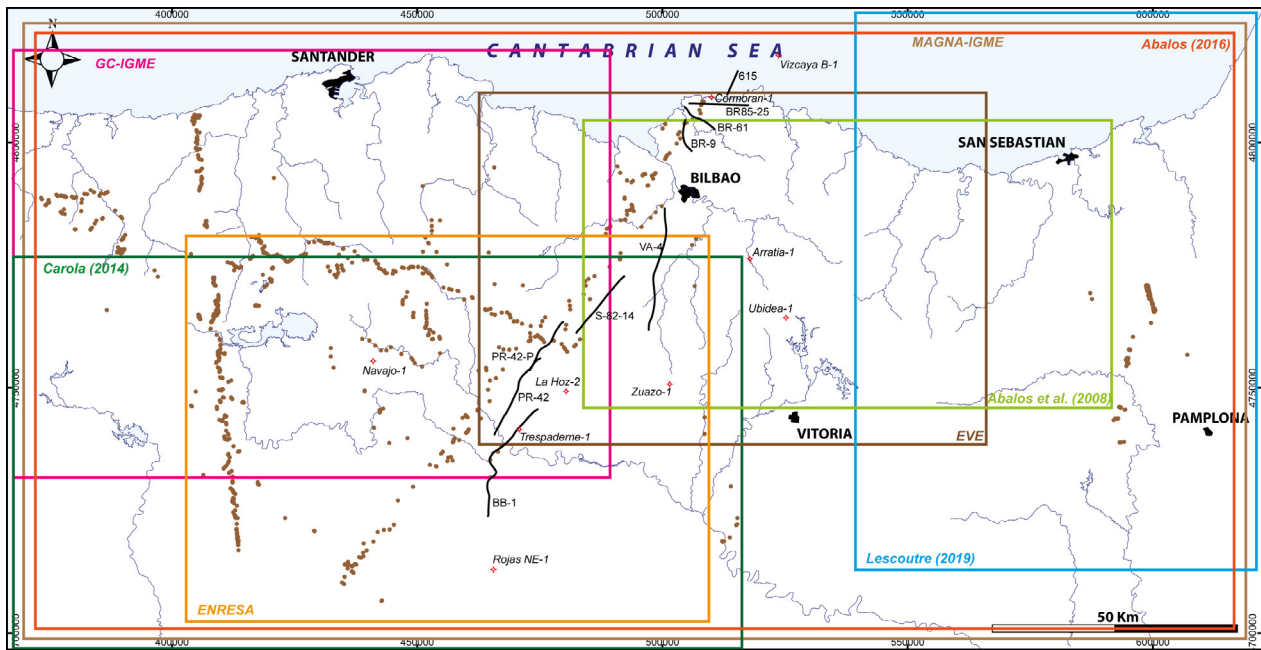


Figure A1.4 : Geological map of the Basque – Cantabrian Pyrenees with the location of seismic lines, drill holes, and field data (i.e. measurements and observations) in brown dots presented in this work. The geological maps compiled to build the thematic map presented in this work are also located: MAGNA-IGME: geological map at 1:50.000 scale from Instituto Geológico y Minero de España (IGME), GC-IGME: geological map at 1:25.000 scale from Gobierno de Cantabria and IGME, EVE: geological map at 1:25.000 scale from Ente Vasco de la Energía, ENRESA: geological map at 1:25.000 from Empresa Nacional de Residuos Radioactivos S.A., Ábalos, B. (2016), Lescoutre, R. (2019) and Carola, E. (2014). See Annex 2.3 for a detailed bibliography.

1.4. GEOLOGICAL MAP OF THE BASQUE – CANTABRIAN REGION

The extensional models proposed to explain the formation of the Basque – Cantabrian Basin summarized above need to be further discussed in the light of the new ideas developed on the formation and evolution of rifted margins. Therefore, new thematic maps need to be developed analysing the tectono-stratigraphic sequences in order to accompany the new interpretations and concepts. Many studies in the literature have addressed and described the stratigraphy observed in the Basque – Cantabrian Pyrenees and the structures affecting the area (Triassic: García-Mondéjar et al., 1986; Espina, 1996; Gómez et al., 2007. Jurassic: Quesada et al., 1991, 1993; Aurell et al., 2003; Quesada et al., 2005. Early Cretaceous: Pujalte, 1979, 1981, 1982; García-Mondéjar, 1989; García-Mondéjar et al., 1996; Hernandez et al., 1999; Bodego et al., 2015. Late Cretaceous: Pujalte, 1989; Rodríguez-Lázaro et al., 1998; Pujalte et al., 2000; Castañares et al., 2001; López-Horgue et al., 2014. Cenozoic: Riba & Jurado, 1992; Quintà & Tavani, 2012, among many others) and the geological knowledge coming out has been captured in multiple geological maps (e.g. Ábalos et al., 2016; Carola et al., 2015).

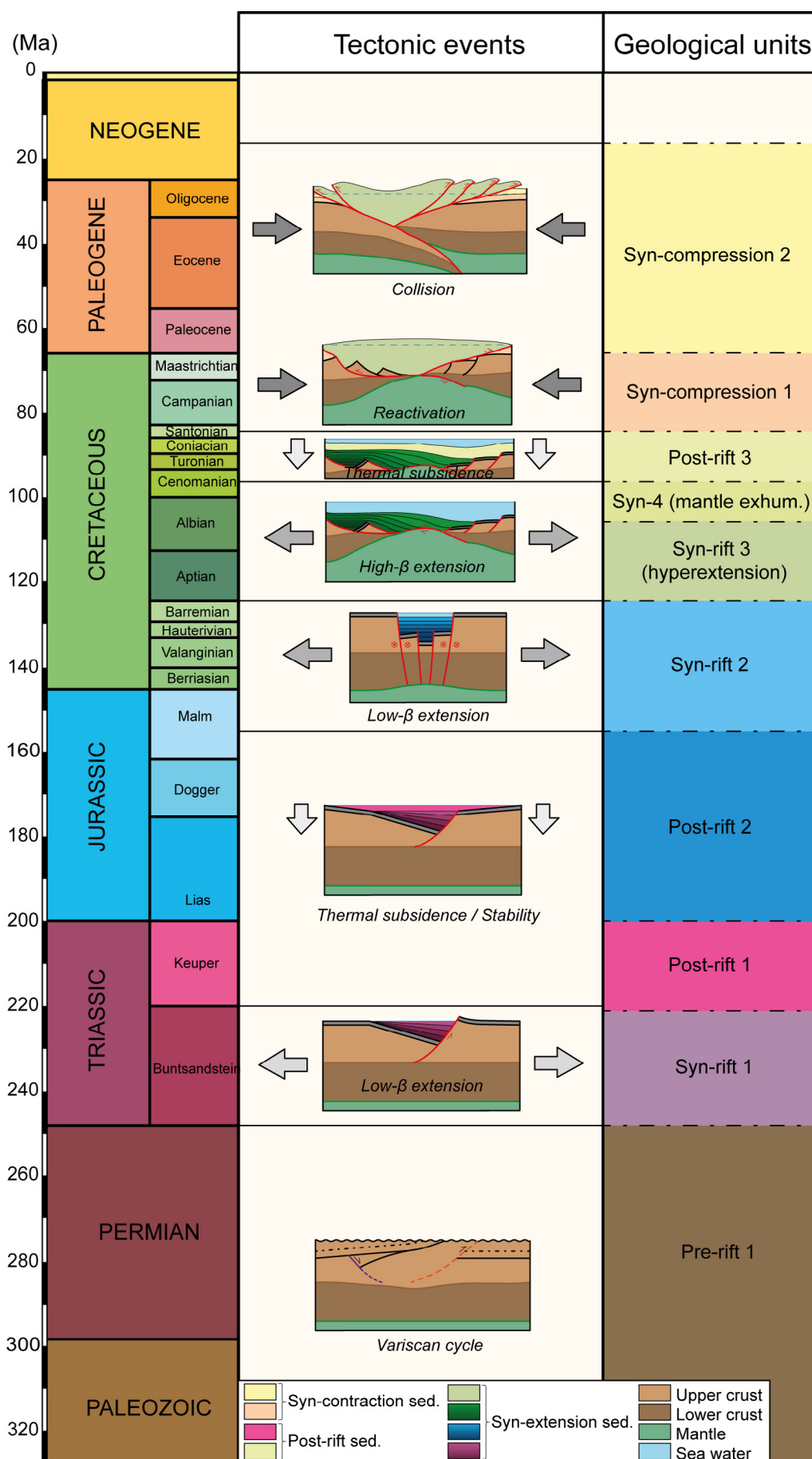


Figure A1.5 : Tectonic events documented in the Basque – Cantabrian Pyrenees from Paleozoic to present-day reported in the literature with the geological units grouped in this report.

In this section, the tectonic evolution of the area and its stratigraphic response is summarized (Fig. A1.5). Therefore, a re-organization of units is proposed that reflects and allows to address further interpretations based on the recent developed concepts of rifted margins pointed out before (i.e. multistage and polyphase evolution). As a result, the thematic map presented in this work aims to be the basis for the upcoming studies addressing the formation and reactivation of the Basque – Cantabrian Pyrenees, as well as surrounding areas in the OROGEN project. Some of these interpretations that are based on the proposed legend of this paper can be found in this volume [(Lescoutre and Manatschal, 2020 (in this volume) and Cadenas et al. (in this volume)] or they are related to ongoing investigations (Miró *et al.* subm., Lescoutre *et al.* subm.). This map, therefore, represents a modification of existing maps combined with the revision of existing data sets as well as more than 1200 new field observations (e.g. dip-data measurements, lineation and contact observations).

The presented map (Annex 2.4) is a graphic representation at 1:300'000 scale covering an area of 33'300 km² limited to the north by the Cantabrian Sea, to the south by the Ebro and Duero Tertiary Basins and to the east and west by Paleozoic massifs (Basque Massif and Asturian Massif, respectively). The organization of the legend has been defined based on the main tectonic phases recognized in the study area and its stratigraphic response (Fig. A1.5), as it is explained hereafter rather than by geological ages (classical geological maps).

The oldest unit (i.e. basement, pre-rift 1) groups all the rocks from Paleozoic up to Permian. As the focus of the map is the Alpine cycle (i.e. Mesozoic to present-day), the previous events are not addressed in detail. The overlying Permo-Mesozoic to Cenozoic succession has been subdivided into syn-rift, post-rift and syn-compressional sequences, which can be further subdivided. The first sequence is the Lower Triassic extensional phase (i.e. Syn-rift 1), characterized by continental clastic sediments (Robles, 2004; Robles & Pujalte, 2004) and the late Triassic evaporites (i.e. Post-rift 1) (Serrano & Martínez del Olmo, 2004), which have been identified as a separate sequence due to its importance for the subsequent tectonic evolution. During Early to Middle Jurassic, a period of relative tectonic quiescence governed the northern Iberian domain (i.e. Post-rift 2). This phase is characterized by large carbonate platforms and marly successions defined as a unit itself in the map (Aurell et al., 2003; Quesada et al., 2005). The Late Jurassic to Barremian is characterized in the northern Iberian domain by a large-scale transtensional episode (Rat, 1988; Espina, 1994; Robles et al., 1996), resulting in a syn-rift sequence localized in small, but kilometre-deep, depocenters (i.e. Syn-rift 2) (e.g. Asturian Basin, Cadenas et al., 2018). The previous event

contrasts with the next Aptian to Middle Cenomanian event that is linked to the major extensional phase structuring the Basque-Cantabrian Pyrenees. The sediments linked to the major extensional event were deposited leading to widely distributed depocenters that are either overlapping or forming away from the previous Late Jurassic to Barremian depocenters (Robles et al., 1988; García-Mondéjar et al., 1996; Lescoutre, 2019). The Aptian to Middle Albian extensional period is comprised in two units: the Aptian to Middle Albian succession (i.e. Syn-rift 3) and the Upper Albian to Middle Cenomanian (i.e. Syn-rift 4). The latter is unconformably overlying the previous sediments (Peropadre et al., 2012) and it is related to a phase of mantle exhumation (Tugend et al., 2014a; Pedrera et al., 2017). A post-rift (i.e. Post-rift 3) sequence recording thermal subsidence of Late Cenomanian to Early Santonian age is observed and manifested by shallow carbonate platforms established in the margins of the main depocenters, whereas a marly sedimentation was occurring basinwards (Floquet, 2004). Onset of convergence occurred at Middle Santonian time and coincided with a reestablishment of clastic sedimentation (i.e. Syn-compression 1). Finally, the Cenozoic period (i.e. Syn-compression 2) is known as the major compressional phase (mostly Eocene to Miocene) (Puigdefàbregas et al., 1992; Pedrera et al., 2017; Martín-Chivelet et al., 2019).

1.5. COMPOSITE SECTION ACROSS THE BASQUE – CANTABRIAN PYRENEES

A SSW – NNE composite seismic section from the Ebro Basin in the south to the Landes High offshore in the north is presented in Fig. A1.6. It provides a first order view of the architecture and nature of depocenters composing the Basque – Cantabrian Pyrenees on its central segment. Moreover, results of refraction seismic surveys (Fernández-Viejo et al., 2000; Pedreira et al., 2003; Ruiz et al., 2017), and the source that is the origin of the gravimetric and magnetic anomalies (Pedreira et al., 2007) have been projected in the section to have a complete crustal scale section crossing the entire Basque – Cantabrian Pyrenees.

In the section, the top basement interface corresponds to a major change in the reflectivity and can therefore be described as a main reflection across the composite line. The top basement is flat underneath the Duero Basin at about 3800m depth, as confirmed by drill hole Rojas NE-1 (Figs. A1.6 and A1.7), projected 12km from the south. Beneath the Tesla Mountains and all along the imbricates related to the Sierra de Cantabrian Frontal Thrust, this interface appears slightly dipping to the north, being at 4000 m depth in the Navajo-1 drill hole (Fig. A1.6 and A1.7). The top basement keeps dipping to the north with about

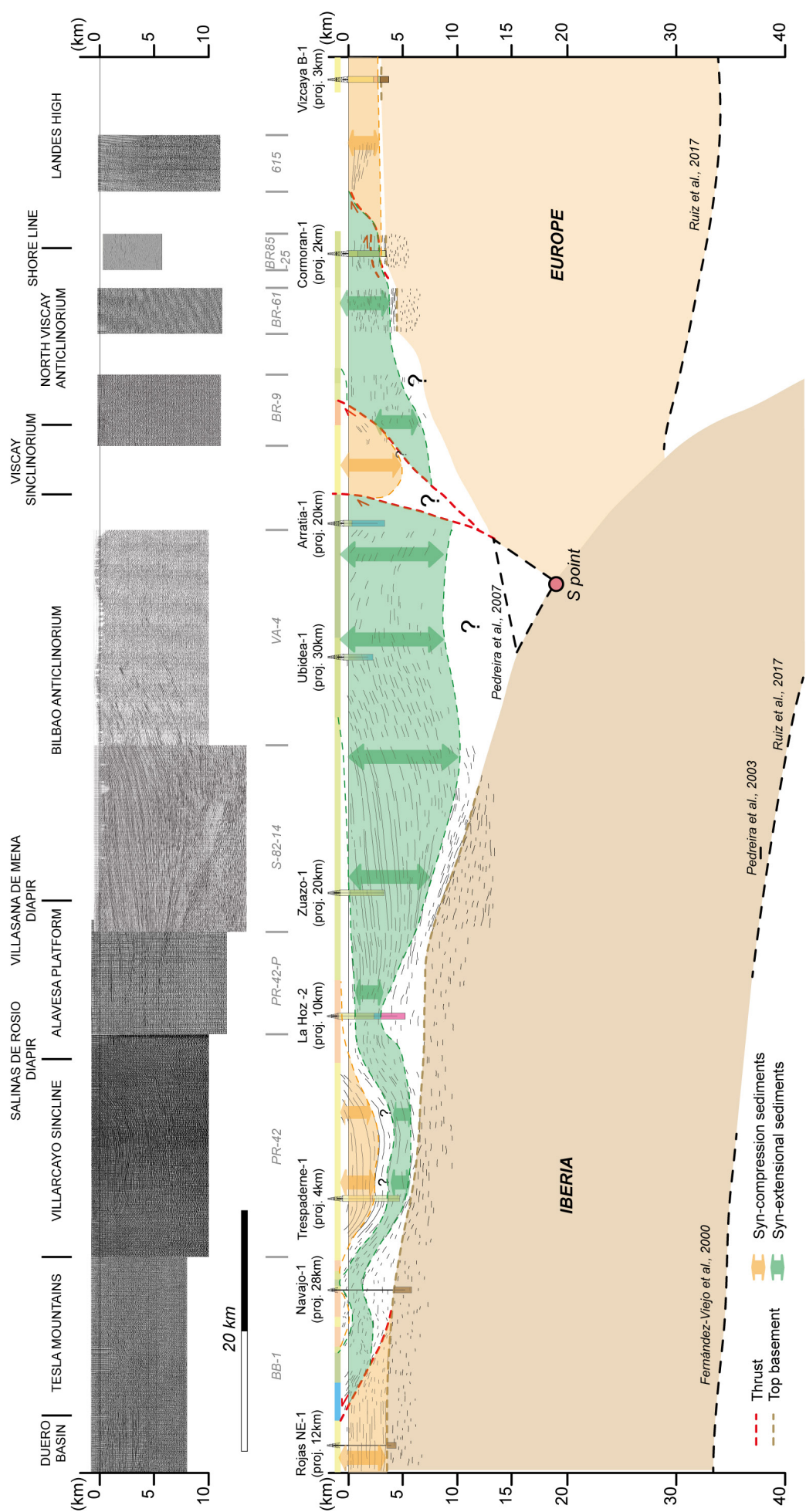


Figure A1.6 : Composite reflection seismic line and its line drawing crossing the Basque - Cantabrian Pyrenees from south (left) to north (right) with nine boreholes and refraction seismic data projected. The surface geology and the main sedimentary successions of syn-extensional sediments and syn-compressional sediments are showed together with the main structures of the area. See the text and Annex 2.1 for further details.

5° degrees until the diapir alignment of Villasana de Mena – Orduña – Murgia, where the dip attitude changes, showing northward steeply dipping reflections. From that point to the north, the depocenter of the Basque-Cantabrian Basin s.s. thickens significantly, coinciding with the northward increase of the dipping of top basement. In the North Biscay Anticlinorium, top basement is flat and located at 4000m, whereas at the shoreline, this contact is at 3300m depth, as confirmed by the Cormoran-1 drill hole (Figs. A1.6 and A1.7). In the Landes High, top basement was drilled at 2800m below sea level at the Biscaya B-1 well (Figs. A1.6 and A1.7).

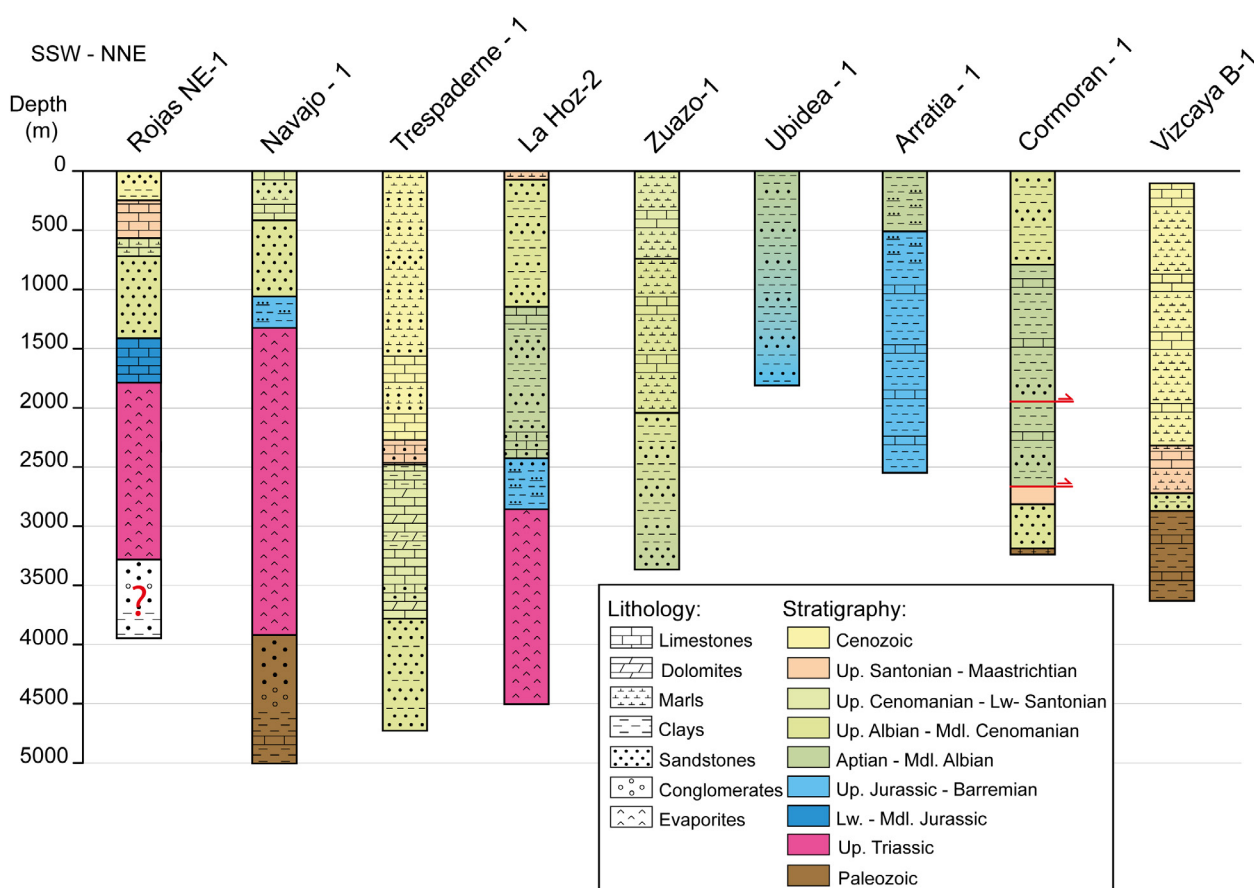


Figure A1.7 : Stratigraphic logs of nine drill holes from the Basque – Cantabrian Pyrenees. All of them start in the same reference level (0 meters) even if they are located at different topographic elevations. The vertical axis shows depth in meters. See Annex 2.2 for further details of each drill hole.

In contrast to the top basement, the sedimentary cover is more deformed, which clearly argues for a strong decoupling between sediments and basement. Nevertheless, the sediments in the Ebro Basin are flat lying on top of the basement until the Sierra de Cantabria Frontal Thrust, where a panel of reflectors is dipping to the north representing the hanging wall of such frontal thrusts (Fig. A1.6). The Tesla Mountain area is deformed by thrusts and related folds and therefore the response in the seismic line is not clear (Annex 2.4 and Fig. A1.6). However, some folded reflectors resulting from the compressional reactivation can be identified. As exposed at surface (Annex 2.4), the complete stratigraphic succession in

this area (i.e. Jurassic to Cenozoic) is thin and represented by few kilometres of sediments in total. To the north, a gentle syncline (i.e. Villarcayo Syncline) is recognized and made of a thick syn-compressional sedimentary pile as evidenced by the Trespaderne-1 well that drilled more than 2.000 m of Late Cretaceous to Cenozoic sediments in its core (Figs. A1.6 and A1.7). The northern limb of the Villarcayo Syncline is conditioned by salt structures, such as the Salinas de Rosio – Salinas de Añana salt diapirs, which are the surface expression of a salt inflated area all along the northern limb of this syncline (Annex 4). This is supported by the La Hoz-2 drill hole, which penetrates more than 1500m of continuous evaporites (Fig. A1.7). Immediately to the north, the reflectors of a thick Mesozoic succession are dipping to the south on top of the north dipping basement. This tilted panel defines the southern limb of the Bilbao Anticlinorium (Annex 4 and Fig. A1.6). The surface geology as well as the Ubidea-1 and Arratia-1 drill holes show a thick sedimentary cover of Late Jurassic to Middle Albian sediments forming the Bilbao Anticlinorium (Annex 4 and Figs. A1.6 and A1.7). North of it, the quality of the seismic lines is not as good as further south due to the intense deformation in the area. However, some reflectors are showing the northern limb of the Biscay Sinclorium and some sub-horizontal trends in the northern Biscay anticlinorium area are observed (Fig. A1.6). Finally, close to the shoreline, the presence of more recent seismic lines and the Cormoran-1 drill hole reflects a still deformed sedimentary cover by presenting some repetitions of the stratigraphy on top of Paleozoic basement (Fig. A1.7). The Biscay B-1 drill hole penetrated a thick and flat non deformed Late Cretaceous to Tertiary succession deposited on top of a thin Late Albian to Middle Cenomanian sequence, which is directly on top basement at 2800m in the Landes High (Figs. A1.6 and A1.7).

From a crustal perspective, a normal, about 30km thick Iberian crust is observed to the south beneath the Duero Basin but slightly tilted to the north underneath the frontal thrust and southern Basque – Cantabrian Pyrenees. A constant trend is observed until the northern edge of the Alavesa Platform, where the top basement increases the northward tilting as mentioned above, whereas the base of the crust follows a similar tendency slightly dipping to the north, suggesting a crustal thinning underneath the Bilbao Anticlinorium. However, in the same position, but at shallower level, a high magnetic and gravimetric anomaly is reported (Pedreira et al., 2007). From that anomaly to the north, the European crust is present with a Moho depicted at around 30 km whereas the top basement remains at deeper levels as the thick sediments reported in the Bilbao anticlinorium are on top. Therefore, a thin European crust is assumed to the south whereas to the north its thickness increases up to a normal, about 30km thick crust beneath the Cormoran-1 and Viscaya B-1 boreholes (Fig. A1.6). Geological cross sections partially based on the

previous observations have been published (Muñoz, 2019) suggesting an interpretation of the Basque – Cantabrian Pyrenees with a strong decoupling between basement and sedimentary cover.

1.6. SUMMARY

The goal of this data report is to compile and present an analysis of a data set consisting of a composite seismic line across the Basque – Cantabrian Pyrenees with nine drill holes projected into the seismic transect. A new thematic map of the Basque – Cantabrian Pyrenees at 1:300.000 scale is also provided to better understand the tectonostratigraphic evolution of the area with a simple but robust organisation. This data is presented in order to provide the base for new interpretations on the formation and reactivation of the Basque – Cantabrian Pyrenees. Thus, this data report will be important and can be used to understand how the stacking of the different Mesozoic events recognized in the Basque – Cantabrian Pyrenees are organized and may built the foundation to test new concepts such as multistage and polyphase rift evolutions. Attempts to apply these concepts have been published already in examples presented in this volume.

ACKNOWLEDGEMENTS

This work represents the data-set that has been compiled in the PhD of Jordi Miró and that belongs to the project CGL2017-85532-P of the Ministerio de Economía y Competitividad, the GEOMODELS Research Institute and the Grup de Geodinàmica i Anàlisi de Conques (2014SGR-467). We also thank reviewers Jesús Garcia-Senz and Ruth Soto and editors Olivier Lacombe and Stefano Tavani for helping to improve an earlier version of the report. The Instituto Geologico y Minero de España (I.G.M.E.) is thanked for providing seismic sections and well logs and Midland Valley for providing the academic license of the used Move software.

ANNEX 2

Annex 2.1 List of reflexion seismic lines used in this work with their orientations and coordinates from Instituto Geológico y Minero de España.

Seismic line	Orientation	X coord. S/E (UTM)	Y coord. S/E (UTM)	X coord. N/W (UTM)	Y coord. N/W (UTM)
BB-1	S - N	464298	4723678	474731	4745597
PR-42	S - N	465668	4740456	475119	4756071
PR-42-P	S - N	473519	4754532	479862	4763538
S-82-14	S - N	482407	4761027	492283	4773007
VA-4	S - N	497056	4761749	500576	4786716
BR-9	S - N	506053	4798176	504361	4804998
BR-61	W - E	510646	4803013	504499	4807824
BR85-25	W - E	505734	4808128	517651	4807707
615	S - N	513195	4809718	515656	4814807

See <http://info.igme.es/Hidrocarburos/> for further details

Annex 2.2 List of drill holes used in this work with their coordinates and measured depths from Instituto Geológico y Minero de España.

Drill hole	X coord. (UTM)	Y coord. (UTM)	Z coord. (m)	Measured Depth (m)
Rojas NE-1	465498	4712882	781	3923
Navajo-1	440953	4755514	974	5395
Traspaderne-1	470801	4741584	585	4734
La Hoz-2	480123	4749285	1033	4508
Zuazo-1	501389	4750536	845	3345
Ubidea-1	525246	4764137	611	1812
Arratia-1	517801	4776169	142	2550
Cormoran-1	510000	4809250	14	3305
Vizcaya B-1	523520	4818186	26	3626

See <http://info.igme.es/Hidrocarburos/> for further details

Annex 2.3

List of 1.50.000 maps used to build the map presented in this work published by the Instituto Geológico y Minero de España (IGME). MAGNA Series (1972-2003). The references are ordered according to their sheet numbering.

- Martínez-García, E., 1981. Mapa y Memoria (40 p.) de la Hoja nº 32 (Llanes) del Mapa Geológico de España a escala 1:50.000 (Serie MAGNA). Instituto Geológico y Minero de España, Madrid.
- Portero García, J.M., Ramírez del Pozo, J., Olivé Davó, A. and Martín Alafont, J.M., 1976. Mapa y Memoria (46 p.) de la Hoja nº 33 (Comillas) del Mapa Geológico de España a escala 1:50.000 (Serie MAGNA). Instituto Geológico y Minero de España, Madrid.
- Portero García, J.M., Olivé Davó, A., Martín Alafont, J. and Ramírez del Pozo, J., 1976. Mapa y Memoria (40 p.) de la Hoja nº 34 (Torrelavega) del Mapa Geológico de España a escala 1:50.000 (Serie MAGNA). Instituto Geológico y Minero de España, Madrid.
- Ramírez del Pozo, J., Portero García, J.M., Olivé Davó, A., Martín Alafont, J. and Aguilar Tomás, M.J., 1976. Mapa y Memoria (41 p.) de la Hoja nº 35 (Santander) del Mapa Geológico de España a escala 1:50.000 (Serie MAGNA). Instituto Geológico y Minero de España, Madrid.
- Olivé Davó, A., Martín Alafont, J.M., Ramírez del Pozo, J. and Portero García, J.M., 1982. Mapa y Memoria (31 p.) de la Hoja nº 36 (Castro Urdiales) del Mapa Geológico de España a escala 1:50.000 (Serie MAGNA). Instituto Geológico y Minero de España, Madrid.
- Espejo, J.A. and Pastor, F., 1975. Mapa y Memoria (25 p.) de la Hoja nº 37 (Algorta) del Mapa Geológico de España a escala 1:50.000 (Serie MAGNA). Instituto Geológico y Minero de España, Madrid.
- Espejo Molina, J.A., 1975. Mapa y Memoria (26 p.) de la Hoja nº 38 (Bermeo) del Mapa Geológico de España a escala 1:50.000 (Serie MAGNA). Instituto Geológico y Minero de España, Madrid.
- Espejo Molina, J.A., 1975. Mapa y Memoria (11 p.) de la Hoja nº 39 (Lequeitio) del Mapa Geológico de España a escala 1:50.000 (Serie MAGNA). Instituto Geológico y Minero de España, Madrid.
- Campos Fernández, J., García-Deñás, V., Lamolda Palacios, M. and Pujalte Navarro, V., 1974. Mapa y Memoria (10 p.) de la Hoja nº 40 (Jaizquíbel) del Mapa Geológico de España a escala 1:50.000 (Serie MAGNA). Instituto Geológico y Minero de España, Madrid.
- Campos Fernández, J., García-Deñás, V., Lamolda Palacios, M. and Pujalte Navarro, V., 1974. Mapa y Memoria (13 p.) de la Hoja nº 41 (Irún) del Mapa Geológico de España a escala 1:50.000 (Serie MAGNA). Instituto Geológico y Minero de España, Madrid.
- Martínez-García, E., Marquínez, J., Heredia, N., Navarro, D., Rodríguez Fernández, L.R., 1984. Mapa y Memoria (45 p.) de la Hoja nº 56 (Carreña-Cabrales) del Mapa Geológico de España a escala 1:50.000 (Serie MAGNA). Instituto Geológico y Minero de España, Madrid.
- Carreras Suárez, F., Ramírez del Pozo, J., Aguilar Tomás, M.J. and Pujalte, V., 1978. Mapa y Memoria (47 p.) de la Hoja nº 57 (Cabezón de la Sal) del Mapa Geológico de España a escala 1:50.000 (Serie MAGNA). Instituto Geológico y Minero de España, Madrid.
- Carreras Suárez, F., Portero García, J.M., Del Olmo Zamora, P., Ramírez del Pozo, J. and Aguilar Tomás, M.J., 1979. Mapa y Memoria (38 p.) de la Hoja nº 58 (Los Corrales de Buelna) del Mapa Geológico de España a escala 1:50.000 (Serie MAGNA). Instituto Geológico y Minero de España, Madrid.
- Portero García, J.M., Ramírez del Pozo, J., Olivé Davó, A., del Olmo Zamora, P., Aguilar Tomás, M.J. and Martín Alafont, J., 1978. Mapa y Memoria (46 p.) de la Hoja nº 59 (Villacarriedo) del Mapa Geológico de España a escala 1:50.000 (Serie MAGNA). Instituto Geológico y Minero de España, Madrid.
- Portero García, J.M., Ramírez del Pozo, J., Olivé Davó, A., del Olmo Zamora, P., Aguilar Tomás, M.J. and Martín Alafont, J.M., 1978. Mapa y Memoria (36 p.) de la Hoja nº 60 (Valmaseda) del Mapa Geológico de España a escala 1:50.000 (Serie MAGNA). Instituto Geológico y Minero de España, Madrid.

- Ortiz Ramos, A. and Perconig Genzo, E., 1975. Mapa y Memoria (35 p.) de la Hoja nº 61 (Bilbao) del Mapa Geológico de España a escala 1:50.000 (Serie MAGNA). Instituto Geológico y Minero de España, Madrid.
- Espejo Molina, J.A. and Pignatelli García, R., 1973. Mapa y Memoria (32 p.) de la Hoja nº 62 (Durango) del Mapa Geológico de España a escala 1:50.000 (Serie MAGNA). Instituto Geológico y Minero de España, Madrid.
- Martín Fernández, M., 1975. Mapa y Memoria (17 p.) de la Hoja nº 63 (Éibar) del Mapa Geológico de España a escala 1:50.000 (Serie MAGNA). Instituto Geológico y Minero de España, Madrid.
- Campos Fernández, J. and García-Dueñas, V., 1974. Mapa y Memoria (43 p.) de la Hoja nº 64 (San Sebastián) del Mapa Geológico de España a escala 1:50.000 (Serie MAGNA). Instituto Geológico y Minero de España, Madrid.
- Krausse, H.F., Müller, D., Requadt, H., Campos Fernández, J., García-Dueñas, V., Garrote, A., Navarro-Vilá, F., Velasco, F., Solé Sedó, J. and Villalobos Vilches, L., 1975. Mapa y Memoria (46 p.) de la Hoja nº 65 (Vera de Bidasoa) del Mapa Geológico de España a escala 1:50.000 (Serie MAGNA). Instituto Geológico y Minero de España, Madrid.
- Rodríguez Fernández, L.R., Heredia, N., Navarro, D., Martínez-García, E., Marquínez, J., 1994. Mapa y Memoria (128 p.) de la Hoja nº 81 (Potes) del Mapa Geológico de España a escala 1:50.000 (Serie MAGNA). Instituto Geológico y Minero de España, Madrid.
- Heredia, N., Navarro, D., Rodríguez Fernández, L.R., Wagner, R.H., Pujalte, V. and García Mondéjar, J., 1986. Mapa y Memoria (70 p.) de la Hoja nº 82 (Tudanca) del Mapa Geológico de España a escala 1:50.000 (Serie MAGNA). Instituto Geológico y Minero de España, Madrid.
- Carreras Suárez, F., Portero García, J.M., Del Olmo Zamora, P., Ramírez del Pozo, J. and Aguilar Tomás, M.J., 1978. Mapa y Memoria (35 p.) de la Hoja nº 83 (Reinosa) del Mapa Geológico de España a escala 1:50.000 (Serie MAGNA). Instituto Geológico y Minero de España, Madrid.
- Del Olmo Zamora, P., Ramírez del Pozo, J., Aguilar Tomás, M.J., Portero García, J.M. and Olivé Davó, A., 1978. Mapa y Memoria (44 p.) de la Hoja nº 84 (Espinosa de los Monteros) del Mapa Geológico de España a escala 1:50.000 (Serie MAGNA). Instituto Geológico y Minero de España, Madrid.
- Olivé Davó, A., Ramírez del Pozo, J., del Olmo Zamora, P., Aguilar Tomás, M.J. and Portero García, J.M., 1978. Mapa y Memoria (32 p.) de la Hoja nº 85 (Villasana de Mena) del Mapa Geológico de España a escala 1:50.000 (Serie MAGNA). Instituto Geológico y Minero de España, Madrid.
- Olivé Davó, A., Ramírez del Pozo, J., Aguilar Tomás, M.J. and Carreras Suárez, F.J., 1978. Mapa y Memoria (27 p.) de la Hoja nº 86 (Landaco) del Mapa Geológico de España a escala 1:50.000 (Serie MAGNA). Instituto Geológico y Minero de España, Madrid.
- Olivé Davó, A., Ramírez del Pozo, J. and Del Olmo Zamora, P., 1978. Mapa y Memoria (34 p.) de la Hoja nº 87 (Elorrio) del Mapa Geológico de España a escala 1:50.000 (Serie MAGNA). Instituto Geológico y Minero de España, Madrid.
- Martín García, L y Esnaola Gómez, J.M., 1975. Mapa y Memoria (20 p.) de la Hoja nº 88 (Vergara) del Mapa Geológico de España a escala 1:50.000 (Serie MAGNA). Instituto Geológico y Minero de España, Madrid.
- Campos Fernández, J., Olivé Davó, A., Ramírez Merino, J.I., Solé Sedó, J. and Villalobos Vilches, L., 1986. Mapa y Memoria (47 p.) de la Hoja nº 89 (Tolosa) del Mapa Geológico de España a escala 1:50.000 (Serie MAGNA). Instituto Geológico y Minero de España, Madrid.
- Del Valle Lerchundi, J., Villalobos Vilches, L., Bornhorst, A., de Boer, H.U., Krausse, H.F., Mohr, K., Müller, R., Pilger, A., Requadt, H., Avidad, J., García-Dueñas, V., Garrote, A. and Ramón Lluch, R., 1975. Mapa y Memoria (55 p.) de la Hoja nº 90 (Sumbilla) del Mapa Geológico de España a escala 1:50.000 (Serie MAGNA). Instituto Geológico y Minero de España, Madrid.
- Lobato, L., Rodríguez Fernández, L.R., Heredia, N., Velando, F. and Matas, J., 1985. Mapa y Memoria (98 p.) de la Hoja nº 106 (Camporredondo de Alba) del Mapa Geológico de España a escala 1:50.000 (Serie MAGNA). Instituto Geológico y Minero de España, Madrid.

- Ambrose, T., Carballeira, J., López Rico, J., y Wagner, R.H., 1984. Mapa y Memoria (113 p.) de la Hoja nº 107 (Barruelo de Santullán) del Mapa Geológico de España a escala 1:50.000 (Serie MAGNA). Instituto Geológico y Minero de España, Madrid.
- Del Olmo Zamora, P. and Ramírez del Pozo, J., 1978. Mapa y Memoria (34 p.) de la Hoja nº 108 (Las Rozas) del Mapa Geológico de España a escala 1:50.000 (Serie MAGNA). Instituto Geológico y Minero de España, Madrid.
- Carreras Suárez, F., del Olmo Zamora, P. and Ramírez del Pozo, J., 1979. Mapa y Memoria (42 p.) de la Hoja nº 109 (Villarcayo) del Mapa Geológico de España a escala 1:50.000 (Serie MAGNA). Instituto Geológico y Minero de España, Madrid.
- Martín Alafont, J.M., Ramírez del Pozo, J. and Carreras Suárez, F.J., 1979. Mapa y Memoria (42 p.) de la Hoja nº 110 (Medina de Pomar) del Mapa Geológico de España a escala 1:50.000 (Serie MAGNA). Instituto Geológico y Minero de España, Madrid.
- Del Olmo Zamora, P., Ramírez del Pozo, J. and Aguilar Tomás, M.J., 1979. Mapa y Memoria (35 p.) de la Hoja nº 111 (Orduña) del Mapa Geológico de España a escala 1:50.000 (Serie MAGNA). Instituto Geológico y Minero de España, Madrid.
- Del Olmo Zamora, P., Ramírez del Pozo, J. and Olivé Davó, A., 1978. Mapa y Memoria (34 p.) de la Hoja nº 112 (Vitoria) del Mapa Geológico de España a escala 1:50.000 (Serie MAGNA). Instituto Geológico y Minero de España, Madrid.
- Carreras Suárez, F.J., del Olmo Zamora, P., Portero García, J.M. and Ramírez del Pozo, J., 1978. Mapa y Memoria (33 p.) de la Hoja nº 113 (Salvatierra) del Mapa Geológico de España a escala 1:50.000 (Serie MAGNA). Instituto Geológico y Minero de España, Madrid.
- Ramírez Merino, J.I., Olivé Davó, A., Villalobos Vilches, L., León González, L y Carbayo Olivares, A., 1987. Mapa y Memoria (59 p.) de la Hoja nº 114 (Alsasua) del Mapa Geológico de España a escala 1:50.000 (Serie MAGNA). Instituto Geológico y Minero de España, Madrid.
- Carbayo Olivares, A., León González, L., y Villalobos Vilches, L. 1978. Mapa y Memoria (61 p.) de la Hoja nº 115 (Ansoain) del Mapa Geológico de España a escala 1:50.000 (Serie MAGNA). Instituto Geológico y Minero de España, Madrid.
- Colmenero, J.R., Vargas, I., García-Ramos, J.C., Manjón, M., Crespo, A. and Matas, J., 1982. Mapa y Memoria (75 p.) de la Hoja nº 132 (Guardo) del Mapa Geológico de España a escala 1:50.000 (Serie MAGNA). Instituto Geológico y Minero de España, Madrid.
- López Olmedo, F., Enrile Alvir, A. and Cabra Gil, P., 1997. Mapa y Memoria (162 p.) de la Hoja nº 133 (Prádanos de Ojeda) del Mapa Geológico de España a escala 1:50.000 (Serie MAGNA). Instituto Geológico y Minero de España, Madrid.
- Pendas Fernández, F y Menéndez Casares, E., 1994. Mapa y Memoria (68 p.) de la Hoja nº 134 (Polientes) del Mapa Geológico de España a escala 1:50.000 (Serie MAGNA). Instituto Geológico y Minero de España, Madrid.
- Carreras Suárez, F., Ramírez del Pozo, J. and Aguilar Tomás, M.J., 1979. Mapa y Memoria (37 p.) de la Hoja nº 135 (Sedano) del Mapa Geológico de España a escala 1:50.000 (Serie MAGNA). Instituto Geológico y Minero de España, Madrid.
- Olivé Davó, A., Aguilar Tomás, M.J. and Ramírez del Pozo, J., 1980. Mapa y Memoria (42 p.) de la Hoja nº 136 (Oña) del Mapa Geológico de España a escala 1:50.000 (Serie MAGNA). Instituto Geológico y Minero de España, Madrid.
- Olivé Davó, A., Ramírez del Pozo, J. and Riba Arderiú, O., 1979. Mapa y Memoria (44 p.) de la Hoja nº 137 (Miranda de Ebro) del Mapa Geológico de España a escala 1:50.000 (Serie MAGNA). Instituto Geológico y Minero de España, Madrid.
- Martín Alafont, J.M., Ramírez del Pozo, J. Portero García, J.M., y Riba Arderiú, O., 1978. Mapa y Memoria (44 p.) de la Hoja nº 138 (La Puebla de Arganzón) del Mapa Geológico de España a escala 1:50.000 (Serie MAGNA). Instituto Geológico y Minero de España, Madrid.
- Carreras Suárez, F.J., Ramírez del Pozo, J. and Aguilar Tomás, M.J., 1978. Mapa y Memoria (36 p.) de la Hoja nº 139 (Eulate) del Mapa Geológico de España a escala 1:50.000 (Serie MAGNA). Instituto Geológico y Minero de España, Madrid.

- Ramírez Merino, J.I., Olivé Davó, A., Carbayo Olivares, A., Villalobos Vilches, L. and León González, L., 1987. Mapa y Memoria (46 p.) de la Hoja nº 140 (Estella) del Mapa Geológico de España a escala 1:50.000 (Serie MAGNA). Instituto Geológico y Minero de España, Madrid.
- Del Valle Lerchundi, J., 1978. Mapa y Memoria (23 p.) de la Hoja nº 141 (Pamplona) del Mapa Geológico de España a escala 1:50.000 (Serie MAGNA). Instituto Geológico y Minero de España, Madrid.
- López Olmedo, F., Enrile Alvir, A. and Cabra Gil, P., 1997. Mapa y Memoria (113 p.) de la Hoja nº 165 (Herrera de Pisuerga) del Mapa Geológico de España a escala 1:50.000 (Serie MAGNA). Instituto Geológico y Minero de España, Madrid.
- Pineda Velasco, A., 1997. Mapa y Memoria (89 p.) de la Hoja nº 166 (Villadiego) del Mapa Geológico de España a escala 1:50.000 (Serie MAGNA). Instituto Geológico y Minero de España, Madrid.
- Pineda Velasco, A., 1997. Mapa y Memoria (110 p.) de la Hoja nº 167 (Montorio) del Mapa Geológico de España a escala 1:50.000 (Serie MAGNA). Instituto Geológico y Minero de España, Madrid.
- Portero García, J.M., Hernández Samaniego, A., Ramírez del Pozo, J. and Riba Arderiú, O., 1979. Mapa y Memoria (36 p.) de la Hoja nº 168 (Briviesca) del Mapa Geológico de España a escala 1:50.000 (Serie MAGNA). Instituto Geológico y Minero de España, Madrid.
- Portero García, J.M., Ramírez del Pozo, J. and Aguilar Tomás, M.J., 1978. Mapa y Memoria (41 p.) de la Hoja nº 169 (Casalarreina) del Mapa Geológico de España a escala 1:50.000 (Serie MAGNA). Instituto Geológico y Minero de España, Madrid.
- Portero García, J.M., Ramírez del Pozo, J. and Aguilar Tomás, M.J., 1979. Mapa y Memoria (43 p.) de la Hoja nº 170 (Haro) del Mapa Geológico de España a escala 1:50.000 (Serie MAGNA). Instituto Geológico y Minero de España, Madrid.
- Olivé Davó, A., Ramírez Merino, J.I., Carbayo Olivares, A., Castiella Muruzábal, J. and Solé Sedo, J., 1987. Mapa y Memoria (39 p.) de la Hoja nº 171 (Viana) del Mapa Geológico de España a escala 1:50.000 (Serie MAGNA). Instituto Geológico y Minero de España, Madrid.
- Hernández Samaniego, A., Ramírez del Pozo, J., Carbayo Olivares, A., Castiella Muruzábal, J. and Solé Sedo, J., 1987. Mapa y Memoria (55 p.) de la Hoja nº 172 (Allo) del Mapa Geológico de España a escala 1:50.000 (Serie MAGNA). Instituto Geológico y Minero de España, Madrid.
- Pineda Velasco, A. and Arce Duarte, J.M., 1997. Mapa y Memoria (93 p.) de la Hoja nº 200 (Burgos) del Mapa Geológico de España a escala 1:50.000 (Serie MAGNA). Instituto Geológico y Minero de España, Madrid.
- Olivé Davó, A., Ramírez Merino, J.I. and Ortega, L.I., 1990. Mapa y Memoria (38 p.) de la Hoja nº 201 (Belorado) del Mapa Geológico de España a escala 1:50.000 (Serie MAGNA). Instituto Geológico y Minero de España, Madrid.

List of 1.25.000 maps used in this report published by the Ente Vasco de la Energía (EVE). The references are ordered according to their sheet numbering.

- Garrote Ruiz, A., García Portero, J., Muñoz Jiménez, L., Arriola Garrido, A., Eguiguren Altuna, E., García Pascual, I. and Garrote Ruiz, R., 1993. Mapa y Memoria de la Hoja nº 37-II (Arminza) del Mapa Geológico del País Vasco a escala 1:25.000. Ente Vasco de la Energía-EVE.
- Garrote Ruiz, A., García Portero, J., Muñoz Jiménez, L., Arriola Garrido, A., Eguiguren Altuna, E., García Pascual, I. and Garrote Ruiz, R., 1993. Mapa y Memoria de la Hoja nº 37-III (Zierbena) del Mapa Geológico del País Vasco a escala 1:25.000. Ente Vasco de la Energía-EVE.
- Garrote Ruiz, A., García Portero, J., Muñoz Jiménez, L., Arriola Garrido, A., Eguiguren Altuna, E., García Pascual, I. and Garrote Ruiz, R., 1993. Mapa y Memoria de la Hoja nº 37-IV (Getxo) del Mapa Geológico del País Vasco a escala 1:25.000. Ente Vasco de la Energía-EVE.
- Garrote Ruiz, A., García Portero, J., Arriola Garrido, A., Eguiguren Altuna, E., García Pascual, I. and Garrote Ruiz, R., 1991. Mapa y Memoria de la Hoja nº 38-I (Bermeo) del Mapa Geológico del País Vasco a escala 1:25.000. Ente Vasco de la Energía-EVE.

- Garrote Ruiz, A., García Portero, J., Arriola Garrido, A., Eguiguren Altuna, E., García Pascual, I. and Garrote Ruiz, R., 1992. Mapa y Memoria de la Hoja nº 38-III (Mungia) del Mapa Geológico del País Vasco a escala 1:25.000. Ente Vasco de la Energía-EVE.
- Garrote Ruiz, A., García Portero, J., Arriola Garrido, A., Eguiguren Altuna, E., García Pascual, I. and Garrote Ruiz, R., 1992. Mapa y Memoria de la Hoja nº 38-IV (Elantxobe) del Mapa Geológico del País Vasco a escala 1:25.000. Ente Vasco de la Energía-EVE.
- Garrote Ruiz, A., García Portero, J., Fernández Carrasco, J., Cerezo Arasti, A., Tijero Sanz, F. and Zapata Sola, M., 1986. Mapa y Memoria de la Hoja nº 39-III (Lekeitio) del Mapa Geológico del País Vasco a escala 1:25.000. Ente Vasco de la Energía-EVE.
- Garrote Ruiz, A., Muñoz Jiménez, L., García Pascual, I. and Eguiguren Altuna, E., 1992. Mapa y Memoria de la Hoja nº 60-I-III (Carranza) del Mapa Geológico del País Vasco a escala 1:25.000. Ente Vasco de la Energía-EVE.
- Garrote Ruiz, A., Muñoz Jiménez, L., García Pascual, I. and Eguiguren Altuna, E., 1992. Mapa y Memoria de la Hoja nº 60-II (Turcios) del Mapa Geológico del País Vasco a escala 1:25.000. Ente Vasco de la Energía-EVE.
- Garrote Ruiz, A., Muñoz Jiménez, L., García Pascual, I. and Eguiguren Altuna, E., 1992. Mapa y Memoria de la Hoja nº 60-III (Zalama) del Mapa Geológico del País Vasco a escala 1:25.000. Ente Vasco de la Energía-EVE.
- Garrote Ruiz, A., Muñoz Jiménez, L., García Pascual, I. and Eguiguren Altuna, E., 1992. Mapa y Memoria de la Hoja nº 60-IV (Balmaseda) del Mapa Geológico del País Vasco a escala 1:25.000. Ente Vasco de la Energía-EVE.
- Garrote Ruiz, A., García Portero, J., Muñoz Jiménez, L., Arriola Garrido, A., Eguiguren Altuna, E., García Pascual, I. and Garrote Ruiz, R., 1993. Mapa y Memoria de la Hoja nº 61-I (Santurtzi) del Mapa Geológico del País Vasco a escala 1:25.000. Ente Vasco de la Energía-EVE.
- Garrote Ruiz, A., García Portero, J., Muñoz Jiménez, L., Arriola Garrido, A., Eguiguren Altuna, E., García Pascual, I. and Garrote Ruiz, R., 1993. Mapa y Memoria de la Hoja nº 61-II (Bilbao) del Mapa Geológico del País Vasco a escala 1:25.000. Ente Vasco de la Energía-EVE.
- Garrote Ruiz, A., García Portero, J., Muñoz Jiménez, L., Arriola Garrido, A., Eguiguren Altuna, E., García Pascual, I. and Garrote Ruiz, R., 1993. Mapa y Memoria de la Hoja nº 61-III (Güeñes) del Mapa Geológico del País Vasco a escala 1:25.000. Ente Vasco de la Energía-EVE.
- Garrote Ruiz, A., García Portero, J., Muñoz Jiménez, L., Arriola Garrido, A., Eguiguren Altuna, E., García Pascual, I. and Garrote Ruiz, R., 1993. Mapa y Memoria de la Hoja nº 61-IV (Basauri) del Mapa Geológico del País Vasco a escala 1:25.000. Ente Vasco de la Energía-EVE.
- Garrote Ruiz, A., García Portero, J., Arriola Garrido, A., Eguiguren Altuna, E., García Pascual, I. and Garrote Ruiz, R., 1993. Mapa y Memoria de la Hoja nº 62-I (Lezama) del Mapa Geológico del País Vasco a escala 1:25.000. Ente Vasco de la Energía-EVE.
- Garrote Ruiz, A., García Portero, J., Arriola Garrido, A., Eguiguren Altuna, E., García Pascual, I. and Garrote Ruiz, R., 1992. Mapa y Memoria de la Hoja nº 62-II (Gernika-Lumo) del Mapa Geológico del País Vasco a escala 1:25.000. Ente Vasco de la Energía-EVE.
- Garrote Ruiz, A., García Portero, J., Arriola Garrido, A., Eguiguren Altuna, E., García Pascual, I. and Garrote Ruiz, R., 1993. Mapa y Memoria de la Hoja nº 62-III (Galdakao) del Mapa Geológico del País Vasco a escala 1:25.000. Ente Vasco de la Energía-EVE.
- Garrote Ruiz, A., García Portero, J., Fernández Carrasco, J., Cerezo Arasti, A., Tijero Sanz, F. and Zapata Sola, M., 1993. Mapa y Memoria de la Hoja nº 62-IV (Durango) del Mapa Geológico del País Vasco a escala 1:25.000. Ente Vasco de la Energía-EVE.
- Garrote Ruiz, A., García Portero, J., Fernández Carrasco, J., Cerezo Arasti, A., Tijero Sanz, F. and Zapata Sola, M., 1986. Mapa y Memoria de la Hoja nº 63-I (Ondarroa) del Mapa Geológico del País Vasco a escala 1:25.000. Ente Vasco de la Energía-EVE.
- Garrote Ruiz, A., García Portero, J., Fernández Carrasco, J., Cerezo Arasti, A., Tijero Sanz, F. and Zapata Sola, M., 1986. Mapa y Memoria de la Hoja nº 63-II (Zumaya) del Mapa Geológico del País Vasco a escala 1:25.000. Ente Vasco de la Energía-EVE.

- Garrote Ruiz, A., García Portero, J., Fernández Carrasco, J., Cerezo Arasti, A., Tijero Sanz, F. and Zapata Sola, M., 1991. Mapa y Memoria de la Hoja nº 63-III (Eibar) del Mapa Geológico del País Vasco a escala 1:25.000. Ente Vasco de la Energía-EVE.
- Garrote Ruiz, A., García Portero, J., Fernández Carrasco, J., Cerezo Arasti, A., Tijero Sanz, F. and Zapata Sola, M., 1986. Mapa y Memoria de la Hoja nº 63-IV (Azkoitia) del Mapa Geológico del País Vasco a escala 1:25.000. Ente Vasco de la Energía-EVE.
- Garrote Ruiz, A., García Portero, J., Fernández Carrasco, J., Cerezo Arasti, A., Tijero Sanz, F. and Zapata Sola, M., 1991. Mapa y Memoria de la Hoja nº 86-I (Arceniega) del Mapa Geológico del País Vasco a escala 1:25.000. Ente Vasco de la Energía-EVE.
- Garrote Ruiz, A., García Portero, Arriola Garrido, A., Eguiguren Altuna, E., García Pascual, I. and Garrote Ruíz, R., 1991. Mapa y Memoria de la Hoja nº 86-II (Llodio) del Mapa Geológico del País Vasco a escala 1:25.000. Ente Vasco de la Energía-EVE.
- Garrote Ruiz, A., García Portero, J., Fernández Carrasco, J., Cerezo Arasti, A., Tijero Sanz, F. and Zapata Sola, M., 1991. Mapa y Memoria de la Hoja nº 86-III (Ayala) del Mapa Geológico del País Vasco a escala 1:25.000. Ente Vasco de la Energía-EVE.
- Garrote Ruiz, A., García Portero, Arriola Garrido, A., Eguiguren Altuna, E., García Pascual, I. and Garrote Ruíz, R., 1991. Mapa y Memoria de la Hoja nº 86-IV (Amurrio) del Mapa Geológico del País Vasco a escala 1:25.000. Ente Vasco de la Energía-EVE.
- Garrote Ruiz, A., García Portero, J., Arriola Garrido, A., Eguiguren Altuna, E., García Pascual, I. and Garrote Ruiz, R., 1993. Mapa y Memoria de la Hoja nº 87-I (Igorre) del Mapa Geológico del País Vasco a escala 1:25.000. Ente Vasco de la Energía-EVE.
- Garrote Ruiz, A., García Portero, J., Fernández Carrasco, J., Cerezo Arasti, A., Tijero Sanz, F. and Zapata Sola, M., 1993. Mapa y Memoria de la Hoja nº 87-II (Igorre) del Mapa Geológico del País Vasco a escala 1:25.000. Ente Vasco de la Energía-EVE.
- Garrote Ruiz, A., García Portero, J., Arriola Garrido, A., Eguiguren Altuna, E., García Pascual, I. and Garrote Ruiz, R., 1993. Mapa y Memoria de la Hoja nº 87-III (Gorbea) del Mapa Geológico del País Vasco a escala 1:25.000. Ente Vasco de la Energía-EVE.
- Garrote Ruiz, A., García Portero, J., Muñoz Jiménez, L., Fernández Carrasco, J., Cerezo Arasti, A., Tijero Sanz, F., Zapata Sola, M., García Pascual, I. and Eguiguren Altuna, E., 1994. Mapa y Memoria de la Hoja nº 87-IV (Otxandio) del Mapa Geológico del País Vasco a escala 1:25.000. Ente Vasco de la Energía-EVE.
- Garrote Ruiz, A., García Portero, J., Muñoz Jiménez, L., Fernández Carrasco, J., Cerezo Arasti, A., Tijero Sanz, F. and Zapata Sola, M., 1992. Mapa y Memoria de la Hoja nº 88-I (Bergara) del Mapa Geológico del País Vasco a escala 1:25.000. Ente Vasco de la Energía-EVE.
- Garrote Ruiz, A., Muñoz Jiménez, L., Zapata Sola, M. and Cerezo Arasti, A., 1992. Mapa y Memoria de la Hoja nº 88-II (Zumarraga) del Mapa Geológico del País Vasco a escala 1:25.000. Ente Vasco de la Energía-EVE.
- Garrote Ruiz, A., García Portero, J., Muñoz Jiménez, L., Fernández Carrasco, J., Cerezo Arasti, A., Tijero Sanz, F. and Zapata Sola, M., 1992. Mapa y Memoria de la Hoja nº 88-III (Mondragon) del Mapa Geológico del País Vasco a escala 1:25.000. Ente Vasco de la Energía-EVE.
- Garrote Ruiz, A., Muñoz Jiménez, L., Zapata Sola, M. and Cerezo Arasti, A., 1992. Mapa y Memoria de la Hoja nº 88-IV (Beasain) del Mapa Geológico del País Vasco a escala 1:25.000. Ente Vasco de la Energía-EVE.
- Garrote Ruiz, A., Muñoz Jiménez, L., Arriola Garrido, A., Eguiguren Altuna, E. and García Pascual, I., 1994. Mapa y Memoria de la Hoja nº 112-I (Zuya) del Mapa Geológico del País Vasco a escala 1:25.000. Ente Vasco de la Energía-EVE.
- Garrote Ruiz, A., Muñoz Jiménez, L., Arriola Garrido, A., Eguiguren Altuna, E. and García Pascual, I., 1994. Mapa y Memoria de la Hoja nº 112-II (Legutiano) del Mapa Geológico del País Vasco a escala 1:25.000. Ente Vasco de la Energía-EVE.
- Garrote Ruiz, A., Muñoz Jiménez, Tejerina Lobo, L., Eguiguren Altuna, E. and García Pascual, I., 1992. Mapa y Memoria de la Hoja nº 113-II (Zegama) del Mapa Geológico del País Vasco a escala 1:25.000. Ente Vasco de la Energía-EVE.

Garrote Ruiz, A., Muñoz Jiménez, Tejerina Lobo, L., Eguiguren Altuna, E. and García Pascual, I., 1994. Mapa y Memoria de la Hoja nº 113-I (Santuario de Arantzau) del Mapa Geológico del País Vasco a escala 1:25.000. Ente Vasco de la Energía-EVE.

List of 1.25.000 maps used in this report published by the Instituto Geológico y Minero de España (IGME) and Gobierno de Cantabria. The references are ordered according to their sheet numbering.

- Mediato Arribas, J.F., Larrondo Echevarria, E., Hernaiz Huerta, P.P. and Robador Moreno, A., 2008. Mapa y Memoria de la Hoja nº 18-IV (Cabo de Ajo) del Mapa Geológico de Cantabria a escala 1:25.000. Gobierno de Cantabria and Instituto Geológico y Minero de España, Madrid.
- García Senz, J., Cañas Fernandez, V. and Robador Moreno, A., 2003. Mapa y Memoria de la Hoja nº 32-IV / 33-III (San Vicente de la Barquera) del Mapa Geológico de Cantabria a escala 1:25.000. Gobierno de Cantabria and Instituto Geológico y Minero de España, Madrid.
- García Senz, J., Cañas Fernandez, V. and Robador Moreno, A., 2003. Mapa y Memoria de la Hoja nº 33-IV (Comillas) del Mapa Geológico de Cantabria a escala 1:25.000. Gobierno de Cantabria and Instituto Geológico y Minero de España, Madrid.
- Solé Pont F.J., Mediato Arribas, J.F., Hernaiz Huerta, P.P. and Robador Moreno, A., 2008. Mapa y Memoria de la Hoja nº 34-I (Suances) del Mapa Geológico de Cantabria a escala 1:25.000. Gobierno de Cantabria and Instituto Geológico y Minero de España, Madrid.
- Solé Pont F.J., Mediato Arribas, J.F., Larrondo Echevarria, E., Hernaiz Huerta, P.P. and Robador Moreno, A., 2008. Mapa y Memoria de la Hoja nº 34-II (Muriedas) del Mapa Geológico de Cantabria a escala 1:25.000. Gobierno de Cantabria and Instituto Geológico y Minero de España, Madrid.
- Solé Pont F.J., Mediato Arribas, J.F., Larrondo Echevarria, E., Hernaiz Huerta, P.P. and Robador Moreno, A., 2008. Mapa y Memoria de la Hoja nº 34-III (Torrelavega) del Mapa Geológico de Cantabria a escala 1:25.000. Gobierno de Cantabria and Instituto Geológico y Minero de España, Madrid.
- Larrondo Echevarria, E., Mediato Arribas, J.F., Hernaiz Huerta, P.P. and Robador Moreno, A., 2008. Mapa y Memoria de la Hoja nº 34-IV (Renedo) del Mapa Geológico de Cantabria a escala 1:25.000. Gobierno de Cantabria and Instituto Geológico y Minero de España, Madrid.
- Larrondo Echevarria, E., Mediato Arribas, J.F., Hernaiz Huerta, P.P. and Robador Moreno, A., 2008. Mapa y Memoria de la Hoja nº 35-I (Santander) del Mapa Geológico de Cantabria a escala 1:25.000. Gobierno de Cantabria and Instituto Geológico y Minero de España, Madrid.
- Mediato Arribas, J.F., Larrondo Echevarria, E., Hernaiz Huerta, P.P. and Robador Moreno, A., 2008. Mapa y Memoria de la Hoja nº 35-II (Noja) del Mapa Geológico de Cantabria a escala 1:25.000. Gobierno de Cantabria and Instituto Geológico y Minero de España, Madrid.
- Larrondo Echevarria, E., Mediato Arribas, J.F., Hernaiz Huerta, P.P. and Robador Moreno, A., 2008. Mapa y Memoria de la Hoja nº 35-III (El Astillero) del Mapa Geológico de Cantabria a escala 1:25.000. Gobierno de Cantabria and Instituto Geológico y Minero de España, Madrid.
- Mediato Arribas, J.F., Larrondo Echevarria, E., Hernaiz Huerta, P.P. and Robador Moreno, A., 2008. Mapa y Memoria de la Hoja nº 35-IV (Entrambasaguas) del Mapa Geológico de Cantabria a escala 1:25.000. Gobierno de Cantabria and Instituto Geológico y Minero de España, Madrid.
- Robador Moreno, A., 2011. Mapa y Memoria de la Hoja nº 36-I (Santoña) del Mapa Geológico de Cantabria a escala 1:25.000. Gobierno de Cantabria and Instituto Geológico y Minero de España, Madrid.
- Robador Moreno, A. and Rosales Franco, I., 2011. Mapa y Memoria de la Hoja nº 36-III (Laredo) del Mapa Geológico de Cantabria a escala 1:25.000. Gobierno de Cantabria and Instituto Geológico y Minero de España, Madrid.
- Rosales Franco, I., Robador Moreno, A. and Perucha Atienza, M.A., 2011. Mapa y Memoria de la Hoja nº 36-IV / 37-III (Castro Urdiales-Zierbena) del Mapa Geológico de Cantabria a escala 1:25.000. Gobierno de Cantabria and Instituto Geológico y Minero de España, Madrid.

- Merino Tomé, O.A., Bahamonde, J.R., Fernández, L.P., Rodríguez García, A. and Robador Moreno, A., 2009. Mapa y Memoria de la Hoja nº 56-I / 56-III (Carreña-Sotres) del Mapa Geológico de Cantabria a escala 1:25.000. Gobierno de Cantabria and Instituto Geológico y Minero de España, Madrid.
- Merino Tomé, O.A., Bahamonde, J.R., Bernández Rodríguez, E., Ipas Llorens, J., Rodríguez García, A., Sela del Río, E. and Robador Moreno, A., 2009. Mapa y Memoria de la Hoja nº 56-II (Panés) del Mapa Geológico de Cantabria a escala 1:25.000. Gobierno de Cantabria and Instituto Geológico y Minero de España, Madrid.
- Merino Tomé, O.A., Bahamonde Rionda, J.R., Corrochano Fernández, D., Bernández Rodríguez, E., Ipas Llorens, J., Rodríguez García, A., Sela del Río, E. and Robador Moreno, A., 2009. Mapa y Memoria de la Hoja nº 56-IV (Tama) del Mapa Geológico de Cantabria a escala 1:25.000. Gobierno de Cantabria and Instituto Geológico y Minero de España, Madrid.
- García-Senz, J., Merino Tomé, O.A., Bahamonde Rionda, J.R. and Robador Moreno, A., 2011. Mapa y Memoria de la Hoja nº 57-I (Puentenansa) del Mapa Geológico de Cantabria a escala 1:25.000. Gobierno de Cantabria and Instituto Geológico y Minero de España, Madrid.
- Huerta Carmona, J., Nozal Martín, F. and Robador Moreno, A., 2009. Mapa y Memoria de la Hoja nº 57-II (Cabezón de la sal) del Mapa Geológico de Cantabria a escala 1:25.000. Gobierno de Cantabria and Instituto Geológico y Minero de España, Madrid.
- Bernardez Rodríguez, E., Ipas Llorens, J., Robador Moreno, A. and Nozal Martín, F., 2010. Mapa y Memoria de la Hoja nº 57-III (Cosío) del Mapa Geológico de Cantabria a escala 1:25.000. Gobierno de Cantabria and Instituto Geológico y Minero de España, Madrid.
- Del Olmo Ruiz, J., Nozal Martín, F. and Robador Moreno, A., 2009. Mapa y Memoria de la Hoja nº 57-IV (Valle) del Mapa Geológico de Cantabria a escala 1:25.000. Gobierno de Cantabria and Instituto Geológico y Minero de España, Madrid.
- Huerta Carmona, J., Nozal Martín, F. and Robador Moreno, A., 2009. Mapa y Memoria de la Hoja nº 58-I (Los corrales de Buelna) del Mapa Geológico de Cantabria a escala 1:25.000. Gobierno de Cantabria and Instituto Geológico y Minero de España, Madrid.
- Ipas Llorens, J.F., Nozal Martín, F. and Robador Moreno, A., 2009. Mapa y Memoria de la Hoja nº 58-II (Puente Viesgo) del Mapa Geológico de Cantabria a escala 1:25.000. Gobierno de Cantabria and Instituto Geológico y Minero de España, Madrid.
- Bernardez Rodríguez, E., Nozal Martín, F. and Robador Moreno, A., 2009. Mapa y Memoria de la Hoja nº 58-III (Arenas de Iguña) del Mapa Geológico de Cantabria a escala 1:25.000. Gobierno de Cantabria and Instituto Geológico y Minero de España, Madrid.
- Ipas Llorens, J.F., Nozal Martín, F. and Robador Moreno, A., 2009. Mapa y Memoria de la Hoja nº 58-IV (Santiurde de Toranzo) del Mapa Geológico de Cantabria a escala 1:25.000. Gobierno de Cantabria and Instituto Geológico y Minero de España, Madrid.
- García Senz, J., Mediato Arribas, J., and Robador Moreno, A., 2012. Mapa y Memoria de la Hoja nº 59-I (Sarón) del Mapa Geológico de Cantabria a escala 1:25.000. Gobierno de Cantabria and Instituto Geológico y Minero de España, Madrid.
- García Senz, J. and Robador Moreno, A., 2012. Mapa y Memoria de la Hoja nº 59-II (Arredondo) del Mapa Geológico de Cantabria a escala 1:25.000. Gobierno de Cantabria and Instituto Geológico y Minero de España, Madrid.
- Robador Moreno, A. and Cañas Fernández, V., 2013. Mapa y Memoria de la Hoja nº 59-III (Selaya) del Mapa Geológico de Cantabria a escala 1:25.000. Gobierno de Cantabria and Instituto Geológico y Minero de España, Madrid.
- Robador Moreno, A. and Cañas Fernández, V., 2013. Mapa y Memoria de la Hoja nº 59-IV (Veguilla) del Mapa Geológico de Cantabria a escala 1:25.000. Gobierno de Cantabria and Instituto Geológico y Minero de España, Madrid.
- García Senz, J. and Robador Moreno, A., 2008. Mapa y Memoria de la Hoja nº 60-I (Ramales de la Victoria) del Mapa Geológico de Cantabria a escala 1:25.000. Gobierno de Cantabria and Instituto Geológico y Minero de España, Madrid.

- Robador Moreno, A., 2008. Mapa y Memoria de la Hoja nº 60-II / 61-I (La Iglesia - Santurtzi) del Mapa Geológico de Cantabria a escala 1:25.000. Gobierno de Cantabria and Instituto Geológico y Minero de España, Madrid.
- García Senz, J. and Robador Moreno, A., 2008. Mapa y Memoria de la Hoja nº 60-III (Concha) del Mapa Geológico de Cantabria a escala 1:25.000. Gobierno de Cantabria and Instituto Geológico y Minero de España, Madrid.
- Robador Moreno, A., 2008. Mapa y Memoria de la Hoja nº 60-IV (Balmaseda) del Mapa Geológico de Cantabria a escala 1:25.000. Gobierno de Cantabria and Instituto Geológico y Minero de España, Madrid.
- Rodríguez Fernández, L.R., Merino Tomé, O. López Olmedo, F., Nozal, F. and Robador Moreno, A., 2008. Mapa y Memoria de la Hoja nº 81-I (Camaleño) del Mapa Geológico de Cantabria a escala 1:25.000. Gobierno de Cantabria and Instituto Geológico y Minero de España, Madrid.
- López Olmedo, F., Rodríguez Fernández, L.R., Rodríguez García, A., and Robador Moreno, A., 2010. Mapa y Memoria de la Hoja nº 81-II (Potes) del Mapa Geológico de Cantabria a escala 1:25.000. Gobierno de Cantabria and Instituto Geológico y Minero de España, Madrid.
- Rodríguez Fernández, L.R., Toyos, J.M., and Robador Moreno, A., 2009. Mapa y Memoria de la Hoja nº 81-III (Portilla de la Reina) del Mapa Geológico de Cantabria a escala 1:25.000. Gobierno de Cantabria and Instituto Geológico y Minero de España, Madrid.
- Rodríguez Fernández, L.R., Toyos, J.M., and Nozal Martín, F., 1996. Mapa y Memoria de la Hoja nº 81-IV (Pesaguero) del Mapa Geológico de Cantabria a escala 1:25.000. Gobierno de Cantabria and Instituto Geológico y Minero de España, Madrid.
- Corrochano, D., Bernárdez, E., Ipas, J., Robador Moreno, A. and Nozal Martín, F., 2010. Mapa y Memoria de la Hoja nº 82-I (Tudanca) del Mapa Geológico de Cantabria a escala 1:25.000. Gobierno de Cantabria and Instituto Geológico y Minero de España, Madrid.
- Bernárdez, E., Ipas, J., Robador Moreno, A., 2009. Mapa y Memoria de la Hoja nº 82-II (Los Tojos) del Mapa Geológico de Cantabria a escala 1:25.000. Gobierno de Cantabria and Instituto Geológico y Minero de España, Madrid.
- Corrochano, D., Bernárdez, E., Robador Moreno, A. and Nozal Martín, F., 2010. Mapa y Memoria de la Hoja nº 82-III (Valdeprado) del Mapa Geológico de Cantabria a escala 1:25.000. Gobierno de Cantabria and Instituto Geológico y Minero de España, Madrid.
- Corrochano, D., Bernárdez, E., Ipas, J., and Robador Moreno, A., 2009. Mapa y Memoria de la Hoja nº 82-IV (Espinilla) del Mapa Geológico de Cantabria a escala 1:25.000. Gobierno de Cantabria and Instituto Geológico y Minero de España, Madrid.
- Solé Pont, F.J., Sarrionandía Eguidazu, F., Mediato Arribas, J.F., Hernaiz Huerta, P.P., and Robador Moreno, A., 2008. Mapa y Memoria de la Hoja nº 83-I (Molledo) del Mapa Geológico de Cantabria a escala 1:25.000. Gobierno de Cantabria and Instituto Geológico y Minero de España, Madrid.
- Solé Pont, F.J., Sarrionandía Eguidazu, F., Mediato Arribas, J.F., Hernaiz Huerta, P.P., and Robador Moreno, A., 2008. Mapa y Memoria de la Hoja nº 83-II (San Miguel de Luena) del Mapa Geológico de Cantabria a escala 1:25.000. Gobierno de Cantabria and Instituto Geológico y Minero de España, Madrid.
- Sarrionandía Eguidazu, F., Solé Pont, F.J., Mediato Arribas, J.F., Hernaiz Huerta, P.P., and Robador Moreno, A., 2008. Mapa y Memoria de la Hoja nº 83-III (Reinosa) del Mapa Geológico de Cantabria a escala 1:25.000. Gobierno de Cantabria and Instituto Geológico y Minero de España, Madrid.
- Sarrionandía Eguidazu, F., Solé Pont, F.J., Mediato Arribas, J.F., Hernaiz Huerta, P.P., and Robador Moreno, A., 2008. Mapa y Memoria de la Hoja nº 83-IV (La Costana) del Mapa Geológico de Cantabria a escala 1:25.000. Gobierno de Cantabria and Instituto Geológico y Minero de España, Madrid.
- Robador Moreno, A., and Cañas Fernández, V., 2013. Mapa y Memoria de la Hoja nº 84-I (Vega de Pas) del Mapa Geológico de Cantabria a escala 1:25.000. Gobierno de Cantabria and Instituto Geológico y Minero de España, Madrid.

- Robador Moreno, A., 2011. Mapa y Memoria de la Hoja nº 84-II (Bárcenas) del Mapa Geológico de Cantabria a escala 1:25.000. Gobierno de Cantabria and Instituto Geológico y Minero de España, Madrid.
- Robador Moreno, A., 2010. Mapa y Memoria de la Hoja nº 84-III (Pedrosa de Valdeporres) del Mapa Geológico de Cantabria a escala 1:25.000. Gobierno de Cantabria and Instituto Geológico y Minero de España, Madrid.
- García Senz, J., and Robador Moreno, A., 2009. Mapa y Memoria de la Hoja nº 85-I (Bercedo) del Mapa Geológico de Cantabria a escala 1:25.000. Gobierno de Cantabria and Instituto Geológico y Minero de España, Madrid.
- Bernárdez, E., Robador Moreno, A., and Nozal Martín, F., 2010. Mapa y Memoria de la Hoja nº 107-I (San Salvador de Cantamuda/Brañosera) del Mapa Geológico de Cantabria a escala 1:25.000. Gobierno de Cantabria and Instituto Geológico y Minero de España, Madrid.
- Bernárdez, E., and Robador Moreno, A., 2010. Mapa y Memoria de la Hoja nº 107-IV (Barruelo de Santullán) del Mapa Geológico de Cantabria a escala 1:25.000. Gobierno de Cantabria and Instituto Geológico y Minero de España, Madrid.
- García Senz, J., Perucha, M.A., and Robador Moreno, A., 2012. Mapa y Memoria de la Hoja nº 108-I (Matamorosa) del Mapa Geológico de Cantabria a escala 1:25.000. Gobierno de Cantabria and Instituto Geológico y Minero de España, Madrid.
- García Clariana, P., Cañas, V., and Robador Moreno, A., 2008. Mapa y Memoria de la Hoja nº 108-II (Arija/Soncillo) del Mapa Geológico de Cantabria a escala 1:25.000. Gobierno de Cantabria and Instituto Geológico y Minero de España, Madrid.
- López Olmedo, F., and Robador Moreno, A., 2011. Mapa y Memoria de la Hoja nº 108-III (Mataporquera) del Mapa Geológico de Cantabria a escala 1:25.000. Gobierno de Cantabria and Instituto Geológico y Minero de España, Madrid.
- Montes Santiago, M.J., and Robador Moreno, A., 2008. Mapa y Memoria de la Hoja nº 108-IV (Espinosa de Bricia/Manzanedo) del Mapa Geológico de Cantabria a escala 1:25.000. Gobierno de Cantabria and Instituto Geológico y Minero de España, Madrid.
- Peropadre Medina, C., Mediato Arribas, J.F., Hernaiz Huerta, P.P., and Robador Moreno, A., 2011. Mapa y Memoria de la Hoja nº 134-I (Pomar de Valdivia) del Mapa Geológico de Cantabria a escala 1:25.000. Gobierno de Cantabria and Instituto Geológico y Minero de España, Madrid.
- Peropadre Medina, C., Mediato Arribas, J.F., Hernaiz Huerta, P.P., and Robador Moreno, A., 2011. Mapa y Memoria de la Hoja nº 134-II (Polientes/Escalada) del Mapa Geológico de Cantabria a escala 1:25.000. Gobierno de Cantabria and Instituto Geológico y Minero de España, Madrid.

List of 1:25.000 maps used in this report done by Empresa Nacional de Residuos Radioactivos S.A. (ENRESA). The references are in alphabetic order.

- INGEMISA, 1990. Mapa Geológico Diapiros Vasco-Burgalesa Hoja Salinas de Añana a escala 1:25.000. Empresa Nacional de Residuos Radioactivos S.A., Madrid.
- INGEMISA, 1990. Mapa Geológico Diapiros Vasco-Burgalesa Hoja Salinas de Rosio a escala 1:25.000. Empresa Nacional de Residuos Radioactivos S.A., Madrid.
- INGEMISA, 1990. Mapa Geológico Diapiros Vasco-Burgalesa Hoja Villasana de Mena a escala 1:25.000. Empresa Nacional de Residuos Radioactivos S.A., Madrid.
- Informes y Proyectos S.A. (INYPESA), 1994. Mapa Geológico Banda Plegada código: 46.93-SK-01-TE-GE-1 a escala 1:25.000. Empresa Nacional de Residuos Radioactivos S.A., Madrid.
- Informes y Proyectos S.A. (INYPESA), 1994. Mapa Geológico Banda Plegada código: 46.93-SK-01-TE-GE-2 a escala 1:25.000. Empresa Nacional de Residuos Radioactivos S.A., Madrid.
- Informes y Proyectos S.A. (INYPESA), 1994. Mapa Geológico Pantano del Ebro código: 46.93-SK-04-TE-GE-0 a escala 1:25.000. Empresa Nacional de Residuos Radioactivos S.A., Madrid.

Informes y Proyectos S.A. (INYPSA), 1994. Mapa Geológico Plataforma Burgalesa código: 46.93-SK-05-TE-GE-0 a escala 1:25.000. Empresa Nacional de Residuos Radioactivos S.A., Madrid.

List of maps used in this report from other scientific publications (i.e. PhD thesis and papers). The references are in alphabetic order.

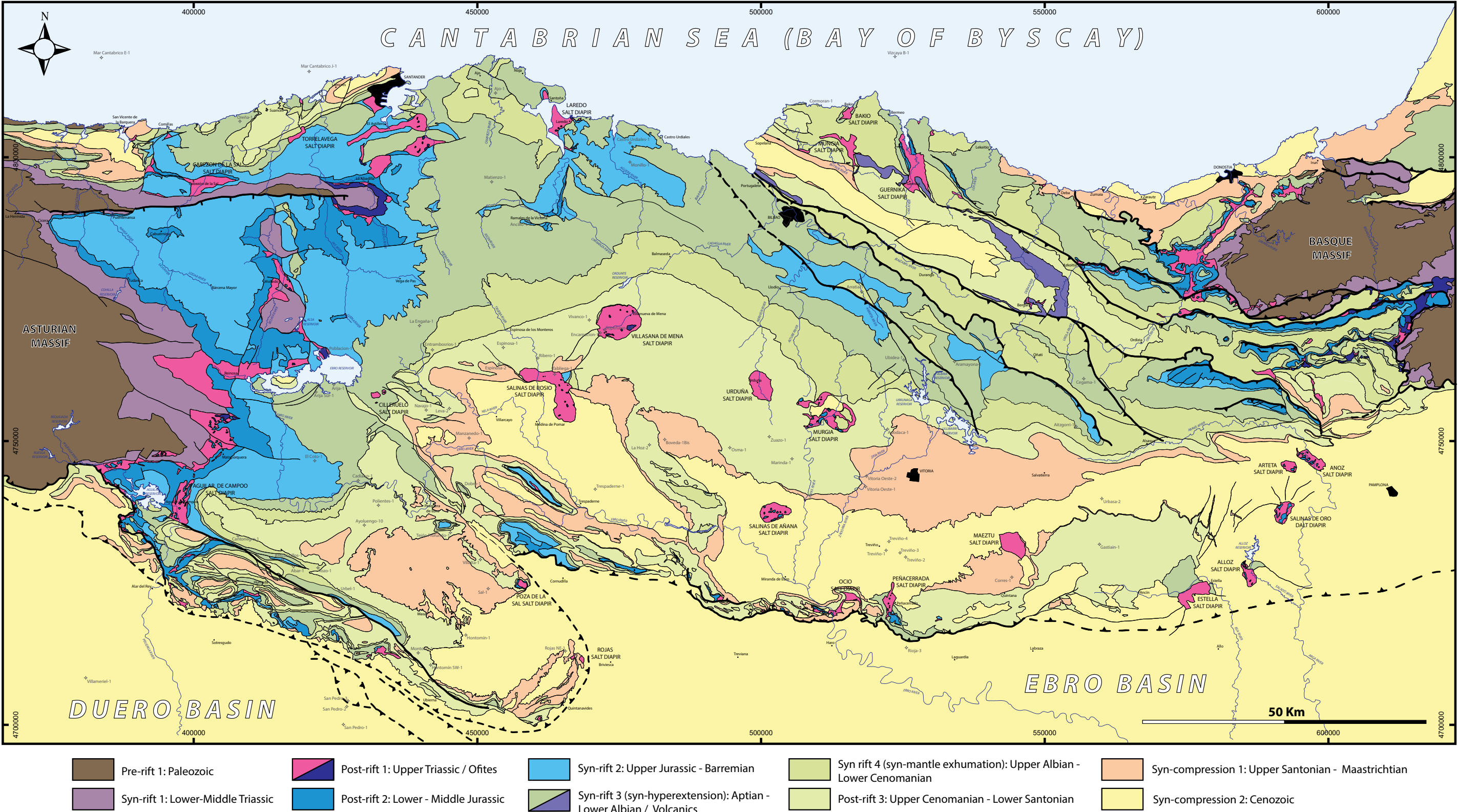
Ábalos, B., 2016. Geologic map of the Basque-Cantabrian Basin and a new tectonic interpretation of the Basque Arc. *International Journal of Earth Sciences*, 105(8), 2327-2354.

Ábalos, B., Alkorta, A., & Iríbar, V., 2008. Geological and isotopic constraints on the structure of the Bilbao anticlinorium (Basque–Cantabrian basin, North Spain). *Journal of Structural Geology*, 30(11), 1354-1367.

Carola, E., 2014. The transition between thin-to thick-skinned styles of deformation in the western Pyrenean Belt. Tesis Doctoral, Universidad de Barcelona, 245 p.

Lescoutre, R., 2019. Formation and reactivation of the Pyrenean – Cantabrian rift system: inheritance, segmentation and thermal evolution. PhD Thesis. University of Strasbourg, 256p.

Annex 2.4



ANNEX 3: STRIKE-SLIP CORRIDORS IN MICROPLATE KINEMATICS: THE IBERIA RESTORATION PARADIGM REVISED (PEER REVIEW)

Tracking no:

Authors:

Gianluca Frasca

Abstract:

Disclaimer: This is a confidential document and must not be discussed with others, forward in any form, or posted on websites without the express written consent of the Geological Society of America.

1 **Strike-slip corridors in microplate kinematics: the Iberia** 2 **restoration paradigm revised**

3 Gianluca Frasca^{1,2}, Gianreto Manatschal², Patricia Cadenas^{2,3}, Jordi Miro^{2,4}, Rodolphe
 4 Lescoutre^{2,5}

5 ¹*IGG, CNR, Via Valperga Caluso 35, 10125 Torino, Italy*

6 ²*IPGS, EOST-CNRS, Université de Strasbourg, 1 Rue Blessig, 67084 Strasbourg, France*

7 ³*BCSI, ICM, CSIC, 37 Passeig Marítim de la Barceloneta, 08003 Barcelona, Spain*

8 ⁴*Institut de Recerca Geomodels, DDTO, Universitat de Barcelona, Barcelona 08028, Spain*

9 ⁵*Department of Earth Sciences, Uppsala University, Villavägen 16, 75236 Uppsala, Sweden*

10

11 **ABSTRACT**

12 Despite considerable progress in restoring rifted margins, none of the current kinematic
 13 models can restore Iberia in full agreement with the circum-Iberian geology. This conflict claims
 14 for a revision of the restoration method. Iberia has a unique geological dataset that allows
 15 calibration and testing of kinematic restorations, representing an ideal candidate for the revision
 16 of paradigmatic intracontinental restoration approaches. Mesozoic left-lateral motion of Africa
 17 relative to Europe occurred while Iberia was diverging from North America. We identify
 18 deforming regions with strike-slip corridors that surround rigid blocks and segment
 19 intracontinental rifts. Relying on recently published data, we constrain the timing and motion
 20 along these strike-slip corridors, and we propose new Euler poles for Iberia and confining
 21 microplates. The resulting kinematics of Iberia is broadly consistent with the Mesozoic circum-

Iberian geology. We conclude that large-scale intracontinental strike-slip corridors may offer a robust boundary condition for reconstructing microplate motions during oblique rifting.

INTRODUCTION

Great efforts have been directed recently in the plate kinematic community to consider the pre-breakup evolution in kinematic reconstructions of divergent plate boundaries. A robust kinematic description appears crucial to a physics-based understanding of continental rifting (Williams et al., 2019). Kinematic restoration of divergent plates relies on a common frame of procedure, a paradigm, which includes: 1) tight-fit of seafloor magnetic anomalies, defining the position of diverging plates through time; 2) oceanic fracture zones, interpreted as flowlines, determining the direction of the motion; 3) necking zones, defining the tightest-fit solutions of reconstructions; and 4) paleomagnetic data from continental undeformed regions, outlining rotation and latitudinal shifts (e.g. Müller et al., 2019).

This four-step paradigmatic approach achieved outstanding results in reconstructing the global plate motions. However, it fails to restore intracontinental deformation of diverging microplates, when tested against onshore regional geology, as shown for the Iberian case (Barnett-Moore et al., 2016a; Tavani et al., 2018). The oceanic nature and isochron character of first magnetic anomalies of the M-series (e.g. J anomaly) are debated and onshore paleomagnetic declinations do not harmonize with tomographic data in the Pyrenees (Nirrengarten et al., 2017; Chevrot et al., 2018).

Here, we propose that the left-lateral drag of Africa vs. Europe since Late Triassic drove the kinematics of Iberia and controlled the evolution of the interleaving Flemish and Ebro microplates. We define the Newfoundland, Flemish Pass, and Bay of Biscay-Iberian Rift

corridors characterized by strike-slip motion parallel to their dominant trend. Relying on the use of these corridors as flowlines for kinematic restorations, we build a new kinematic model for the southern North Atlantic and the Bay of Biscay, and we reconstruct the kinematics of Iberia from Late Triassic to Late Cretaceous (Anomaly C34).

GEOLOGICAL SETTING

Iberia (IB) is surrounded by the major North America (NAM), European (EU) and NW African (AFR) plates and by smaller rigid microplates such as Flemish Cap (FL), Porcupine (PR), Morocco (MO) and Ebro (EBR). Figure 1 summarizes the stage Euler poles reported for plates and microplates by previous authors. The Mesozoic template is mainly preserved on the Atlantic and Bay of Biscay (Bi) margins, enabling to quantify the displacement. In the east, Mesozoic fossil remnants are preserved in the Pyrenees (Pyr) and in the Iberian Rift System (IRS), allowing for an evaluation of the output of the kinematic models.

Three large-scale strike-slip corridors can be identified around IB: (1) the Newfoundland corridor, (2) the Flemish Pass corridor, and (3) the Bay of Biscay-Iberian Rift corridor, BIR (Reid, 1988; Sandoval et al., 2019; Angrand et al., 2020) (Fig. 1). The Newfoundland corridor separates Central and Northern Atlantic and evolved eventually to a transform margin bounded by oceanic crust, allowing the use of magnetic anomalies to define timing. The Flemish Pass corridor edges southward the E and W Orphan basins and coincides with a NW-SE elongated hyperextended basin. The BIR corridor defines the boundary between IB and EU-EBR and borders northward the basins of the IRS. Its prolongation towards Bi is parallel to the northern Bi margin. Syn-kinematic sedimentary sequences from hyperextended and rift basins have been described along the Flemish Pass and BIR corridors (Tugend et al., 2014; Sandoval et al., 2019).

METHOD

The experiment is designed to respect boundary conditions defined by (1) orientation and timing of the strike-slip corridors, inferred from major structural trend and the age of rift-related basins respectively, and by (2) the global motion of the larger plates around IB, as described by Müller et al. 2019 (Fig. 2, first column). We also include independent and robust input data from the Atlantic to constrain the timing of the motion of IB. We incorporate the extensional template of Gómez-Romeu et al. (2020), which provides extension values for FL and NAM relative to IB, in strong agreement with values proposed by Sutra et al. (2013) (Fig. 2). Moreover, we use the alinement of the M0 magnetic anomaly between southern North Atlantic and Central Atlantic (Fig. 1) to suggest that IB and AFR moved with a similar direction after 120 Ma (Szameitat et al., 2020). Position and timing of present-day edges of continental crust and the landward limits of the oceanic crust also support the reconstruction of the deforming kinematic model (e.g., ECC and LaLOC lines as defined in Nirrengarten et al., 2018, Fig. 3).

RESTORATION OF IBERIA

The initial condition of the model is the widely accepted position of the four main plates (NAM, IB, EU; AFR) at anomaly C34 (Fig. 3A). The synchronous movement along all strike-slip corridors during Late Jurassic to Aptian is critical to define a coherent motion of AFR relative to NAM, NAM relative to FL and IB relative to EU. The strike-slip corridors broadly have the same trend at 83 Ma (Fig. 3A). We modelled backward from this first step at 83 Ma assuming a relative motion during continental rifting parallel to the strike-slip corridors (Fig. 3,

Data repository¹). Then, we completed the restoration of the Atlantic margins to a full continental tight-fit for the southernmost part of the N-Atlantic (Fig. 3H).

Model results for the Iberia-Europe-Ebro region

In our deforming model (Gurnis et al., 2018), the lateral motion of IB relative to EBR is (1) 370 km from 155 to 112 Ma, resulting into the development of Late Jurassic to Aptian depocenters on the IRS (Salas et al., 2001) and (2) 320 km from 112 to 83, suggesting that strike-slip motion should be localized slightly northwards of the IRS (Angrand et al., 2020). No motion is reported before 126 Ma between EBR and EU and 80 km of N-S directed extension between EBR and EU are reported from 126 to 83 Ma, consistently with values inferred from hyperextended basins at Bi (see Tugend et al., 2015). The onset of extension into the Pyrenean domain indicates a shift of the extensional deformation from the NW-SE trending BIR corridor to the E-W trending Pyr segment (see Lescoutre and Manatschal, 2020) (Fig. 3B to 3D).

Location of both pre- and post- Albian strike-slip motion needs further investigations. Complex overprint of (1) post-Late Aptian N-S extension in Bi and (2) post-83 Ma Alpine shortening and related sedimentation could hamper its recognition. However, our kinematic model reproduces for the first time the proposed strike-slip deformation followed by orthogonal N-S extension (Jammes et al., 2009; Tugend et al., 2015) (Fig. 3B to 3D). Our kinematic model predicts that M-series magnetic anomalies in the Bi do not correspond to isochrons (Fig. 3B to 3E). The lateral propagation of the anomalies is similar to what has been shown by Szameitat et al. 2020 for the southern N-Atlantic (Fig. 3C to 3B).

Model results for the southern North Atlantic

The southern N-Atlantic, even if mainly an input region, can be also used to test the model output. The parallelism between the computed FL-IB motion path and the trend of the displacement zone drawn (Mohn et al., 2015) from Late Jurassic to Mid Cretaceous is striking. Similarly, the reconstructed Jurassic IB-AFR motion path is parallel to fracture zones inferred by Fernàndez et al. (2019). Both structural trends fit with the motion path and confirm the validity of our approach (Fig. 1).

The computed total ~185 km of extension for the Orphan Basin during the Mesozoic (Fig. 2 and Figs. 3F,3G) is compatible with the reported observations (MacMahon et al., 2020). Our orthogonal setting has a NAM-FL pole of rotation far from Flemish Cap, in contrast to previous estimations (Sibuet et al., 2007; see Fig. 1). In the southern N-Atlantic, the progressive northward oceanization is compatible with observations reported by Szameitat et al. (2020). At 200 Ma, we derive a full NAM-IB continental tight-fit, implying a crustal overlap for the Flemish Cap-Iberia segment.

The average motion path AFR-NAM derived from Müller et al. (2019) is not perfectly fitting the Newfoundland transform trend for its intracontinental part. We invoke thus an independent motion of Morocco as a deforming promontory of NW Africa during Early Jurassic. The modified motion of Morocco implies a dextral-lateral displacement of 80 km in the Atlas during the early Jurassic and a left-lateral movement south of Iberia during the whole Cretaceous after the docking of Morocco and NW Africa (Fig. 3G), in agreement with geological data (Gimeno-Vives et al., 2019).

Differences with previous plate kinematic reconstructions

The approach to reconstruct the Atlantic - Iberian margins was traditionally based on two end-member approaches. A first method used magnetic anomalies (e.g., J magnetic anomaly) as isochrons (Sibuet et al., 2004; Vissers and Meijer, 2012; Fig. 4A) and a second method used tight fit restorations of continental crust at the end of the Triassic (Barnett-Moore et al., 2016; Nirrengarten et al., 2018; Fig. 4B). Resulted models imply: (1) an acceleration of IB relative to Africa during mid-Cretaceous and thus a dextral shearing in the deforming region south of IB; and (2) significant shortening, triggering subduction during mid-Cretaceous in the Pyrenees (first model) or in the Tethys (second model) (Figs. 4A and 4B). Our workflow privileges as foundation first order on- and off-shore regional observations that favor a third solution: the BIR separates the IB and EBR running north of the Balearic Islands and out of the Pyrenean domain, and EBR corresponds to an independent deforming promontory of EU (Fig. 4C). Furthermore, no subduction resulted north or east of Iberia in agreement with circum-Iberian data. The stage Euler poles are further away from the deformed area between Africa and EU and less scattered than previously assessed (stage rotation poles in Fig. 1).

Iberia paradigm revision and future challenges in restoration of continental rifting

Our method appears suitable for regions where strong oblique motions preclude tight-fit restorations or where significant magmatic additions prevent robust quantification of the original volumes of continental crust (e.g. Mozambique-Antarctica). In contrast to previous restorations (e.g., Nirrengarten et al., 2018), we do not use the criteria as a base for the model and we restrict the use of the continental tight-fit to the orthogonal opening of conjugate hyperextended segments. In our model, gaps and overlaps in restored edges of continental crust (RECC of Nirrengarten et al., 2018) are observed in the Bay of Biscay and in the northernmost southern N-

Atlantic (Fig. 3H). Discrepancies are expected in such an oblique setting, as underlined by Peace et al. (2019). Furthermore, gaps at 200 Ma can be justified with previous Triassic extension (Van Hinsbergen et al., 2020). However, the similarity in size of these gaps and overlaps asks for a mechanism that could explain a shift of crustal material.

The main strike-slip corridors are inside or bounding continental deforming regions, which can be locally up to 300 km wide (white in Fig. 3). In the deforming regions, small rigid blocks may rotate in a book-shelf manner along antithetic faults with an opposite sense of shear (Fig. 4D), or synthetic Riedel-type faults may show trend or sense of shear different from the main strike-slip corridors that accommodate the large-scale plate displacement (Fig. 4E and 4F)(Fossen, 2016). The three exemplified cases show that local structures, even up to 50 km long, can give erroneous kinematic indications if not interpreted on a large-scale kinematic frame. Furthermore, these structures can trigger anomalous local rotations. It asks, therefore, for a careful upscaling of field observations.

The absence of large-scale features such as oceanic fracture zones and the uncertain nature of first magnetic anomalies make the pre-lithosphere breakup extremely problematic for kinematic reconstructions. Our practice overcomes the classical paradigm for reconstruction of IB, (1) showing the importance of the dragging action of major plates on minor intervening microplates and (2) proposing a new approach for intracontinental deformation based on the definition of strike-slip corridors.

CONCLUSIONS

Strike-slip corridors are marked by (1) a sharp contrast between continental and magmatic crust or (2) by alignments of strike-slip basins. We assume that intracontinental strike-

slip corridors materialize, as flowlines, the relative motion of plates and microplates during intracontinental deformation. The resulting reconstruction of Iberia agrees with circum-Iberian plate-scale geological data, suggesting that intracontinental strike-slip corridors may be robust boundary conditions to restore segmented-orthogonal and oblique rifts. We call for caution in upscaling of local onshore field observations in plate kinematic reconstructions. The plate-scale left-lateral motion of Africa relative to Europe appears indeed crucial to control the Mesozoic kinematics of Iberia. Once identified robust and large-scale strike-slip corridors, our method might apply to other deforming continental regions in oblique settings worldwide where large tectonic plates move laterally.

AKNOWLEDGEMENTS

Thanks to B. Petri and S. Tomasi for discussions. GF and GM were supported by M5 consortium, and PC, JM, RL and GM by OROGEN Project.

FIGURE CAPTIONS

Figure 1. Present-day location of strike-slip corridors and magnetic anomalies. Euler stage poles represent relative motions for plates and microplates (different colors). Symbols refer to our and previous global kinematic models. Full or empty symbols indicate the time span: respectively syn- or post- Flemish Cap plate. AFR= NW Africa; Bi= Biscay; EBR= Ebro; EU= Europe; FL= Flemish Cap; MO= Morocco; NAM=North America; PR= Porcupine; Pyr= Pyrenees; IRS= Iberian Rift System. White squares refer to the location of data in columns of Fig. 2 and onset of arrows in Fig. 3.

Figure 2. Main tectonic events in the NAM-AFR-EUR area around IB as defined by Müller et al. 2019 in the first column. Computed values of displacement in km for the points shown in Fig. 1 and time span represented in maps of Fig. 3. Input data are in black, while output are grey. Computed values and 2σ method explained in Data Repository. Colors in the background show evolution from rifting to drifting.

Figure 3. Tectonic restorations of Iberia and surrounding plates. Present-day geographic configuration is shown for the stable parts of the plates, deforming continental regions are white. Each map represents the incremental deformation in the time span between the same and the previous map, reported in Fig. 2. Necking lines in grey and exhumed mantle region in green, first oceanic crust and magnetic anomalies in light and dark blue. (A) ~83 Ma: magnetic anomaly C34 and onset of AFR-IB-EU convergence. (B) ~97 Ma: mantle exhumation in the Pyrenees and post-rift in Iberian Range basins. (C) ~112 Ma: mantle exhumation in northern Southern North Atlantic and syn-rift in Iberian Range. (D) ~120 Ma: magnetic anomalies appear in S N Atlantic. (E) ~133 Ma: Break-up in southernmost North Atlantic. (F) ~145 Ma: Onset thinning continental crust in northernmost southern N Atlantic. (G) ~165 Ma: Break-up in the Central Atlantic and onset IB-EUR relative motion. (H) ~200 Ma: Tight-fit IB-NAM for southernmost North Atlantic. Necking lines in grey and edge of the continental crust region in green, first oceanic crust and magnetic anomalies in light and dark blue. Size arrows is proportional to the stage velocities.

Figure 4. Sketch view of three end-member solutions for the motion of Iberia: (A) based on the J magnetic anomaly (e.g. Van Hinsbergen et al., 2020); (B) based on tight-fit of restored

227 *continental crust (e.g. Nirrengarten et al. 2018); (C) based on strike-slip corridors, our solution.*
 228 *Possible local deformation patterns in or along sinistral strike-slip corridors: (D) bookshelf*
 229 *sliding with antithetic (dextral) faults. Note the possible extension in collapsing areas; (E)*
 230 *dextral or (F) sinistral large-scale shear bands may appear as mechanical instabilities at*
 231 *different angles from the main displacement surface (redrawn after Fossen, 2016).*

232
 233 ¹GSA Data Repository item 201Xxxx, with Method supplements, GPlates files and
 234 reconstruction movie, is available online at www.geosociety.org/pubs/ft20XX.htm, or on request
 235 from editing@geosociety.org.

236

237 **References Cited**

- 238 Barnett-Moore, N., Hosseinpour, M., and Maus, S., 2016a, Assessing discrepancies between
 239 previous plate kinematic models of Mesozoic Iberia and their constraints: *Tectonics*, v.
 240 35, p. 2015TC004019, doi:10.1002/2015TC004019.
- 241 Barnett-Moore, N., Müller, D.R., Williams, S., Skogseid, J., and Seton, M., 2016b, A
 242 reconstruction of the North Atlantic since the earliest Jurassic: *Basin Research*, p. n/a-n/a,
 243 doi:10.1111/bre.12214.
- 244 Chevrot, S. et al., 2018, The non-cylindrical crustal architecture of the Pyrenees: *Scientific*
 245 *Reports*, v. 8, p. 9591, doi:10.1038/s41598-018-27889-x.
- 246 Fernández, M., Torne, M., Vergés, J., Casciello, E., and Macchiavelli, C., 2019, Evidence of
 247 Segmentation in the Iberia–Africa Plate Boundary: A Jurassic Heritage? *Geosciences*, v.
 248 9, p. 343.

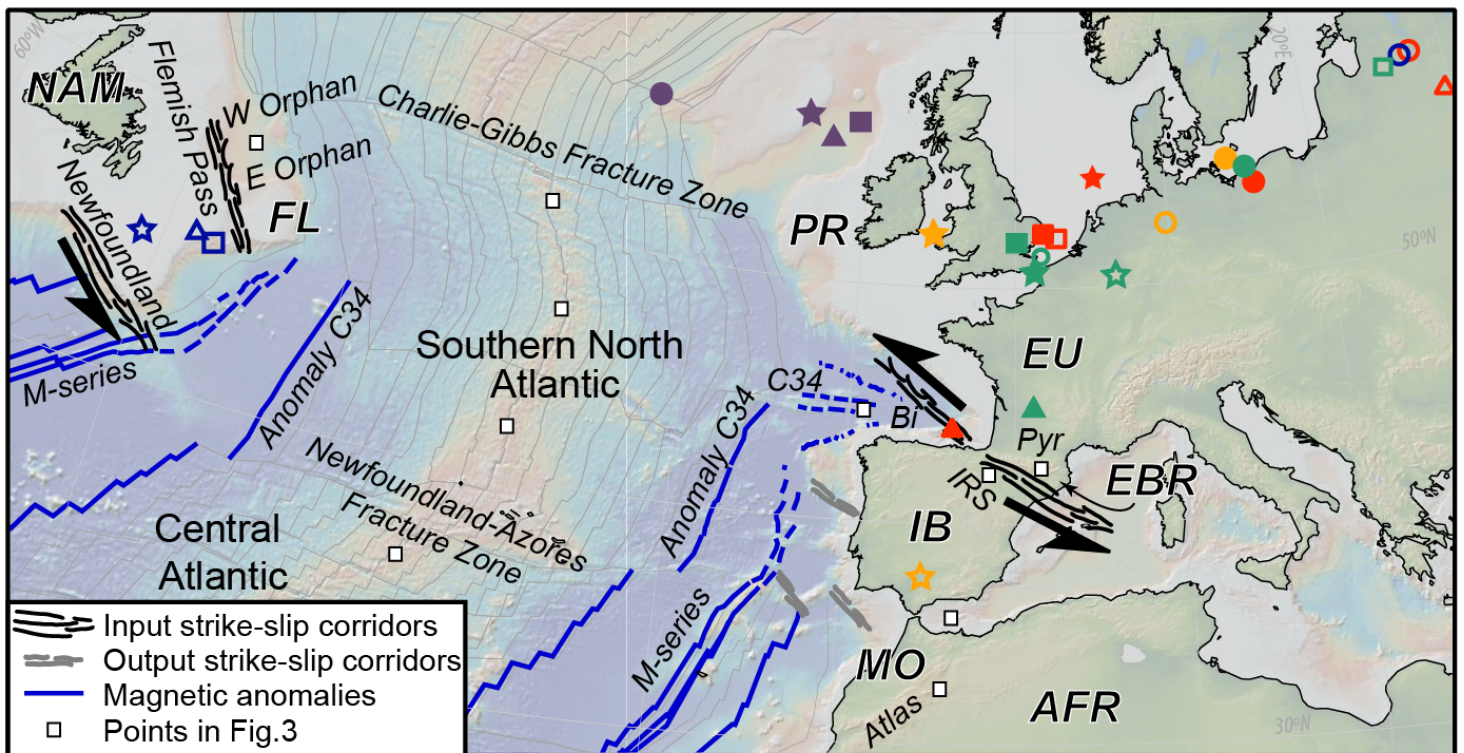
- 249 Fossen, H., 2016, Structural geology: Cambridge University Press.
- 250 Gimeno-Vives, O., Mohn, G., Bosse, V., Haissen, F., Zaghloul, M.N., Atouabat, A., and Frizon
251 de Lamotte, D., 2019, The Mesozoic Margin of the Maghrebian Tethys in the Rif Belt
252 (Morocco): Evidence for Polyphase Rifting and Related Magmatic Activity: *Tectonics*, v.
253 38, p. 2894–2918, doi:10.1029/2019TC005508.
- 254 Gómez-Romeu, J., Kuszniir, N., Roberts, A., and Manatschal, G., 2020, Measurements of the
255 extension required for crustal breakup on the magma-poor Iberia-Newfoundland
256 conjugate margins: *Marine and Petroleum Geology*, v. 118, p. 104403,
257 doi:10.1016/j.marpetgeo.2020.104403.
- 258 Gurnis, M., Yang, T., Cannon, J., Turner, M., Williams, S., Flament, N., and Müller, R.D., 2018,
259 Global tectonic reconstructions with continuously deforming and evolving rigid plates:
260 *Computers & Geosciences*, v. 116, p. 32–41, doi:10.1016/j.cageo.2018.04.007.
- 261 Jammes, S., Manatschal, G., Lavier, L., and Masini, E., 2009, Tectonosedimentary evolution
262 related to extreme crustal thinning ahead of a propagating ocean: Example of the western
263 Pyrenees: *Tectonics*, v. 28, p. 1–24, doi:10.1029/2008TC002406.
- 264 Lescoutre, R., and Manatschal, G. Role of rift-inheritance and segmentation for orogenic
265 evolution: example from the Pyrenean-Cantabrian system: *Bull. Soc. Géol. Fr*,
266 doi:10.1051/bsgf/2020021.
- 267 MacMahon, H., Welford, J.K., Sandoval, L., and Peace, A.L., 2020, The Rockall and the Orphan
268 Basins of the Southern North Atlantic Ocean: Determining Continuous Basins Across
269 Conjugate Margins: *Geosciences*, v. 10, p. 178.

- 270 Mohn, G., Karner, G.D., Manatschal, G., and Johnson, C.A., 2015, Structural and stratigraphic
271 evolution of the Iberia–Newfoundland hyper-extended rifted margin: a quantitative
272 modelling approach: Geological Society, London, Special Publications, v. 413, p. 53,
273 doi:10.1144/SP413.9.
- 274 Müller, R.D. et al., 2019, A Global Plate Model Including Lithospheric Deformation Along
275 Major Rifts and Orogens Since the Triassic: Tectonics, v. 38, p. 1884–1907,
276 doi:10.1029/2018TC005462.
- 277 Nirrengarten, M., Manatschal, G., Tugend, J., Kusznir, N., and Sauter, D., 2018, Kinematic
278 Evolution of the Southern North Atlantic: Implications for the Formation of
279 Hyperextended Rift Systems: Tectonics, v. 37, p. 89–118, doi:10.1002/2017TC004495.
- 280 Nirrengarten, M., Manatschal, G., Tugend, J., Kusznir, N.J., and Sauter, D., 2017, Nature and
281 origin of the J-magnetic anomaly offshore Iberia–Newfoundland: implications for plate
282 reconstructions: Terra Nova, v. 29, p. 20–28.
- 283 Peace, A.L., Welford, J.K., Ball, P.J., and Nirrengarten, M., 2019, Deformable plate tectonic
284 models of the southern North Atlantic: Journal of Geodynamics, v. 128, p. 11–37,
285 doi:10.1016/j.jog.2019.05.005.
- 286 Reid, I., 1988, Crustal structure beneath the southern Grand Banks: seismic-refraction results and
287 their implications: Canadian Journal of Earth Sciences, v. 25, p. 760–772,
288 doi:10.1139/e88-071.

- 289 Salas, R., Guimerà, J., Mas, R., Martín-Closas, C., Meléndez, A., and Alonso, A., 2001,
290 Evolution of the Mesozoic central Iberian Rift System and its Cainozoic inversion
291 (Iberian chain): *Peri-Tethys Memoir*, v. 6, p. 145–185.
- 292 Sandoval, L., Welford, J.K., MacMahon, H., and Peace, A.L., 2019, Determining continuous
293 basins across conjugate margins: The East Orphan, Porcupine, and Galicia Interior basins
294 of the southern North Atlantic Ocean: *Marine and Petroleum Geology*, v. 110, p. 138–
295 161, doi:10.1016/j.marpetgeo.2019.06.047.
- 296 Sibuet, J.-C., Srivastava, S., Enachescu, M., and Karner, G., 2007, Early Cretaceous motion of
297 Flemish Cap with respect to North America: Implications on the formation of Orphan
298 Basin and SE Flemish Cap-Galicia Bank conjugate margins: *Geological Society, London*,
299 *Special Publications*, v. 282, p. 63–76, doi:10.1144/SP282.4.
- 300 Sibuet, J.-C., Srivastava, S.P., and Spakman, W., 2004, Pyrenean orogeny and plate kinematics:
301 *Journal of Geophysical Research: Solid Earth*, v. 109, p. 1–18,
302 doi:10.1029/2003JB002514.
- 303 Sutra, E., Manatschal, G., Mohn, G., and Unternehr, P., 2013, Quantification and restoration of
304 extensional deformation along the Western Iberia and Newfoundland rifted margins:
305 *Geochemistry, Geophysics, Geosystems*, v. 14, p. 2575–2597, doi:10.1002/ggge.20135.
- 306 Tavani, S., Bertok, C., Granado, P., Piana, F., Salas, R., Vigna, B., and Muñoz, J.A., 2018, The
307 Iberia-Eurasia plate boundary east of the Pyrenees: *Earth-Science Reviews*, v. 187, p.
308 314–337, doi:10.1016/j.earscirev.2018.10.008.

- 309 Tugend, J., Manatschal, G., and Kuszniir, N.J., 2015, Spatial and temporal evolution of
310 hyperextended rift systems: Implication for the nature, kinematics, and timing of the
311 Iberian-European plate boundary: *Geology*, v. 43, p. 15–18, doi:10.1130/G36072.1.
- 312 Tugend, J., Manatschal, G., Kuszniir, N.J., Masini, E., Mohn, G., and Thinon, I., 2014, Formation
313 and deformation of hyperextended rift systems: Insights from rift domain mapping in the
314 Bay of Biscay-Pyrenees: *Tectonics*, v. 33, p. 1239–1276, doi:10.1002/2014TC003529.
- 315 Vissers, R.L.M., and Meijer, P.Th., 2012, Mesozoic rotation of Iberia : Subduction in the
316 Pyrenees ? *Earth Science Reviews*, v. 110, p. 93–110,
317 doi:10.1016/j.earscirev.2011.11.001.
- 318 Williams, S.E., Whittaker, J.M., Halpin, J.A., and Müller, R.D., 2019, Australian-Antarctic
319 breakup and seafloor spreading: Balancing geological and geophysical constraints: *Earth-*
320 *Science Reviews*, v. 188, p. 41–58, doi:10.1016/j.earscirev.2018.10.011.
- 321

Figure 1



- | | | |
|--|--|--|
| <ul style="list-style-type: none"> AFR-EU IB-EBR IB-EU FL-NAM NAM-AFR | <ul style="list-style-type: none"> ○ Our work: 165 to 112 Ma ● Our work: 112 to 83 Ma □ Barnett-Moore et al. 2016: 144 to 120 Ma ■ Barnett-Moore et al. 2016: 120 to 83 Ma | <ul style="list-style-type: none"> ☆ Nirrengarten et al. 2018: 140 to 120 Ma ★ Nirrengarten et al. 2018: 120 to 83 Ma △ Van Hinsbergen et al. 2020: 155 to 126 Ma ▲ Van Hinsbergen et al. 2020: 126 to 83 Ma |
|--|--|--|

Figure 2

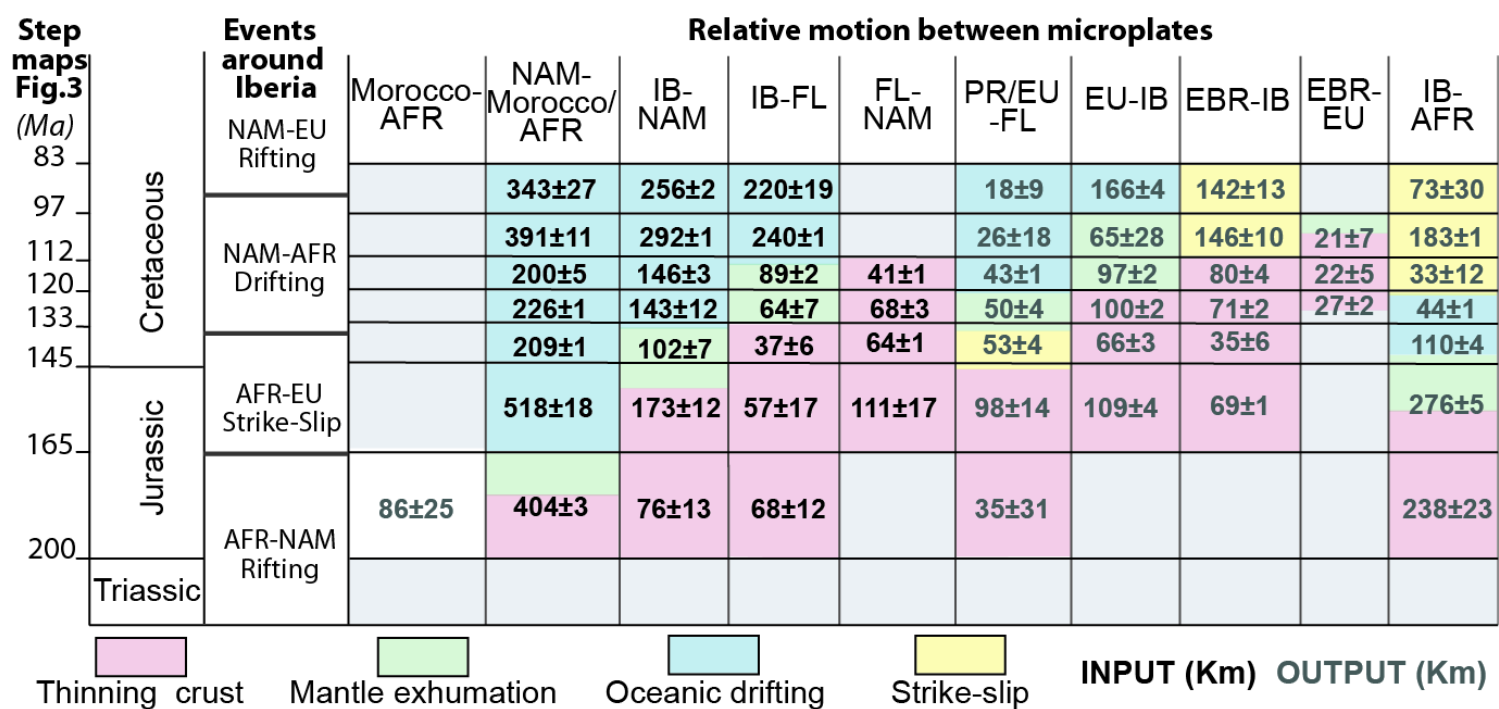


Figure 3

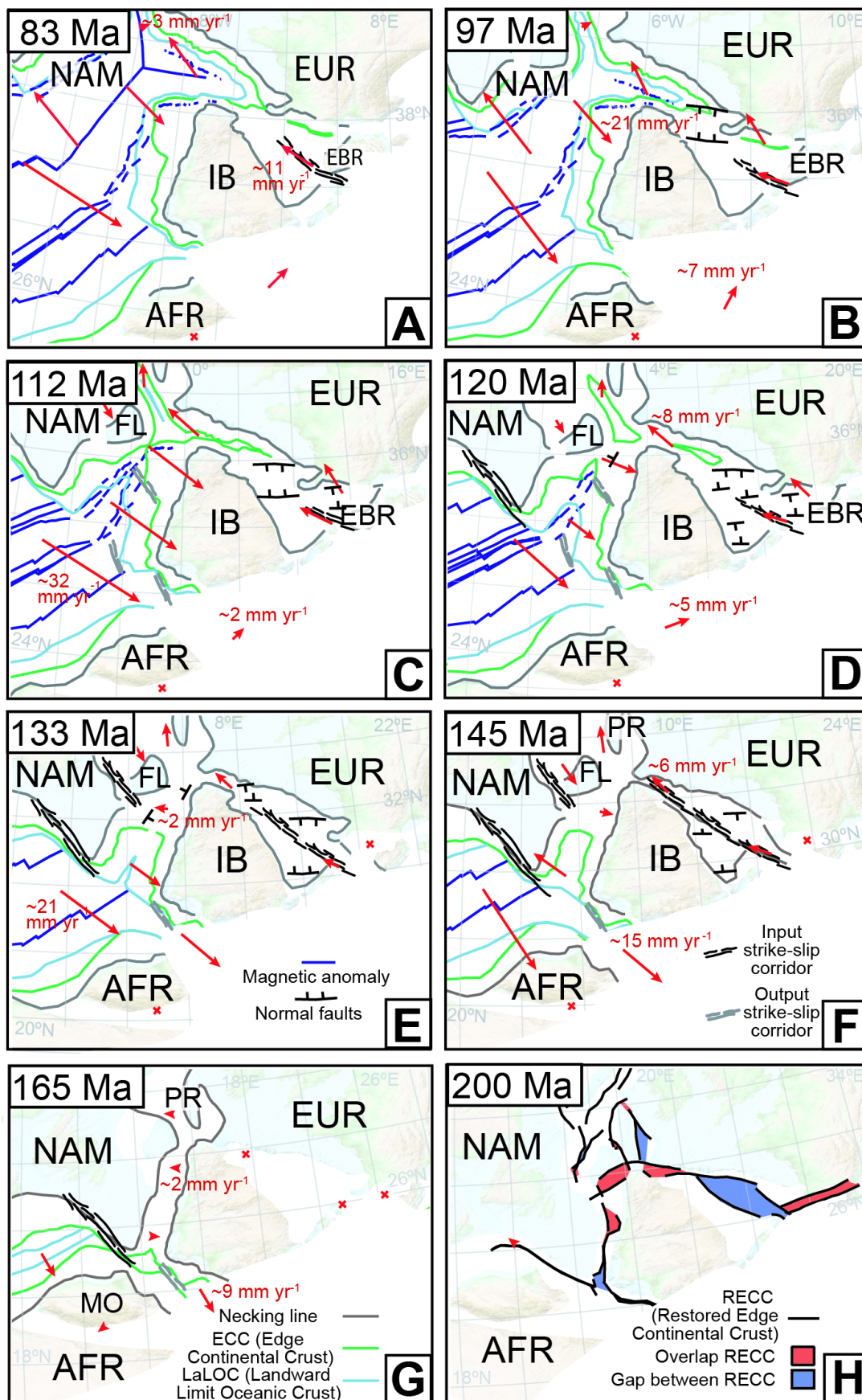
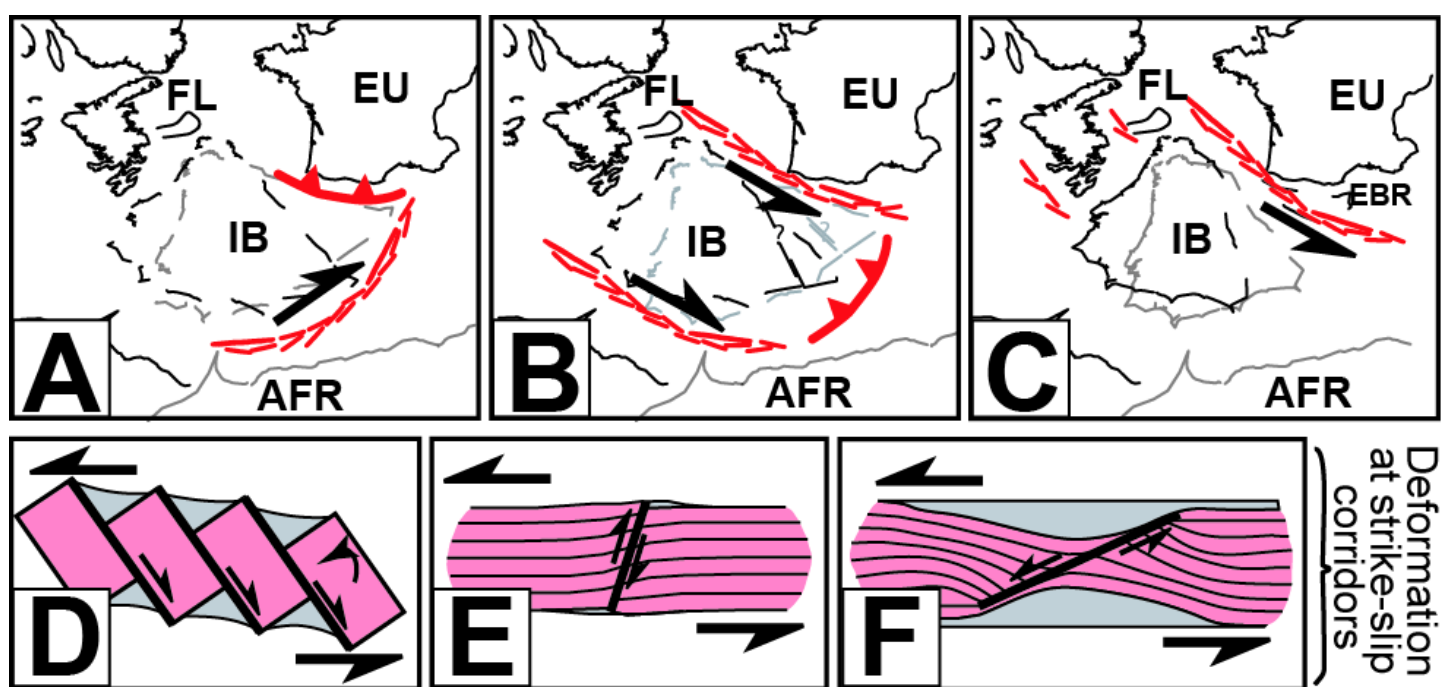


Figure 4



List of Figures

INTRODUCTION

31

- Figure I.1 : Classical view of the Wilson Cycle with possible short-cuts (stripped line). Modified after Petri (2014) and Chenin et al. (2019). 32
- Figure I.2 : Lithospheric scale sections showing (a) an idealized lithosphere made of a thermally equilibrated layer cake and (b) a “real” post-orogenic lithosphere showing inherited structural and compositional complexity. From Manatschal et al. (2015). 33
- Figure I.3 : 3D block to schematize a (a) pure shear extension (symmetric) and (b) a simple shear extension (asymmetric). Modified after Frisch et al. (2010) 34
- Figure I.4 : First order architecture of a volcanic margin (left) and a non-volcanic margin (right). From Peron-Pinvidic et al. (2019). 36
- Figure I.5 : Conceptual model of the evolution of a polyphase rifting. (a) Stretching mode characterized by high angle normal faults associated to half-graben subsidence. Continental crust may be slightly stretched, and sedimentary basins developed independently from each other. (b) Thinning phase is characterized by a conjugate decoupling system of detachment faults that accommodated exhumation of deeper crustal levels. Deformation goes from a distributed to localized extension. (c) Exhumation phase is observed where detachment faults crosscut the embrittled crust and exhume serpentinized mantle rocks. (d) Sea floor spreading is the final phase where a proto-ridge is developed. Modified after Peron-Pinvidic and Manatschal (2009). 37
- Figure I.6 : Simplified architecture of a passive margin hyperextended with the characterized domains and its main characteristics. Modified after Tugend (2013). 38
- Figure I.7 : Conceptual model of (a) polyphase rift system, (b) multistage rift system and (c) multistage and polyphase rift system in both map view (upper part) and section view (lower part). 38
- Figure I.8 : Diagram showing a possible classification of orogens by temperature and magnitude. From Jamieson and Beaumont (2013). 40
- Figure I.9 : Geological sketch of the ECORS geological cross section of the Central Pyrenees with the main terminology of a fold and thrust belt. From Muñoz et al., (2018). 41
- Figure I.10 : Geological sketch of the Sevier and Laramides orogens in North America to illustrate a thin-skinned structural style vs a thick-skinned structural style. Modified after Wyoming State Geological Survey (2020). 42
- Figure I.11 : Geological cross section along the Pallaresa valley (central Pyrenees s.s.) based on the ECORS-Pyrenees cross section. From Muñoz et al. (2018). 43
- Figure I.12 : Mountain belts of the western portion of the Himalayan – Alpine orogenic system labelled in black and main tectonic plates labelled

in white. From Carola (2014).	44
Figure I.13 : Crustal scale geological cross section along the Pyrenean Orogen showing the main architecture along strike. (1) ECORS-Pyrenees, (2) ECORS-Arzaq, (3) Basque-Cantabrian Pyrenees – Parentis and (4) Asturian Massif – Armorican Margin. Modified after Muñoz (2019).	45
Figure I.14 : Common terminology used in the literature to refer to different parts of the Pyrenean orogen. Modified from Barnolas and Pujalte (2004).. .	46
Figure I.15 : Map of the Variscan orogeny in the western Europe with the main sutures identified and the different tectonic plates involved. Modified after Martínez-Catalán et al. (2007).	47
Figure I.16 : Plate tectonic reconstruction of the Alpine realm at (a) Late Triassic and (b) Late Jurassic stages. Symbols: 1: passive margin; 2: magnetic or synthetic anomalies; 3: seamount; 4: intra-oceanic subduction; 5: mid-ocean ridge; 6: active margin; 7: active rift; 8: inactive rift (basin); 9: collision zone; 10: thrust; 11: suture. Oceanic lithosphere in black. See Stampfli and Hochard (2009) for the meaning of abbreviations. From Stampfli and Hochard (2009)..	48
Figure I.17 : Different models proposed for the geodynamic evolution of the Iberia-Eurasia plate boundary at Late Jurassic-Aptian and at Aptian-Santonian times (modified after Tavani et al., 2018). Orthogonal rifting model after Tugend et al. (2015); Strike-slip model after Stampfli & Borel (2002); Scissor-type model after Sibuet et al. (2004). Modified after Lescoutre (2019)..	50
Figure I.18 : Different plate reconstructions for the Iberian and NW African/Moroccan plate. Red line: Macchiavelli et al., 2017; blue line: Vissers and Meijer (2012); green line: Rosenbaum et al. (2002); purple line: Srivastava et al. (1990). Present-day coastlines (grey areas) are shown for reference. From Macchiavelli et al. (2017).	51
Figure I.19 : Hydrographical base map with the location of the main datasets used in this thesis.. . . .	53
Figure I.20 : Geomodels Analogue Modelling Laboratory of the University of Barcelona where the experimental program was run.	55

CHAPTER 1: REACTIVATION OF A HYPEREXTENDED RIFT SYSTEM: THE BASQUE-CANTABRIAN PYRENEES CASE

61

Figure 1.7 : Onshore a structural map of the Pyrenees and surrounding areas with the main terminology used in this work (modified from Carola et al., 2013). The offshore geology is represented by the rift domains (from Tugend et al., 2014 and Cadenas et al., 2018). Mesozoic rift basins are labelled in white and the orange line shows the position of the seismic line CS-146 modified in this work.	63
Figure 1.8 : a) Classification of extensional rift basins. b) Theoretical sketch showing the rift system variability (see the text for further details).	65
Figure 1.9 : Tectono-stratigraphic map of the Basque – Cantabrian Pyrenees and surroundings with the location of the different seismic line and	

wells shown in this work as well as the position of the Central and Western sections presented in this study (figures 11 and 12). BCB: Basque – Cantabrian Basin; CB: Cabuérniga Basin; PB: Polientes Basin. 67

Figure 1.10 : N-S seismic sections in the (a) Folded Band, (b) Burgalesa Platform and (c) Sierra de Cantabria Frontal Thrusts - Montes de Tesla areas with the projection of Tozo and Villalta wells as well as the field data and outcropping units showing the structure of the southern Central section. FT: frontal thrust; UF: Ubierna Fault; SCFT: Sierra de Cantabria Frontal Thrust. See Fig. 3 for location. 70

Figure 1.11 : a) N-S seismic section in the Alavesa Platform and Bilbao Anticlinorium areas showing the overlapping of Mesozoic syn-rift depocenters shifting to the south. See Fig. 3 and b) for location. b) Map of the different Mesozoic syn-rift depocenters of more than 2 km thick in the Basque – Cantabrian Pyrenees build from seismic interpretation and field observations. See colour legend in Fig. 5a. 72

Figure 1.12 : a) Aerial photograph from the Sopela beach with the interpretation of the thrust weld and a field image of the detailed weld with the characteristic shear deformation. See location in Fig. 3 and b). b) Geological cross section in the northern Central section modified from Roca et al., subm. with the integration of field data, observations coming from BR85-25 and HZV-81-19 interpreted seismic lines and the projections of Cormoran-1, Gaviota B-a and Vizcaya B-1 boreholes. 73

Figure 1.13 : N-S seismic sections (a and b) and E-W seismic section (c) in the Polientes Mesozoic Basin with the projection of the Cantonegro-1, El Coto-1 and Cadialso-1 boreholes and the surface data and geology. The E-W (c) section shows the thick- to thin-skin transition in the Western Basque – Cantabrian Pyrenees and the plunge observed in the sediments at surface controlled by the basement at depth. See Fig. 3 for location. 74

Figure 1.14 : a) N-S seismic section in the Santander Block area with the projection of the field data and surface geology as well as the Oreña-1 borehole and the Ajo-1 borehole to link the onshore with the offshore sections. CB: Cabuérniga Fault. b) Field image of the northern limit of the Cabuérniga Basin with the view to the Cabuérniga Fault. See location in Fig. 3. 75

Figure 1.15 : Northern part of the Western section combining the STC-13 seismic line (Fig. 8) and a modified depth converted interpretation from the CS-146 seismic line of Cadenas et al. (2020). See Figs. 1 and 3 for location. . . 76

Figure 1.16 : Compiling of the published geophysical data along the central section (a) and Western section (b) coming from seismic, borehole and refraction data. 77

Figure 1.17 : a) Present-day crustal-scale cross section across the central Basque – Cantabrian Pyrenees (modified from Muñoz et al., 2019). See Fig. 3 for location. b) Restoration of the Central section at Middle Cenomanian times (end of multistage and polyphase extension) with the rift domains depicted on top. c) Restoration of the Central section at Barremian times (end of the first rift stage). 81

Figure 1.18 : a) Present-day crustal-scale cross section across the western Basque – Cantabrian Pyrenees to the Bay of Biscay. See Fig. 3 for location. b) Restoration of the Western section at middle Cenomanian times (end of polyphase extensional event) with the rift domains depicted on top. Dashed lines show the future compressional structures. c) Restoration of the Western section at Barremian times (end of the first monophasic rift stage). 82

Figure 1.19 : The three basic concepts for a proper restoration of a hyperextended rifted margin. a) Crustal areal conservation and pre-rift length conservation. b) Rheological component by considering the different decoupling levels may influence such evolution. c) Isostasy, considering the crustal thickness vs total accommodation space relation. . . 84

Figure 1.20 : Theoretical distribution of decoupling levels at the end of extension that will control the reactivation of a hyperextended margin. From the reactivation of the serpentinized mantle occurring at first in the more distal domains initiating the underthrusting, to the reactivation of a mid-crustal decoupling in the necking domain to the final decoupling of the sedimentary cover in the salt where it is available. 87

CHAPTER 2: ROLE OF INHERITANCE IN A THICK- TO THIN-SKIN TRANSITION: INSIGHTS FROM ANALOGUE MODELLING AND BASQUE – CANTABRIAN PYRENEES 93

Figure 2.1 : Structural map of the Pyrenean Orogen and surrounding areas with crustal cross sections depicting the main structural changes along the fold and thrust belt. Offshore, rift domains are mapped. 1: Asturian Massif – Armorican Margin; 2: Basque – Cantabrian Pyrenees – Parentis; 3: ECORS-Arzaq; 4: ECORS-Pyrenees. Modified from Carola et al. (2013) and Cadenas et al. (2018). 96

Figure 2.2 : Tectonostratigraphic map of the Basque – Cantabrian Pyrenees – Asturian Massif junction and geological cross section showing the along strike variability of the structural style, thick-skinned to the west and thin-skinned to the east. Cross section 1 from Alonso et al. (1996). 98

Figure 2.3 : 3D (left) and top view (right) schemes of the experimental setup. A) 3D diagram showing the disposition of the rigid blocks at the base of the model. B) top view of the previous 3D diagram. C) final organization of the setup with transparency of various sand-layers. Note the limit of basement and pinch-out of the polymer as indicated in d). D) top view of model with basement sand and polymer to show the overlapping area and the limits of both units which defines the different structural domains. E) section view of the coupled and decoupled domains located in d). 100

Figure 2.4 : Top view evolution of Model-1. Illumination comes from the left. Shadowed areas are surface-breaching faults dipping to right (north) and illuminated areas are surface-breaching faults dipping to left (south). The position of the basement rigid blocks is showed in grey dotted lines and the pinch-out of the salt (P.S.) and the limit of basement blocks (L.B.) in white dotted lines. A) top view after 5 mm of extension. B) top view after 25

mm of extension. C) top view after 70 mm of extension. D) top view after 115 mm of extension. See text for details.	102
Figure 2.5 : Cross sections at the end of the extensional deformation (127 mm). A) coupled domain; B) transitional domain; C) decoupled domain. See Fig. 4d for location of sections.....	104
Figure 2.6 : Top view evolution of Model-2. Illumination comes from the left. The position of the basement rigid blocks is showed in grey dotted lines and the pinch-out of the salt (P.S.) and the limit of basement blocks (L.B.) in white dotted lines. A) top view after 21 mm of compression. B) top view after 78 mm of compression. C) top view after 138 mm of compression. D) top view at the end of compression (200 mm). See text for details.	106
Figure 2.7 : Cross sections at the end of the compressional deformation (200 mm). A) coupled domain; B) transitional domain; C) decoupled domain. See Fig. 6d for location of sections.....	108
Figure 2.8 : Top view evolution of Model-3. Illumination comes from the left. The position of the basement rigid blocks is showed in grey dotted lines and the pinch-out of the salt (P.S.) and the limit of basement blocks (L.B.) in white dotted lines. A) top view after 21 mm of compression. B) top view after 78 mm of compression. C) top view after 138 mm of compression. D) top view at the end of compression (200 mm). See text for details.....	109
Figure 2.9 : Cross sections at the end of the compressional deformation (200 mm). A) coupled domain; B) transitional domain; C) decoupled domain. See Fig. 8d for location of sections.....	110
Figure 2.10 : The upper part shows a top view evolution of the transitional domains: a) after 22mm of compression, b) after 46 mm of compression, c) after 88 mm of compression, d) after 166mm of compression. E) top view at the end of compression (200 mm) with the location of the detailed evolution in black square (a to d). f) W-E cross section to the north (see location in e). G) W-E cross section to the south (see location in e).	113
Figure 2.11 : a) top view at the end of compressional deformation with the location of detailed sections displayed below. B) to D) detailed cross sections from east (b) to west (d) showing the changing of vergence in structures from the decoupled to transitional domains. In section c) structures with both vergence coexist.....	114
Figure 2.12 : a) top view of Model-3 at the end of compression. B) tectonostratigraphic map of the Basque – Cantabrian Pyrenees – Asturian Massif junction. C) cross section of the coupled domain showing the thick-skinned architecture in Model-3. D) cross section through the Asturian Massif showing the thick-skinned architecture similar to what observed in the model. E) section through the decoupled domain in Model-3. F) geological cross section across the southern Basque – Cantabrian Pyrenees showing the thin-skinned character.	115

CHAPTER 3: CONTROL OF RIFT-INHERITANCE ON THE NUCLEATION AND GROWTH OF AN OROGEN: INSIGHTS FROM THE PYRENEAN OROGEN **121**

Figure 3.1 : Rift domain map of the Pyrenean – BoB area. STS: Santander Transfer System, W: Western section, C: Central section; E: Eastern section. Modified from Tugend et al., 2014 and Cadenas et al., 2018 122

Figure 3.2: Present-day and restoration to onset of compression and end of extension of the BoB - BCP represented by rift domain maps to the left and three representative sections to the right showing three different scenarios. Sections modified from Miró et al., subm. and Lescoutre et al. subm. 125

Figure 3.3 : Reactivation of a hyperextended rift margin model in section view (top) and map view (bottom). Note the distribution of the main decollements and the link between rift domains and evolution (i.e. timing) of an orogen. 129

ANNEX 1: THE BASQUE - CANTABRIAN PYRENEES: REPORT OF DATA ANALYSIS **187**

Figure A1.1 : Geographic terminology and some examples of geological terminology used in the Pyrenees. Modified from Barnolas and Pujalte (2004) and Carola et al. (2013). 190

Figure A1.2 : a) Tectonic map of the Pyrenean – Bay of Biscay realm with the main structural features resulted from the Alpine orogeny and the presence of the main Mesozoic basins labelled in white: AM: Armorican Margin Basin, Ar-Ma: Arzaq-Mauleon Basin, As: Asturian Basin, BC: Basque – Cantabrian Basin s.s., BoB: Bay of Biscay Basin, Ca: Cameros Basin, Cb: Cabuerniga Basin, Po: Polientes Basin, Or: Organyà Bain, Ma: Maestrat Basin, Pa: Parentis Basin. Labelled in black Paleozoic Massifa: BM: Basque Massif, DE: Demanda Massif. Modified after Masini *et al.* (2014). b) Rift basin models described in the literature. 193

Figure A1.3 : Simplified geological map of the Basque – Cantabrian Pyrenees with the main domains labelled in capital letters and minor domains labelled in black. Modified after Ábalos et al. (2008). 193

Figure A1.4 : Geological map of the Basque – Cantabrian Pyrenees with the location of seismic lines, drill holes, and field data (i.e. measurements and observations) in brown dots presented in this work. The geological maps compiled to build the thematic map presented in this work are also located: MAGNA-IGME: geological map at 1:50.000 scale from Instituto Geológico y Minero de España (IGME), GC-IGME: geological map at 1:25.000 scale from Gobierno de Cantabria and IGME, EVE: geological map at 1:25.000 scale from Ente Vasco de la Energia, ENRESA: geological map at 1:25.000 from Empresa Nacional de Residuos Radioactivos S.A., Ábalos, B. (2016), Lescoutre, R. (2019) and Carola, E. (2014). See Annex 2.3 for a detailed bibliography. 195

Figure A1.5 : Tectonic events documented in the Basque – Cantabrian Pyrenees from Paleozoic to present-day reported in the literature with the geological units grouped in this report. 196

Figure A1.6 : Composite reflexion seismic line and its line drawing crossing the Basque – Cantabrian Pyrenees from south (left) to north (right) with nine boreholes and refraction seismic data projected. The surface geology and the main sedimentary successions of syn-extensional sediments and syn-compressional sediments are showed together with the main structures of the area. See the text and Annex 2.1 for further details.	199
Figure A1.7 : Stratigraphic logs of nine drill holes from the Basque – Cantabrian Pyrenees. All of them start in the same reference level (0 meters) even if they are located at different topographic elevations. The vertical axis shows depth in meters. See Annex 2.2 for further details of each drill hole..	200

List of Tables

Table 1 : Scaling parameters used in the experimental program	101
Table 2 : Experimental program.....	101

Rift-inheritance, segmentation and reactivation of the North Iberian rift system in the Basque - Cantabrian Pyrenees

RÉSUMÉ

Alors que les systèmes de subduction et les « fold-and-thrust-belts » ont été largement étudiés, la transition entre les deux, englobant l'incorporation d'anciens systèmes/marges de rift, reste mal comprise. Cette étude utilise des données géologiques et géophysiques dans les Pyrénées Basco – Cantabriques afin de proposer un nouveau cadre tectono-stratigraphique reliant l'état orogénique actuel au modèle hérité de rift « multistage » et « polyphase ».

L'étude montre que la variabilité structurale et d'architecture le long de l'axe orogénique est héritée des premières étapes de la réactivation qui sont contrôlées par le modèle de rift « multistage » caractérisé par la segmentation et l'existence d'un manteau serpentinisé exhumé contrôlant l'emplacement de la proto-subduction. Alors que la présence de sel du Trias épais et continu peut expliquer le découplage et le style « thin-skin » de la déformation lors de la collision dans les Pyrénées Basco – Cantabriques, la faible quantité de sel dans le Massif asturien a favorisé la réactivation des niveaux de découplage dans la croûte moyenne impliquant un style de collision dit « thick-skin », et conduisant à une liaison complexe entre les deux domaines telle que soutenue par des expériences de modélisation analogique.

Cette étude révèle que la formation et la réactivation des systèmes de rift segmentés et leur incorporation dans les orogènes collisionnels sont au premier ordre contrôlées par l'architecture de rift et les niveaux de découplage hérités, un résultat qui doit être pris en compte dans les futures études traitant des systèmes orogéniques.

Mots clefs : héritage, segmentation, réactivation, « thick- et thin-skin », Pyrénées Basco – Cantabriques

ABSTRACT

While subduction systems and fold and thrust belts have been widely studied, the transition between the two, embracing the incorporation of former rift systems/margins remains poorly understood. This study used geological and geophysical datasets from the Basque – Cantabrian Pyrenees to propose a new tectono-stratigraphic framework that links the present orogenic state with the inherited multistage and polyphase rift template.

The study shows that the along strike variability is inherited from the early stages of reactivation that are controlled by the multistage rift template characterized by segmentation and the existence of exhumed serpentinized mantle controlling location of the proto-subduction. While the presence of thick and continuous Triassic salt can explain the decoupling and thin-skinned style throughout collision in the Basque – Cantabrian Pyrenees, the occurrence of less salt in the Asturian Massif favoured the reactivation of mid-crustal levels and thus a thick-skinned collision style, leading to a complex linkage of both domains, a result that is supported by analogue modelling experiments.

This study reveals that the formation and reactivation of segmented rift systems and its incorporation into collisional orogens is to a first order controlled by the rift template and inherited decoupling levels, a result that needs to be taken into account in future studies of orogenic systems.

Key words: rift-inheritance, segmentation, reactivation, thick- and thin-skin, Basque-Cantabrian Pyrenees